
**Pacific Northwest
National Laboratory**

Operated by Battelle for the
U.S. Department of Energy

Dust Plume Modeling at Fort Bliss: Move-Out Operations, Combat Training and Wind Erosion

(Contract No. 50026A)

E. G. Chapman
J. P. Rishel
F. C. Rutz
T. E. Seiple
R. K. Newsom
K. J. Allwine

September 2006

Prepared for the U. S. Army Fort Bliss Directorate of Environment
under a Related Services Agreement with the U.S. Department of
Energy under contract DE-AC05-76RL01830



DISCLAIMER

This report was prepared as an account of work sponsored by an agency of the United States Government. Neither the United States Government nor any agency thereof, nor Battelle Memorial Institute, nor any of their employees, makes **any warranty, express or implied, or assumes any legal liability or responsibility for the accuracy, completeness, or usefulness of any information, apparatus, product, or process disclosed, or represents that its use would not infringe privately owned rights.** Reference herein to any specific commercial product, process, or service by trade name, trademark, manufacturer, or otherwise does not necessarily constitute or imply its endorsement, recommendation, or favoring by the United States Government or any agency thereof, or Battelle Memorial Institute. The views and opinions of authors expressed herein do not necessarily state or reflect those of the United States Government or any agency thereof.

PACIFIC NORTHWEST NATIONAL LABORATORY
operated by
BATTELLE
for the
UNITED STATES DEPARTMENT OF ENERGY
under Contract DE-AC05-76RL01830

Printed in the United States of America

**Available to DOE and DOE contractors from the
Office of Scientific and Technical Information,
P.O. Box 62, Oak Ridge, TN 37831-0062;
ph: (865) 576-8401
fax: (865) 576 5728
email: reports@adonis.osti.gov**

**Available to the public from the National Technical Information Service,
U.S. Department of Commerce, 5285 Port Royal Rd., Springfield, VA 22161
ph: (800) 553-6847
fax: (703) 605-6900
email: orders@nits.fedworld.gov
online ordering: <http://www.ntis.gov/ordering.htm>**

Dust Plume Modeling at Fort Bliss: Move-Out Operations, Combat Training and Wind Erosion

(Contract No. 50026A)

E. G. Chapman
J. P. Rishel
F. C. Rutz
T. E. Seiple
R. K. Newsom
K. J. Allwine

September 2006

Prepared for the U. S. Army Fort Bliss Directorate of Environment
under a Related Services Agreement with the U.S. Department of
Energy under contract DE-AC05-76RL01830

Pacific Northwest National Laboratory
Richland, Washington 99352

Summary

The potential for air-quality impacts from heavy mechanized vehicles operating in the training ranges and on the unpaved main supply routes at Fort Bliss was investigated. This report details efforts by the staff of Pacific Northwest National Laboratory for the Fort Bliss Directorate of Environment in this investigation. Dust emission and dispersion from typical activities, including move outs and combat training, occurring on the installation were simulated using the atmospheric modeling system DUSTRAN. Major assumptions associated with designing specific modeling scenarios are summarized, and results from the simulations are presented. Major findings include the following:

- Move-outs produce substantially higher PM_{10} concentration contributions than combat training under the same meteorological conditions.
- Impacts from move-outs tend to be highly localized, and the impact location is dependent on the prevailing wind direction in relation to the direction of vehicle travel along the move-out route.
- Low-wind-speed days generally result in higher 24-hour average PM_{10} concentration contributions when compared to high-wind-speed days, especially for combat training scenarios.

Finally, this report examines concentration contributions from dust generated by wind erosion within the Fort Bliss installation. Factors contributing to wind-generated dust are summarized, and Fort Bliss-specific vegetation cover and surface soil texture datasets are described. Results from two DUSTRAN wind erosion simulations—a high- and low-wind speed case—are contrasted and used to quantify the range of wind-generated dust concentrations that might be expected from the Fort Bliss site.

Acronyms

BFIST	Bradley Fire Support Vehicle
BRAC	base realignment and closure
DoD	U.S. Department of Defense
EP	emission potential
EPA	U.S. Environmental Protection Agency
ESE	east-south-east
ESRI	Environmental System Research Institute
GIS	Geographical Information System
GPSMET	Global Positioning System Meteorology
HBCT	heavy brigade combat team
HEMTT	heavy expanded mobility tactical truck
HMMWV	high-mobility multipurpose wheeled vehicle
kph	km per hour
NMED	New Mexico Environmental Department
NWS	National Weather Service
PNNL	Pacific Northwest National Laboratory
PSD	prevention of significant deterioration
RAWS	remote automated weather stations
SERDP	Strategic Environmental Research and Development Program
TCEQ	Texas Commission on Environmental Quality
WNW	west-north-west
WSMR	White Sands Missile Range

Contents

Summary	iii
Acronyms	v
1.0 Introduction.....	1.1
2.0 DUSTRAN Modeling System	2.1
3.0 Determination of Simulation Periods.....	3.1
3.1 Meteorology.....	3.1
3.2 Ambient PM ₁₀ Concentrations.....	3.5
3.3 Selected Simulation Periods	3.6
4.0 Scenarios for Vehicle-Generated Dust.....	4.1
4.1 Brigade Characteristics.....	4.1
4.2 Move-Out Activities	4.3
4.3 Combat Training Activities	4.7
4.4 Vehicle-Emission Factors.....	4.11
5.0 Scenarios for Wind-Generated Dust	5.1
6.0 Simulations of Vehicle-Generated Dust	6.1
7.0 Simulations of Wind-Generated Dust.....	7.1
8.0 List of Persons Consulted	8.1
9.0 References.....	9.1
Appendix A: Wind Roses	A.1
Appendix B: Measured Ambient PM ₁₀ Concentrations.....	B.1
Appendix C: Mapping of HBCT Vehicles to DUSTRAN Vehicle Types.....	C.1
Appendix D: Simulated 24-h-Average PM ₁₀ Concentrations for McGregor Move-Out	D.1
Appendix E: Simulated 24-h-Average PM ₁₀ Concentrations for Dona Ana Move-Out.....	E.1
Appendix F: Simulated 24-h-Average PM ₁₀ Concentrations for Combat Training.....	F.1
Appendix G: Simulated Peak 1-h-Average PM ₁₀ Concentrations for Combat Training	G.1
Appendix H: DUSTRAN 10-m-Above-Ground Wind Fields for March 12 through 16, 2005	H.1

Appendix I: DUSTRAN 10-m-Above-Ground Wind Fields for April 25 through 30, 2005	I.1
Appendix J: DUSTRAN 10-m-Above-Ground Wind Fields for July 20 through 24, 2005	J.1
Appendix K: DUSTRAN 10-m-Above-Ground Wind Fields for November 25 through 29, 2005	K.1

Figures

3.1. Meteorological Stations in the Vicinity of Fort Bliss	3.2
3.2. Mean PM10 Concentration (black) and Wind Speed (red) at TCEQ CAMS37	3.4
3.3. The Left Panel Shows the Time Series of Hourly PM ₁₀ Concentration (Black Dots) for 2005 at TCEQ CAMS12	3.5
3.4. Time Series of Hourly Ambient PM ₁₀ Concentrations at Two Sites and Wind Measurements at One Site for 2005	3.7
4.1. Dona Ana and McGregor Move-Out Routes	4.4
4.2. Normalized Dust Emissions as a Function of Time for One (Blue) and Three (Red) Line Segments Approximating the Release from a Long-Line Source	4.6
4.3. Fort Bliss Battalion Maneuver Boxes	4.9
4.4. DUSTRAN Representation of Battalion Maneuver Boxes Used In Combat Training Scenarios	4.10
5.1. Olson Vegetation Classes for the Fort Bliss Site	5.3
5.2. Zobler Soil Texture Categories for the Fort Bliss Site	5.4
6.1. 24-Hour-Average PM ₁₀ Concentration Contributions on April 30, 2005, for the Dona Ana Move-Out (Left) and Combat Training (Right) Scenarios as Simulated in DUSTRAN	6.3
6.2. 24-Hour-Average PM ₁₀ Concentration Contributions for the McGregor (Left) and Dona Ana (Right) Move-Out Scenarios on April 25, 2005, as Simulated in DUSTRAN	6.4
6.3. Peak 1-Hour- and 24-Hour-Average PM ₁₀ Concentration Contributions for the Combat Training Scenario on April 30, 2005, as Simulated in DUSTRAN	6.5
6.4. 24-Hour-Average PM ₁₀ Concentration Contributions on July 23, 2005, (Left) and July 21, 2005 (Right) for the Combat Training Scenario as Simulated in DUSTRAN	6.6
7.1. 24-Hour-Average PM ₁₀ Concentration Contributions on April 25, 2005, (Left) and April 30, 2005 (Right) from Wind-Generated Dust within the Fort Bliss Site as Simulated in DUSTRAN	7.3
7.2. 10-Meter Wind Field at 1000 MST on April 25, 2005 (Left) and April 30, 2005, (Right) for the Fort Bliss Site as Calculated by DUSTRAN	7.4

Tables

3.1. Information on Meteorological and Air Quality Stations in the Fort Bliss Vicinity	3.3
3.2. Periods in 2005 Selected for DUSTRAN Simulations	3.6
4.1. DUSTRAN Vehicle Types	4.2
4.2. Overall Mapping of All Heavy Brigade Combat Team Vehicles to DUSTRAN Vehicle Types....	4.2
5.1. Olson Vegetation Classes and Associated Dust Production Factor Used in DUSTRAN.....	5.1
5.2. Fort Bliss Olson Vegetation Classes and Associated Dust-Production Factor	5.2
5.3. Fractions of the Soil Texture Classes in each Zobler Soil Category	5.2

1.0 Introduction

Potential air-quality impacts from heavy mechanized vehicles operating in the training ranges and on the unpaved main supply routes at Fort Bliss are being investigated. Fort Bliss is a multi-mission U.S. Army installation covering approximately 1.12 million acres stretching over two states, Texas and New Mexico. The installation lies mainly within the Tularosa Basin, one of the largest valleys in the Rio Grande rift. From south to north along the installation eastern boundary lie the Hueco Mountains, the Otero Mesa, and the Sacramento Mountains. On the installation southwest boundary lie the Franklin Mountains, while the Organ Mountains lie toward the western edge. The main cantonment or city portion of the installation is in El Paso County, Texas, with the installation and El Paso City sharing a common boundary. The Fort Bliss Training Complex covers the vast majority of the installation land area and is composed of three large geographic segments: the South Training Area, the Dona Ana Range-North Training Area, and the McGregor Range.

Recent recommendations by the Base Realignment and Closure (BRAC) Commission will lead to additional personnel and equipment being assigned to Fort Bliss. These recommendations also may require increasing land areas available for off-road training and maneuver. Dust emissions from military activities on both established and newly opened training areas have the potential to drift off the installation and impact air quality in the local airshed.

This report summarizes efforts by the staff of Pacific Northwest National Laboratory (PNNL) for the Fort Bliss Directorate of Environment to investigate the potential for possible air quality impacts from military activities. The investigation was conducted using the atmospheric dispersion modeling system DUSTRAN (Version 1.0) to simulate dust emission and dispersion from typical activities occurring on the installation. Although the emphasis of the study was on dust generated from vehicle movements, wind-generated dust (i.e., particulates generated via wind erosion) was also investigated. This report 1) briefly describes the DUSTRAN modeling system, 2) summarizes the meteorological analysis that was used to identify suitable time periods for sample simulations, 3) summarizes the development of military activity scenarios to be simulated with DUSTRAN along with the assumptions used in these scenarios, and 4) presents results of model simulations conducted using these scenarios. Example simulations of wind-generated dust from within the Fort Bliss installation are also presented, and concentration contributions are compared to results from vehicular activities.

2.0 DUSTRAN Modeling System

DUSTRAN was developed under the U.S. Department of Defense's (DoD's) Strategic Environmental Research and Development Program (SERDP) to create an atmospheric dispersion modeling system to assist the DoD in addressing particulate air quality issues at military training and testing ranges (Allwine et al. 2004; Allwine et al. 2006). DUSTRAN is a comprehensive dispersion modeling system, consisting of a dust-emissions model, a diagnostic meteorological model, and dispersion models that are integrated seamlessly into Environmental System Research Institute's (ESRI's) ArcMap Geographical Information System (GIS) software. DUSTRAN functions as a console application within ArcMap and allows the user to interactively create a release scenario and run the underlying models. Through the process of data layering, the model domain, sources, and results—including the calculated wind vector field and plume contours—can be displayed with other spatial and geophysical data sources to aid in analyzing and interpreting the scenario.

Fundamental to DUSTRAN is a dust-emissions model that includes algorithms for calculating dust emissions from both vehicle activity and wind erosion. Vehicle-generated dust includes activities on paved and unpaved surfaces of roadways. The emissions model includes the Gillies et al. (2005a; 2005b) particulate emission factors for various wheeled military vehicles and the widely-used AP-42 emission factors (EPA 2005). The experiments to derive the Gillies et al. (2005a; 2005b) wheeled military vehicle-emission factors were conducted at Fort Bliss during the spring of 2001 and the spring of 2002. Wind-generated dust over a user-specified modeling region is a function of surface wind stress, soil type, and vegetation type. For both vehicle-generated and wind generated dust, emissions are calculated for explicit particle-size classes of $PM_{2.5}$, PM_{10} , PM_{15} , and PM_{30} .

In DUSTRAN, dust transport, diffusion, and deposition are simulated using one of two regulatory (40 CFR Part 51, Appendix W) dispersion models—the CALifornia PUFF (CALPUFF) model or the CALifornia GRID (CALGRID) model. The use of two dispersion models arises from their frame-of-reference used in calculating plume transport, which leads to inherent strengths in simulating different source types. The CALPUFF (Scire et al. 2000a) dispersion model is used for vehicle-generated dust emissions where explicit source-types can be identified using well-defined area or line-source configurations. The CALGRID (Scire et al. 1989) dispersion model is used for wind-generated dust emissions where the entire model domain is a potential emission source.

A diagnostic meteorological model, called the CALifornia METeorological (CALMET) model (Scire et al. 2000b), is also integrated in DUSTRAN. The main function of CALMET is to create gridded fields of wind and boundary-layer parameters from observed meteorological data. These gridded fields are then supplied to the CALPUFF and CALGRID dispersion models, which perform the plume advection, diffusion, and deposition calculations.

Numerous data preprocessors interface CALMET, CALPUFF, and CALGRID to standard terrain elevation and land-use datasets for use in model calculations. A post-processing program, called CALifornia POST (CALPOST), is also available for computing average (greater than 1 hour) concentration and deposition values. All model components are dynamically linked and managed by the DUSTRAN interface. For the current application, Fort Bliss Directorate of Environment staff provided geo-reference data layers (e.g., roads, tank trails, installation boundaries, and training areas) for

visualizing model results and detailed, high-resolution GIS soils and vegetation data layers for use in wind-generated dust simulations.

Further details on DUSTRAN and the dispersion models and processors that comprise it can be found in Allwine et al. (2006), Scire et al. (1989), Scire et al. (2000a), and Scire et al. (2000b).

3.0 Determination of Simulation Periods

Meteorological conditions are important in dust simulations because they govern the transport, diffusion, and deposition of dust particles released into the atmosphere. This section reviews wind and ambient PM₁₀ measurement from sites near Fort Bliss, summarizes the results of analyses of selected wind and PM₁₀ data, and identifies four periods for the DUSTRAN simulations. The four simulation periods represent meteorological conditions conducive to potentially high PM₁₀ concentrations from dust generated from vehicle activities and wind erosion at Fort Bliss.

3.1 Meteorology

Meteorological and PM₁₀ monitoring stations located in the vicinity of Fort Bliss include those managed or operated by the Texas Commission on Environmental Quality (TCEQ), the New Mexico Environmental Department (NMED), and the National Weather Service (NWS). The TCEQ sites are scattered throughout El Paso County while the NMED sites are situated primarily along the Rio Grande Valley in Dona Ana County, New Mexico. The NMED and TCEQ sites are primarily for air quality measurements; however, each station also provides basic meteorological observations, which can be used in DUSTRAN simulations. Additional surface observations are available at two sites operated by the White Sands Missile Range (WSMR) and by two interagency Remote Automated Weather Stations (RAWS). The WSMR sites include a Global Positioning System Meteorology (GPSMET) station and the Orogrande tower station. The RAWS stations include one located near Dripping Springs at the base of the western side of the Organ Mountains and one located further north in the San Andres Mountains. In addition to the surface observations, twice daily soundings of winds, temperature, pressure, and relative humidity are provided by rawinsondes launched from the local NWS office in Santa Teresa, NM. Figure 3.1 shows the location of the surface and upper air meteorological stations used in this study, while Table 3.1 lists the sites along with their latitude and longitude and provides a brief description of the type of measurements performed. The Orogrande tower station is not included in either Figure 3.1 or Table 3.1 because these data were not available at the time DUSTRAN simulations were performed. The WSMR has since provided the data, which have been processed so that they can be used in future DUSTRAN simulations.

It is clear from Figure 3.1 that most of the meteorological stations in the greater Fort Bliss area are concentrated to the south and west of the base (i.e., metropolitan El Paso and along the Rio Grande Valley towards Las Cruces, NM). To our knowledge, there are no sources of archived meteorological data available within or immediately east of Fort Bliss.

Winds are the single most important meteorological variable affecting the transport and diffusion of airborne particulate matter. Understanding the local wind patterns is a pre-requisite to running dispersion simulations. An analysis of the local wind climatology was performed to determine both seasonal and diurnal trends in the wind patterns. This information was then used to identify candidate periods in 2005 that were used in DUSTRAN dispersion simulations.

Table 3.1. Information on Meteorological and Air Quality Stations in the Fort Bliss Vicinity

Station ID	Operator	Latitude	Longitude	Relevant Measurements
CAMS12	TCEQ ^(a)	-106.5011	31.7681	Hourly surface meteorology, PM ₁₀ , PM _{2.5}
CAMS414	TCEQ	-106.3242	31.7864	Hourly surface meteorology
CAMS72	TCEQ	-106.4258	31.8939	Hourly surface meteorology
CAMS37	TCEQ	-106.4028	31.7467	Hourly surface meteorology, PM ₁₀ , PM _{2.5}
CAMS49	TCEQ	-106.3031	31.6622	Hourly surface meteorology, PM ₁₀
LOMN5	RAWS ^(b)	-106.5867	32.3233	Hourly surface meteorology
SNDN5	RAWS	-106.5250	32.5800	Hourly surface meteorology
WSMN5	GPSMET ^(c)	-106.3500	32.4100	Hourly surface meteorology
EPZ	NWS ^(d)	-106.7000	31.9000	Twice daily soundings
KALM	NWS	-105.9833	32.8333	Hourly surface meteorology
KELP	NWS	-106.3758	31.8111	Hourly surface meteorology
KLRU	NWS	-106.9219	32.2894	Hourly surface meteorology
6O	NMED ^(e)	-106.6306	31.9306	Hourly surface meteorology
6ZG	NMED	-106.5575	31.7958	Hourly surface meteorology, PM ₁₀ , PM _{2.5}
6ZL	NMED	-106.6742	32.4247	Hourly surface meteorology, PM ₁₀
6ZK	NMED	-106.4092	32.0411	Hourly surface meteorology, PM ₁₀
6ZM	NMED	-106.5839	31.7961	Hourly surface meteorology
6ZN	NMED	-106.6828	31.7878	Hourly surface meteorology
6WM	NMED	-106.8644	32.2781	Hourly surface meteorology, PM ₁₀

(a) TCEQ = Texas Commission on Environmental Quality

(b) RAWS = Remote Automated Weather Station

(c) GPSMET = Global Positioning System Meteorology

(d) NWS = National Weather Service

(e) NMED = New Mexico Environment Department

The figures in Appendix A summarize the results of our wind climatology analysis in the form of a series of wind rose charts. These results were compiled from 4 years (2002 through 2005) of hourly surface wind measurements at three TCEQ continuous air monitoring stations (CAMS12, CAM72, and CAMS414). Each figure in Appendix A displays wind roses for a given month for each of these three stations. Results are further broken down into nighttime and daytime statistics.

We examined wind statistics from CAMS72 and CAMS414 based on their close proximity to the main cantonment at Fort Bliss and the major population center of El Paso. CAMS72 is located near the eastern base of the Franklin Mountains in northeast El Paso, and the CAMS414 site is located on the eastern outskirts of the El Paso area (see Figure 3.1). CAMS12 is located on the University of Texas at El Paso campus, at the western base of the Franklin Mountains. Terrain effects are expected at CAMS12 and CAMS72 because of their proximity to the Franklin Mountains. This is particularly true for CAMS12, where channeling may occur because of the relatively narrow constriction in the Rio Grande Valley on the west side of El Paso. Such terrain effects must be recognized and accounted for in dispersion modeling. Terrain effects are expected to be less significant at CAMS414 because this site is located in a relatively flat area, furthest from any major terrain feature.

A few of the more salient features illustrated in the wind roses of Appendix A are highlighted here:

- Regardless of season, the wind statistics at CAMS12 display a strong tendency for west-north-west (WNW) or east-south-east (ESE) flow. This is consistent with a channeling effect through the relatively narrow valley on the west side of El Paso.
- All the stations indicate that the strongest flows are from the west. Interestingly, CAMS72 consistently shows stronger westerly winds. This may be associated with bora-like events in which strong but shallow flows descend along the east slope of the Franklins.
- When comparing daytime versus nighttime wind roses for March and April at CAMS414, where terrain effects are much less significant, there is a distinctive diurnal variation in the wind speeds. Daytime wind roses show strong westerly winds, whereas night-time wind roses indicate much weaker winds. A diurnal variation in wind speed is a characteristic of this area in the spring. As the boundary layer depth increases during the day, higher momentum air is mixed down to the surface. At night, when vertical mixing subsides because of increased stability, the winds near the surface decrease significantly. This diurnal evolution in the boundary layer results in calm mornings followed by gusty afternoons at the surface.
- By June, wind speeds have subsided (compared to the spring season), but the strongest winds are still westerly. Starting in July, there is a shift toward southerly flow during the daytime. This is particularly evident in the data from CAMS414 and CAMS72. This pattern persists through August and is associated with the summer monsoon season that brings much needed precipitation in the form of afternoon thunderstorms.

Figure 3.2 shows the seasonal variation in the mean wind speeds. This figure clearly shows that the spring windy season is associated with increased PM₁₀ concentration, probably because of dust generated from wind erosion in the general region.

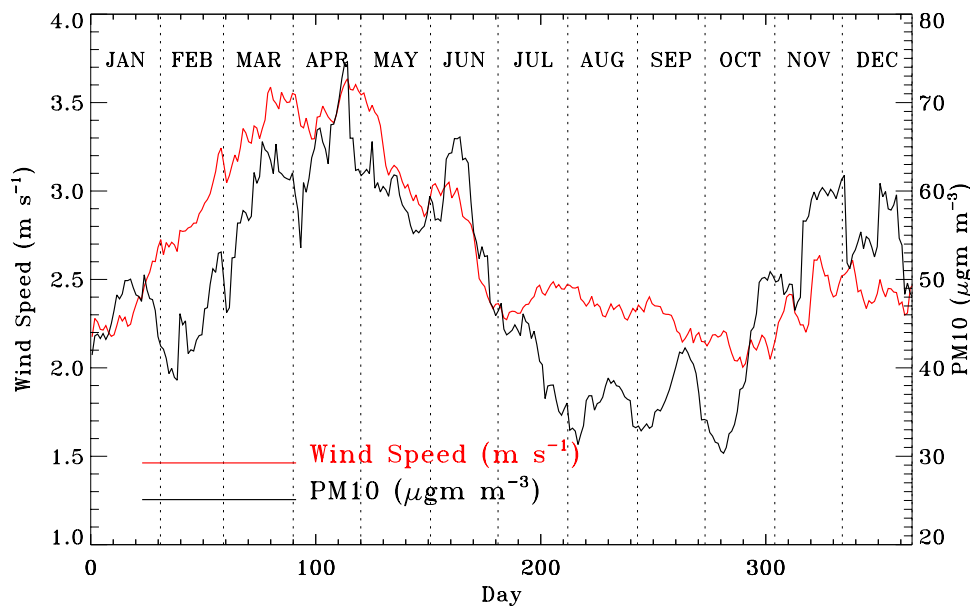


Figure 3.2. Mean PM₁₀ Concentration (black) and Wind Speed (red) at TCEQ CAMS37. Plots are created from 4 years (from 2002 through 2005) of hourly data using a 20-day sliding average.

3.2 Ambient PM₁₀ Concentrations

Particulate concentration data from three monitoring stations in the vicinity of Fort Bliss were analyzed. These stations include two TCEQ sites (CAMS12, and CAMS37) and one NMED site (6ZK). The latter site is of particular interest in this study because it is located in Chaparral, NM, and is relatively close to major Fort Bliss training areas.

Figure 3.2 shows the seasonal variation of 20-day-average PM₁₀ concentrations over the year at the TCEQ CAM37 site. This figure was generated from 4 years of hourly data using a 20-day sliding averaging window to compute a smoothed time series of PM₁₀ concentrations. The results show a clear seasonal trend, with PM₁₀ levels reaching a maximum during the spring windy season. Typical 20-day-mean concentrations range from about 35 $\mu\text{g m}^{-3}$ in the fall to nearly 75 $\mu\text{g m}^{-3}$ in April.

An inspection of hourly PM₁₀ data at the TCEQ CAMS12 site indicates a distinctive diurnal variation. To verify, power spectra of PM₁₀ time series were computed for years 2002 through 2005. Spectra clearly show peaks at a frequency of 1 cycle per day, corresponding to a period of 1 day. To establish the magnitude of the typical diurnal variation in PM₁₀ concentration, the mean PM₁₀ concentration was computed as a function of time of day over the entire 4-year data set. The right panel of Figure 3.3 shows the result of that analysis. Typical minimum PM₁₀ concentrations of roughly 30 $\mu\text{g m}^{-3}$ occurred between 0300 and 0500 MST, and typical maximum concentrations of about 90 $\mu\text{g m}^{-3}$ occurred around 1900 MST. However, it was not unusual for hourly-average PM₁₀ concentrations to reach well above 200 $\mu\text{g m}^{-3}$ at the CAM12 site as revealed by the hourly values plotted in the left panel of Figure 3.3.

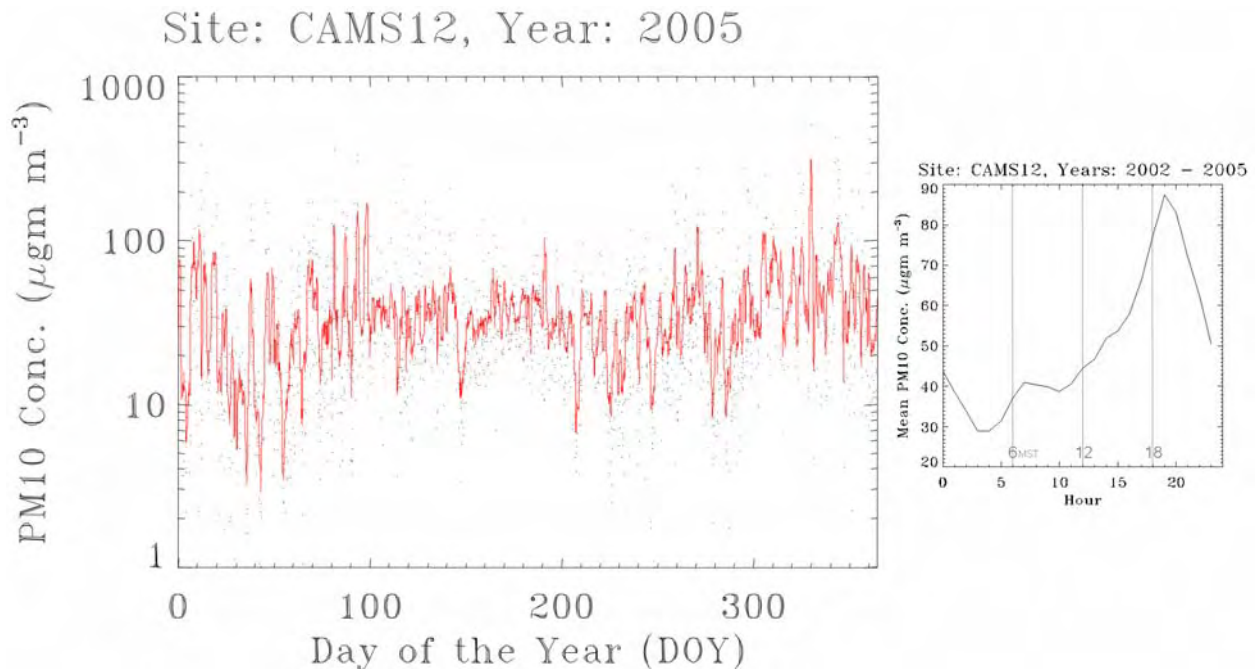


Figure 3.3. The Left Panel Shows the Time Series of Hourly PM₁₀ Concentration (Black Dots) for 2005 at TCEQ CAMS12. The red curve is smoothed hourly data. The diurnal variation in PM₁₀ concentration (right) averaged from 2002 through 2005 at CAMS12 is shown in the right panel.

3.3 Selected Simulation Periods

Simulation periods were selected based on an examination of surface and upper-air meteorological data from 2005. Table 3.2 lists four simulation periods that were selected; these simulation periods were chosen based on two primary selection criteria:

- Availability of quality measurements from all surface and upper-air meteorological stations shown in Figure 3.1, for periods spanning several complete days, and
- Climatologically representative periods.

The first criterion alone eliminated many potential simulation periods. Ideally, we wanted to find periods with continuous data records lasting several days from a distribution of monitoring stations over the modeling domain. As part of this quality control process, we examined time series of PM₁₀ and meteorological data for consistency among various monitoring sites.

As indicated above, the second important selection criterion was based on climatology. We focused on finding climatologically representative periods where both higher and lower ambient dust concentrations throughout the entire Fort Bliss region were likely. The higher concentrations typically occur in periods of average-to-high wind conditions. Thus, we selected two simulation periods during the spring months, a season characterized by dry conditions and strong afternoon winds. We also selected one period that contains an exceptionally high wind event associated with a frontal passage in late November. For both the spring and November cases, the winds were mostly westerly; the predominant wind direction in the Fort Bliss area. For contrast, when lower ambient dust conditions are likely, we chose one period from late July where the winds were weaker and more southerly, as is typical of the summer monsoon in the southwestern United States.

Table 3.2. Periods in 2005 Selected for DUSTRAN Simulations

Period	Start		End	
	Date (2005)	Time (LST) ^(a)	Date (2005)	Time (LST)
1	March 12	0000	March 16	2400
2	April 25	0000	April 30	2400
3	July 20	0000	July 24	2400
4	November 25	0000	November 29	2400

(a) Local Standard Time

Figure 3.4 shows the selected simulation periods with time series of hourly ambient PM₁₀ concentrations and winds from the TCEQ CAMS37 monitoring site and hourly ambient PM₁₀ concentrations from the NMED 6ZK site. PM₁₀ concentrations greater than 1000 µg m⁻³ were measured at the two sites during the November high-wind-speed period. Time series of winds, temperature, and PM₁₀ at NMED station 6ZK are shown for each simulation period in Appendix B.

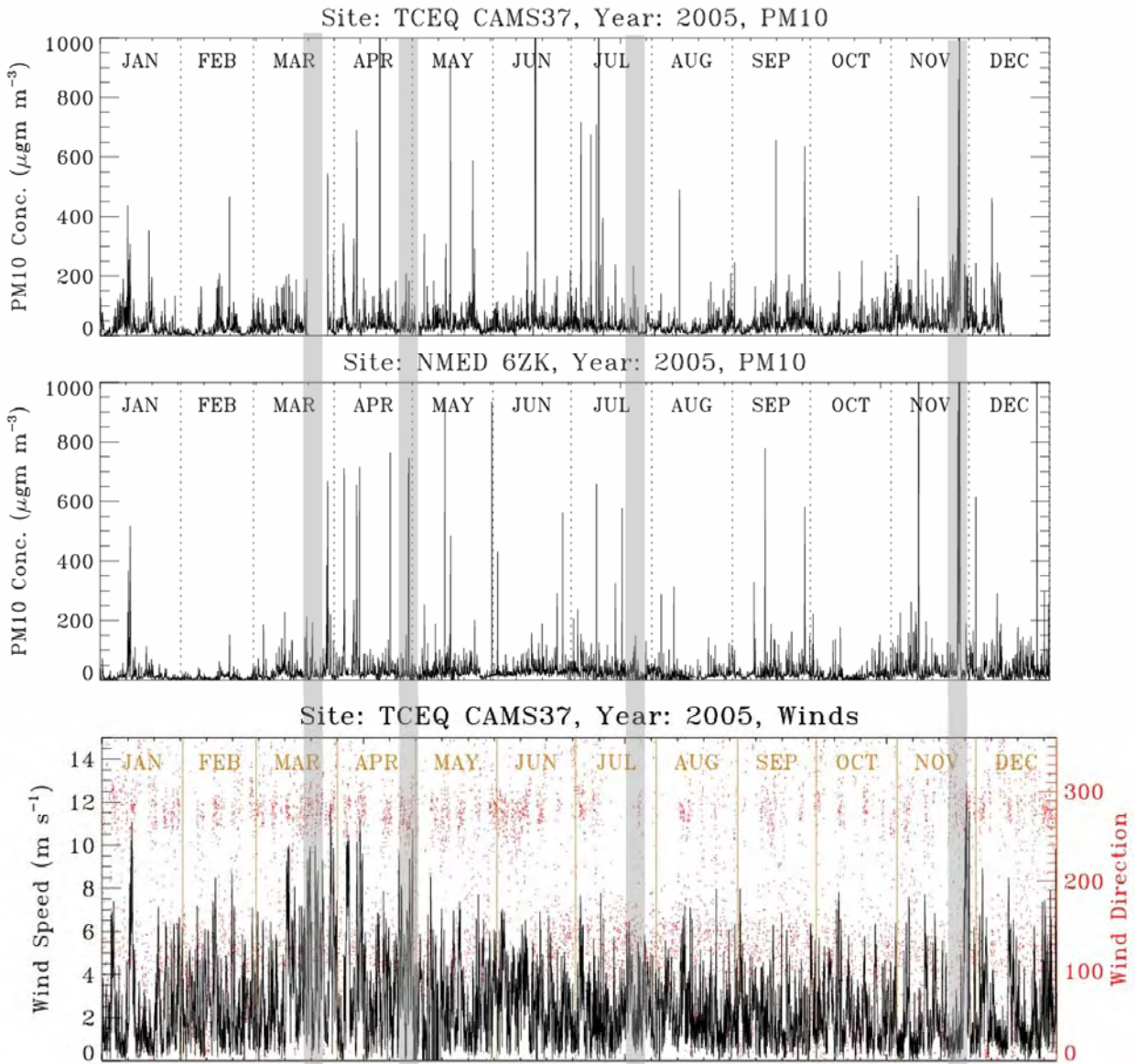


Figure 3.4. Time Series of Hourly Ambient PM₁₀ Concentrations at Two Sites and Wind Measurements at One Site for 2005. The red dots in the lower panel represent hourly wind directions. The DUSTRAN simulation periods are highlighted in gray.

4.0 Scenarios for Vehicle-Generated Dust

Using DUSTRAN to simulate dust emissions from vehicle activity requires the specification of meteorological conditions, vehicle information in terms of the number and type of vehicles involved in the activity (i.e., the type of brigade involved), and information on the location, timing, and duration of the activity (i.e., brigade activity). A meteorological summary for the Fort Bliss area was provided in Section 3, including the rationale for selecting the four simulation periods (March 12–16, April 25–April 30, July 20–24, and November 25–29, 2005). Meteorological data from stations listed in Table 3.1 and located as shown in Figure 3.1 were archived for these periods and used in the DUSTRAN simulations. This section focuses on the selection of a brigade type and the development of vehicle activity scenarios for various brigade activities. A complete description of the vehicle dust-emission algorithms are provided in the DUSTRAN User’s Manual (Allwine et al. 2006).

Based on discussions with Fort Bliss personnel, the three major brigade activities identified as of most interest in assessing Fort Bliss contributions to PM₁₀ air quality are:

- Move-out of an entire Heavy Brigade Combat Team (HBCT) from the main Fort Bliss cantonment to the McGregor Range Camp,
- Move-out of an entire HBCT from the main cantonment to the Dona Ana Range Camp, and
- Combat training in the three main battalion maneuver areas, Dona Ana 1, McGregor, and South.

The description of the brigade being simulated is given next followed by descriptions of the move-out and combat-training activities to be simulated.

4.1 Brigade Characteristics

Fort Bliss staff provided the report entitled “Prevention of Significant Deterioration (PSD) Analysis” and an accompanying Excel spreadsheet prepared by Booz Allen Hamilton (2005). The spreadsheet included a summary of the number and type of vehicles associated with brigades typically training at Fort Bliss (e.g., Heavy Brigade Combat Team, Aviation Brigade, and Fire Brigade). Of the brigade types listed in the spreadsheet, the HBCT had by far the greatest total number of vehicles associated with it (758 wheeled and 354 tracked vehicles). Because the presence of more moving vehicles generally translates into more dust emissions, the HBCT type was selected for use in the simulations.

At the time of conducting the simulations described in this report, the DUSTRAN modeling system included the 10 default vehicle types listed in Table 4.1. To perform DUSTRAN simulations, it was necessary to “map” the HBCT vehicles into the DUSTRAN vehicle types. This process was performed using vehicle descriptions and weight as the major mapping criteria. For example, the Booz Allen Hamilton spreadsheet description of a “Truck utility: S20 shelter carrier 4×4 w/e (high-mobility multipurpose wheeled vehicle [HMMWV])” suggests that this type of vehicle best maps to the HMMWV in DUSTRAN. The Booz Allen Hamilton spreadsheet description of a “Fire support team vehicle: Bradley (BFIST)” does not immediately suggest a mapping, but an Internet search using the key words “military vehicles” and “BFIST” reveals websites reporting that a typical weight for this type of vehicle is on the order of 58,000 lb (26,300 kg). This weight, in turn, suggests that this type of vehicle can be represented in DUSTRAN as one freightliner loaded with a Patriot missile battery. Appendix C gives the

assigned mapping of HBCT vehicles, as presented in the Booz Allen Hamilton spreadsheet, to individual DUSTRAN vehicle types. Table 4.2 summarizes the overall mapping of all HBCT vehicles in a single HBCT to DUSTRAN vehicle types. Note that the 758 wheeled vehicles present in a HBCT are mapped to a total of 758 wheeled DUSTRAN vehicles, while the 354 tracked vehicles present in a HBCT are mapped to a total of 548 DUSTRAN vehicles. The number of DUSTRAN vehicles representing tracked vehicles is larger than the actual HBCT total because in some instances the tracked vehicles are heavier than representative DUSTRAN vehicle types and must be mapped as multiple DUSTRAN vehicles (see Appendix C).

Table 4.1. DUSTRAN Vehicle Types

Vehicle Type	Weight (kg)
Dodge Neon, 2002 Civilian vehicle with Eagle GA Touring M+S P185/165R 85T tires	1176
Dodge Caravan, 2002 Civilian vehicle with GoodYear Integrity M+S 215/70R15 98S tires	1759
Ford Taurus, 2002 Civilian vehicle with Firestone M+S P215/60R16 94T tires	1516
GMC G20 Van, DRI TRAKER vehicle used for measuring dust emissions in real time	3100
GMC C5500, 1999 Civilian vehicle 6 wheels with GoodYear and Michelin tires	5227
HMMWV, Military Vehicle 4 wheels with tires	2445
M923A2 (5-Ton), Military Vehicle 2 front wheels and 8 rear wheels on dual axles	14318
M1078 LMTV, 2.5 Ton Military vehicle with 4 wheels and tires	8060
M977 HEMTT, Military vehicle with 8 wheels and tires	17727
Freightliner, Tractor trailer rig with 22 wheels and tires loaded with Patriot missile batteries	23636

Table 4.2. Overall Mapping of All Heavy Brigade Combat Team Vehicles to DUSTRAN Vehicle Types

Vehicle Type	HMMWV	GMC G20 Van	GMC C550	M923A2 (5-Ton)	M977 HEMTT	Loaded Freightliner
Wheeled Vehicles	562	55	24	102	0	15
Tracked Vehicles	0	0	0	63	35	450
Total	562	55	24	165	35	465

Using vehicle weight to perform the mapping is consistent with the findings of Gillies et al. (2005a; 2005b). They observed that vehicle weight and vehicle speed are the only two variables that matter significantly in calculating PM₁₀ military wheeled vehicle-emission factors for unpaved roads. We note that DUSTRAN calculations are relatively insensitive to the exact DUSTRAN vehicle chosen for use in a particular military vehicle mapping as long as the overall military vehicle weight is approximated. For example, consider a situation where 50 military vehicles weighing 10,000 kg each must be mapped to available DUSTRAN vehicles. The total weight of 500,000 kg is approximately equal to 21 freightliners loaded with Patriot missile batteries, each weighing 23,636 kg (note that DUSTRAN does not allow fractional vehicle numbers). To simulate the effects of these fifty 10,000-kg vehicles, 21 “Loaded Freightliners” thus could be entered into DUSTRAN. The 21 “Loaded Freightliners” would yield a total weight of 496,356 kg, a difference of 0.7% from the true weight of 500,000 kg. Alternatively, if the weight of a HMMWV (2,445 kg) were used for the mapping, 205 “HMMWVs” could be entered into DUSTRAN to represent the fifty 10,000-kg vehicles. The 205 “HMMWVs” would yield a total weight of 501,225 kg, a difference of 0.2% from the true weight of 500,000 kg. Because of the linear nature of the Gilles et al. (2005a; 2005b) equations, a small difference from “true” weight will carry through the

calculations and cause a comparable difference in calculated source strength. In this example, entering 21 “Loaded Freightliners” would yield a source strength 0.7% lower than the “true” best estimate source strength, while entering 205 “HMMWVs” would yield a source strength 0.2% higher than the “true” best estimate source strength. Such small differences will have a negligible effect on DUSTRAN concentration contours. In short, the mapping process allows vehicles currently included in DUSTRAN to be used as surrogates for other vehicles. If a lighter vehicle type is chosen as the surrogate, a greater numbers of vehicles will be entered than if a heavier vehicle type had been chosen as the surrogate.

DUSTRAN has recently been upgraded to allow the user to specify a list of vehicles with accompanying weights. This does not necessarily improve the accuracy of DUSTRAN, but rather eliminates the somewhat confusing step of mapping all simulated vehicles to a limited set of vehicle types that may, at times, appear to have no common characteristics with the simulated vehicles, other than weight.

4.2 Move-Out Activities

The McGregor and Dona Ana move-out activities are simulated as line sources in DUSTRAN and involve all vehicles in a HBCT, as mapped to standard DUSTRAN vehicle types as discussed above. All vehicles are assumed to begin the move-out at the Biggs Army Airfield near the main cantonment and to travel exclusively on unpaved installation roads. Figure 4.1 indicates the move-out routes. Consistent with the stated desire of Fort Bliss staff to include potential worst-case situations, the Dona Ana move-out route was deliberately chosen to be on unpaved roads located essentially at the Fort Bliss borders, thus maximizing the potential for off-installation drift. Move-outs are assumed to include all HBCT vehicles traveling directly on unpaved road surfaces; it is assumed there is no transport of military vehicles on flatbed trucks or railcars.

DUSTRAN does not treat the notion of individual vehicles, but rather takes a “bulk” approach to dust emissions from vehicle activities. That is, the dust emissions from all vehicles active on a roadway over a specified time are assumed to be released uniformly from the road at a constant rate throughout the duration of the activity. For the McGregor move-out, it was assumed that the first vehicle departed Biggs Airfield at 0600 MST, and the last vehicle reached the McGregor Range Camp just before 1400 MST. For the longer Dona Ana move-out, it was assumed that the first vehicle departed Biggs Airfield at 0600 MST, and the last vehicle reached the range camp just before 1800 MST.

Move-out routes could be modeled in DUSTRAN as one long-line source with 1306 vehicles (the total number of equivalent DUSTRAN vehicles in an HCBT; see Table 4.2) active for 8 hours (0600 to 1400 MST) on the McGregor move-out and 12 hours (0600 to 1800 MST) on the Dona Ana move-out. However, for a move-out traversing a sufficiently long route (i.e., much longer than the vehicles can physically travel in 1 hour), this approximation may be unrealistic because not all vehicles will initially be active (i.e., they will be queued), and those vehicles that are active cannot traverse the entire length of the route during the first few hourly time steps. Similarly, towards the end of the move out, not all vehicles will be active (i.e., they will have already reached the camp), and those vehicles that are active will be nearer to the end of the route during the last few hourly time steps. To better approximate vehicular dust emissions for a long move-out route, then, one can construct a series of line segments that are placed end-to-end with differing start times. The overall effect of segmenting a long-line source is to more realistically represent the timing and spatial distribution of the vehicle movement and thus the associated dust emissions that are generated along the route.

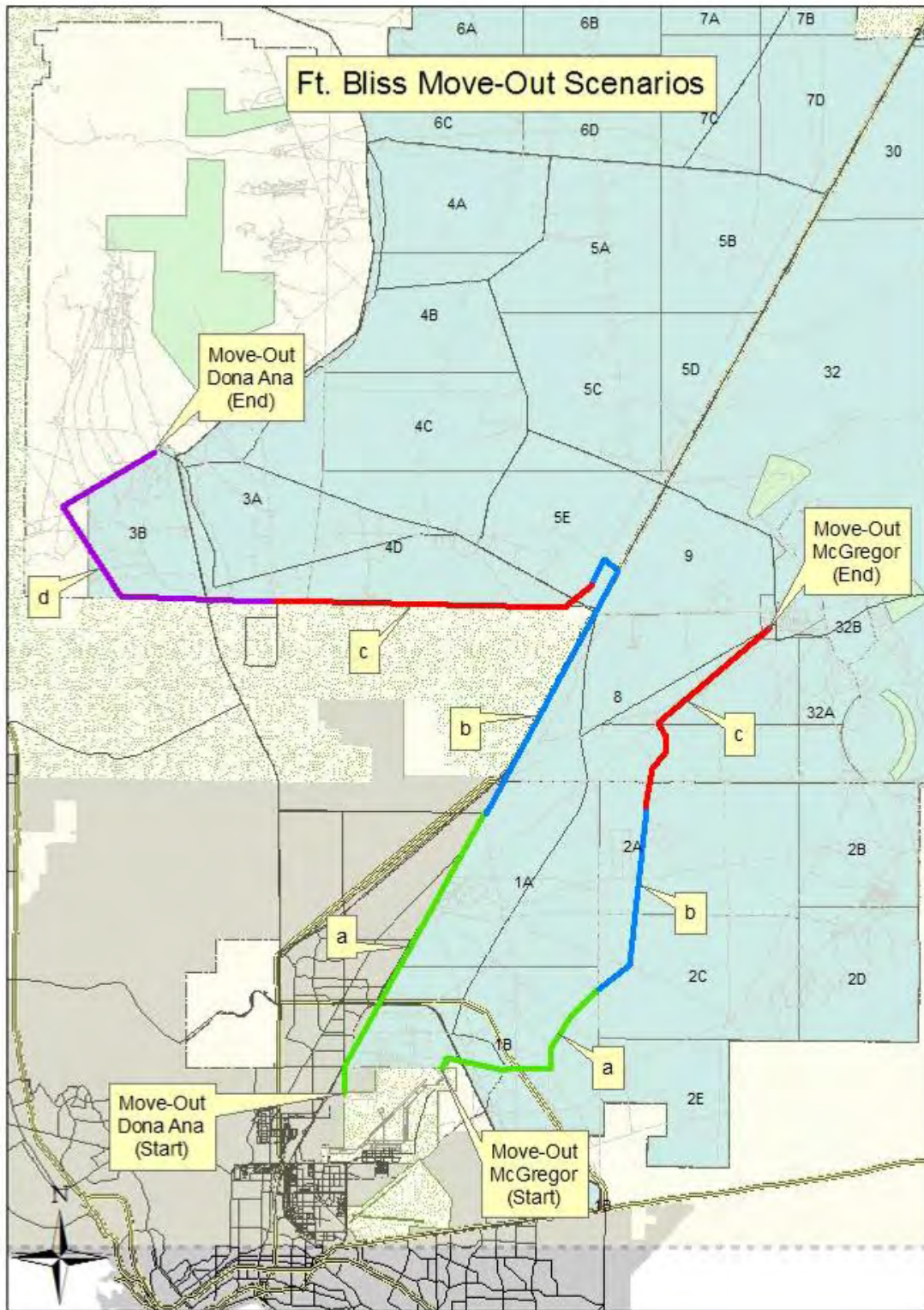


Figure 4.1. Dona Ana and McGregor Move-Out Routes. The McGregor route is divided into three contiguous segments (labeled *a*, *b* and *c*) while the Dona Ana route is divided into four contiguous line segments (labeled *a*, *b*, *c* and *d*).

For example, consider a situation where the McGregor move-out route is divided into three contiguous line segments, “a,” “b,” and “c,” of roughly equal length (Figure 4.1) where the assumptions of the first convoy vehicle leaving Biggs Airfield at 0600 MST and the last convoy vehicle reaching McGregor Range at 1400 MST are maintained. Assume further that the first convoy vehicle reaches the start of segment “b” at 0700 MST and the start of segment “c” at 0800 MST. Segment “a” will experience the passage of 1306 equivalent DUSTRAN vehicles during the period from 0600 to 1200 MST, segment “b” from 0700 to 1300 MST, and segment “c” from 0800 to 1400 MST. Activity duration on each segment is thus 6 hours.

Figure 4.2 compares the hourly dust emissions (normalized by the total emissions for the entire release) from the approach using three contiguous equal line segments with the hourly emissions from the approach using one long-line segment for this scenario. The one long-line segment results in a “step” function for emission source strength, whereas the three contiguous equal line sources result in more of a “bell” shape for emission source strength. Physically, the approach using a one-line segment assumes that the emissions are constant in both space and time, while the multi-segment approach allows for emissions to increase as vehicles enter the roadway, peak once all vehicles are on the roadway, and finally decrease as vehicles reach their destination. In either case, the total emissions are the same (i.e., the areas under both the one- and three-segment curves are equal) and are just distributed differently in both space and time, with the multi-segmented approach more closely simulating the temporal and spatial distribution of dust emission that would occur during a move-out.

It should be noted that it may not be necessary to divide a long road into segments to more realistically predict the time- and space-varying dust emissions. For example, considering the 8-hour-long McGregor move-out described above, treating the move-out as three linked road segments staggered in time will result in no difference in the predicted 24-hour-average PM_{10} concentrations over treating the move-out as one long segment if the meteorological conditions change minimally with time. However, it is probably best to develop move-out scenarios as realistic as practical to foster more realistic predictions of PM_{10} concentrations during any possible meteorological conditions. That is the approach taken in this analysis.

For move-out scenario simulations conducted for this report, the McGregor move-out route is modeled as three contiguous line segments, while the longer Dona Ana move-out is modeled as four contiguous line segments. Vehicle speeds assumed for the scenarios reflect known constraints, such as the 10-mile-per-hour speed limit (16.2 kilometers per hour) along portions of roads near the Fort Bliss main cantonment and the length of each line segment. For the McGregor move-out, it was assumed that vehicles travel at a constant speed of 16 kilometers per hour (kph) during the entire move-out. For the Dona Ana move-out, vehicle speeds were varied slightly depending on the exact lengths of the segments. Vehicles were assumed to travel at 16 kph on segment “a,” 17 kph on segments “b” and “c,” and 19 kph on segment “d.”

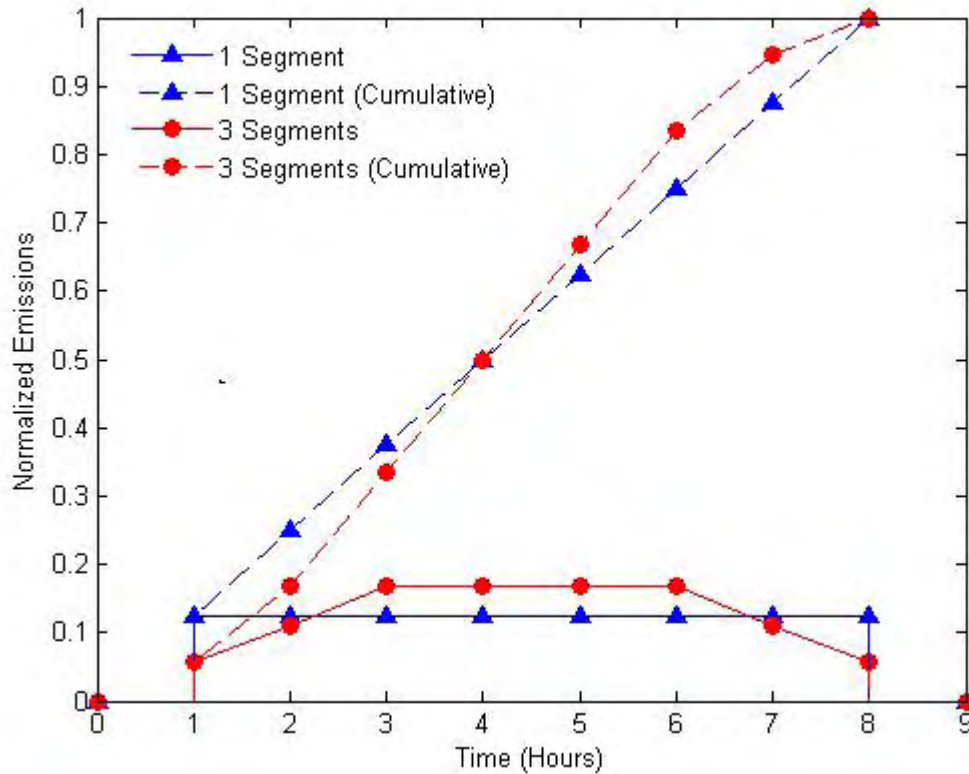


Figure 4.2. Normalized Dust Emissions as a Function of Time for One (Blue) and Three (Red) Line Segments Approximating the Release from a Long-Line Source

The one-line segment has an 8-hour release duration (0600–1400 MST). The three equal-length line segments are contiguous and have a 6-hour release duration that is offset 1-hour in time (i.e., 0600–1200, 0700–1300, and 0800–1400 MST, respectively). In both cases, the cumulative emissions sum to one (dashed curves), but are apportioned differently in both space and time.

Move-out scenario assumptions are summarized below.

Move-Out To McGregor Range Camp

- All vehicles associated with the HBCT travel.
- Move-out route is divided into three segments; “a,” “b,” and “c” (see Figure 4.1).
- First vehicle leaves Biggs Army Airfield (start of segment “a”) at 0600 MST, reaching the start of segment “b” at 0700 MST and the start of segment “c” at 0800 MST.
- Each segment of the move-out route has vehicles on it for a total of 6 hours.
- Mean speed for each type of vehicle along all segments is 16 kilometers per hour (equivalent to 9.9 miles per hour).
- Vehicle types are uniformly mixed throughout the convoy.

Move-Out Dona Ana Range Camp

- All vehicles associated with the HBCT travel.
- Move-out route is divided into four segments; “a”, “b”, “c”, and “d” (see Figure 4.1).

- First vehicle leaves Biggs Army Airfield (start of segment “a”) at 0600 MST, reaching the start of segment “b” at 0700 MST, the start of segment “c” at 0800 MST, and the start of segment “d” at 0900 MST.
- Each segment of the move-out route has vehicles on it for a total of 9 hours.
- Mean speed for each type of vehicle is 16 kilometers per hour (9.9 miles per hour) along segment “a,” 17 kilometers per hour (10.6 miles per hour) along segments “b” and “c,” and 19 kilometers per hour (11.8 miles per hour) along segment “d.”
- Vehicle types are uniformly mixed throughout the convoy.

4.3 Combat Training Activities

Combat training activities are simulated as area sources in DUSTRAN. As with line sources, DUSTRAN does not treat the motion of individual vehicles in an area source but takes a “bulk” approach—dust emissions from all vehicles active within a training area over a specified time are assumed to be released uniformly from the area at a constant rate throughout the duration of the activity. Based on discussions with Fort Bliss staff, a combat training scenario was developed involving the simultaneous use of three training areas, termed the “Full Training” scenario. The “Full Training” scenario, with simulation results using the April 25 through 30, 2005, period of archived meteorological data, also is discussed in a companion report (Chapman et al. 2006).

In the Full Training scenario, two full HBCTs operate in the Dona Ana and McGregor Ranges while one third of a HBCT (i.e., one battalion) operates in the South Training Area. Figure 4.3 shows the approximate locations and sizes of the three maneuver areas. Figure 4.4 shows the DUSTRAN representation of these areas. To facilitate more realistic plume production within the model, each of the three relatively large maneuver boxes is divided into sub-areas. The Dona Ana 1 Combat Training area is divided into four roughly square sub-areas (labeled “a,” “b,” “c,” and “d” in Figure 4.4). The South Combat Training area is divided into two sub-areas (labeled “a” and “b” in Figure 4.4). The McGregor Combat Training region is over three times larger than either the Dona Ana or South Training maneuver boxes and is divided into seven sub-areas (labeled “a,” “b,” “c,” “d,” “e,” “f,” and “g” in Figure 4.4).

The Dona Ana 1 and South Training Combat Training areas shown in Figure 4.4 are relatively simple shapes that translate easily into DUSTRAN area sources. However, the McGregor Combat Training area is irregularly shaped, and modifications are necessary to represent this region within DUSTRAN, as can be seen by comparing Figures 4.3 and 4.4. For example, circular borders were made more angular. These modifications were driven by the fact that area sources within DUSTRAN must be defined by up to four-point areas, making curved edges difficult to mimic. The “stair step” boundary pattern in the northeastern part of the McGregor Range also was smoothed because including the “steps” would lead to multiple small sub-areas that vary by orders of magnitude in size from other sub-areas. We tried to match the overall extent of the indicated McGregor region within the constraints of DUSTRAN area-source definition algorithms.

Military training guidelines suggest that during combat training activities, wheeled vehicles travel approximately 20 miles per day (equivalent to 32.2 km per day) while tracked vehicles travel approximately 13 miles per day (equivalent to 20.9 km per day) (Walter Christensen, personal communication to E. Chapman). Based on this information, within DUSTRAN, a total travel distance of 32 km per day per vehicle was assigned to all the HMMWVs, GMC G20 Vans, and GMC C550 vehicles as well as to 102 of the M923A2 (5-ton) and 15 loaded freightliner vehicles. A total travel distance of

21 km per day per vehicle was assigned to all the M977 HEMTT and to 63 of the M923A2 (5-ton) and 450 loaded freightliner vehicles. These assignments mirror the wheeled and tracked vehicle numbers given in Table 4.2. For all combat training simulations, it was assumed that all vehicles travel at a speed of 40 kilometers per hour when moving. It was further assumed that vehicles are already located in the training areas when activities commence (i.e., no travel to training areas from Range Camps) and that combat training begins at 0700 MST and lasts for 10 hours.

Combat training assumptions are summarized below.

- All vehicles associated with one HBCT are located in the region labeled “Combat Training Dona Ana 1” in Figure 4.4.
- All vehicles associated with one HBCT are located in the region labeled “Combat Training McGregor” in Figure 4.4.
- Vehicles associated with one-third of a HBCT (i.e., one battalion) are located in the region labeled “Combat Training South” in Figure 4.4.
- Within each training area and sub-area, uniform distributions of vehicle type and vehicle numbers exist.
- Vehicles are already located in the training areas when activities commence (i.e., no travel to training areas from the McGregor or Dona Ana Range Camps).
- All combat training begins at 0700 MST.
- Vehicle movement occurs uniformly over a 10-hour period.
- The total distance traveled by each wheeled vehicle over the course of a training day is 32 km, or approximately 20 miles.
- The total distance traveled by each tracked vehicle over the course of a training day is 21 km, or approximately 13 miles.
- When moving, all vehicles travel at a speed of 40 km per hour.

The “Full Training” scenario also is discussed in a companion report (Chapman et al. 2006). This companion report includes simulation results generated using different variations on activity duration and uses the April 25 through 30, 2005, period of archived meteorological data.

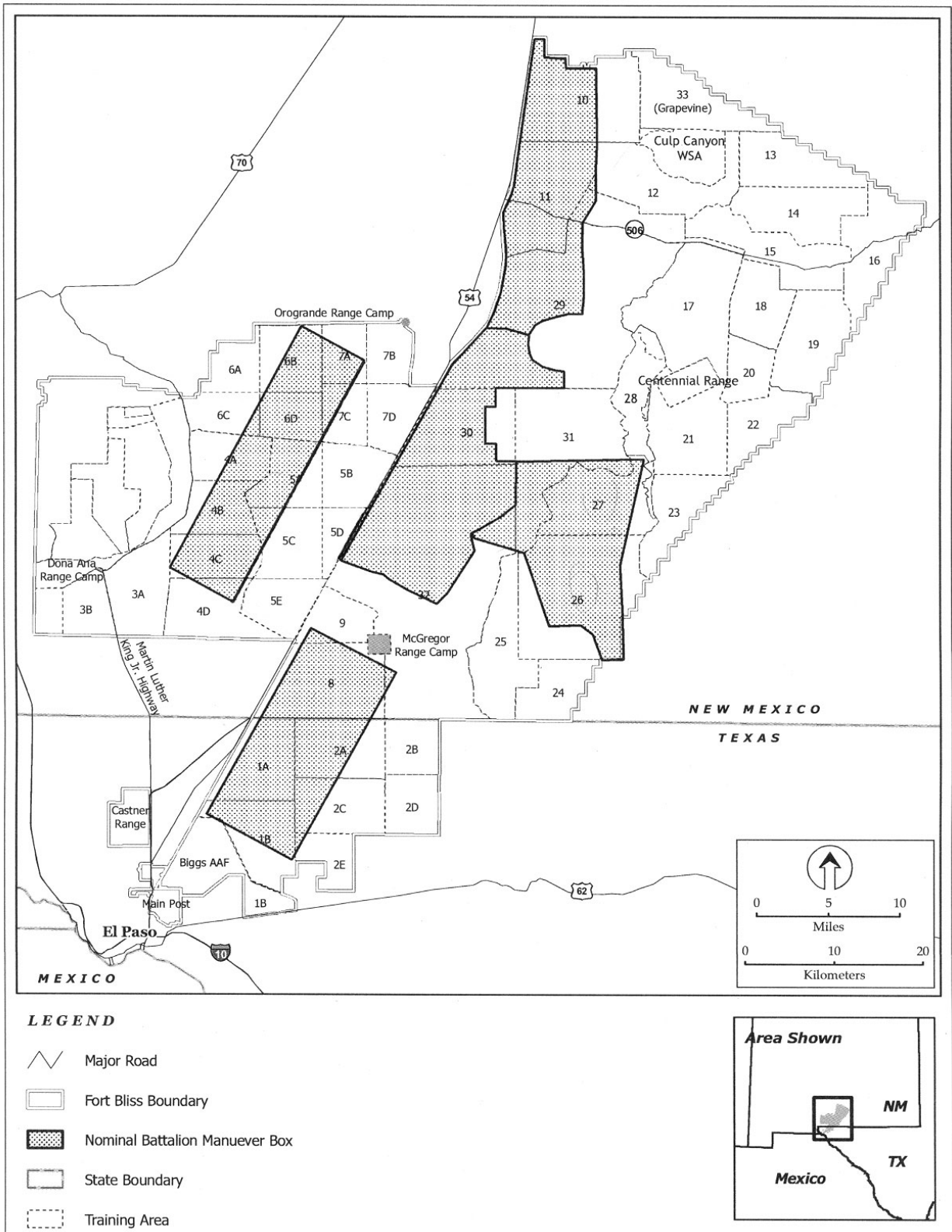


Figure 4.3. Fort Bliss Battalion Maneuver Boxes

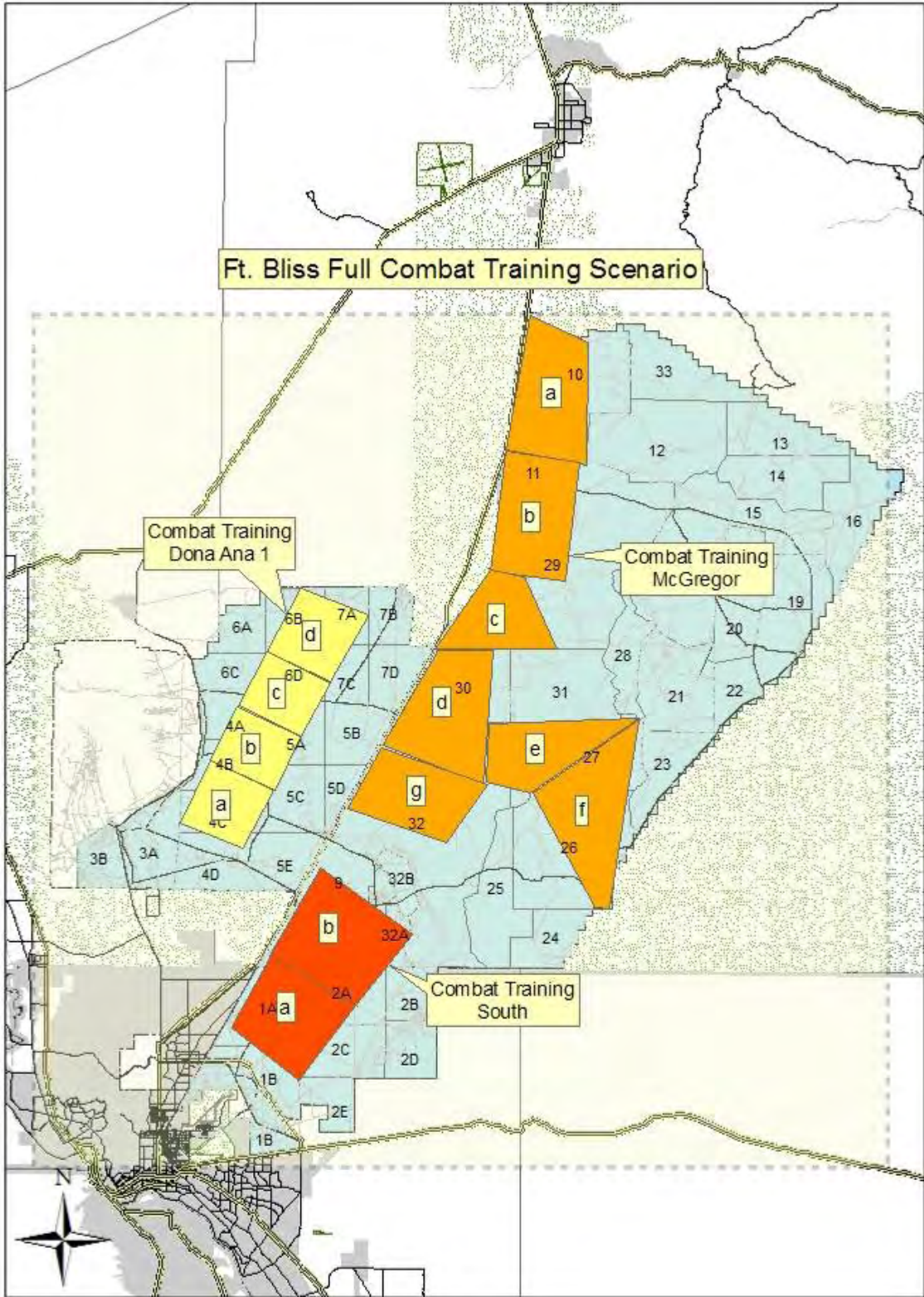


Figure 4.4. DUSTRAN Representation of Battalion Maneuver Boxes Used In Combat Training Scenarios

4.4 Vehicle-Emission Factors

As noted previously, DUSTRAN incorporates emission factors for various wheeled military vehicles as developed by Gillies et al. (2005a; 2005b). Dust-emission factors specific to tracked military vehicles do not currently exist. Under a current SERDP research project, Dr. Jack Gillies and associates of the Desert Research Institute are determining such factors through a series of field experiments similar to those conducted to determine the emission factors for wheeled military vehicles. Emission factors for tracked military vehicles will be incorporated into DUSTRAN when available.

The possibility of identifying AP-42 emission factors that could serve as an acceptable interim surrogate for emission factors for tracked military vehicles was investigated. The only dust-emission factors from tracked vehicles located in AP-42 dealt with the bulldozing of overburden and uncontrolled open dust sources at western surface coal mines (EPA 2005). The active scraping of material covering a coal seam by a bulldozer blade is not a suitable surrogate for the travel movement of tanks and other tracked vehicles, and it must be concluded that no acceptable surrogates within AP-42 exist.

All DUSTRAN simulations conducted for this report used the emission factors for wheeled military vehicles developed by Gillies et al. (2005a; 2005b) for both wheeled and tracked military vehicles. Therefore, an assumption in the move-out scenarios is that the emission factors for tracked military vehicles traveling on unpaved roads can be approximated by the emission factors for wheeled military vehicles traveling on unpaved roads, while an assumption in combat training scenarios is that the emission factors for tracked military vehicles operating off-road can be approximated by the emission factors for wheeled military vehicles traveling on unpaved roads.

The vehicle-emission factor experiments of Gillies et al. (2005a; 2005b) were conducted at Ft. Bliss during the Spring of 2001 and the Spring of 2002. As part of this work, the PM_{10} emission potential (EP) of selected unpaved roads on Fort Bliss was also evaluated (Kuhns et al. 2005). The EP is used to normalize the effect of vehicle speed on dust emissions and allows comparison of vehicle-generated dust emissions from different roads. Approximately 72 km of unpaved roads, mainly in the South Training Area, were tested and compared to the instrumented tower section of road used in the emission factor experiments. Sixty percent of all measured EPs fell in the range of 6.7 to 9.6 grams/vehicle-kilometer-traveled per meter/second (g/vkt)/(m/s), with an average EP and standard deviation of 8 ± 2 (g/vkt)/(m/s). The EP potential of the instrumented tower section was approximately twice this average value. The lower EPs observed by Kuhns et al. (2005) suggest that the source strength of dust emissions caused by vehicular movement on some unpaved Fort Bliss roads as calculated in DUSTRAN potentially may be high by a factor of two, with calculated concentration contributions high by a similar factor. Given the uncertainty in the exact locations of lower EP road surfaces and the desire to be conservative in estimating vehicular generated dust contributions, no EP adjustments were made in the simulations.

5.0 Scenarios for Wind-Generated Dust

Using DUSTRAN to simulate wind-generated dust requires specifying meteorological conditions, vegetation classification, and soil texture classes. Meteorological conditions are used to quantify the magnitude of the wind stress over a surface, with higher wind stress leading to greater dust generation potential. Meteorological periods were identified previously, and the datasets listed in Table 3.1 are available for use in a given wind-generated dust simulation. This section focuses on describing the vegetation classification scheme that is used to define areas that are capable of dust production as well as the soil texture classes that determine the dust-particle-size distribution. A complete description of the wind-generated dust algorithms are provided in the DUSTRAN User’s Manual (Allwine et al. 2006).

A vegetation classification scheme is used in DUSTRAN to define areas that are capable of producing wind-generated dust. Essentially, more vegetation cover results in less wind-generated dust from the surface. In DUSTRAN, vegetation classes are defined using the Olson World Ecosystem (Olson 1992), which defines 59 distinct classes of vegetation. For a given vegetation class, a particulate productivity factor is assigned that ranges from zero (no production capability) to one (complete production capability). Of the 59 classes, only four have sufficiently exposed soil to allow for wind erosion, and they include two desert categories and two semi-desert categories. Because of the sparseness of vegetation in deserts, the vegetation productivity factor for those categories has a value of 1.0. The semi-desert categories have more widespread vegetation in the form of shrubs and grasses and so are assigned a factor of 0.5. Table 5.1 lists the Olson vegetation classes and associated production factors used in the wind-generated dust-emission model within DUSTRAN.

Table 5.1. Olson Vegetation Classes and Associated Dust Production Factor Used in DUSTRAN

ID #	Olson Vegetation Class Description	Production Factor
8	Desert, mostly bare stone, clay and sand	1.0
50	Sand desert, partly blowing dunes	1.0
51	Semi-desert/desert, scrub/sparse grass	0.5
52	Cool/cold shrub, semi-desert/steppe	0.5

A GIS file, supplied by Fort Bliss personnel, provided a map of vegetation classes in and around the Fort Bliss site. The vegetation classes in the Fort Bliss area did not directly correspond to the Olson Classes, necessitating a conversion of the vegetation classes in the provided file to the Olson vegetation classes. Figure 5.1 displays a map of the Olson vegetation classes over the Fort Bliss region. The figure shows that seven Olson codes define the Fort Bliss site, of which only two classes (#8-red and #51-pink) have any potential for dust emission. The other categories (#25-light green, #41-dark brown, #47-light brown, #48-blue, and #56-dark green) have a productivity factor of zero and have no potential for dust emission. Table 5.2 summarizes the seven Olson codes within the Fort Bliss site, as well as a description of the category and the associated dust-productivity factor.

Table 5.2. Fort Bliss Olson Vegetation Classes and Associated Dust-Production Factor

ID #	Olson Vegetation Class Description	Production Factor
8	Desert, mostly bare stone, clay and sand	1.0
25	Snowy deciduous forest, summergreen	0.0
41	Mild/warm/hot grass/shrub	0.0
47	Dry or highland scrub or open woodland	0.0
48	Dry evergreen woodland or low forest	0.0
51	Semi-desert/desert, scrub/sparse grass	0.5
56	Forest/field complex	0.0

In a manner similar to the vegetation classification, a soil texture classification scheme is used to determine the particle-size distribution for wind-generated dust. In DUSTRAN, the soil texture class (i.e., clay, small silt, large silt, and sand) is determined from the Zobler soil texture category (Staub and Rosenzweig 1992), whereby the soil is divided into seven possible soil texture categories. Table 5.3 lists the Zobler soil categories along with the fractional percent of clay, small silt, large silt, and sand content found in that soil texture category. Once the Zobler soil texture category has been determined, the particle-size distribution of wind-generated dust is estimated using the particle diameter ranges of 1 to 2 μm for clay, 2 to 20 for small silt, 20 to 50 for large silt and 50 to 100 for sand (Nickovic et al. 2001).

Table 5.3. Fractions of the Soil Texture Classes in each Zobler Soil Category

Zobler Soil Categories	Soil Texture Classes			
	Clay	Small Silt	Large Silt	Sand
coarse	0.12	0.04	0.04	0.80
medium	0.34	0.28	0.28	0.10
fine	0.45	0.15	0.15	0.25
coarse-medium	0.12	0.09	0.09	0.70
coarse-fine	0.40	0.05	0.05	0.50
medium-fine	0.34	0.18	0.18	0.30
coarse-medium-fine	0.22	0.09	0.09	0.60

Figure 5.2 displays a GIS file that defines the Zobler soil texture categories for the Fort Bliss site. All seven categories occur within the Fort Bliss site, with the Zobler soil category of 1 (coarse) predominant. This category is generally made up of sand (0.80), but also contains clay (0.12), small silt (0.04), and large silt (0.04).

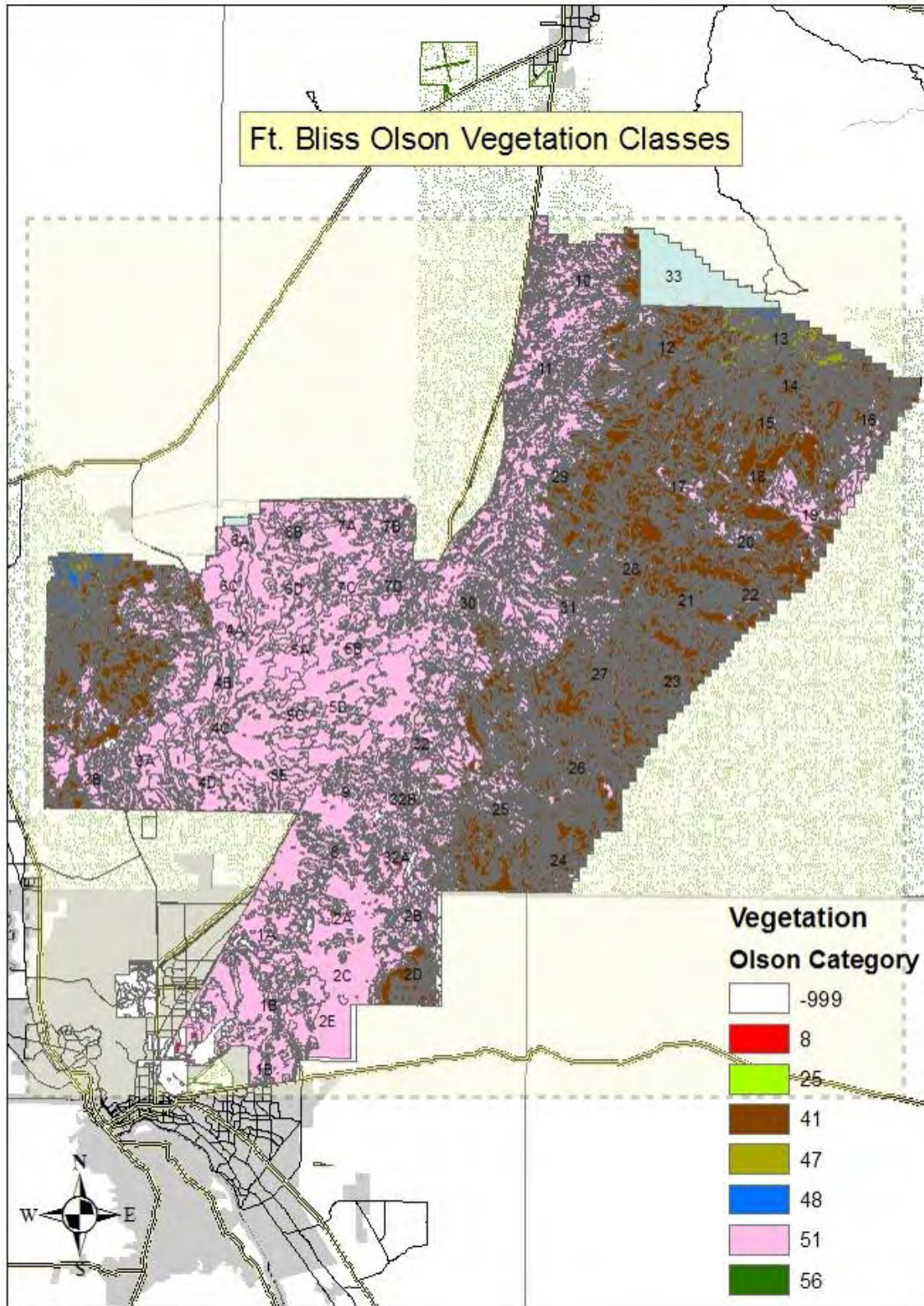


Figure 5.1. Olson Vegetation Classes for the Fort Bliss Site

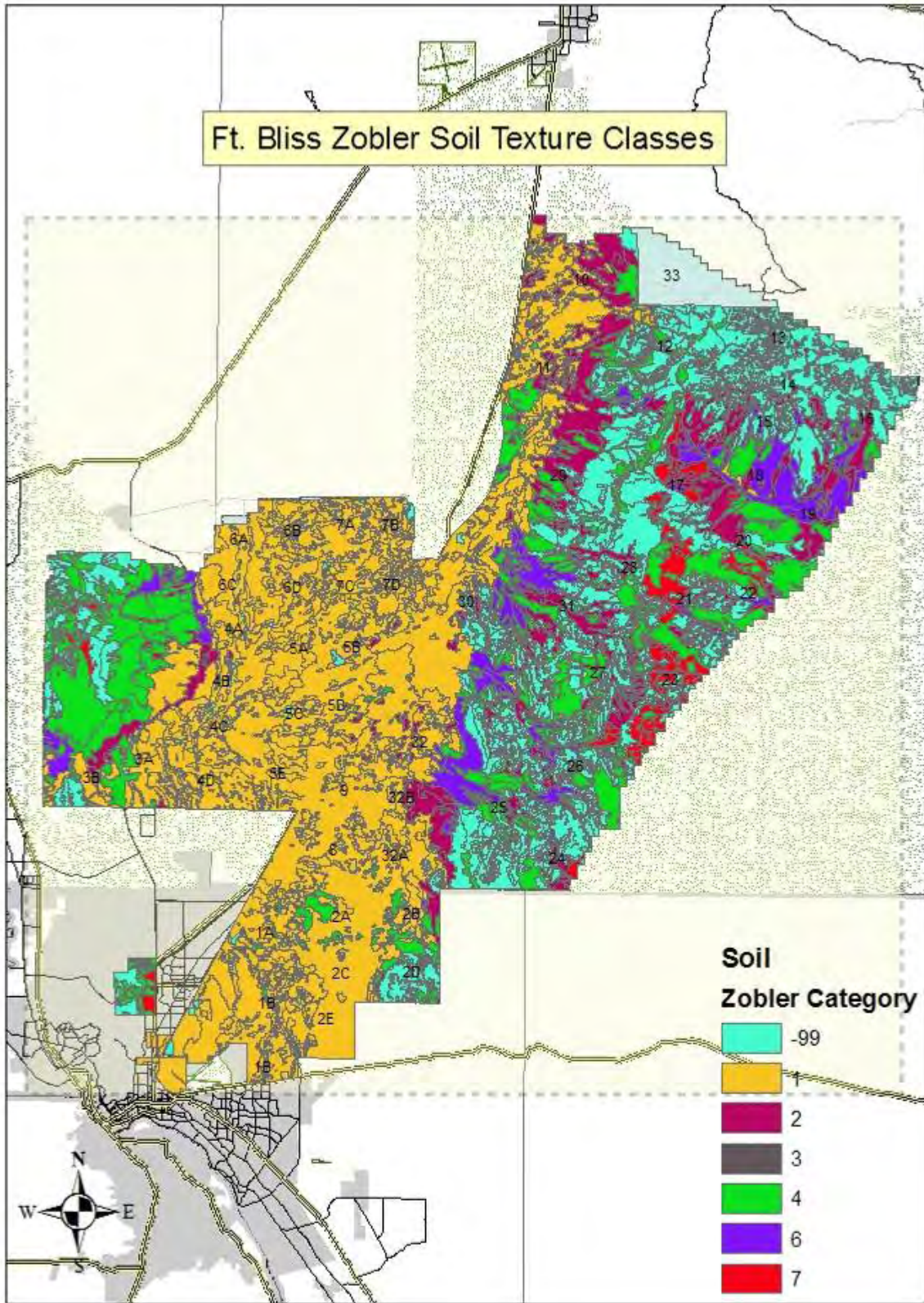


Figure 5.2. Zobler Soil Texture Categories for the Fort Bliss Site

6.0 Simulations of Vehicle-Generated Dust

This section gives the results of the PM₁₀ concentrations from DUSTRAN simulations for the dust emissions from the vehicle activity scenarios. The results represent contributions from the specified sources, not total ambient PM₁₀ concentrations. For example, concentrations reported for move-outs or combat training represent the contributions from that activity alone. Background particulate concentrations in an incoming air mass and particulates generated via wind erosion and from disturbed soils also contribute to total ambient PM₁₀ concentrations, but are not accounted for in these simulations. We refer to the model predictions as *concentration contributions* to emphasize this point.

Simulations for the McGregor move-out, Dona Ana move-out, and combat training scenarios were conducted on a 100 km by 100 km domain encompassing the Fort Bliss installation (see Figure 3.1). Individual grid cells were 2 km by 2 km in horizontal extent with six vertical levels geometrically spaced to extend from the surface to 3300 meters. All simulations were initiated at midnight and ran for 24 hours so that the 24-hour average concentration could be calculated. The vehicle-generated dust simulations include results from all four meteorological periods (see Table 3.2 for individual day specification) and represent a wide range of stability classes, wind speeds, and directions.

Results from vehicle activity simulations, including the McGregor move-out, Dona Ana move-out, and combat training, are presented in Appendix D through F, respectively. Within a given appendix, the 24-hour average PM₁₀ concentration plot is provided for each day for the meteorological periods identified earlier in Table 3.2. The combat training also contains peak 1-hour concentrations for each simulated day given in Appendix G. The 10-meter meteorological wind field for select hours (0700, 1000, 1300, 1600, and 1900 MST) of a given simulated day is provided in Appendix H through K. For convenience and ease-of-comparison, some figures from the appendices are duplicated in the following discussions.

Examining the 24-hour average PM₁₀ concentration plots reveals that the move-outs produce substantially higher concentration contributions than combat training under the same meteorological conditions. For example, the April 30, 2005, Dona Ana move-out simulation results in 24-hour-average PM₁₀ concentration contributions that are on the order of 500 µg/m³, whereas the combat training simulation for the same day results in 24-hour average PM₁₀ concentration contributions nearer to 10 µg/m³ (Figure 6.1). The order-of-magnitude difference can largely be explained because dust emissions from move-outs are confined to narrow, well-defined routes, whereas dust emissions from combat training occur over a much broader area. The resulting concentration contributions are therefore higher and more localized for the defined move-out routes.

Both the Dona Ana and McGregor move-out scenarios generally result in comparable 24-hour-average PM₁₀ concentrations on a given day because the vehicle distribution is approximately the same along each route. Figure 6.2 provides a comparison of the Dona Ana and McGregor move-out simulations for April 25, 2005. Different segments result in localized areas of higher or lower concentration because of the angle of the prevailing wind direction relative to the segment for that day, but the overall magnitude of the 24-hour average PM₁₀ concentration contribution (~ 500 µg m⁻³) is the same for both routes.

For the combat training scenario, the Dona Ana1 training range consistently results in higher 24-hour-average PM_{10} concentration contributions than the McGregor or South training range because it has a greater vehicle density. Figure 6.3 is a plot of the peak 1-hour-average and 24-hour-average PM_{10} concentrations for the combat training scenario on April 30, 2005. Note that the Dona Ana1 training range results in higher relative concentrations because it is smaller in geographic area than the McGregor training range and has more vehicles than the South training range.

Meteorological conditions can greatly affect the average concentration contributions for a given source scenario. Specifically, low wind days generally result in higher 24-hour-average PM_{10} concentration contributions when compared to high wind speed days. Under low wind speed conditions, lofted particulates stay in the area of generation and are not readily dispersed. For example, the 24-hour-average concentration contribution from combat training was an order of magnitude higher on July 23, 2005 (a low wind speed day) than on July 21, 2005 (a high wind speed day) due in part to less plume dilution (Figure 6.4). Day-to-day variations in meteorological conditions were found to more greatly affect the magnitude of the 24-hour-average concentration contribution for the combat training scenario than for the move-out training scenarios. In fact, the magnitude of the 24-hour-average PM_{10} concentration contribution for the Dona Ana move-out ($\sim 500 \mu\text{g m}^{-3}$) did not change day-to-day or period-to-period, just the relative location and size of the affected area along the route. In contrast, the combat training scenario resulted in 24-hour-average concentration contributions that varied one order of magnitude ($10 \mu\text{g m}^{-3}$ to $150 \mu\text{g m}^{-3}$) across the range of days that were simulated.

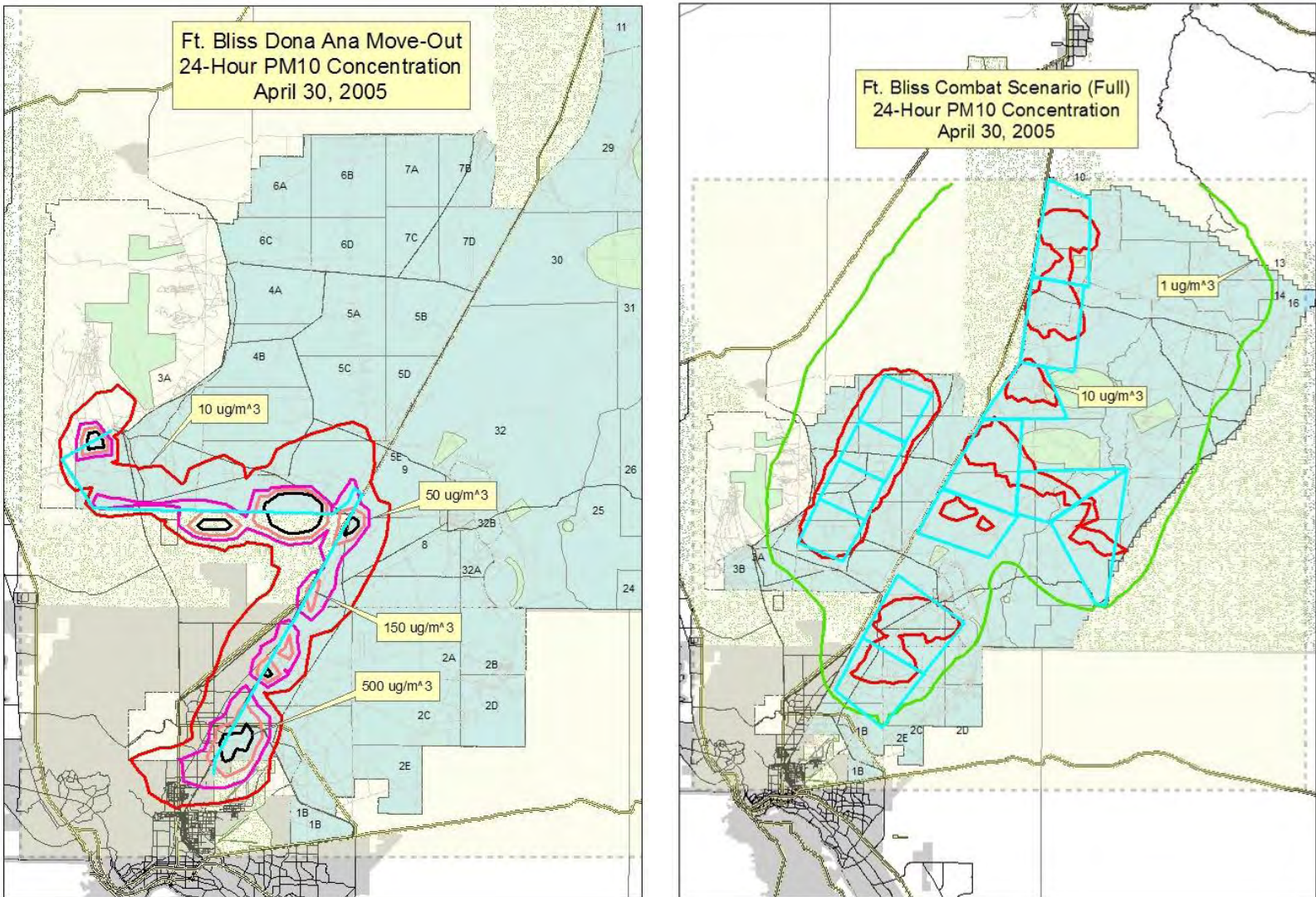


Figure 6.1. 24-Hour-Average PM₁₀ Concentration Contributions on April 30, 2005, for the Dona Ana Move-Out (Left) and Combat Training (Right) Scenarios as Simulated in DUSTAN

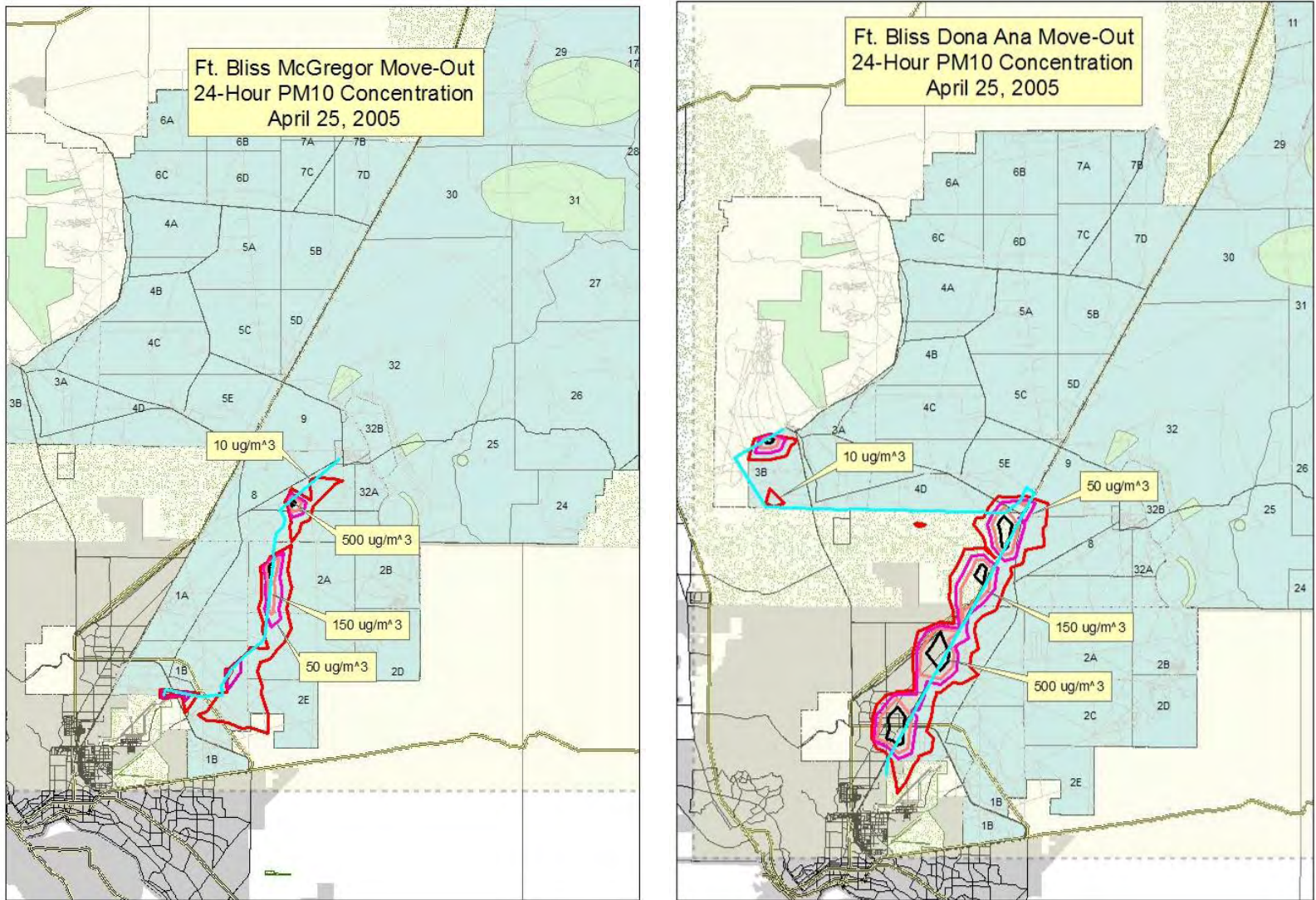


Figure 6.2. 24-Hour-Average PM₁₀ Concentration Contributions for the McGregor (Left) and Dona Ana (Right) Move-Out Scenarios on April 25, 2005, as Simulated in DUSTAN

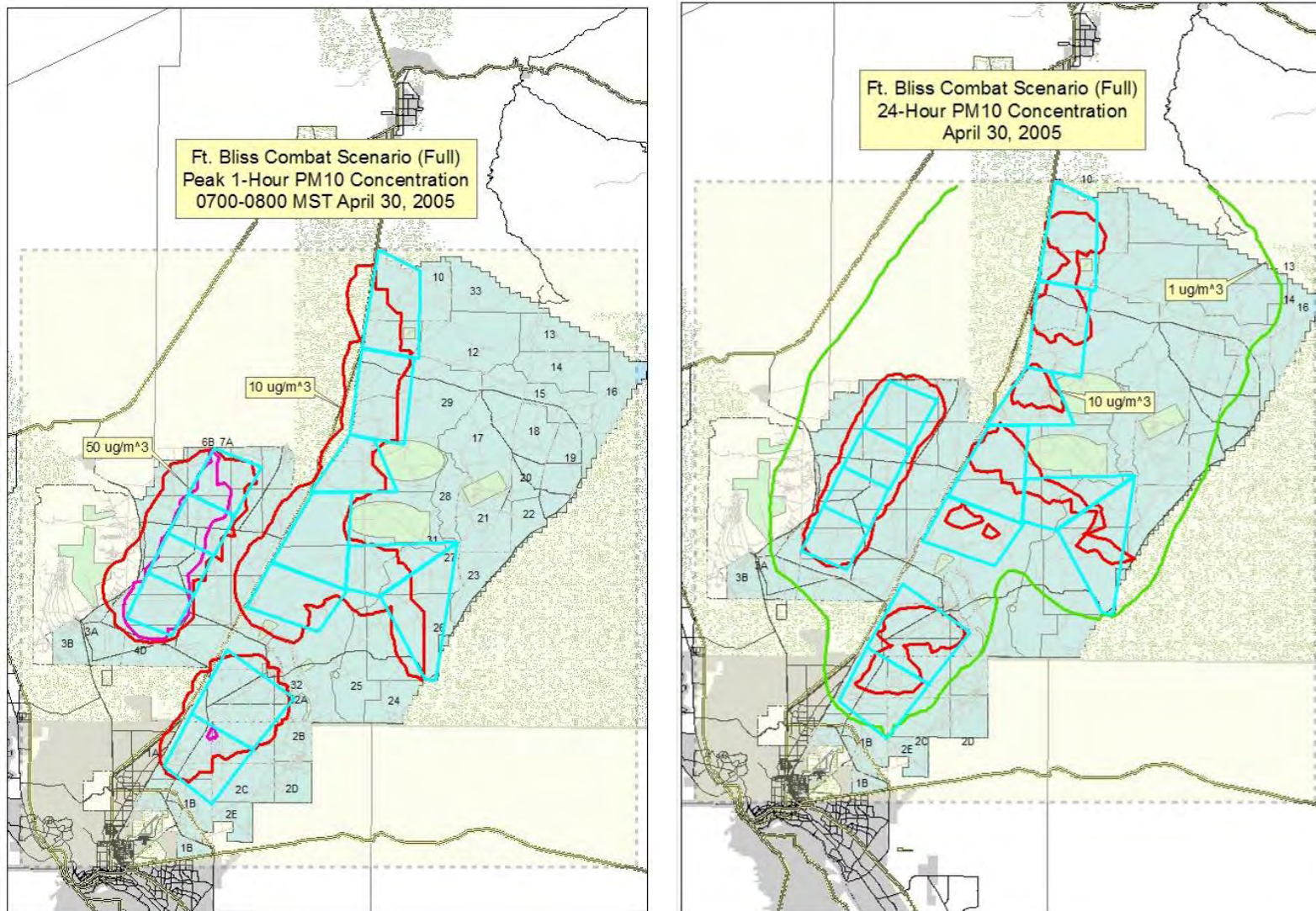


Figure 6.3. Peak 1-Hour- and 24-Hour-Average PM₁₀ Concentration Contributions for the Combat Training Scenario on April 30, 2005, as Simulated in DUSTAN

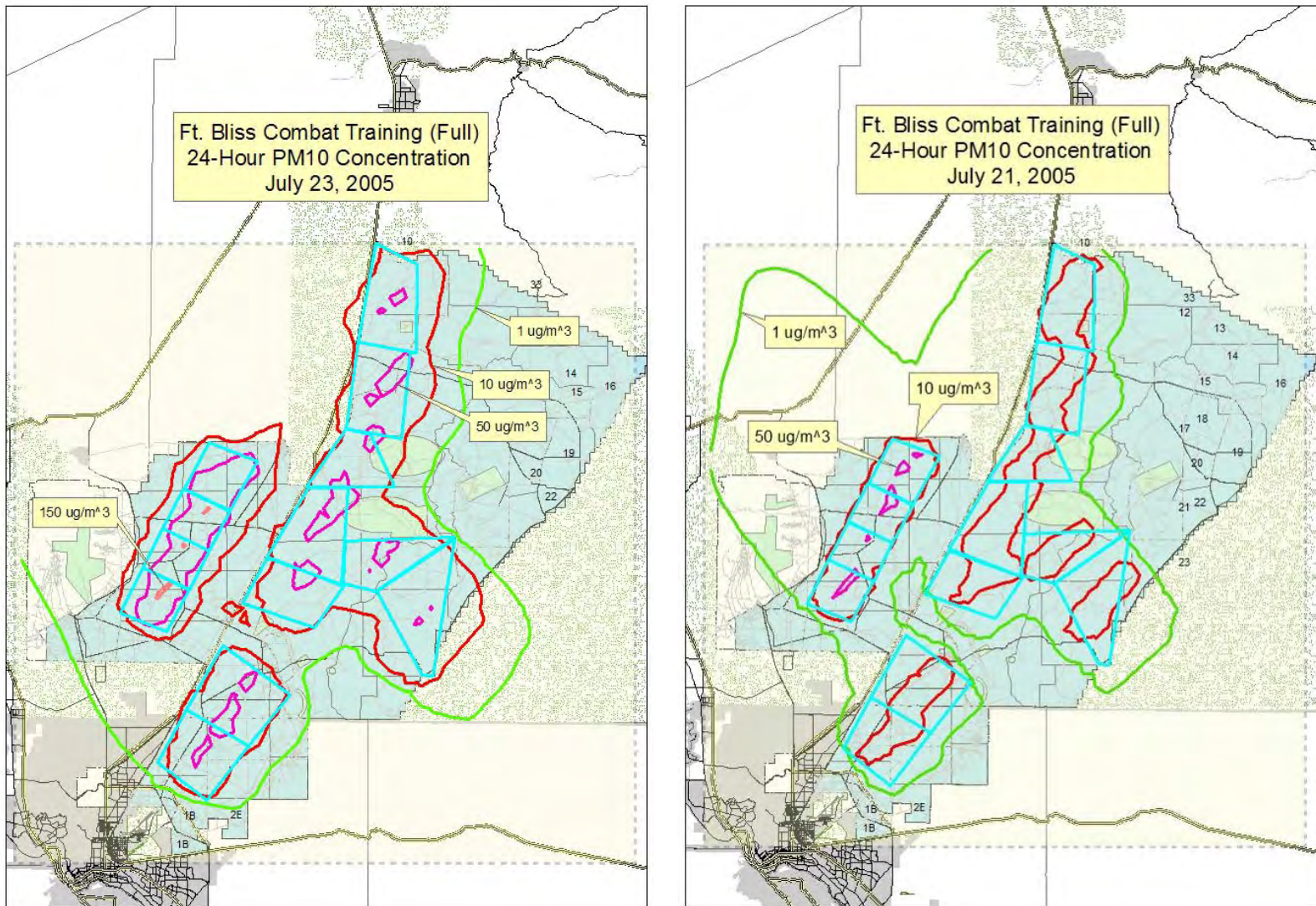


Figure 6.4. 24-Hour-Average PM₁₀ Concentration Contributions on July 23, 2005, (Left) and July 21, 2005 (Right) for the Combat Training Scenario as Simulated in DUSTAN

7.0 Simulations of Wind-Generated Dust

This section gives the results of the PM₁₀ concentrations from DUSTRAN simulations for dust generated by wind erosion. Only two wind-generated dust simulations were performed, and the results from these simulations were used to quantify the range of contribution of wind-generated dust from Fort Bliss to 24-hour-average PM₁₀ concentrations in the vicinity of Fort Bliss. As with the vehicle-generated dust simulations, the predictions for the wind-generated dust simulations represent contributions resulting from particulates generated by wind erosion; neither background particulate concentrations in the incoming air mass nor particulates generated by vehicular activity are accounted for in these simulations.

Simulations of the contribution of wind-generated dust to PM₁₀ air quality for the Fort Bliss site were conducted on a 100 km by 100 km domain encompassing the installation (see Figure 3.1). Individual grid cells were 5 km by 5 km in horizontal extent with six vertical levels geometrically spaced to extend from the surface to 3300 meters. Simulations were initiated at midnight and run for 24 hours so that 24-hour-average concentration could be calculated. Results from wind-generated dust simulations are presented for 2 days—April 25, 2005 (a high wind speed day) and April 30, 2005 (a low wind speed day)—and are meant to quantify the range of the 24-hour-average PM₁₀ concentration contributions that might be expected because of wind-generated dust from within the Fort Bliss installation. In both simulations, it was assumed there was no precipitation and the soil was dry, giving conservative concentration estimates.

Figure 7.1 presents results for the two wind-generated dust simulations. The 10-meter meteorological wind fields for select hours (0700, 1000, 1300, 1600, and 1900 MST) of the 2 days simulated are provided in Appendix I. For convenience, Figure 7.2 presents the 1000 MST wind fields for both days to illustrate that the wind speed was indeed much greater on April 25, 2005, than on April 30, 2005; this was true for all simulated hours.

Comparing the 24-hour-average PM₁₀ concentration plots reveals that the windier day (April 25) resulted in concentration contributions that were approximately one order of magnitude larger than the lower wind speed day (i.e., ~500 μg m⁻³ compared to ~50 μg m⁻³). In either case, the highest concentration contributions occurred where the Olson vegetation class is semi-desert (Olson category #51, Figure 5.1), which is the primary vegetation category within the Fort Bliss installation that is conducive for dust generation.

It should be noted that the contour plots presented in Figure 7.1 give the false impression that the concentrations immediately drop to zero within the Fort Bliss domain, as is evidenced by the closed contours and contour gradient near the outer perimeter of the domain. The reason for this artifact is that the outer-most grid cells in a wind-generated dust simulation are used to establish boundary conditions for the inner grid cells and, as a result, do not have concentrations explicitly calculated and contoured.

Finally, comparing wind-generated dust simulations to vehicle-generated dust simulations reveals that both processes generally contribute equally to the 24-hour-average PM₁₀ concentration (~500 μg m⁻³), with the wind-generated dust simulation impacting a larger area because of the implicitly larger source size. Furthermore, wind-generated dust contributions are higher (lower) when vehicle-generated dust contributions are lower (higher), because of the competing effect of wind speed. Higher wind speeds result in greater wind-generated dust emissions, but they act to dilute vehicle-generated dust emission.

Similarly, lower wind speeds result in lesser wind-generated dust emissions, but they act to limit the dispersion of vehicle-generated dust emissions.

The simulations in this section demonstrate the capability of DUSTRAN to estimate contributions of wind-generated dust to the ambient PM_{10} concentrations. The focus of these simulations was to show the contribution of wind-generated dust from Fort Bliss to local PM_{10} concentrations. Thus, the modeling domain was limited to a 100-km by 100-km domain encompassing the installation. DUSTRAN allows simulations for larger domains up to 400 km by 400 km in size, allowing for longer range air quality impacts to be addressed. For example, the contribution of Fort Bliss dust emissions (both vehicle- and wind-generated) to PM_{10} concentrations at the Guadalupe Mountains National Park can be estimated. For wind-generated dust simulations, DUSTRAN can also account for wind-generated dust emissions over the entire domain using data files (included with DUSTRAN) of vegetation classes and soil texture categories covering the contiguous United States. These files have data at a coarser resolution than the Fort Bliss files discussed in Section 5. By not including the coarser vegetation and soil texture files in a run of DUSTRAN, only the contribution of wind-generated dust from Fort Bliss to air quality at the Guadalupe Mountains National Park can be addressed.

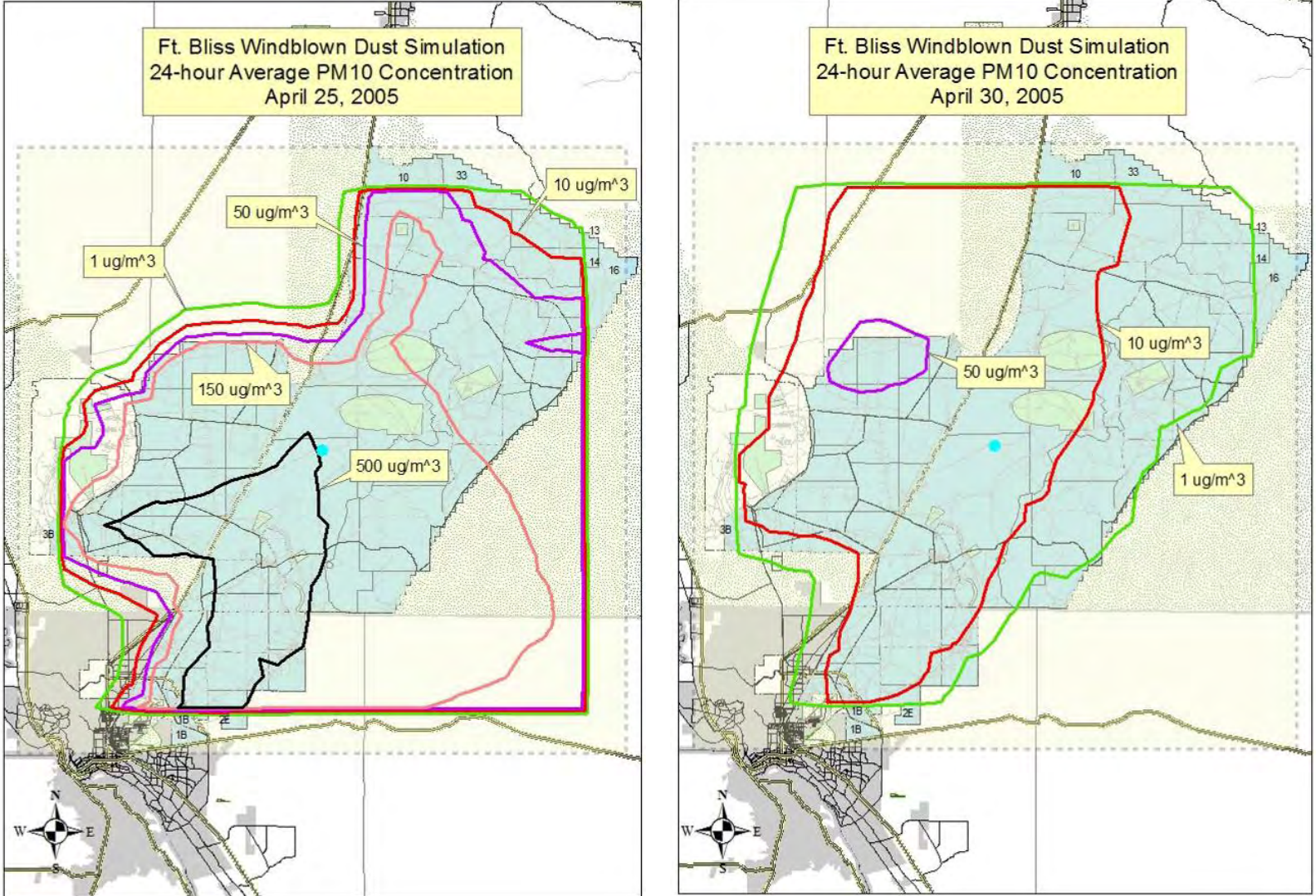


Figure 7.1. 24-Hour-Average PM₁₀ Concentration Contributions on April 25, 2005, (Left) and April 30, 2005 (Right) from Wind-Generated Dust within the Fort Bliss Site as Simulated in DUSTAN

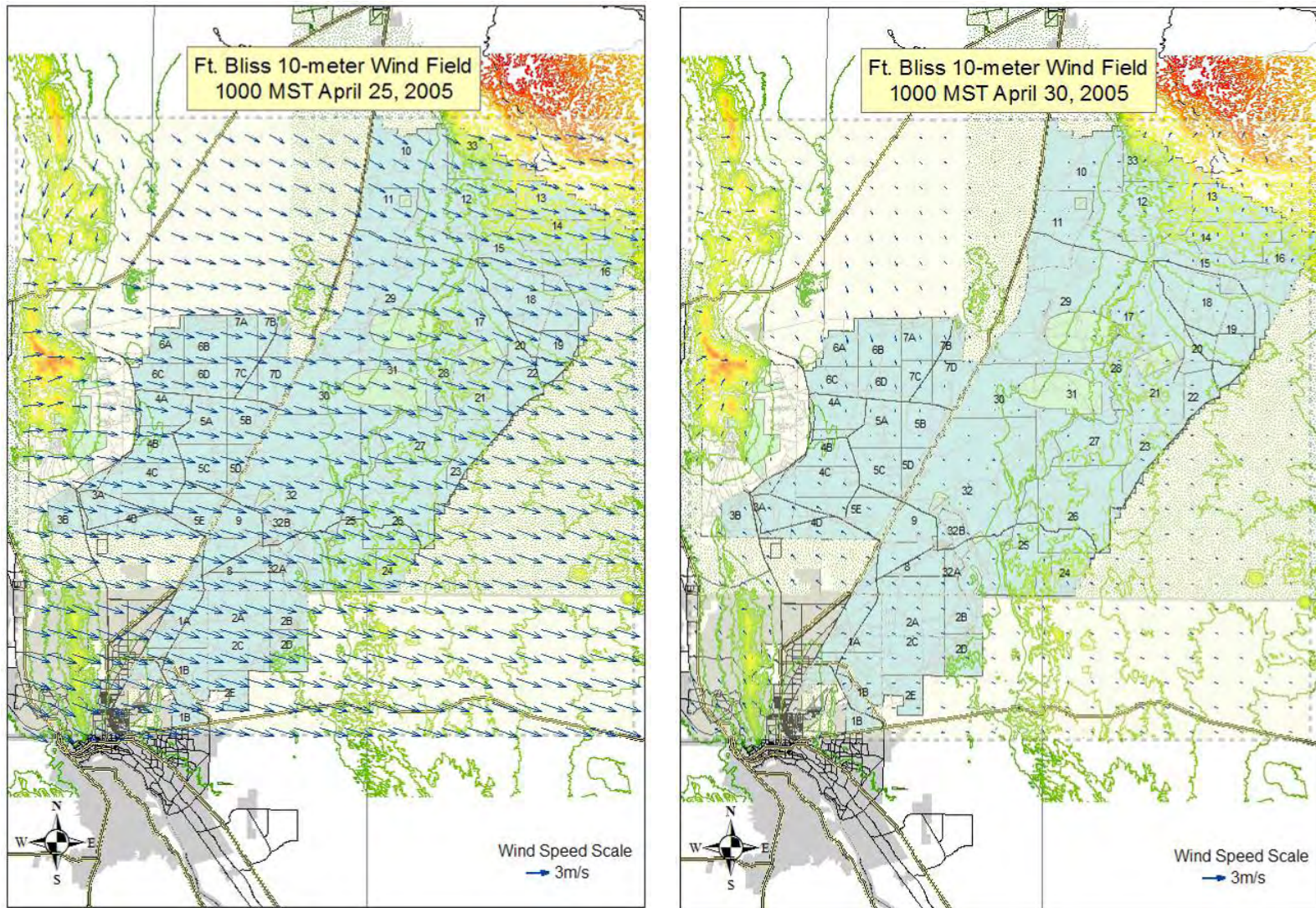


Figure 7.2. 10-Meter Wind Field at 1000 MST on April 25, 2005 (Left) and April 30, 2005, (Right) for the Fort Bliss Site as Calculated by DUSTAN

8.0 List of Persons Consulted

Mr. Dallas Bash, Fort Bliss
Mr. Chuck Carrigan, Fort Bliss
Dr. Jack Gillies, Desert Research Institute
Dr. Hampden Kuhns, Desert Research Institute
Dr. Brian Locke, Fort Bliss
Mr. Charles Maricic, Fort Bliss
Mr. Jesse Moncada, Fort Bliss

Telephone conversations were also held with Dr. Gary Bertolin, SAIC.

9.0 References

- Allwine KJ, FC Rutz, WJ Shaw, BG Fritz, and BL Hoopes. 2004. *Third Annual Progress Report: Development of a GIS-Based Complex Terrain Model for Atmospheric Dust Dispersion*. PNNL-14555, Pacific Northwest National Laboratory, Richland, WA.
- Allwine KJ, FC Rutz, WJ Shaw, JP Rishel, BG Fritz, EG Chapman, BL Hoopes and TE Seiple. 2006. *DUSTRAN 1.0 User's Guide: A GIS-Based Atmospheric Dust Dispersion Modeling System*. PNNL-16055, Pacific Northwest National Laboratory, Richland, WA.
- Booz Allen Hamilton. 2005. *Prevention of Significant Deterioration (PSD) Analysis, Ft. Bliss, Texas, Ft. Bliss, New Mexico*. Report available from Fort Bliss Directorate of Environment, Fort Bliss, TX.
- Chapman, EG, JP Rishel, FC Rutz, TE Seiple, RK Newsom, and KJ Allwine KJ. 2006. *Dust Plume Modeling at Fort Bliss: Full Training Scenario*. PNNL-15935, Pacific Northwest National Laboratory, Richland, WA.
- Gillies JA., V Etyemezian, H Kuhns, D Nikolic, and DA Gillette. 2005a. "Effect of Vehicle Characteristics on Unpaved Road Dust Emissions." *Atmos. Environ.* 39:2341-2347.
- Gillies JA, WP Arnott, V Etyemezian, H Kuhns, H Moosmuller, D DuBois, M Abu-Allaban, G Schwemmer, DA Gillette, WG Nickling, R Varma, T Wilkerson, and R Varma. 2005b. *Characterizing and Quantifying Local and Regional Particulate Matter Emissions from Department of Defense Installations*. Final report prepared for the Strategic Environmental Research and Development Program under Project CP-1191.
- Kuhns H, JA Gillies, V Etyemezian, D Dubois, S Ahonen, D Nikolic, and C Durham. 2005. "Spatial Variability of Unpaved Road Dust PM10 Emission Factors near El Paso, Texas." *J. Air & Waste Manage. Assoc.* 55:3-12.
- Nickovic S, G Kallos, A Papadopoulos, and O Kakaliagou. 2001. "A model for prediction of desert dust cycle in the atmosphere." *J. Geophys. Res.* 106, 18113-18129.
- Olson JS. 1992. "World Ecosystems (WE1.4). Digital Raster Data on a 10-minute Cartesian Orthonormal Geodetic 1080 × 2160 grid." In: *Global Ecosystems Database, Version 2.0*. Boulder, CO. Available at: http://www.ngdc.noaa.gov/seg/cdroms/ged_ii/datasets/a05/ow.htm (accessed 09-27-2006).
- Scire JS, DG Strimaitis, and RJ Yamartino. 2000a. *A User's Guide for the CALPUFF Dispersion Model (Version 5)*. Earth Tech, Inc., Concord, MA.
- Scire JS, FR Robe, ME Fernau, and RJ Yamartino. 2000b. *A User's Guide for the CALMET Meteorological Model (Version 5)*. Earth Tech, Inc., Concord, MA.
- Scire JS, RJ Yamartino, GR Carmichael, and YS Chang. 1989. *CALGRID: A Mesoscale Photochemical Grid Model Volume II – User's Guide*. California Resources Board, Sacramento, CA.

Staub B, and C Rosenzweig. 1992. "Global Zobler Soil Type, Soil Texture, Surface Slope, and Other Properties. Digital Raster Data on a 1-degree Geographic (lat/long) 180 × 360 grid." In: *Global Ecosystems Database Version 2.0*. Boulder, CO, NOAA National Geophysical Data Center. Available at: http://www.ngdc.noaa.gov/seg/cdroms/ged_ii/datasets/a11/sr.htm (accessed 09-27-2006).

U.S. Environmental Protection Agency (EPA). 2005. *Compilation of Air Pollutant Emission Factors (AP-42)*, Fifth Edition, Volume 1: *Stationary Point and Area Sources*. U. S. Environmental Protection Agency, Research Triangle Park, NC. Available at: <http://www.epa.gov/ttn/chief/ap42/> (accessed 09-27-2006).

Appendix A

Wind Roses

Appendix A: Wind Roses

The figures in this appendix summarize the results of our wind climatology analysis in the form of a series of wind rose charts. These results were compiled from 4 years (2002 through 2005) of hourly surface wind measurements from three air monitoring stations (CAMS12, CAM72, and CAMS414) that are operated by the Texas Commission on Environmental Quality (TCEQ). Each figure displays wind roses for a given month for each of these three stations. Results are further broken down into nighttime and daytime statistics. Results for the 12 months of the year are given.

These wind roses give the frequency (%) that winds occur from each direction for seven wind speed categories. Wind direction is divided into eighteen 20-degree sectors. For example, the upper-right plot in Figure A.1 shows the winds are from 110 degrees (~ESE) for approximately 17% of the time during the 2001 to 2005 time period at the CAMS12 measurement location.

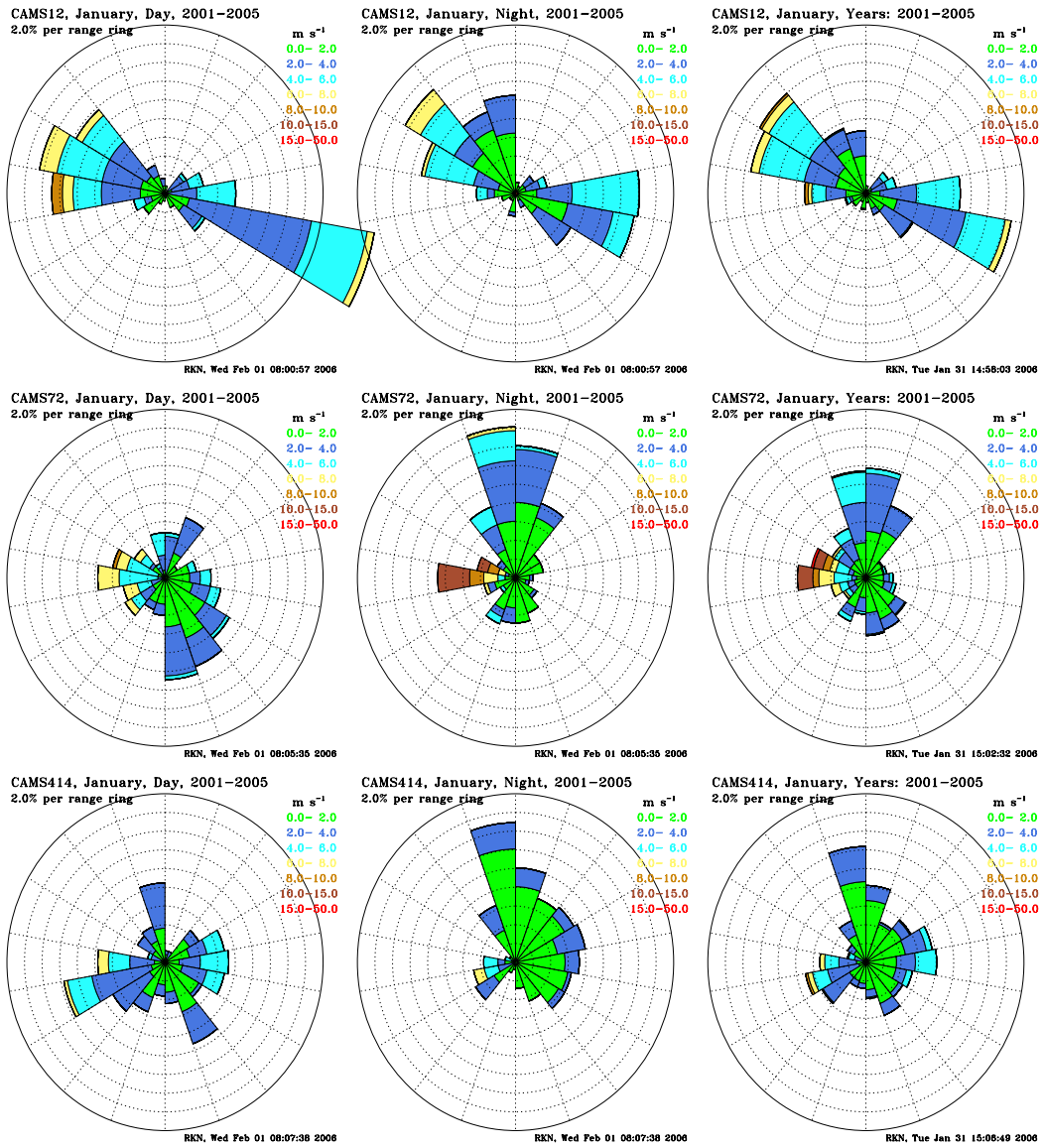


Figure A.1. January Wind Roses for at CAMS12 (top row), CAMS72 (middle row), and CAMS414 (bottom row)

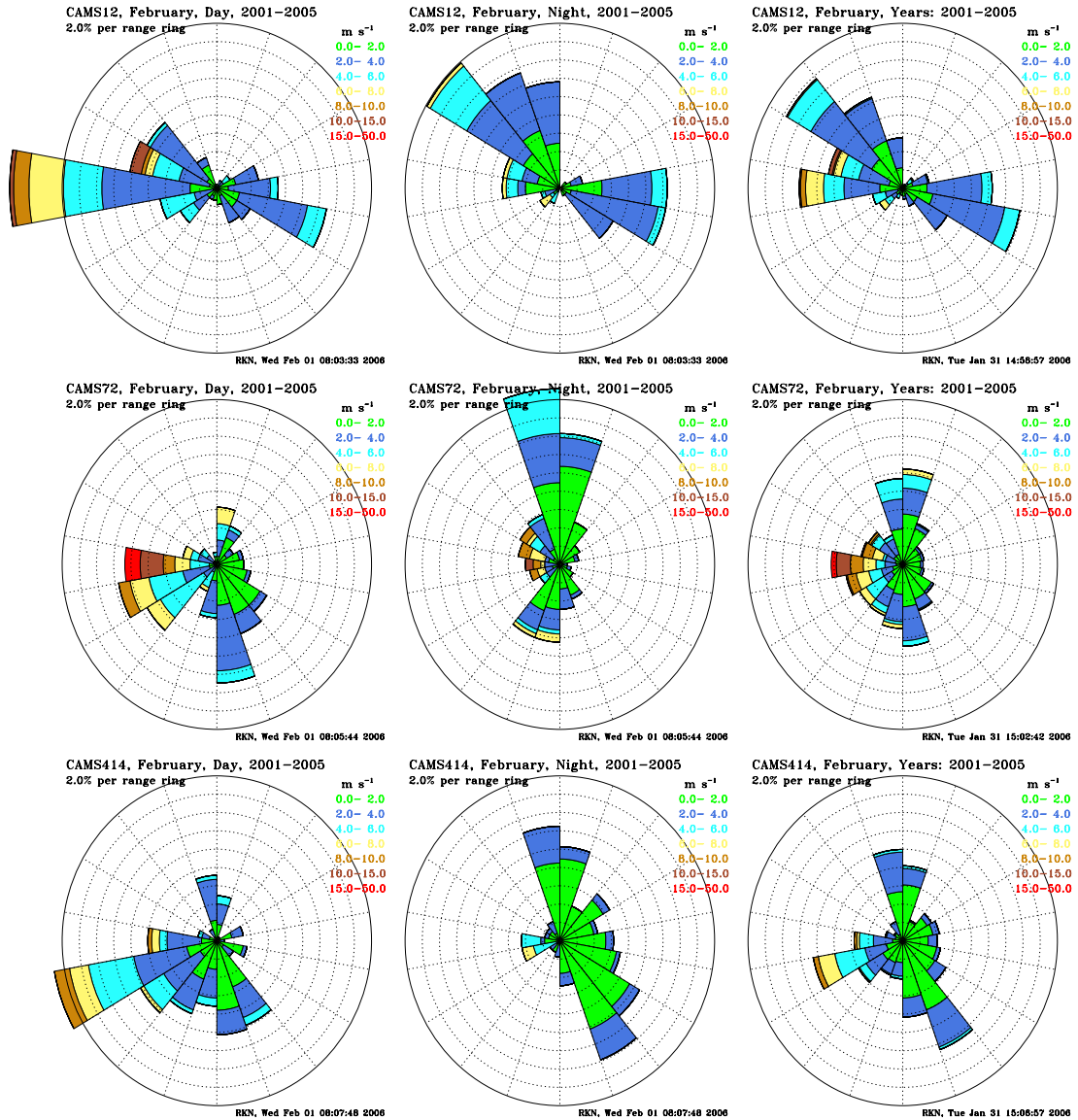


Figure A.2. February Wind Roses for at CAMS12 (top row), CAMS72 (middle row), and CAMS414 (bottom row)

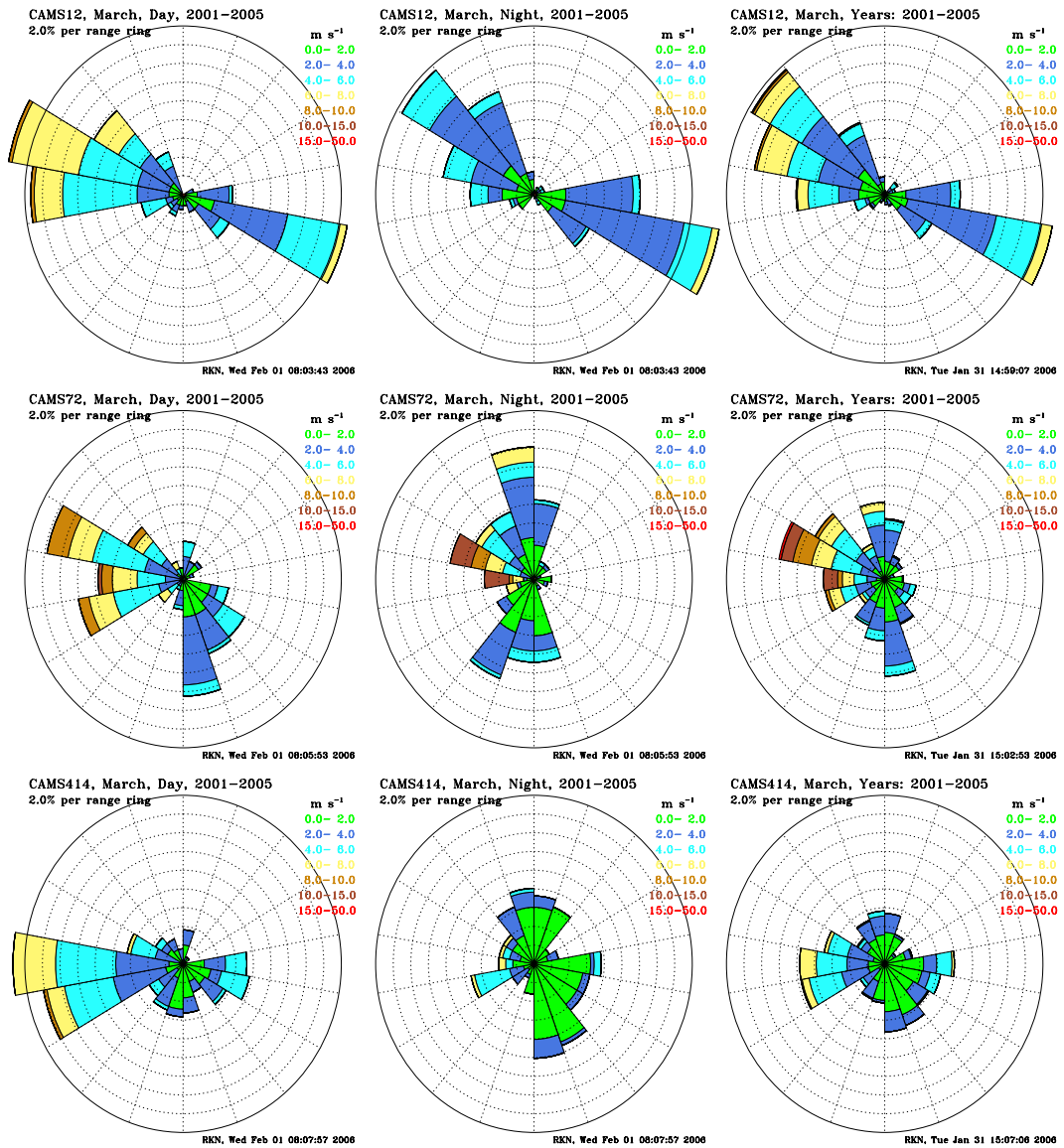


Figure A.3. March Wind Roses for at CAMS12 (top row), CAMS72 (middle row), and CAMS414 (bottom row)

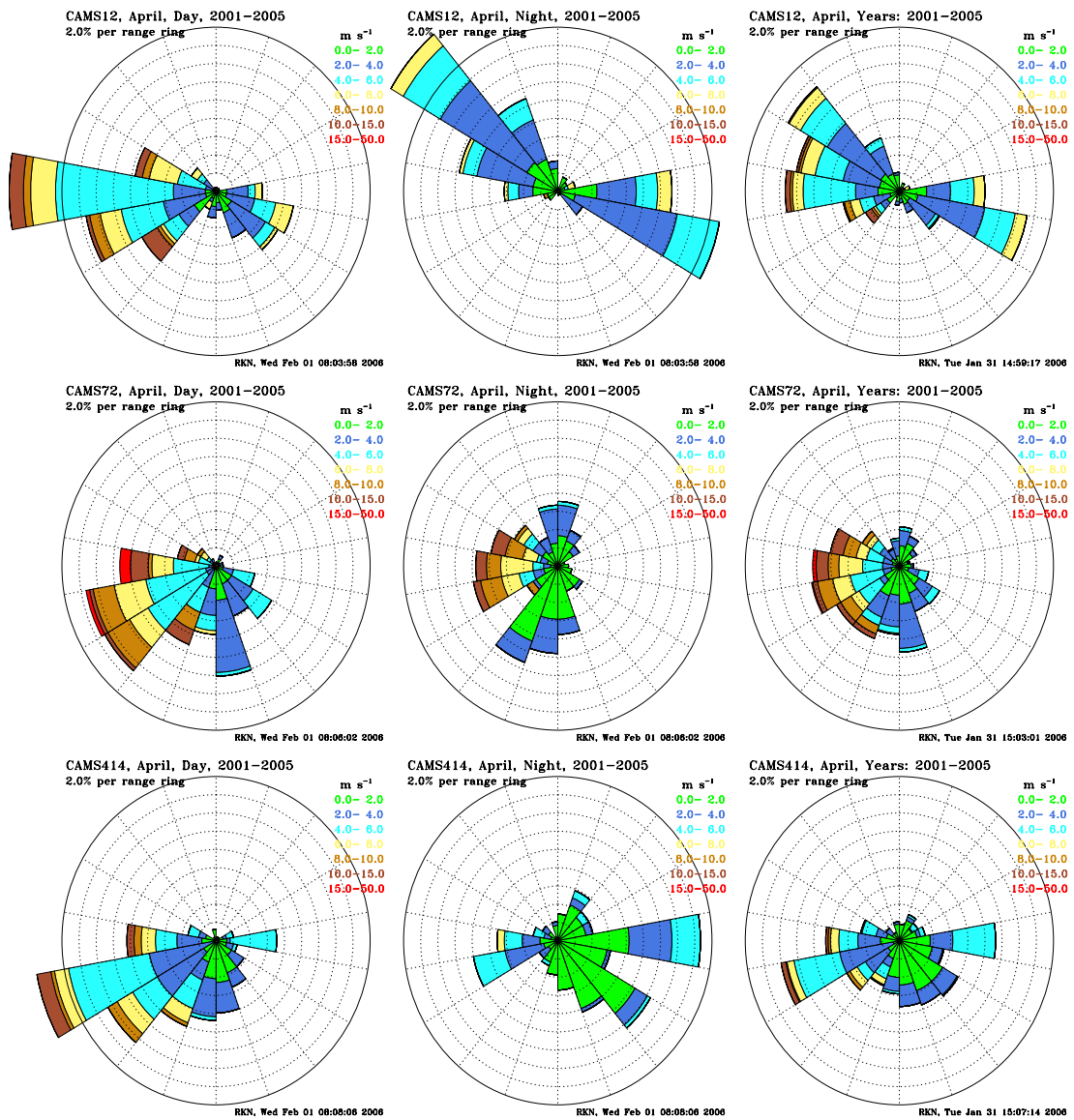


Figure A.4. April Wind Roses for at CAMS12 (top row), CAMS72 (middle row), and CAMS414 (bottom row)

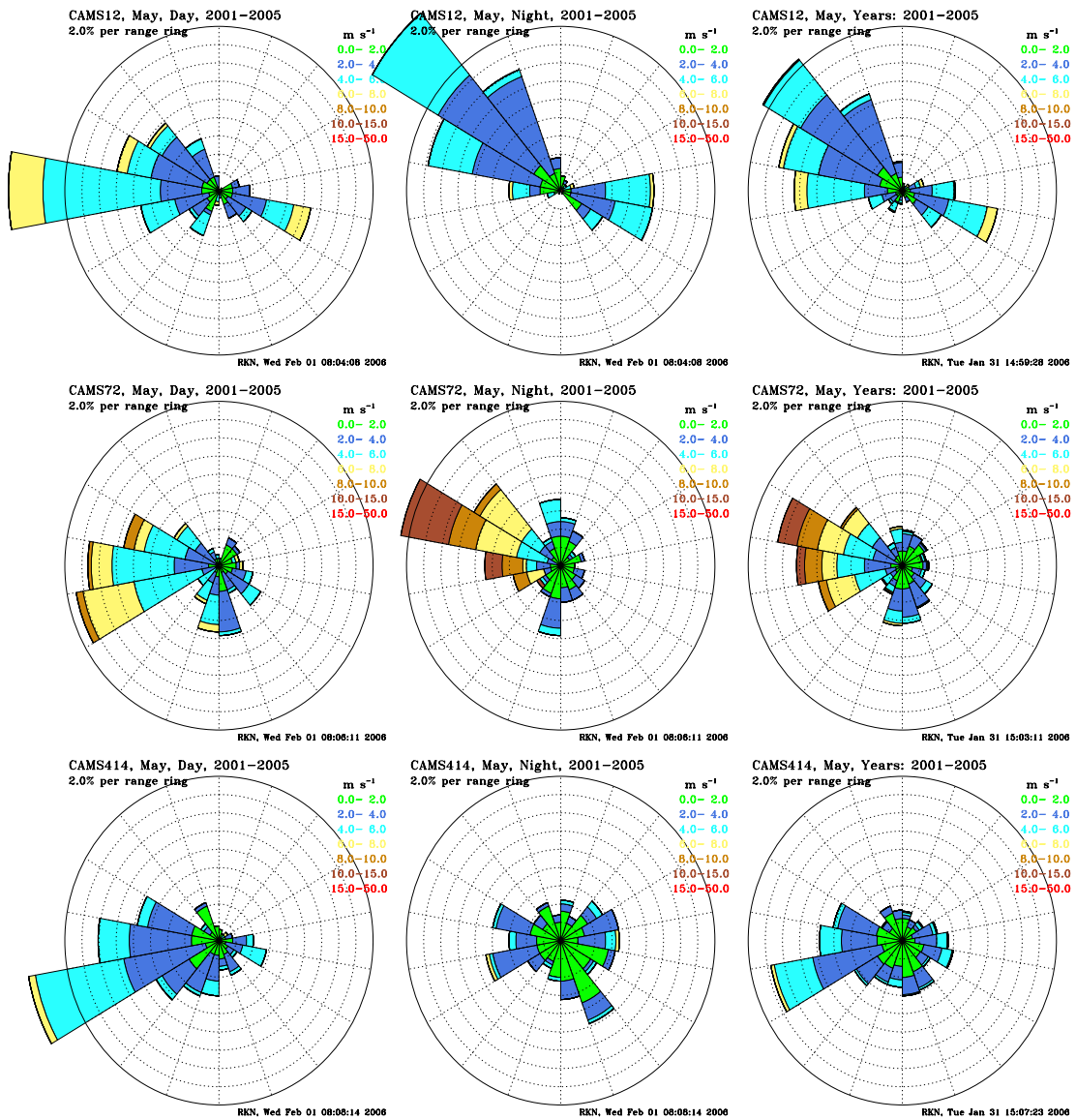


Figure A.5. May Wind Roses for at CAMS12 (top row), CAMS72 (middle row), and CAMS414 (bottom row)

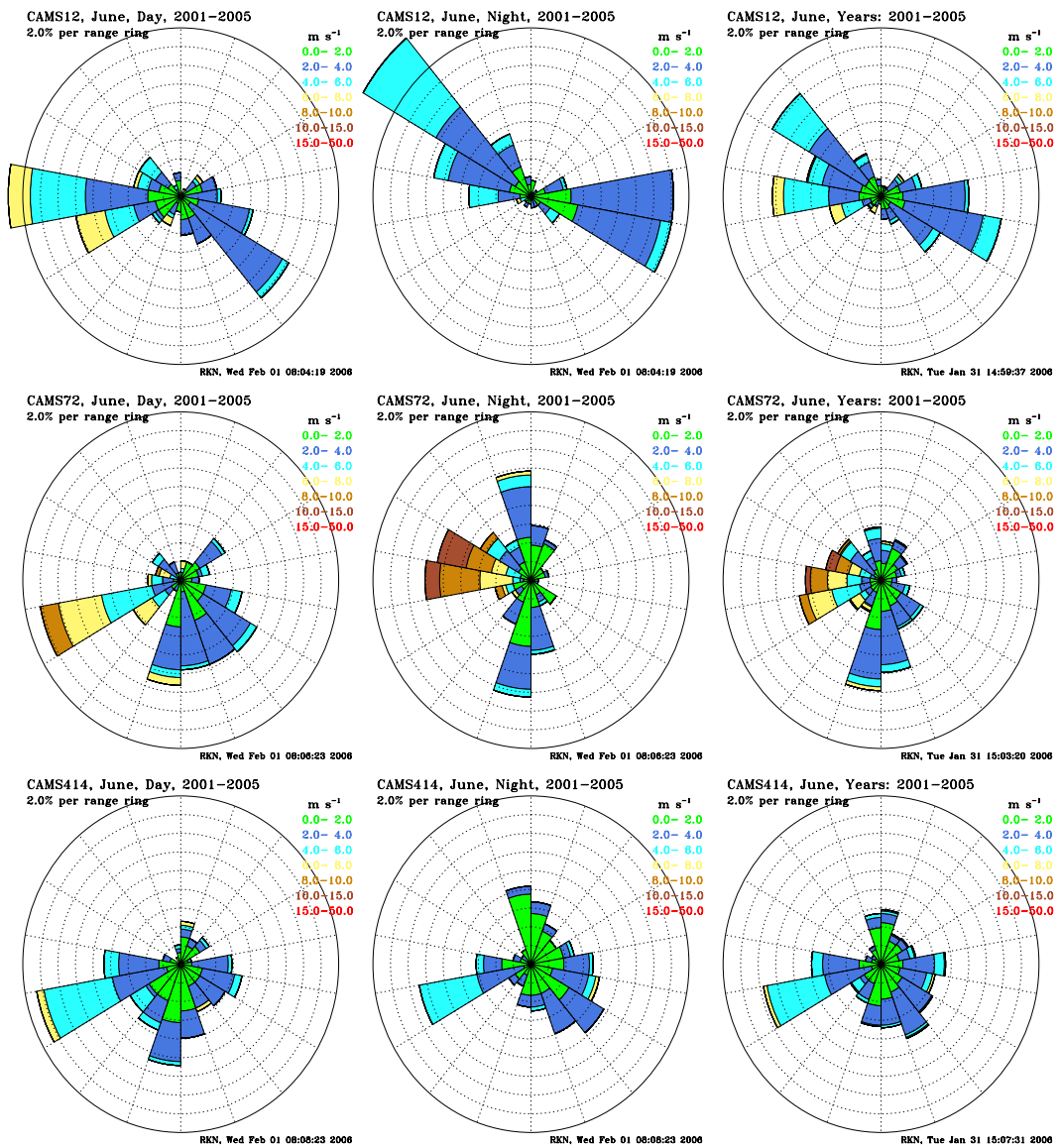


Figure A.6. June Wind Roses for at CAMS12 (top row), CAMS72 (middle row), and CAMS414 (bottom row)

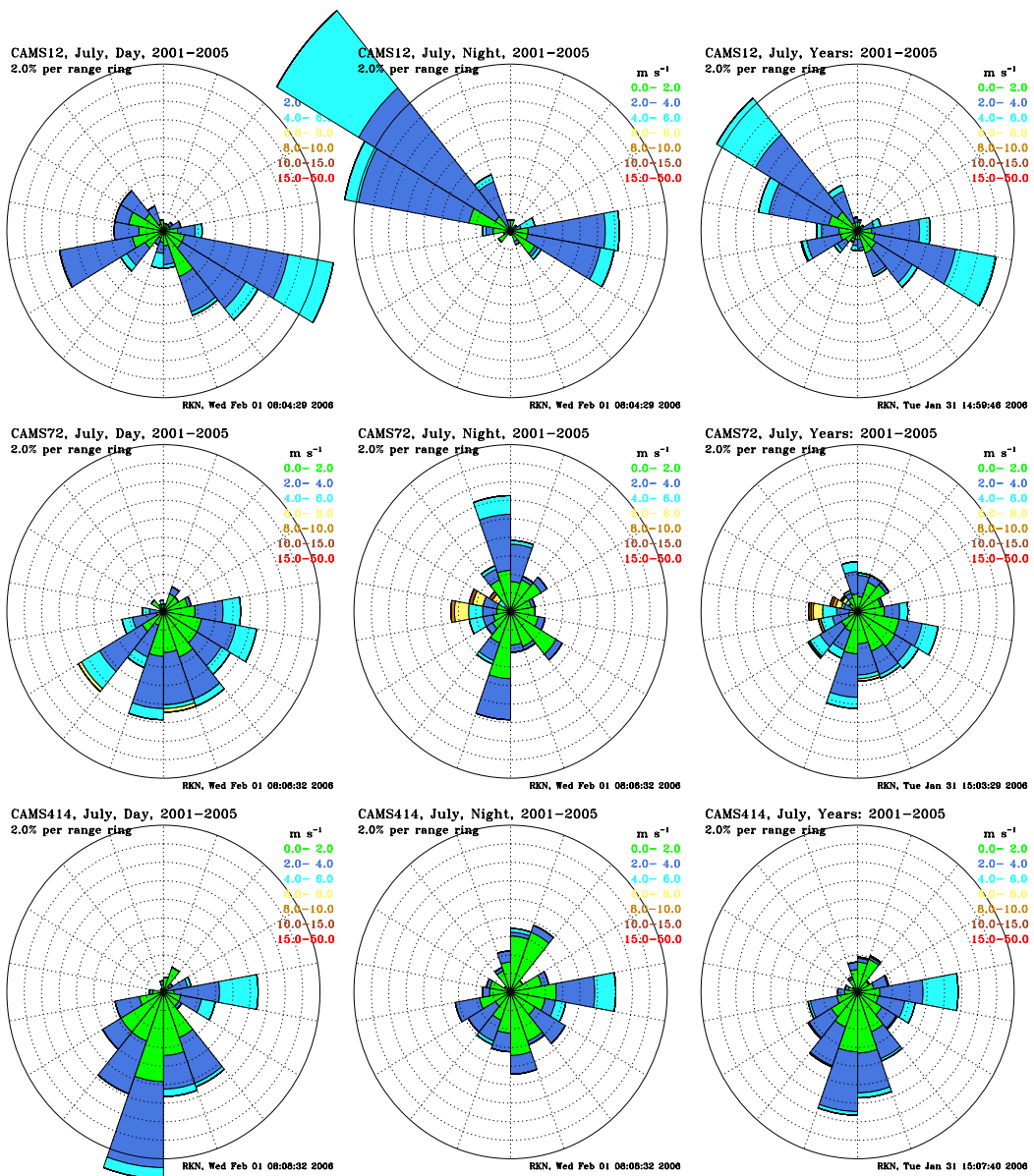


Figure A.7. July Wind Roses for at CAMS12 (top row), CAMS72 (middle row), and CAMS414 (bottom row)

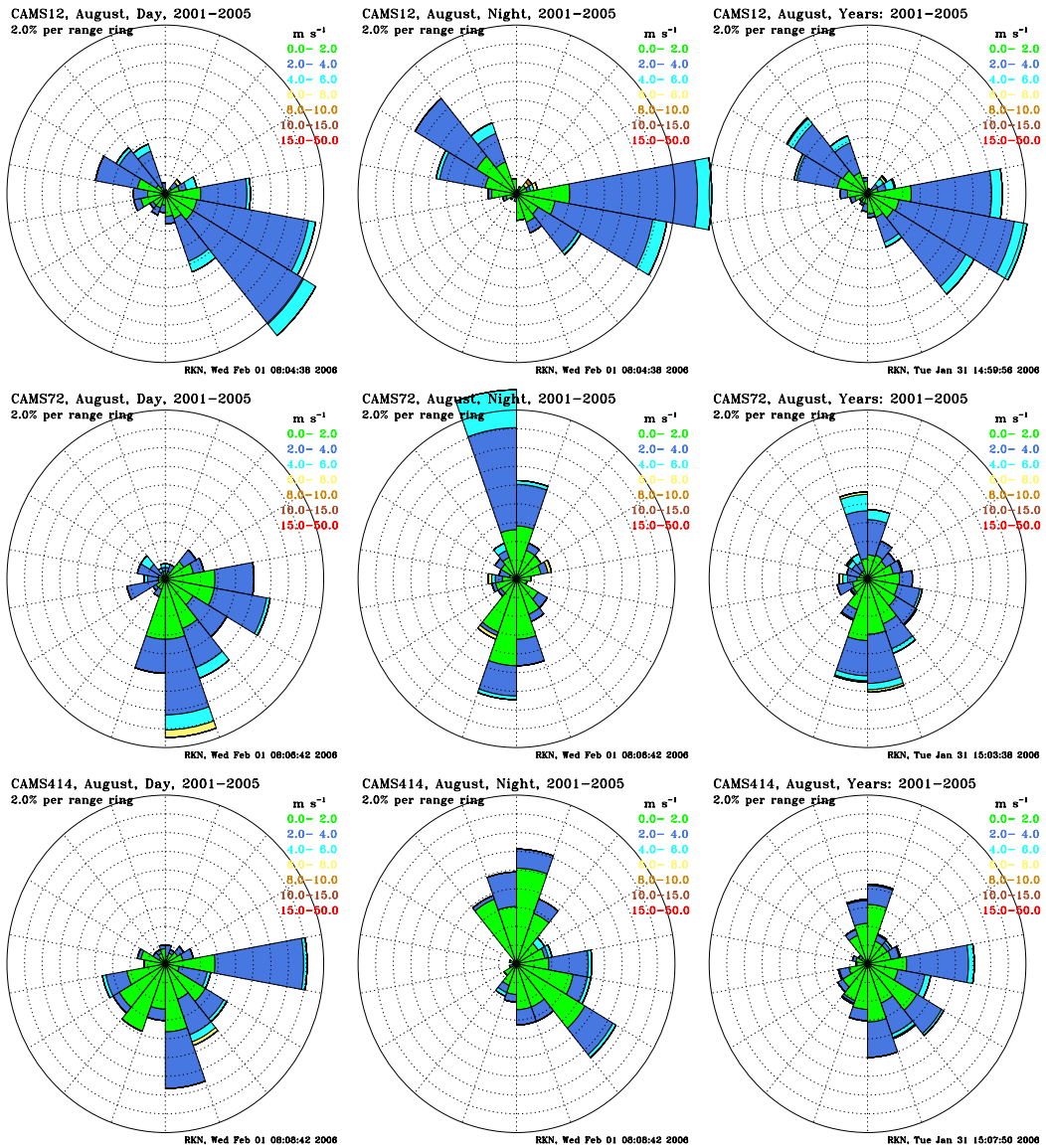


Figure A.8. August Wind Roses for at CAMS12 (top row), CAMS72 (middle row), and CAMS414 (bottom row)

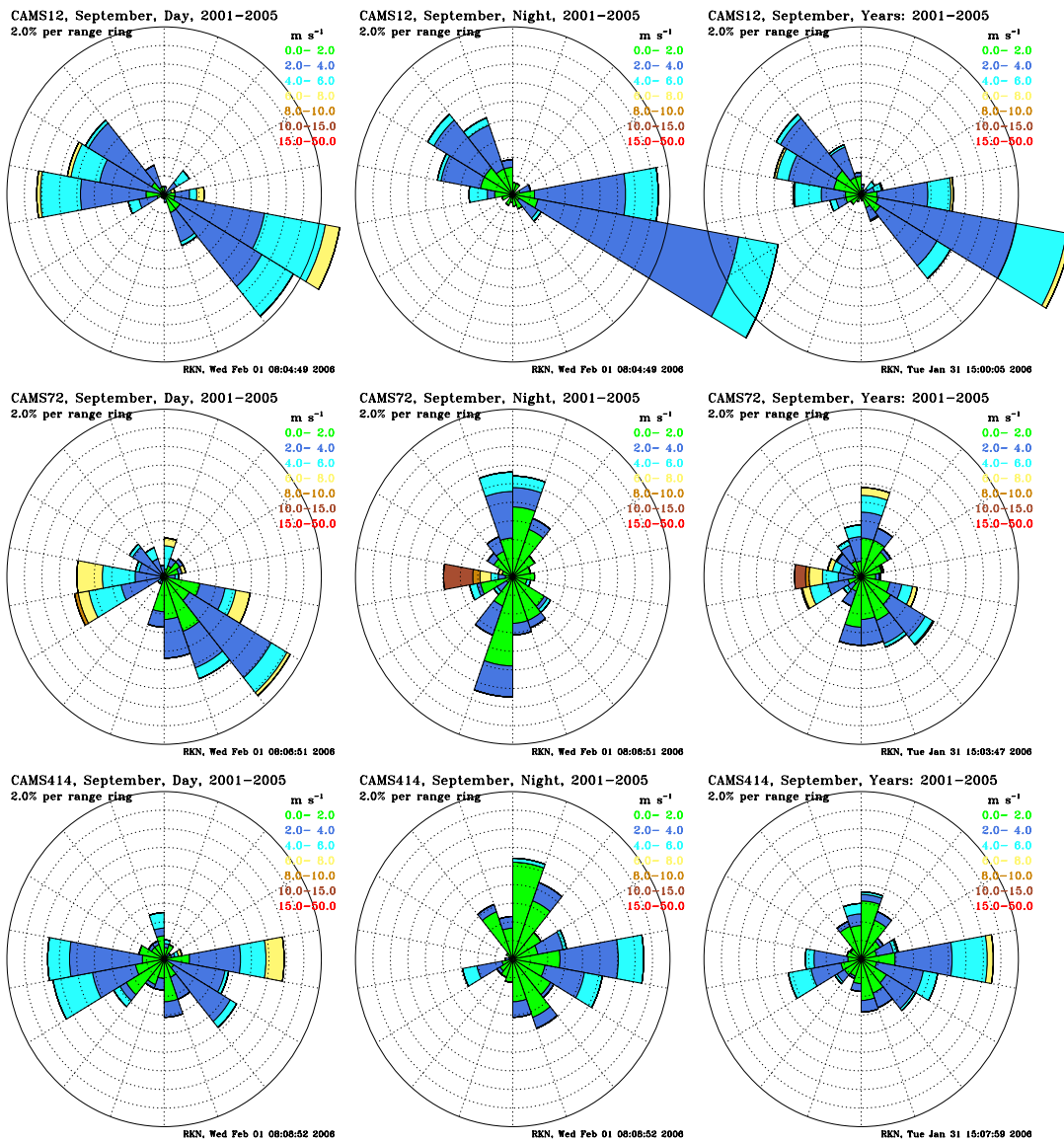


Figure A.9. September Wind Roses for at CAMS12 (top row), CAMS72 (middle row), and CAMS414 (bottom row)

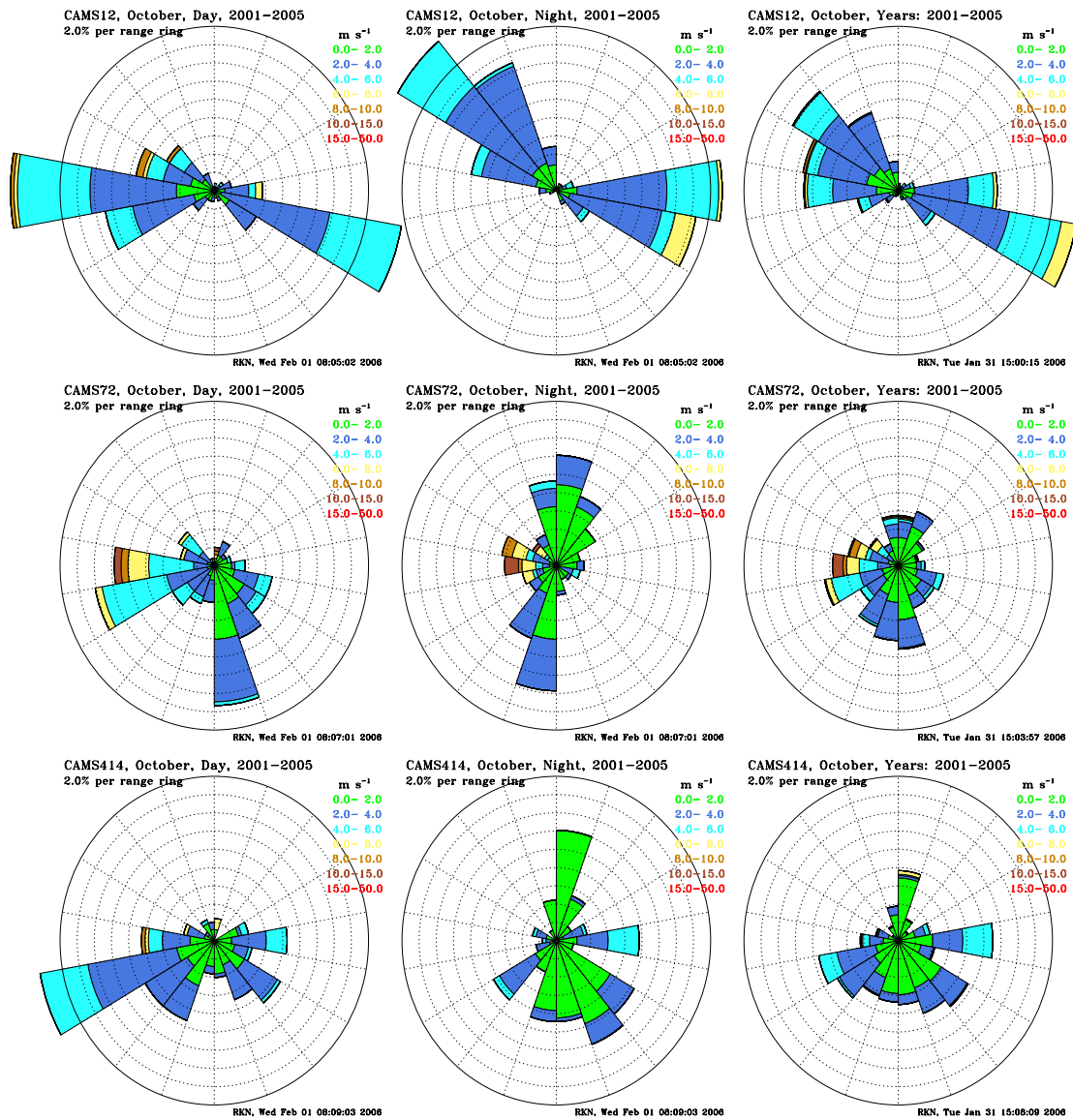


Figure A.10. October Wind Roses for at CAMS12 (top row), CAMS72 (middle row), and CAMS414 (bottom row)

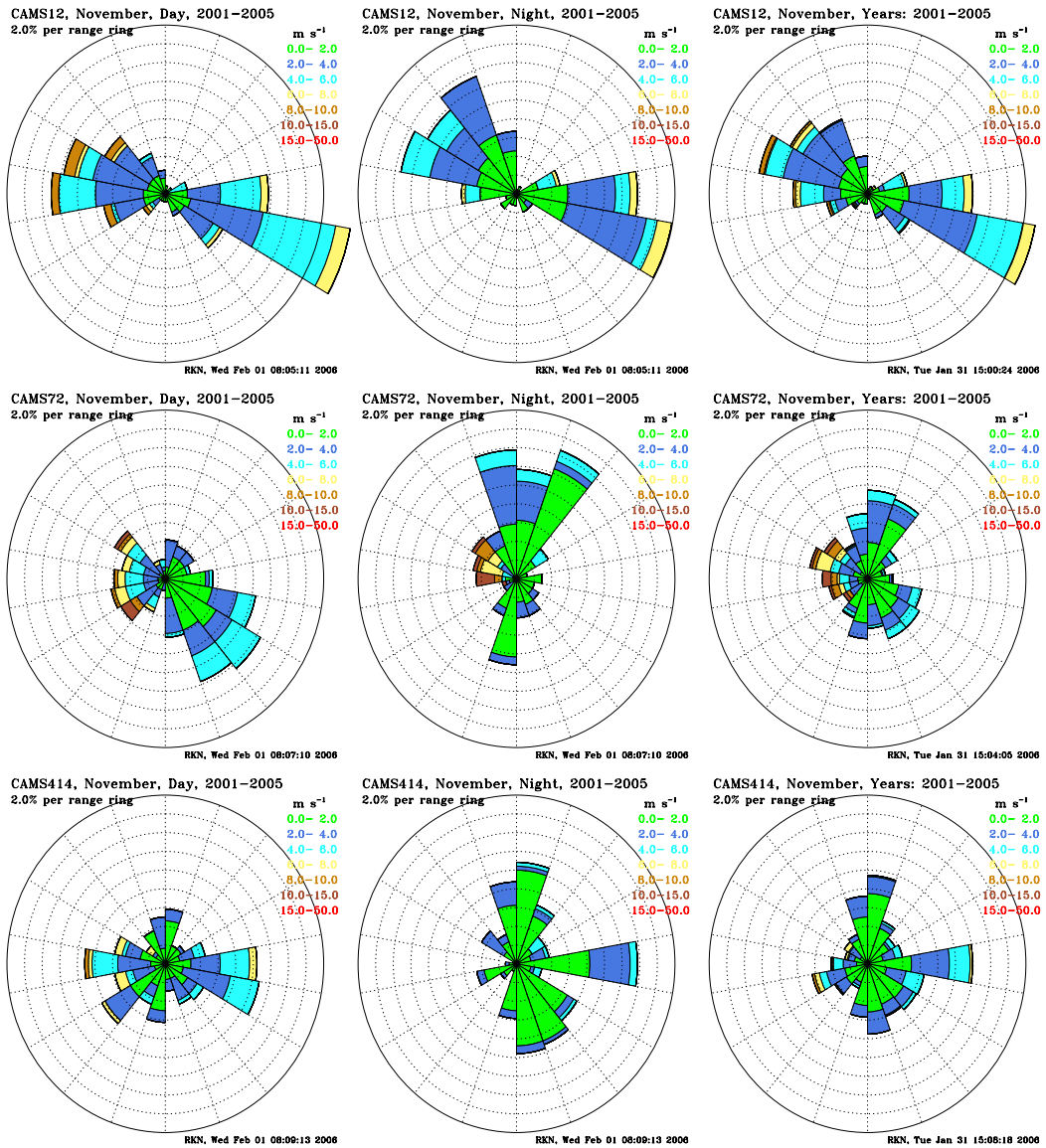


Figure A.11. November Wind Roses for at CAMS12 (top row), CAMS72 (middle row), and CAMS414 (bottom row)

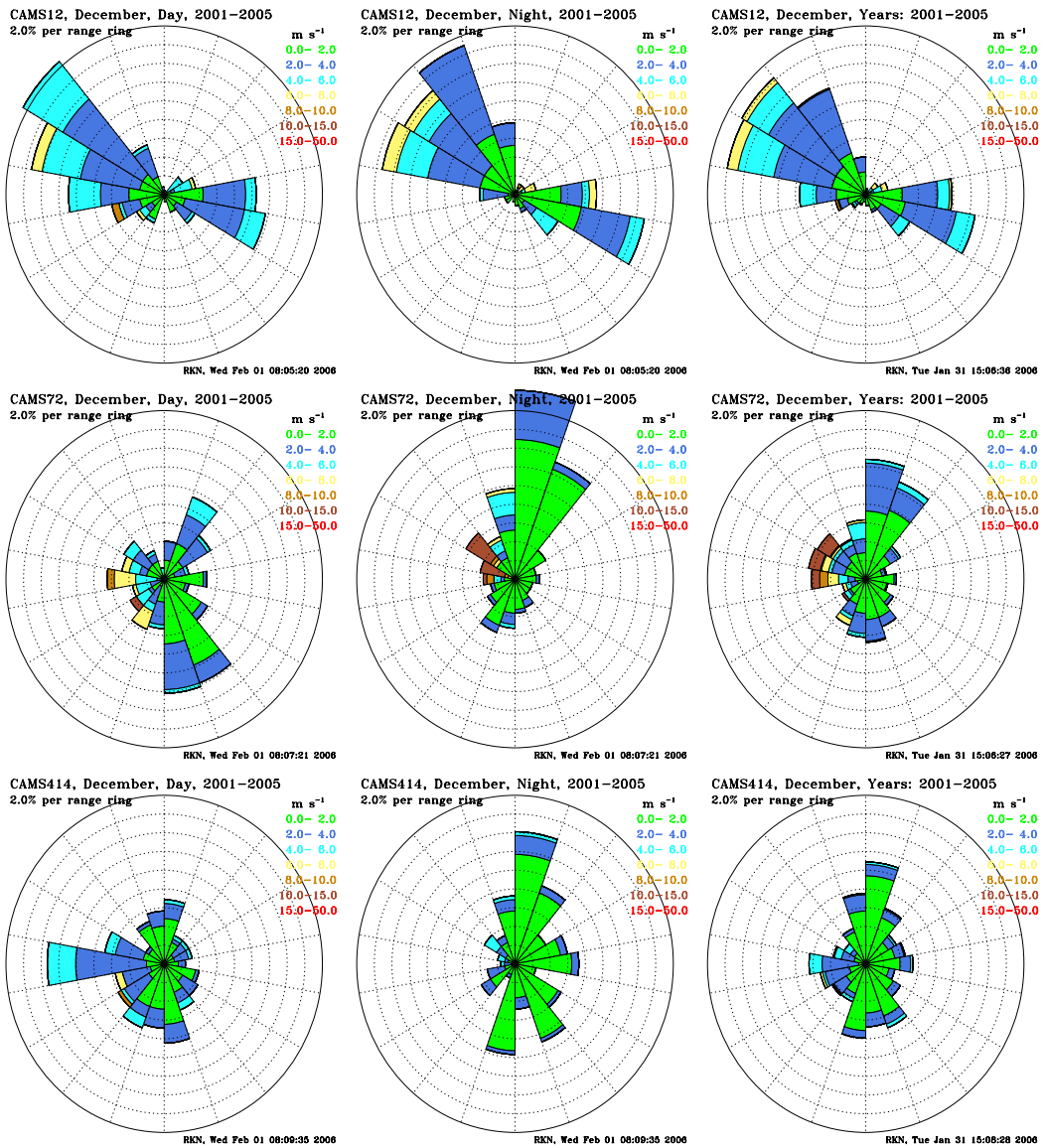


Figure A.12. December Wind Roses for at CAMS12 (top row), CAMS72 (middle row), and CAMS414 (bottom row)

Appendix B

Measured Ambient PM₁₀ Concentrations

Appendix B: Measured Ambient PM₁₀ Concentrations

The following figures give time-series plots of measured hourly wind speed, wind direction, temperature, and PM₁₀ at the New Mexico Environment Department (NMED) station 6ZK for the four DUSTRAN simulation periods. The four simulation periods are March 12–16, April 25–30, July 20–24, and November 25–29, 2005.

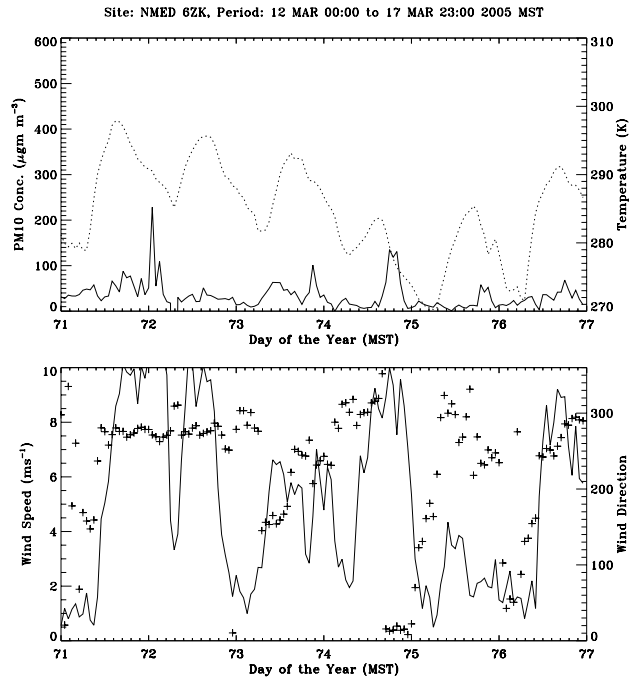


Figure B.1. Time series of PM (top solid), Temperature (top dotted line), Wind Speed (bottom solid), and Wind Direction (+) for the Period from 00:00 MST 12 March to 23:00 MST 17 March

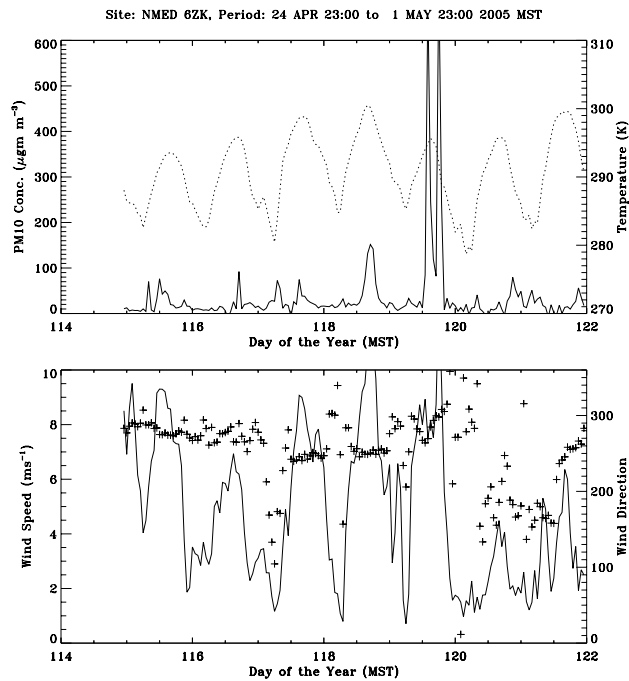


Figure B.2 Time series of PM (top solid), Temperature (top dotted line), Wind Speed (bottom solid), and Wind Direction (+) for the Period from 23:00 MST 24 April to 23:00 MST 1 May, 2005

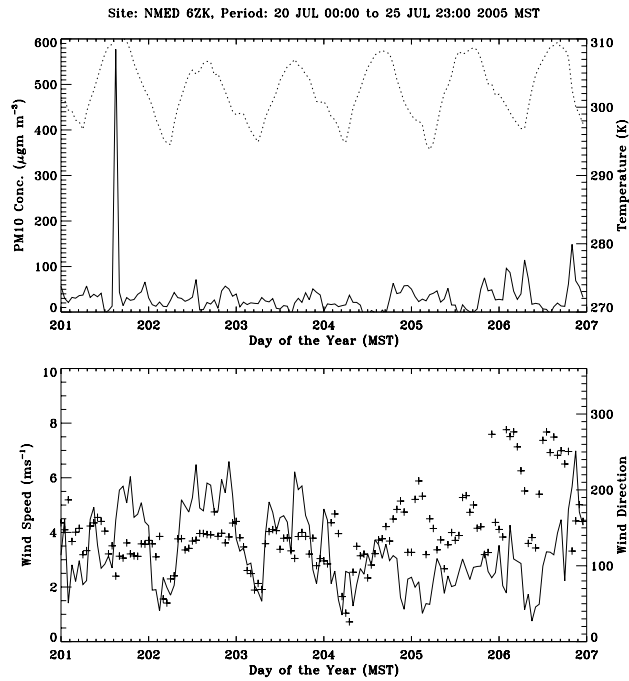


Figure B.3. Time series of PM (top solid), Temperature (top dotted line), Wind Speed (bottom solid), and Wind Direction (+) for the Period from 00:00 MST 20 July to 23:00 MST 25 July, 2005

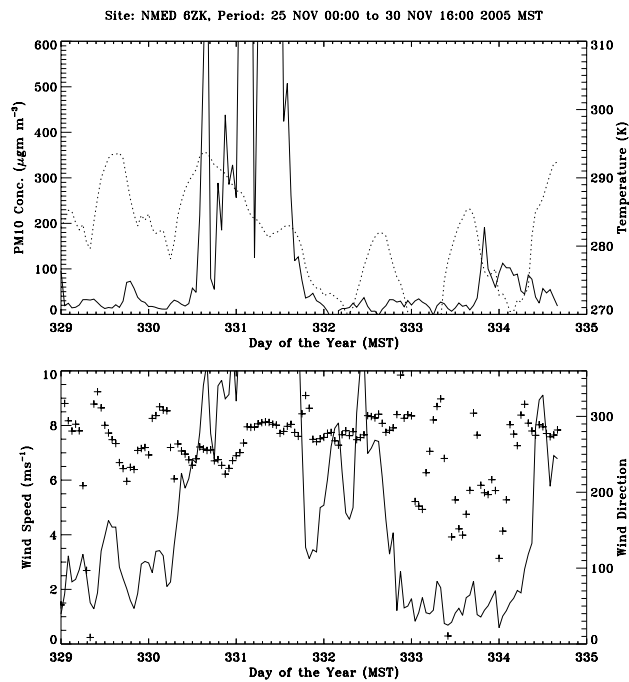


Figure B.4. Time series of PM (top solid), Temperature (top dotted line), Wind Speed (bottom solid), and Wind Direction (+) for the period from November to 16:00 MST 30 November, 2005

Appendix C

Mapping of Heavy Brigade Combat Team (HBCT) Vehicles to DUSTAN Vehicle Types

Appendix C: Mapping of Heavy Brigade Combat Team (HBCT) Vehicles to DUSTRAN Vehicle Types

The following table gives the assigned mapping of HBCT vehicles, as presented in the Booz Allen Hamilton report (2005), to the possibility of 10 default DUSTRAN vehicle types. The 758 wheeled vehicles present in a HBCT are mapped to a total of 758 wheeled DUSTRAN vehicles, while the 354 tracked vehicles present in a HBCT are mapped to a total of 548 DUSTRAN vehicles. The number of DUSTRAN vehicles representing tracked vehicles is larger than the actual HBCT total because in some instances, the tracked vehicles are heavier than representative DUSTRAN vehicle types and must be mapped as multiple DUSTRAN vehicles.

Table C.1. Mapping of Vehicles in One Heavy Brigade Combat Team (HBCT) to Available DUSTAN Vehicle Types. HBCT vehicle types are listed based on Booz Allen Hamilton (2005). The “Freightliner” designation represents loaded freightliners.

Sources	No. Sources	DUSTAN Equivalent (per source)	Comment
Wheeled Vehicle			
SET: CONTACT SUPPORT FIGHTING VEHICLE (TOW)	2	HMMWV	
TRUCK UTILITY: S250 SHELTER CARRIER 4X4 W/E (HMMWV)	2	HMMWV	
TRUCK UTILITY: HEAVY VARIANT HMMWV 4X4 10000 GVW W/E	36	HMMWV	
TRACTOR WHEELED: DSL 4X4 W/EXCAVATOR AND FRONT LOADER	4	GMC G20 VAN	med. Wt 2.5-5 tons
TRUCK AMBULANCE: 4 LITTER ARMD 4X4 W/E (HMMWV)	11	HMMWV	
TRUCK CARGO: TACTICAL 8X8 HEAVY EXPANDED MOBILITY W/W W/LT CRANE	4	GMC C550	hvy Wt. >5tons
TRUCK CARGO: TACTICAL 8X8 HEAVY EXPANDED MOBILITY W/MED CRANE	4	GMC C550	
TRUCK CARGO: HEAVY PLS TRANSPORTER 15-16.5 TON 10X10	43	M923A2(5-ton)	
TRUCK CARGO: HEAVY PLS TRANSPORTER 15-16.5 TON 10X10 W/MHE W/E	12	M923A2(5-ton)	
TRUCK CARGO: MTV W/E W/W	1	HMMWV	
TRUCK TANK: FUEL SERVICING 2500 GALLON 8X8 HEAVY EXP MOB W/WINCH	6	M923A2(5-ton)	
TRUCK CARGO: 4X4 LMTV W/E	23	HMMWV	
TRUCK CARGO: 4X4 LMTV W/E W/W	7	HMMWV	
TRUCK CARGO: MTV LWB W/E	1	HMMWV	
TRUCK CARGO: MTV W/E	50	HMMWV	
TRUCK: CARGO	55	HMMWV	
TRUCK TRACTOR: MTV W/E	26	GMC G20 VAN	med. Wt 2.5-5 tons
TRUCK TRACTOR: MTV W/E W/W	1	GMC G20 VAN	med. Wt 2.5-5 tons
TRUCK UTILITY: CARGO/TROOP CARRIER 1-1/4 TON 4X4 W/E (HMMWV)	206	HMMWV	
TRUCK UTILITY: CARGO/TROOP CARRIER 1-1/4 TON 4X4 W/E W/W (HMMWV)	4	HMMWV	
TRUCK UTILITY: EXPANDED CAPACITY 4X4 W/E HMMWV M1113	50	HMMWV	
TRUCK LIFT: FORK VARIABLE REACH ROUGH TERRAIN	6	HMMWV	
TRUCK TANK: FUEL SERVICING 2500 GALLON 8X8 HEAVY EXP MOB	41	M923A2(5-ton)	
TRUCK TRACTOR: LET 6X6 66000 GVW W/W C/S	4	1 FREIGHTLINER	
TRUCK UTILITY: ARMT CARRIER ARMD 1-1/4 TON 4X4 W/E (HMMWV)	15	HMMWV	
TRUCK UTILITY: ARMT CARRIER ARMD 1-1/4 TON 4X4 W/E W/W (HMMWV)	2	HMMWV	
TRUCK UTILITY: EXPANDED CAPACITY UP ARMORED HMMWV 4X4 W/E	44	HMMWV	
TRUCK VAN: EXPANSIBLE MTV W/E	6	GMC G20 VAN	med. Wt 2.5-5 tons
TRUCK VAN: LMTV W/E	18	GMC G20 VAN	med. Wt 2.5-5 tons
TRUCK WRECKER: MTV W/E W/W	4	GMC C5500	hvy wt. >5tons
TRUCK WRECKER: TACTICAL 8X8 HEAVY EXPANDED MOBILITY W/WINCH	10	GMC C5500	hvy wt. >5tons

Table C.1. (contd)

POWER SUPPLY VEHICLE: HYP-57/TSEC	47	HMMWV	
AUGER EARTH BOOM MOUNTED: HYD SMALL EMPLACEMENT EXCAVATOR (SEE)	2	GMC C5500	
FIRE SUPPORT TEAM VEHICLE: BRADLEY (BFIST)	11	1 FREIGHTLINER	58000lbs/26300kg
Total Wheeled Vehicles	758		
Tracked Vehicle			
RECOVERY VEHICLE FULL TRACKED: MEDIUM	13	2 FREIGHTLINERS	medium' HERCULES 70
RECOVERY VEHICLE FULL TRACKED: HEAVY M88A2	13	3 FREIGHTLINERS	TONS/63500KG
TANK COMBAT FULL TRACKED: 120MM GUN M1A2	58	3 FREIGHTLINERS	ABRAMS 68.4 TONS
TRACTOR FULL TRACKED HIGH SPEED: ARMORED COMBAT EARTHMOVER (ACE)	6	1 FREIGHTLINER	COMBAT WEIGHT 55000lbs/24950kg
CARRIER AMMUNITION: TRACKED VEHICLE (CATV)	16	1 FREIGHTLINER	M992 28.75 tons/57500lbs/26000kg
CARRIER 120 MILLIMETER MORTAR: SELF PROPELLED ARMORED	14	M923A2 (5 ton)	~12,000kg
CARRIER ARMORED COMMAND POST: FULL TRACKED	35	M977 HEMMET	M113 FAMILY 40000lbs/18000kg
CARRIER PERSONNEL FULL TRACKED: ARMORED (RISE)	49	M923A2 (5 ton)	M113A3 APC 27180lbs/12300kg
FIGHTING VEHICLE: FULL TRACKED INFANTRY HI SURVIVABILITY (IFV)	18	1 FREIGHTLINER	M2 Bradley 50000lbs/22700KG
FIGHTING VEHICLE: FULL TRACKED INFANTRY (IFV) M2A3	61	1 FREIGHTLINER	Bradley 58000lbs/26304kg
HOWITZER MEDIUM SELF PROPELLED:	16	1 FREIGHTLINER	M109 A6 Paladin 60000lbs/27211 kg
FIGHTING VEHICLE: FULL TRACKED CAVALRY (CFV) M3A3	29	1 FREIGHTLINER	Bradley 58000lbs/26304kg
RECOVERY VEHICLE FULL TRACKED: MEDIUM	13	2 FREIGHTLINERS	medium' - between Bradley and Hercules
RECOVERY VEHICLE FULL TRACKED: HEAVY M88A2	13	3 FREIGHTLINERS	Hercules 70 tons/63500 kg
Total Tracked Vehicles	354		

Appendix D

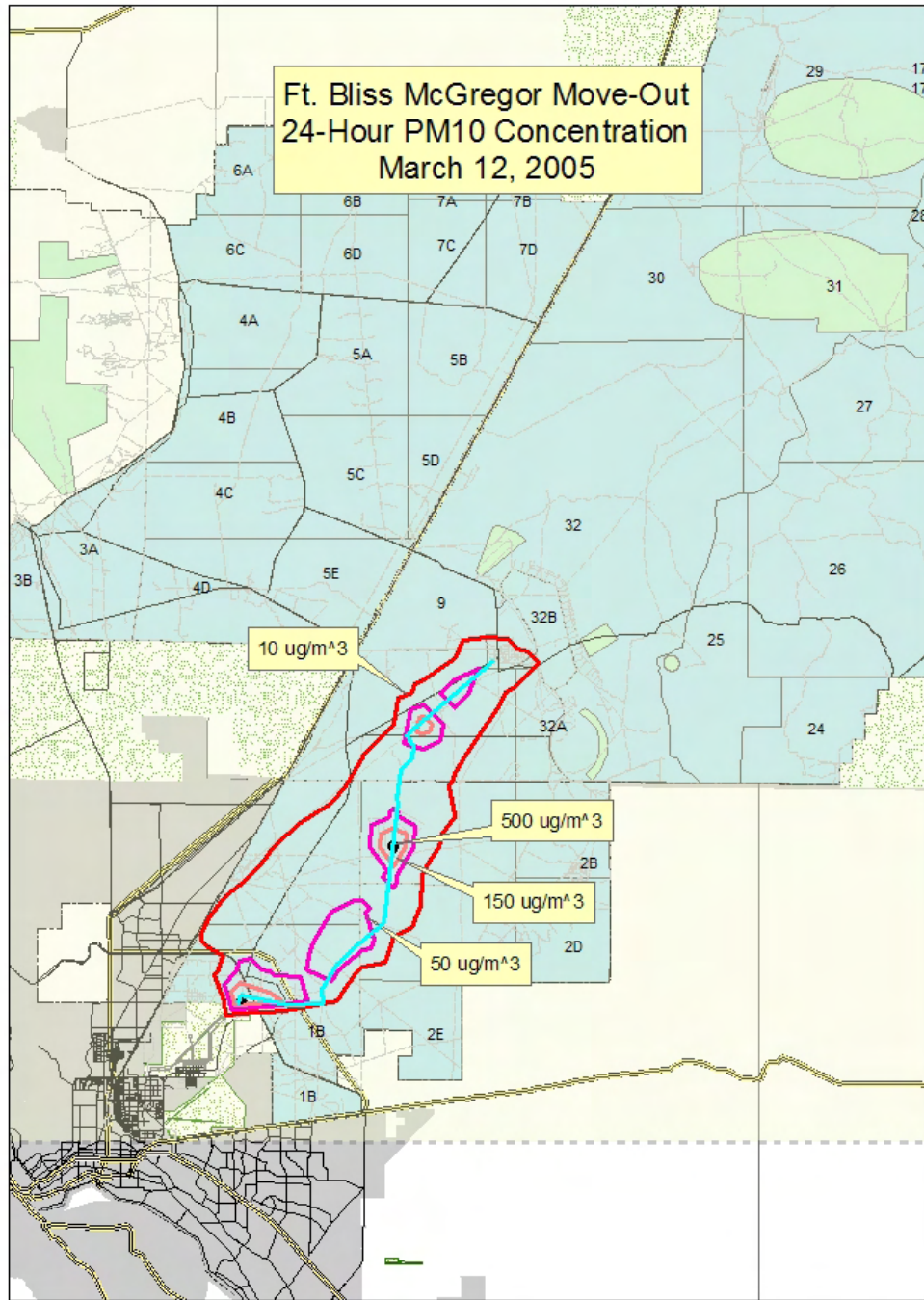
Simulated 24-h-Average PM₁₀ Concentrations for the McGregor Move-Out

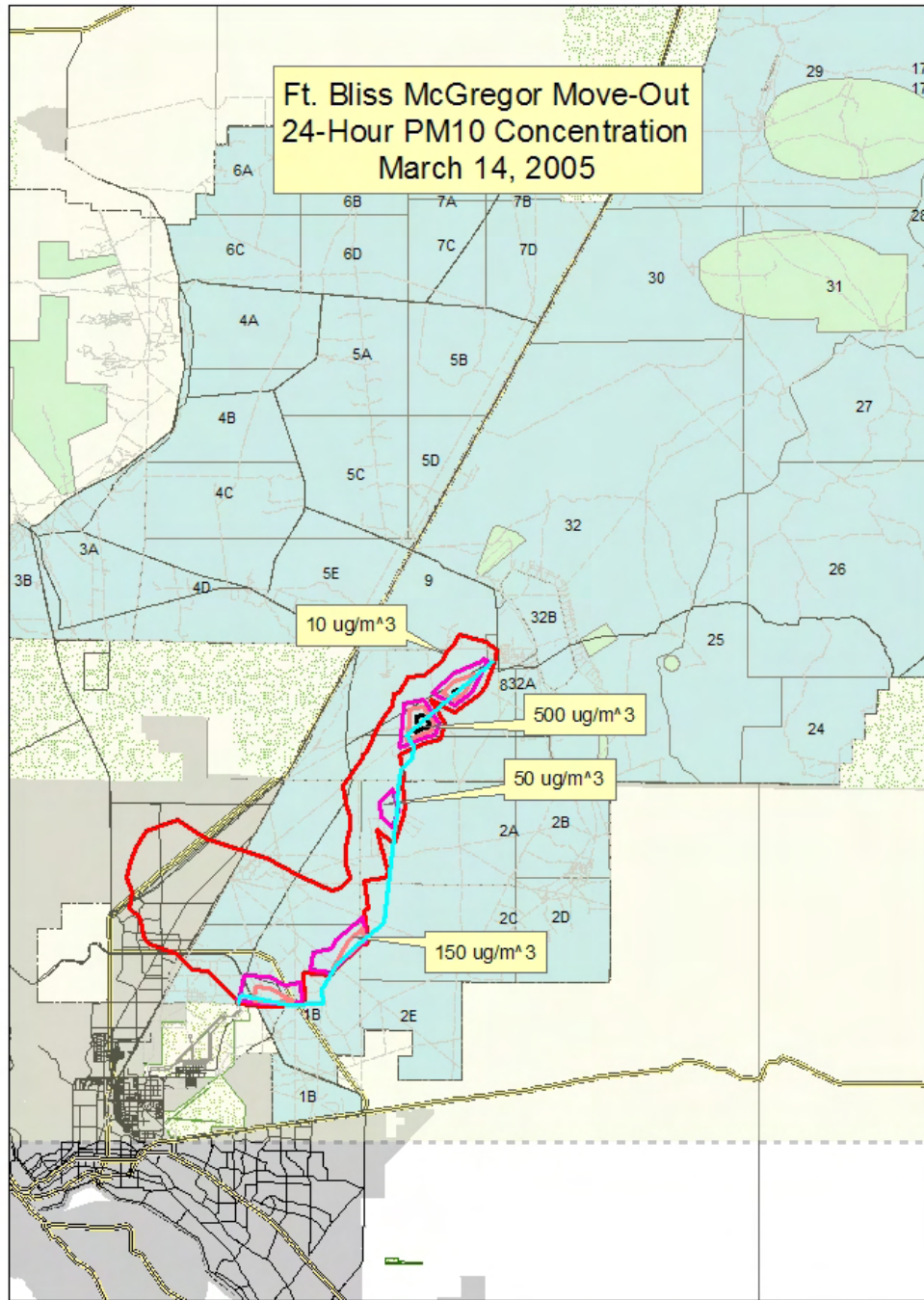
Appendix D: Simulated 24-h-Average PM₁₀ Concentrations for the McGregor Move-Out

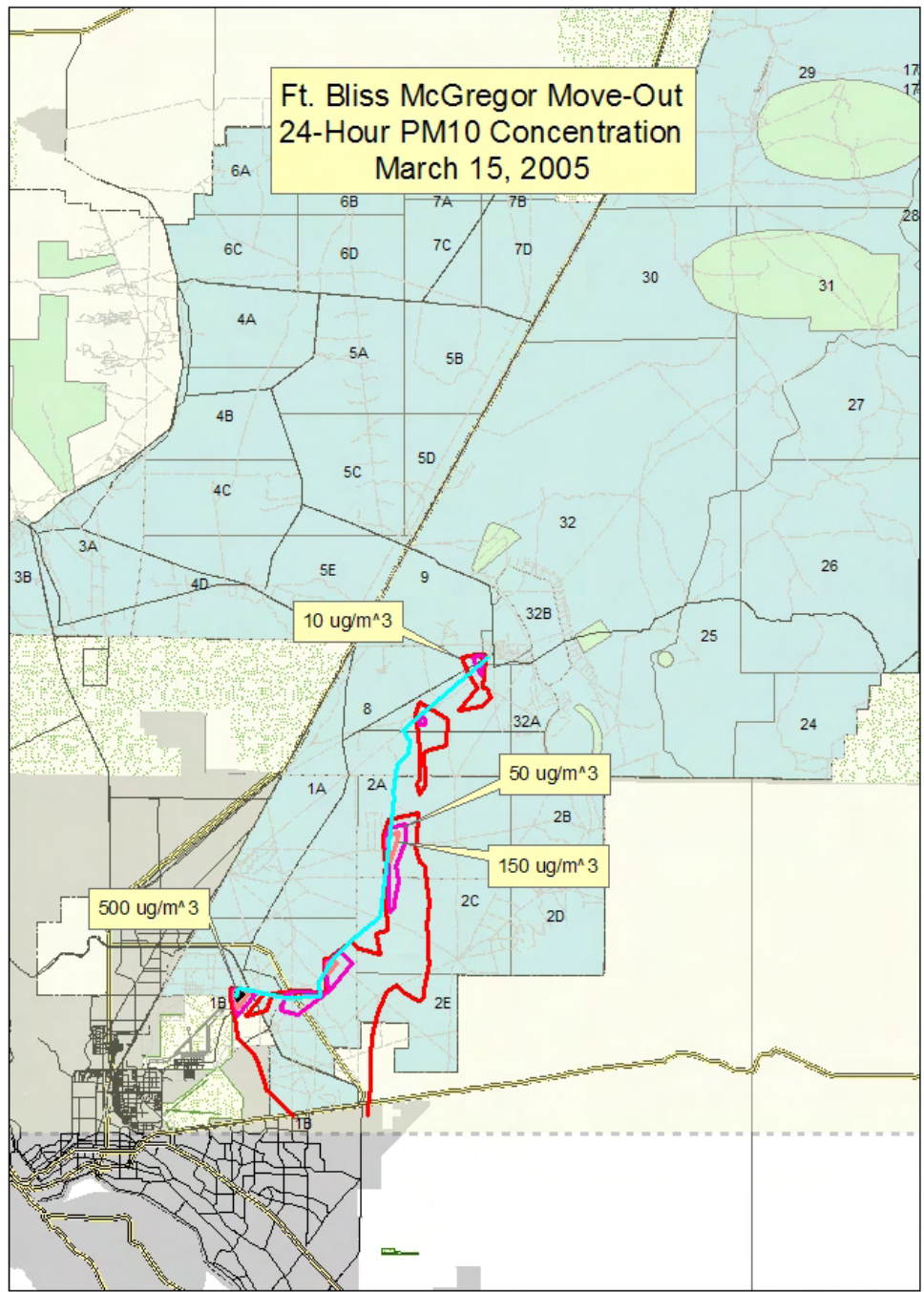
Contour maps of 24-hour-average PM₁₀ concentrations contributed from McGregor move-out operations to air quality in and around Fort Bliss are given for the 21 simulated days (March 12–16, April 25–30, July 20–24, and November 25–29, 2005). McGregor move-out scenario assumptions for DUSTRAN simulations are summarized below.

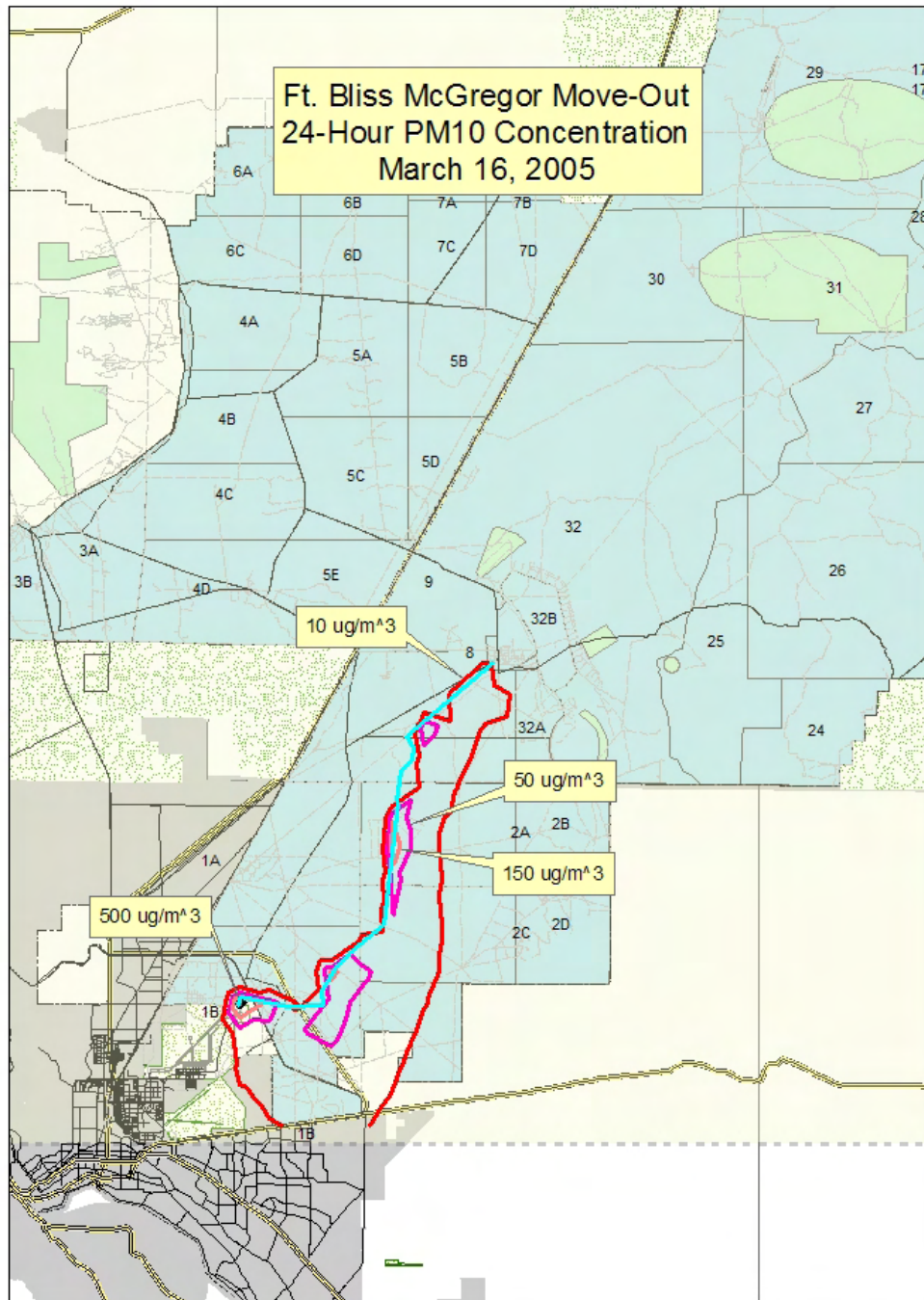
Move-Out To McGregor Range Camp

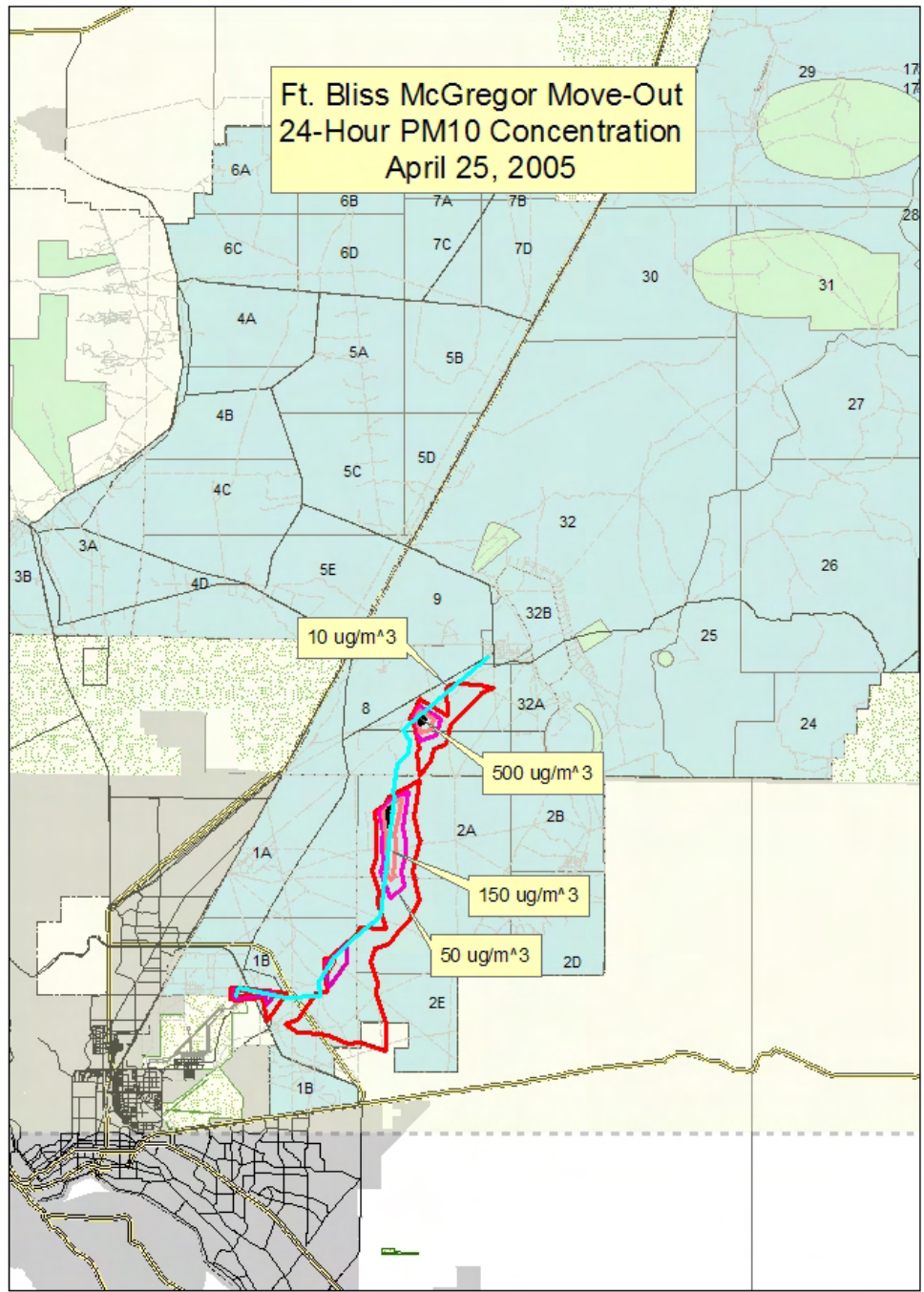
- All vehicles associated with the HBCT travel.
- Move-out route is divided into three segments; “a,” “b,” and “c” (see Figure 4.1).
- First vehicle leaves Biggs Army Airfield (start of segment “a”) at 0600 MST, reaching the start of segment “b” at 0700 MST and the start of segment “c” at 0800 MST.
- Each segment of the move-out route has vehicles on it for a total of 6 hours.
- Mean speed for each type of vehicle along all segments is 16 kilometers per hour (equivalent to 9.9 miles per hour)
- Vehicle types are uniformly mixed throughout the convoy.

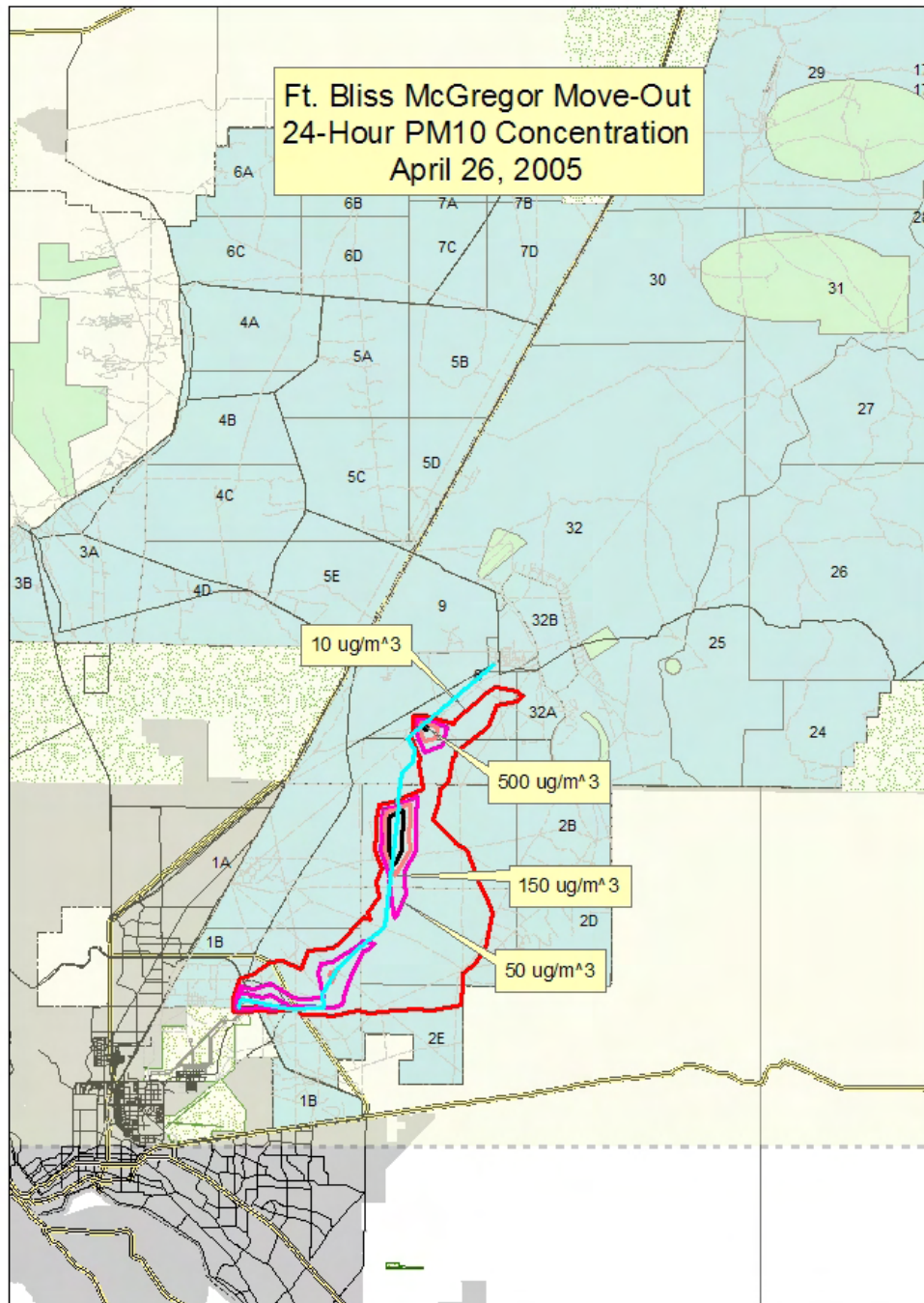


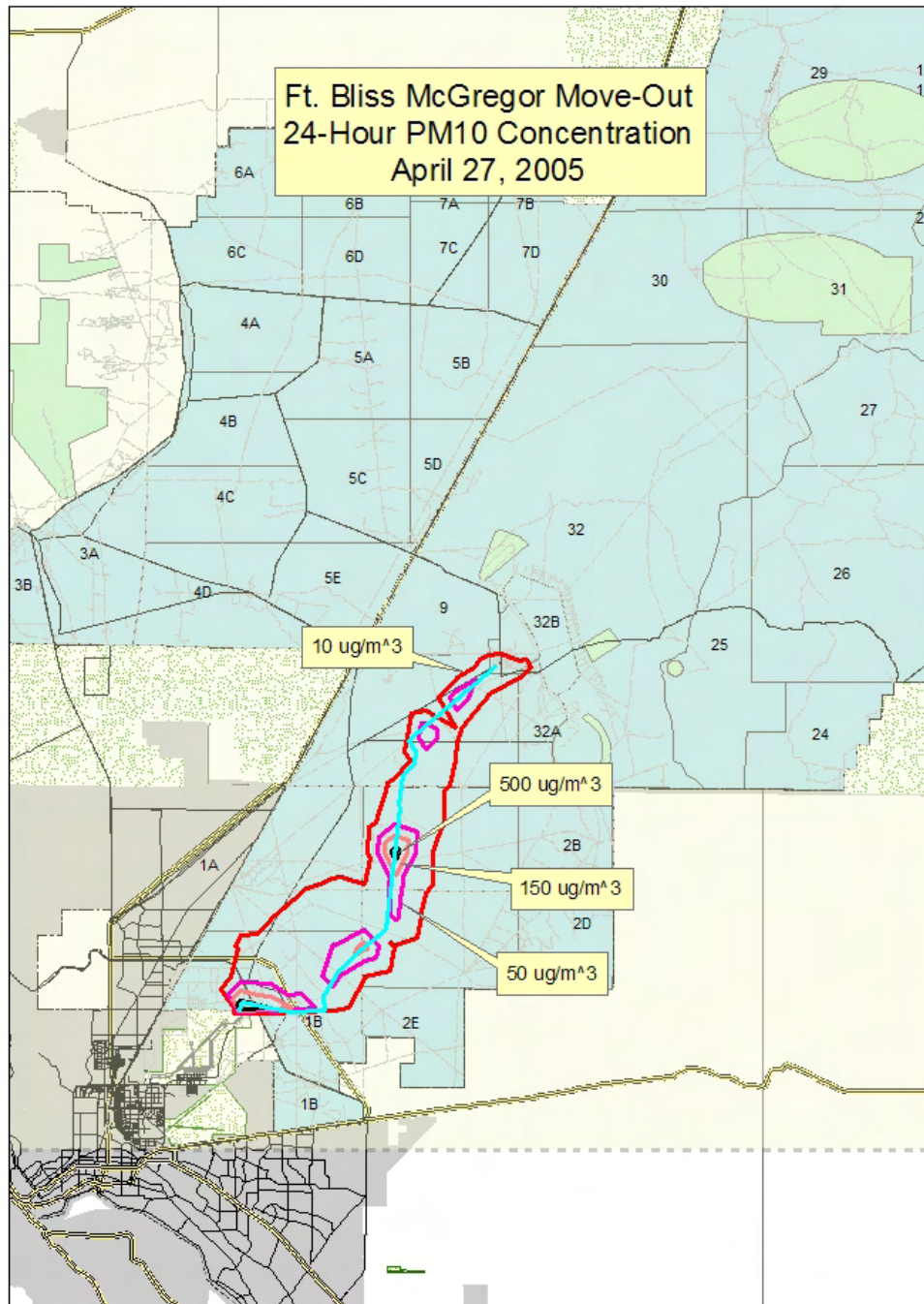


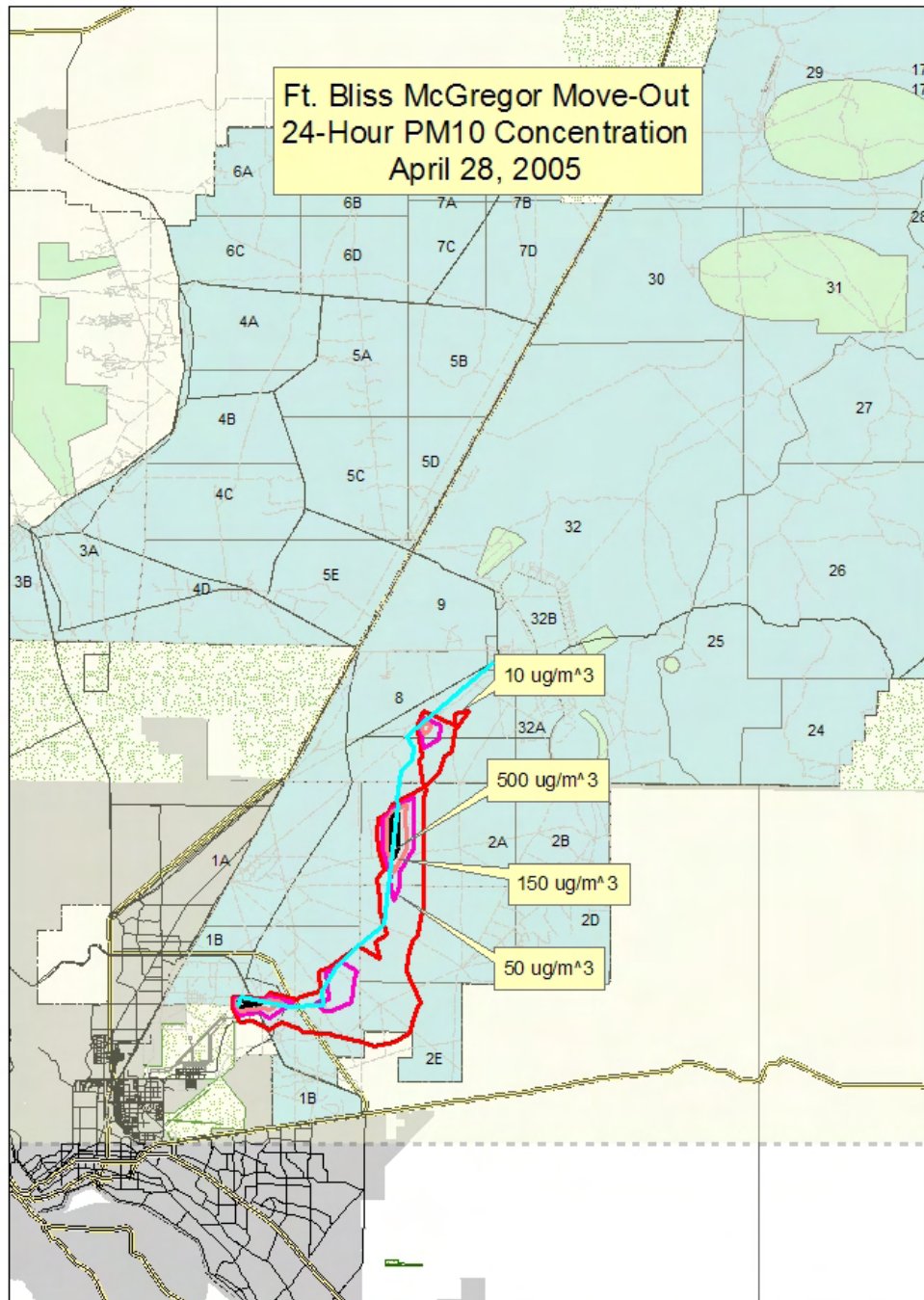


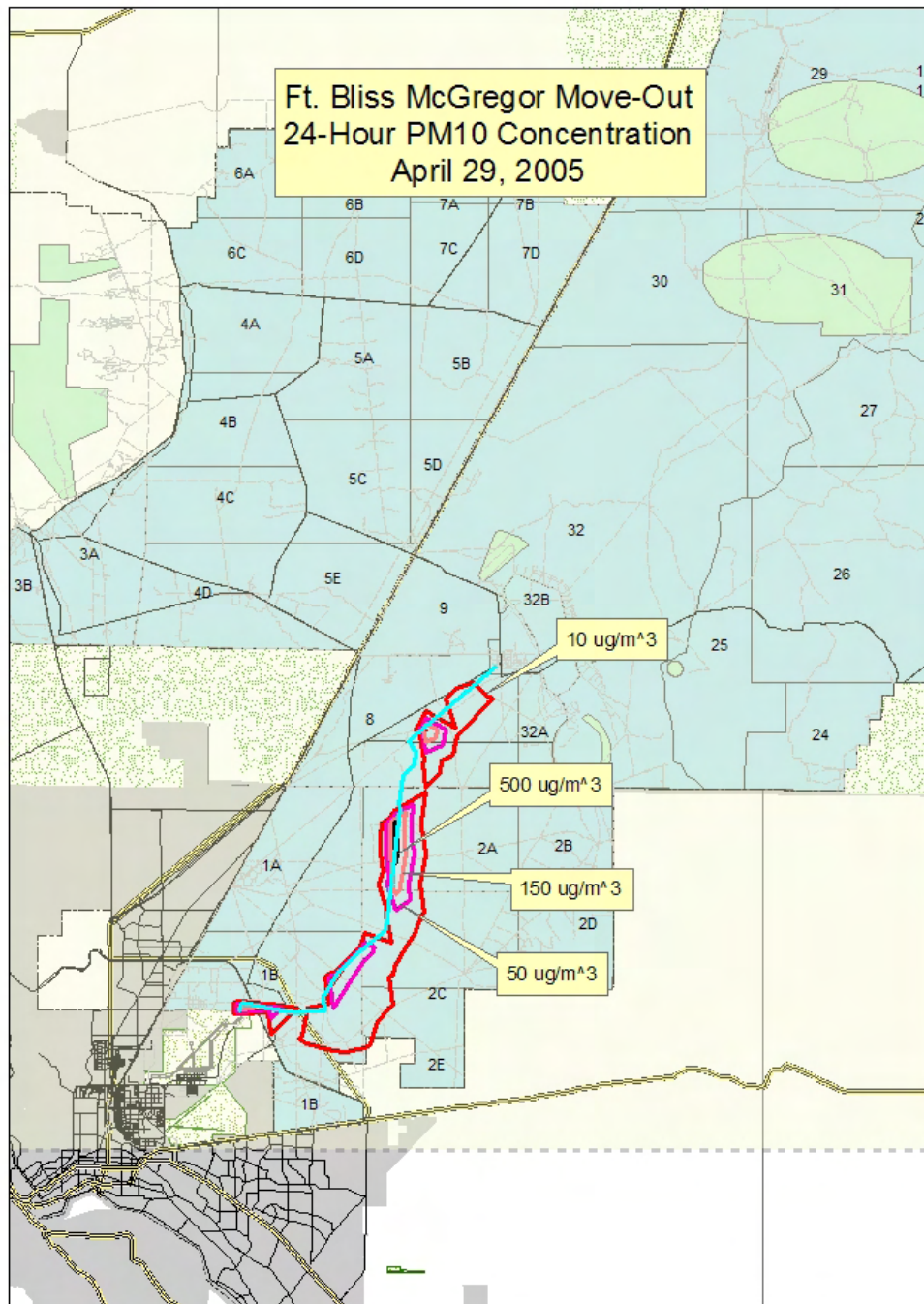


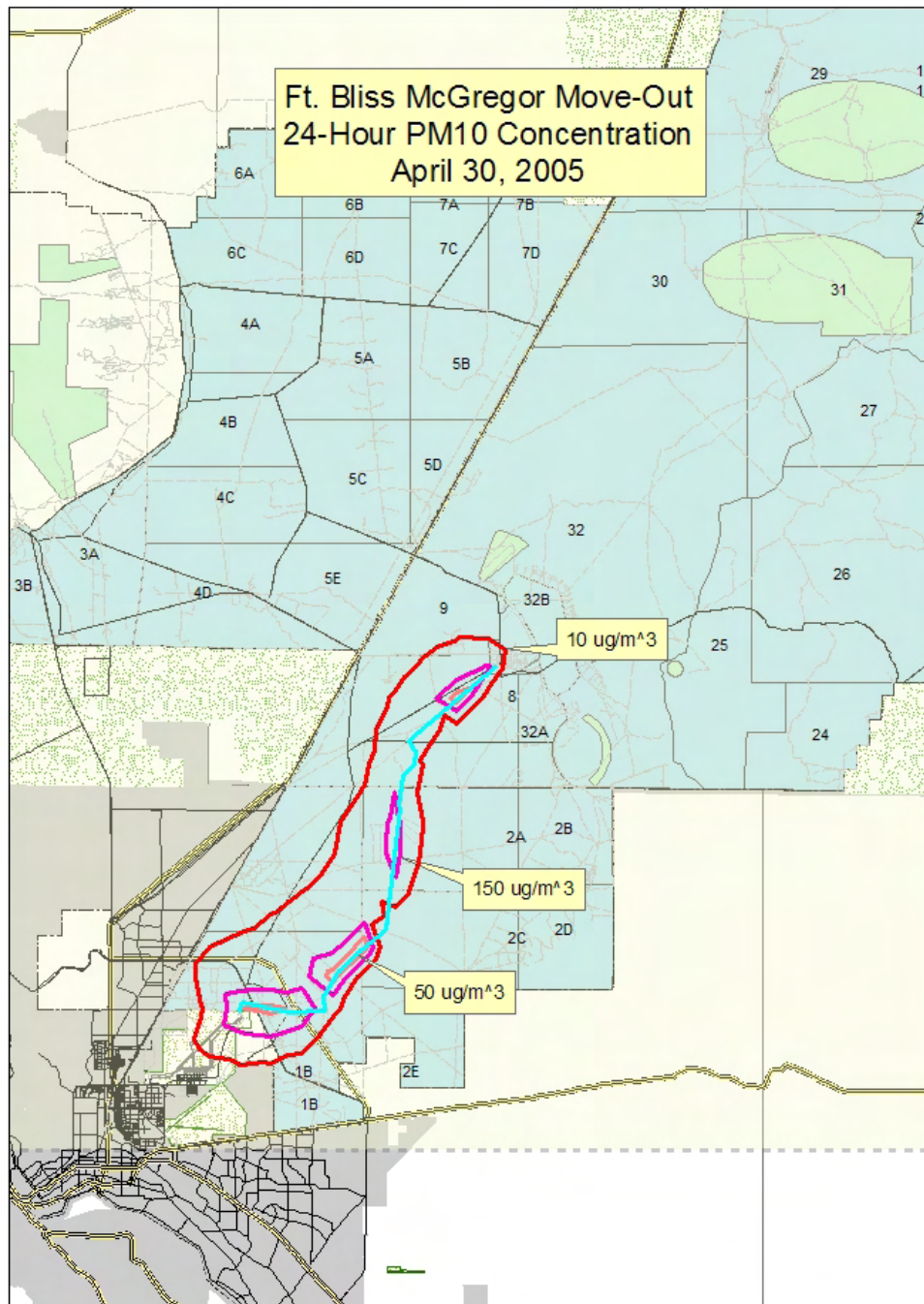


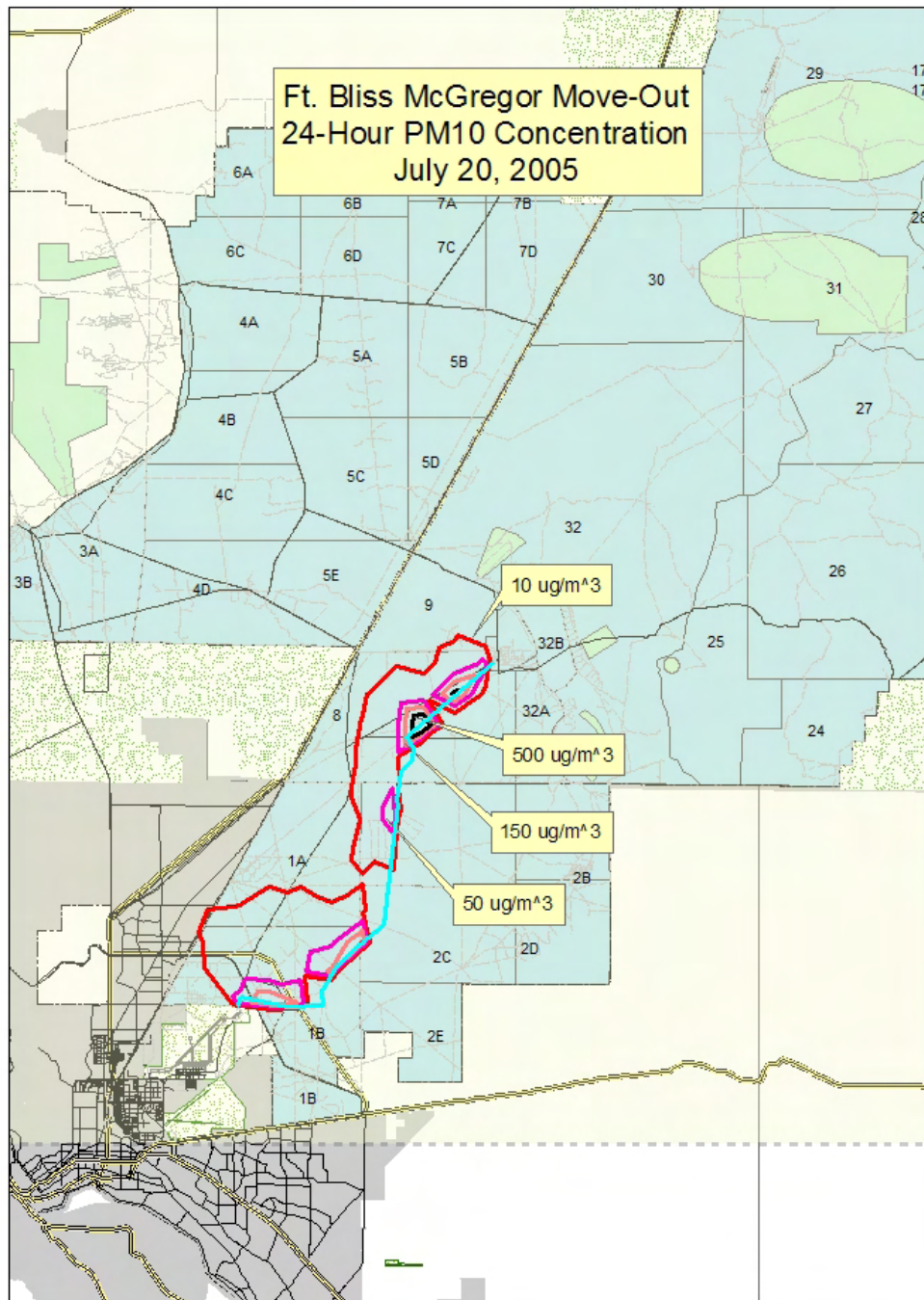


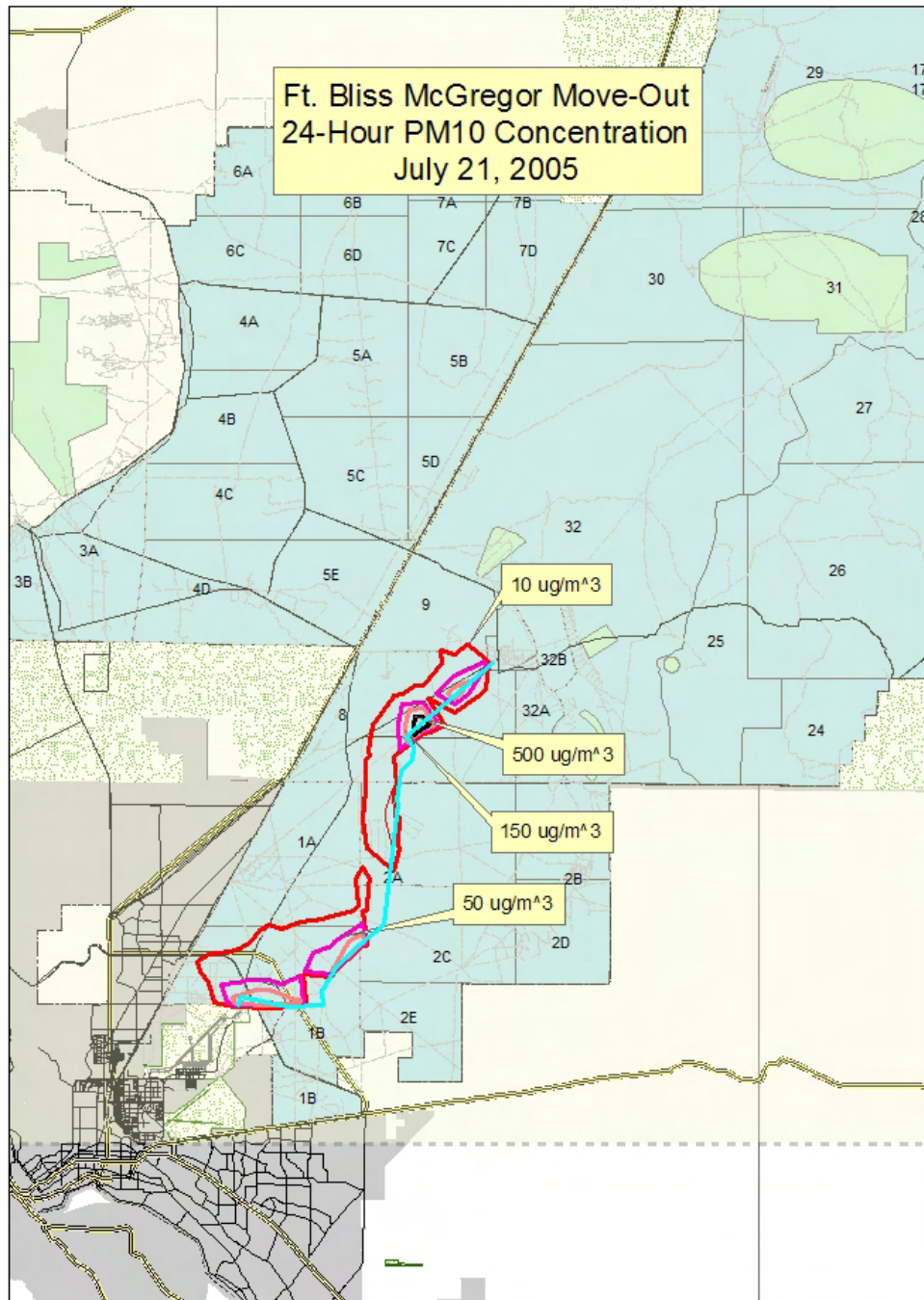


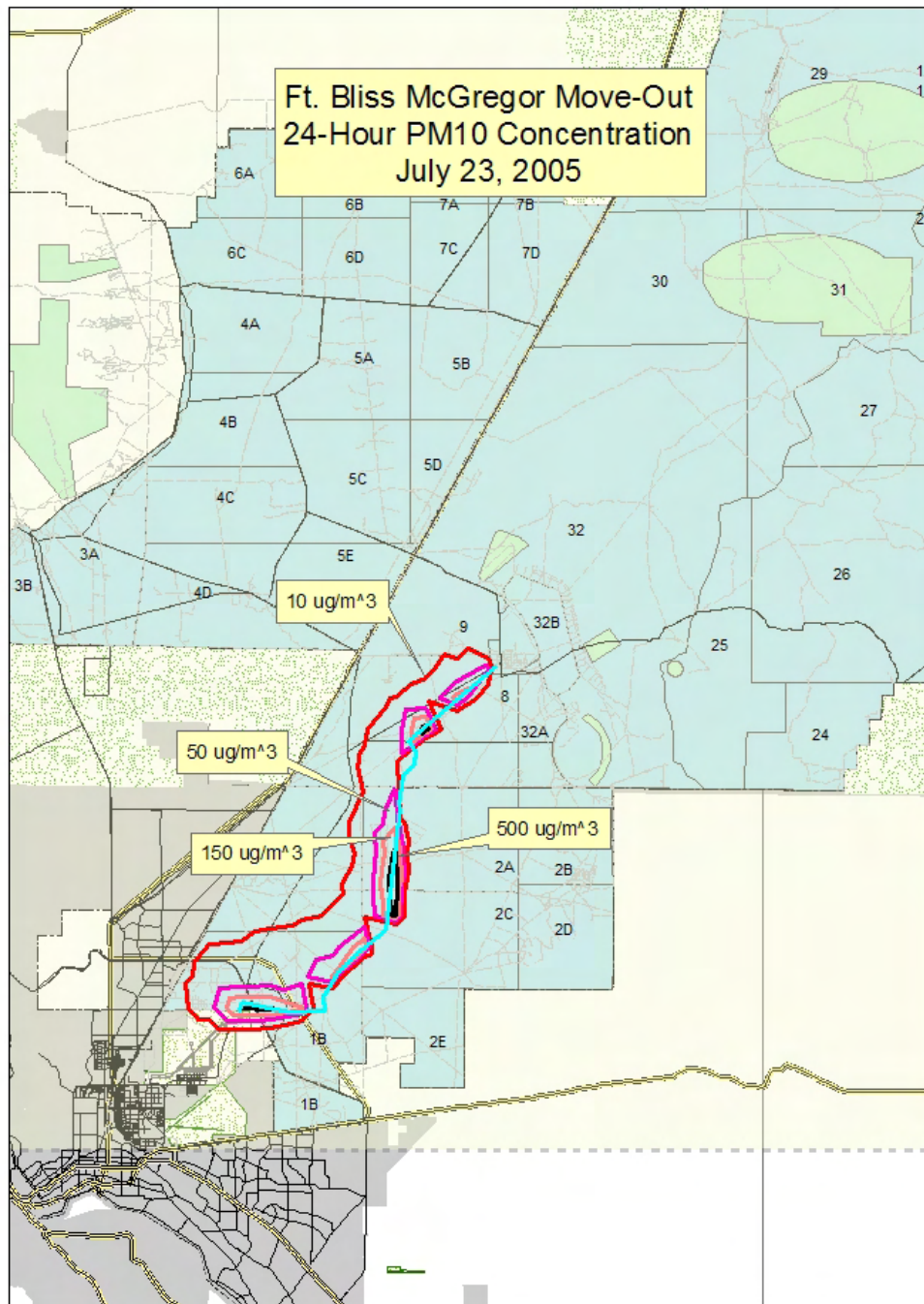


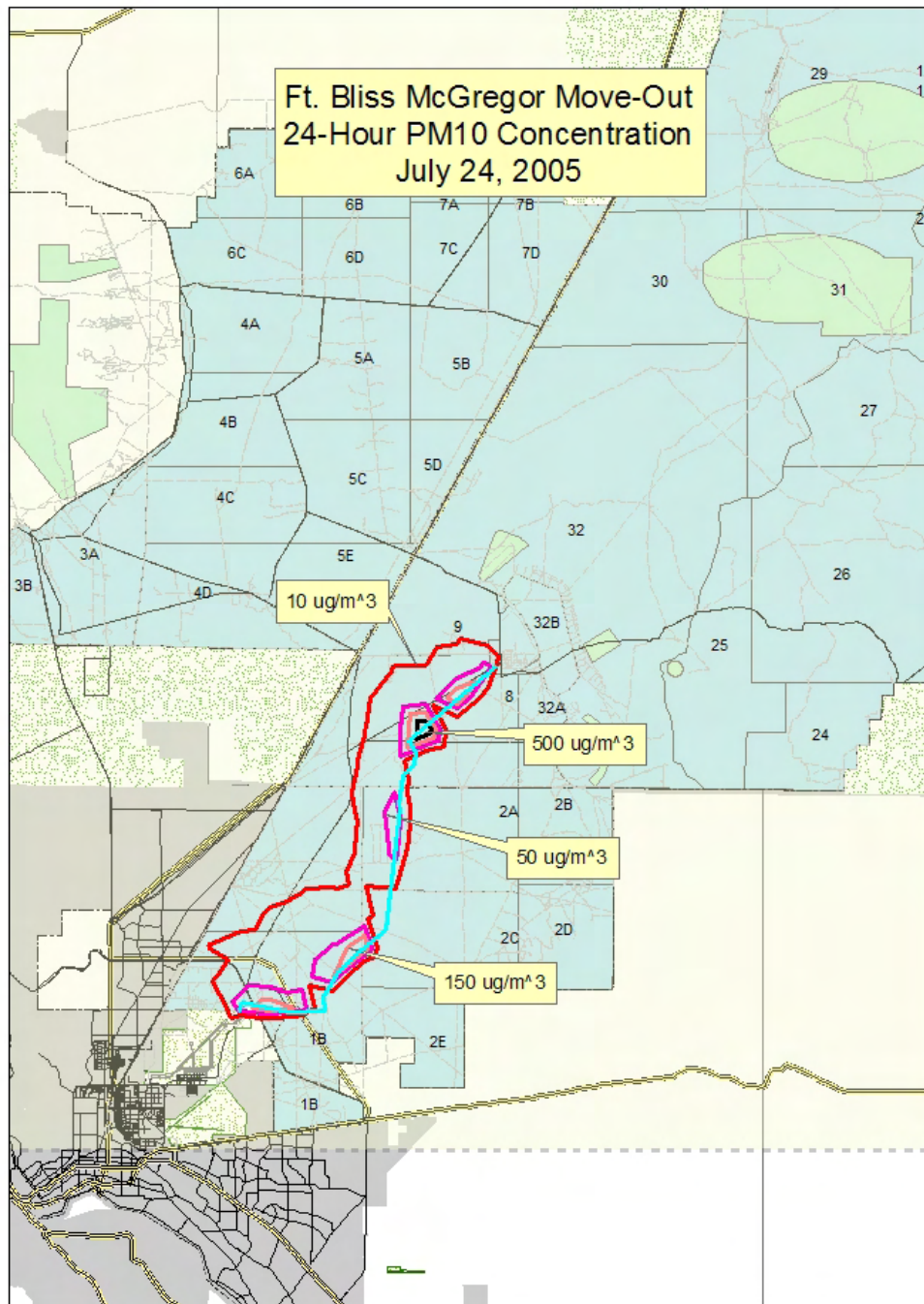


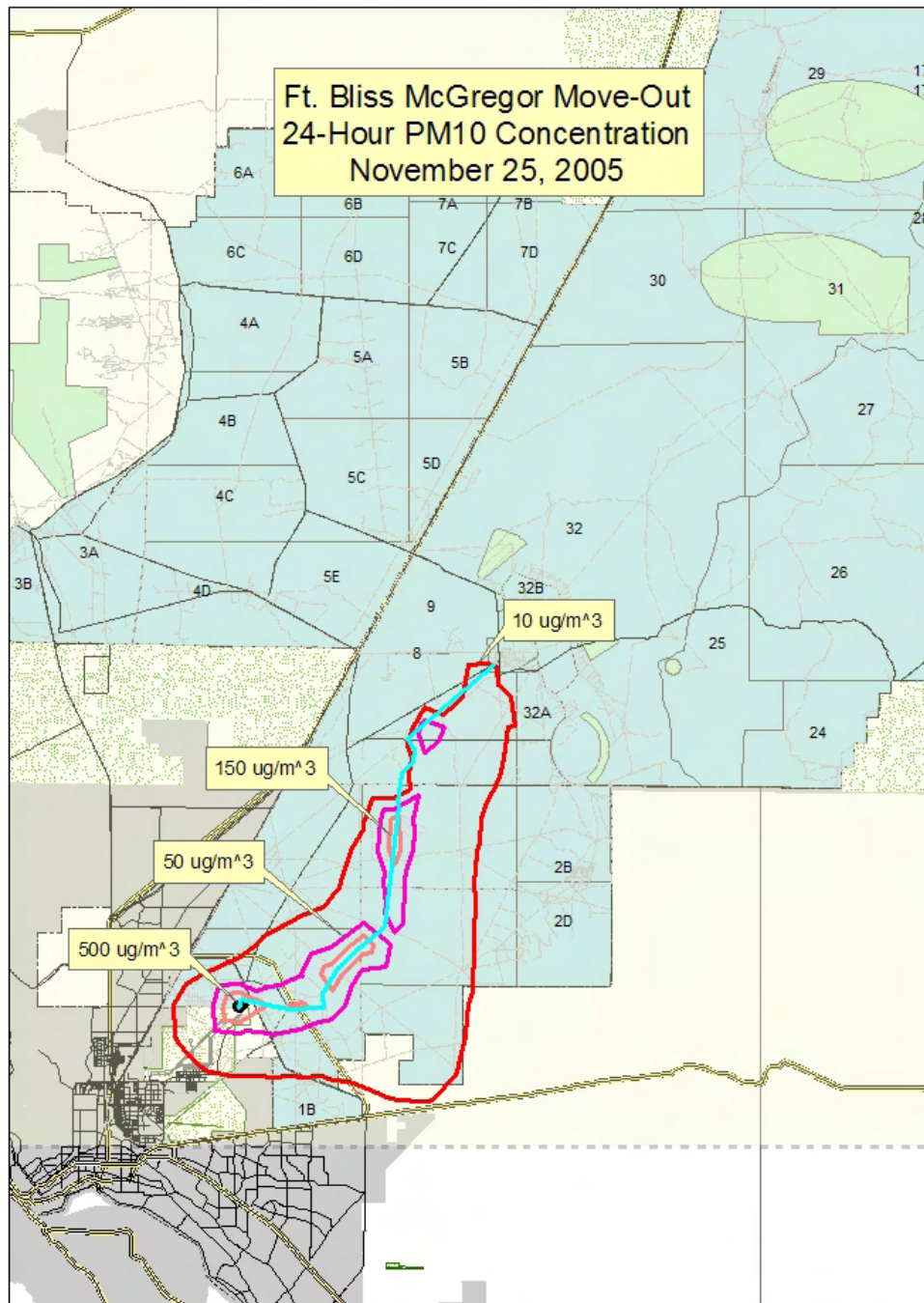


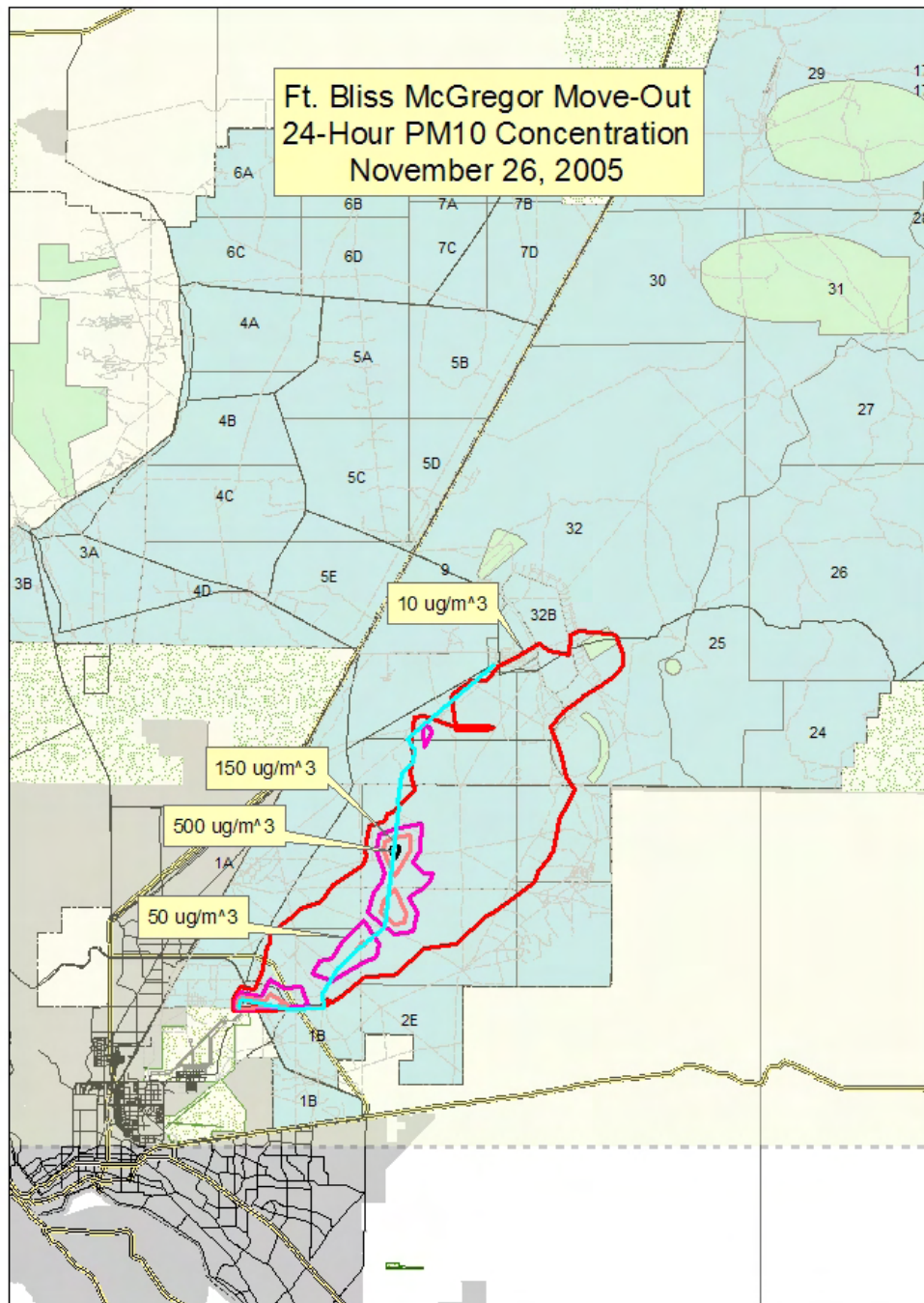


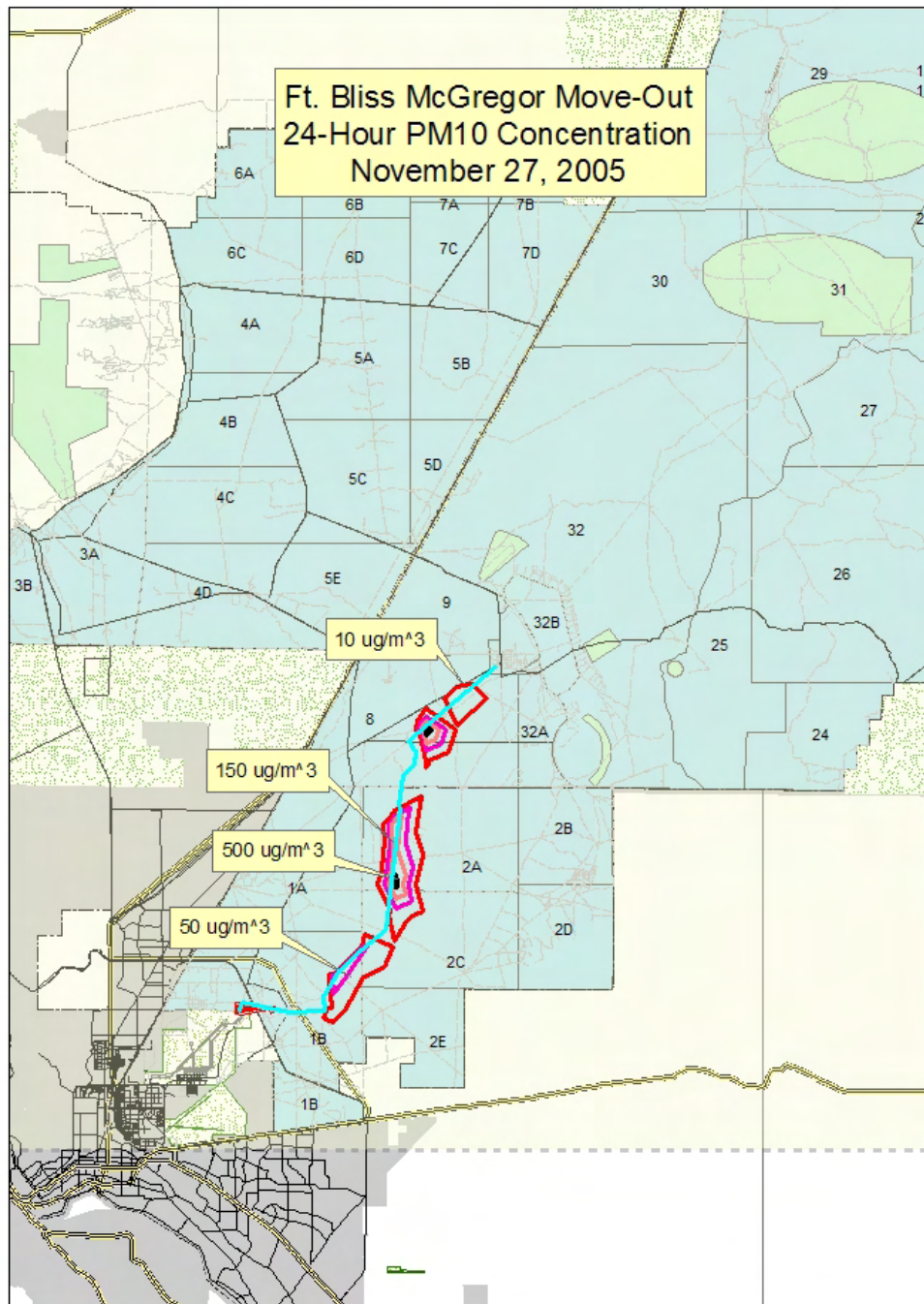


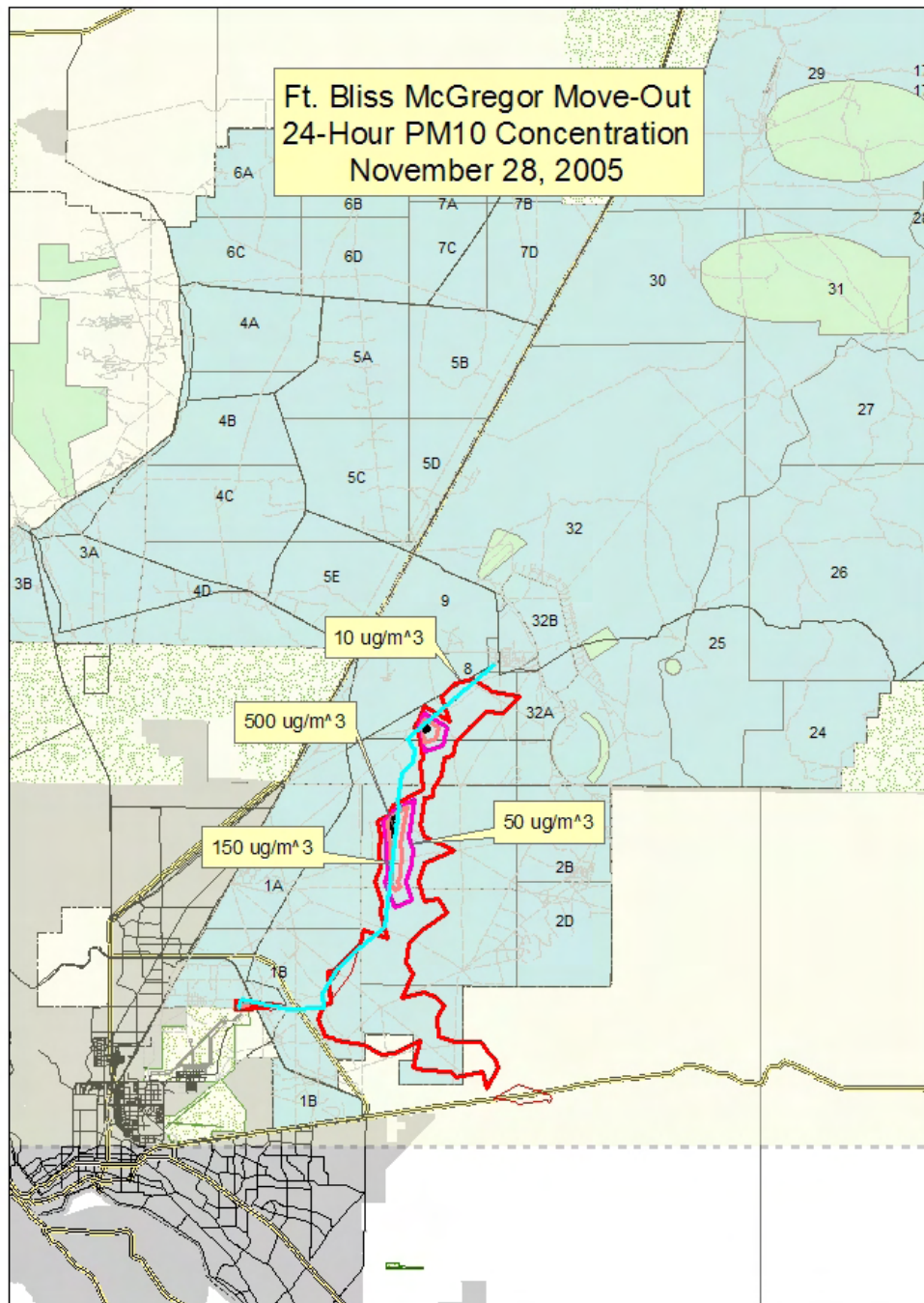


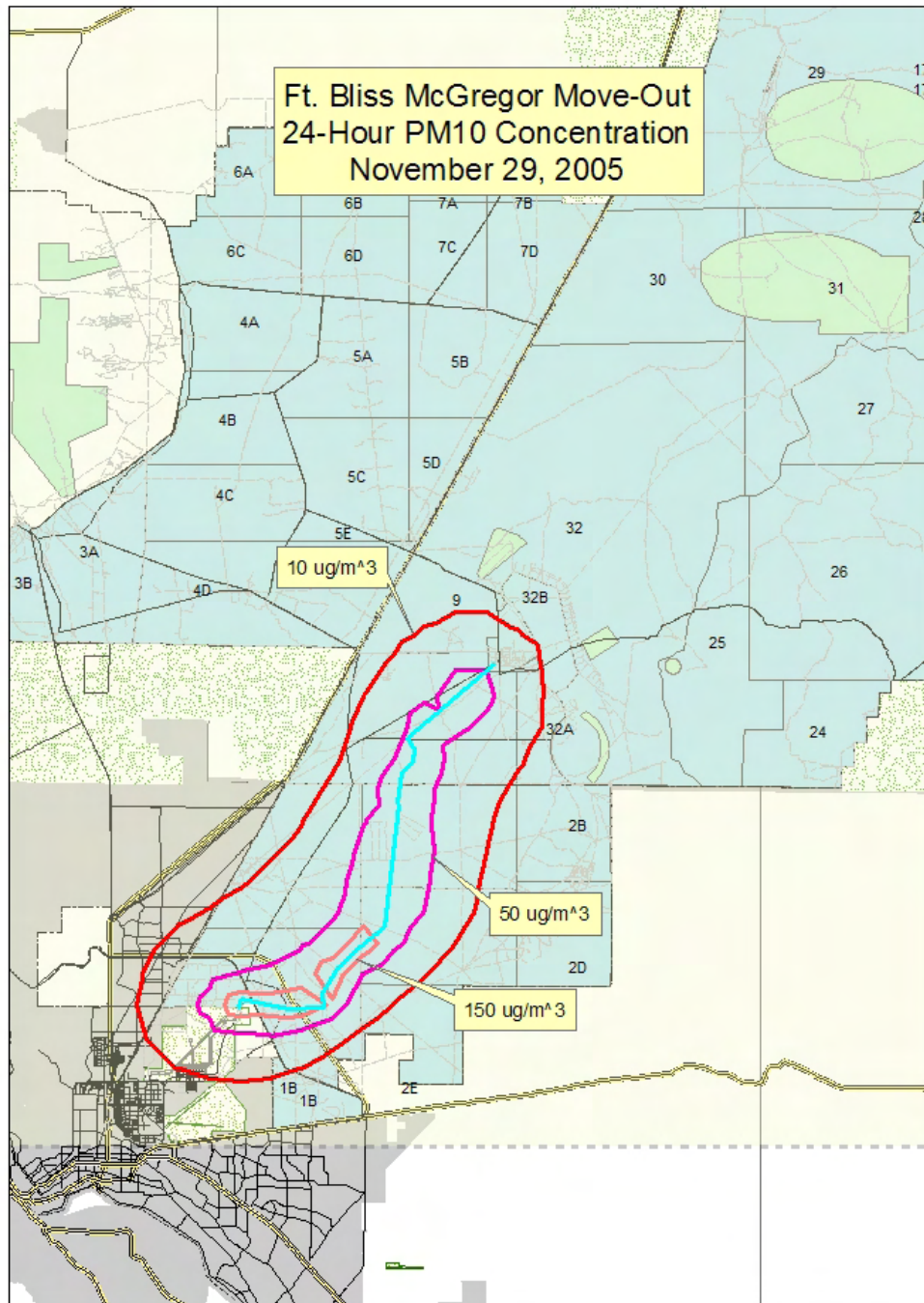












Appendix E

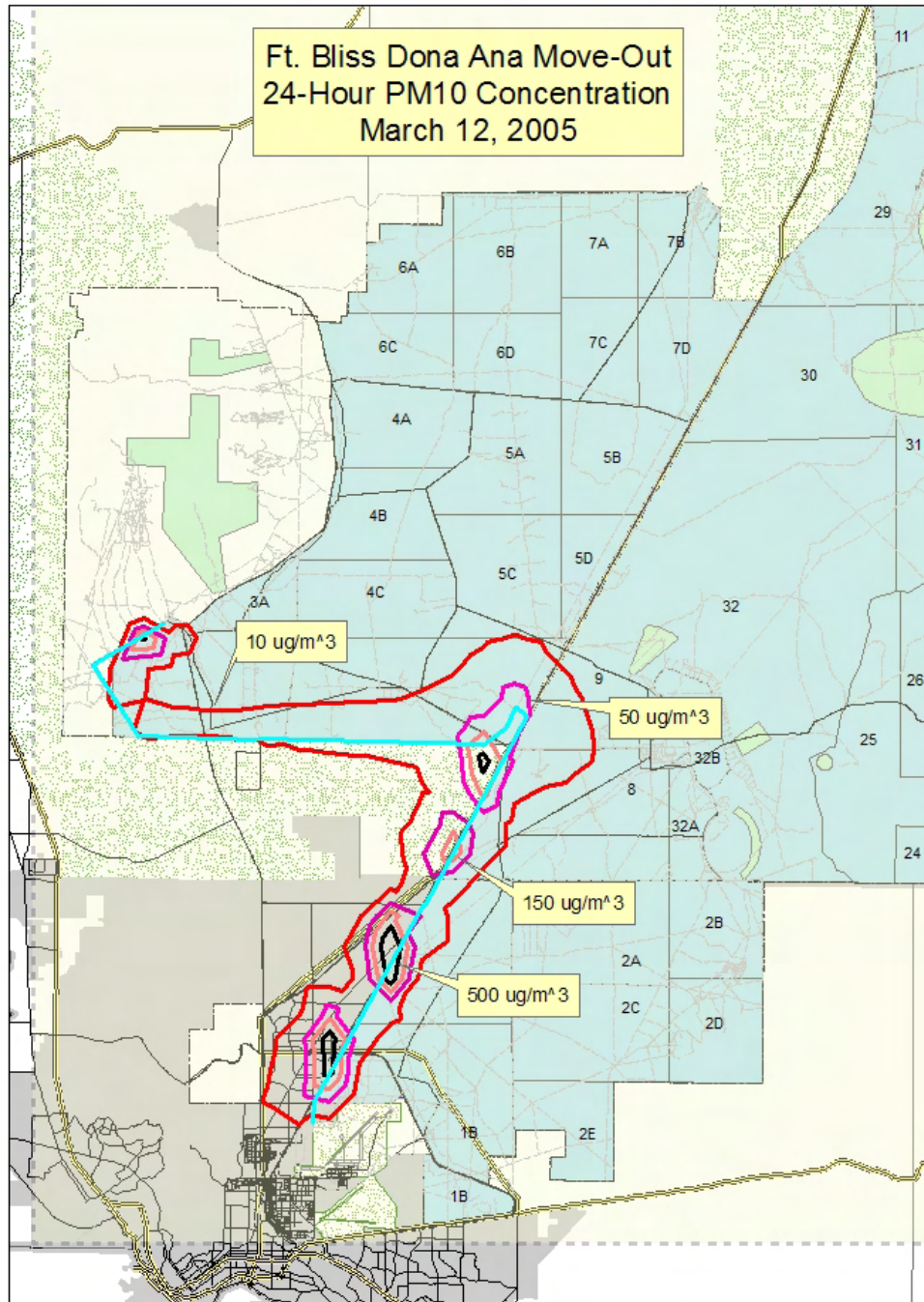
Simulated 24-h-Average PM₁₀ Concentrations for the Dona Ana Move-Out

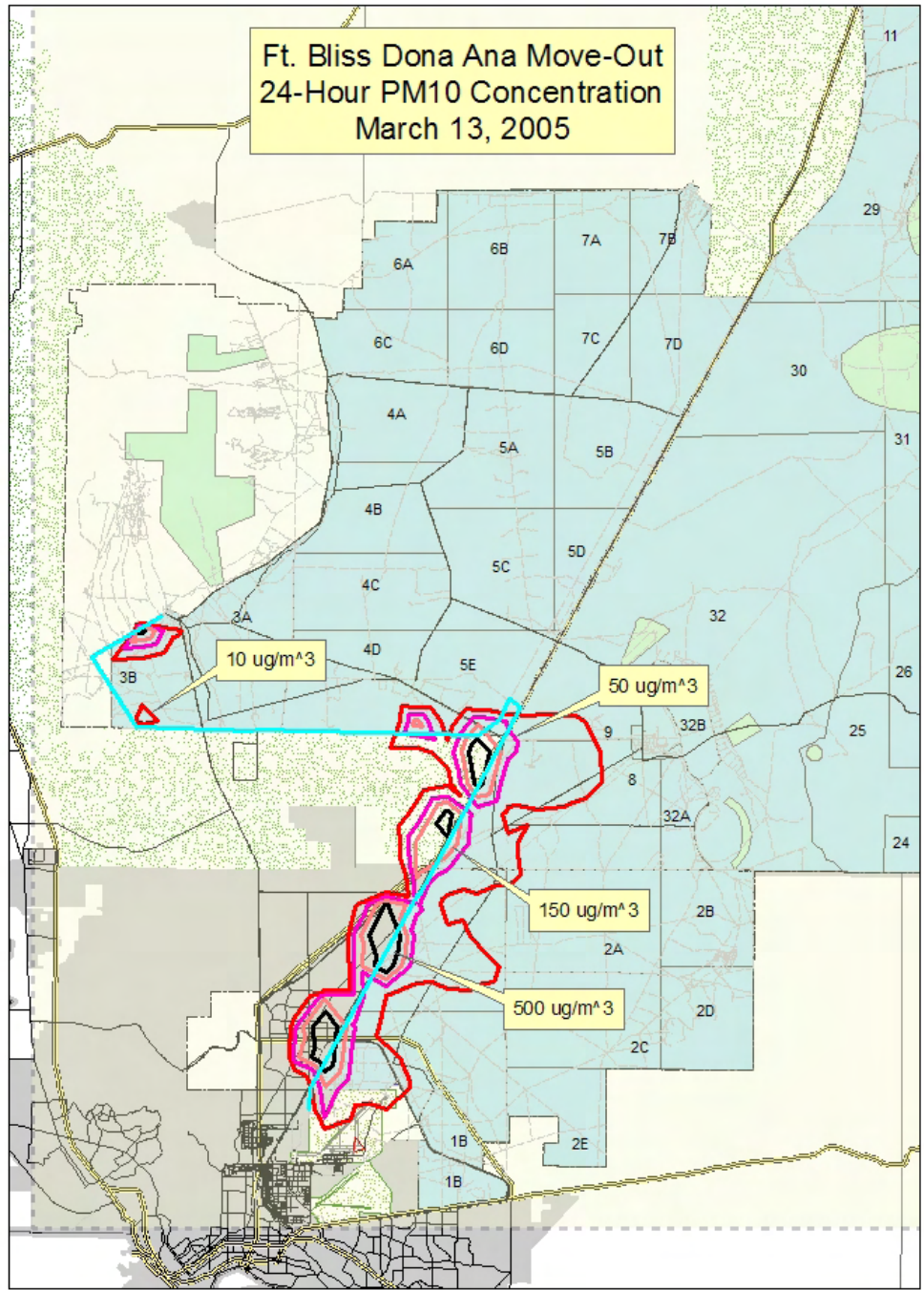
Appendix E: Simulated 24-h-Average PM₁₀ Concentrations for the Dona Ana Move-Out

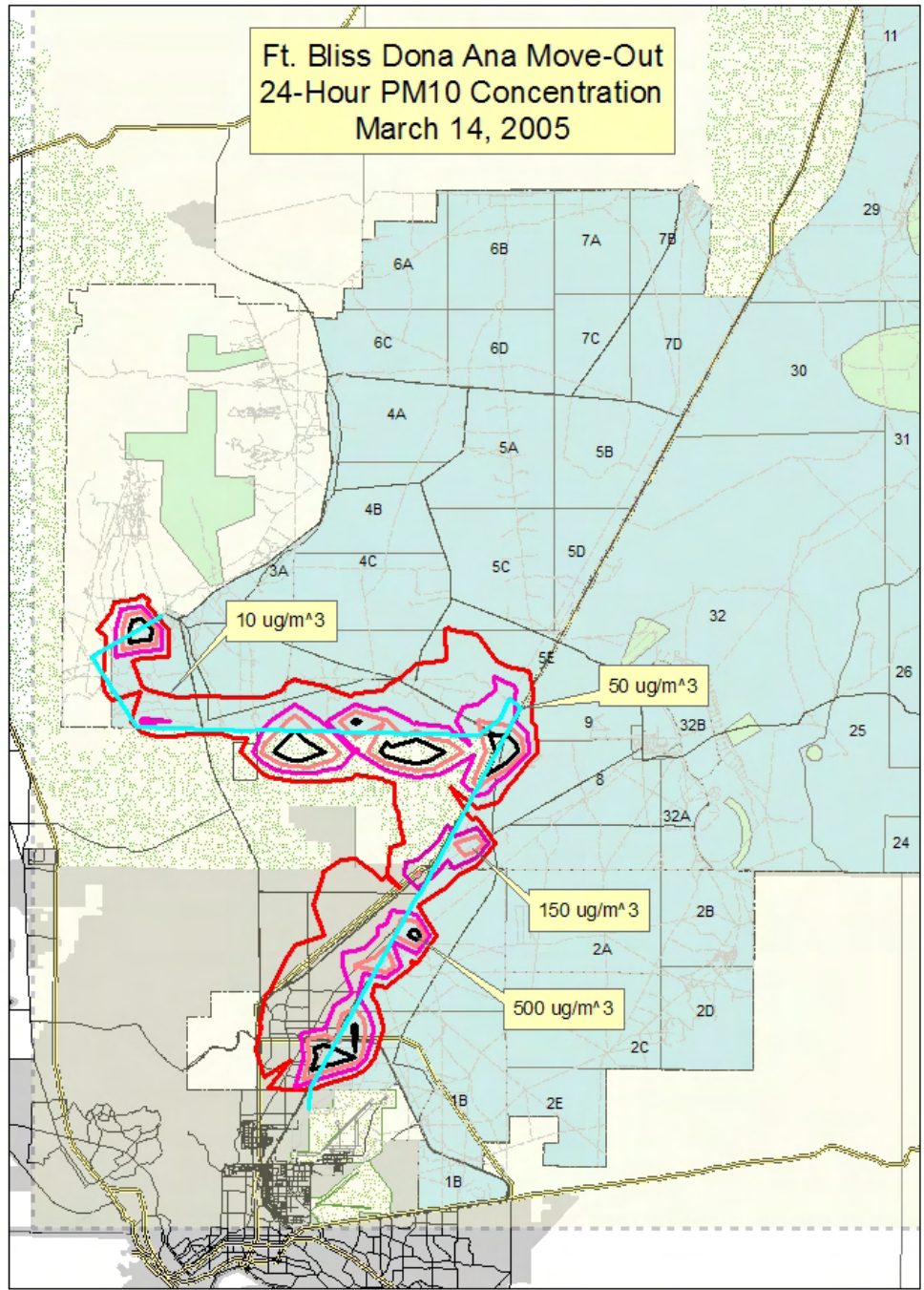
Contour maps of 24-hour-average PM₁₀ concentrations contributed from Dona Ana move-out operations to air quality in and around Fort Bliss are given for the 21 simulated days (March 12–16, April 25–30, July 20–24, and November 25–29, 2005). Dona Ana move-out scenario assumptions for DUSTAN simulations are summarized below.

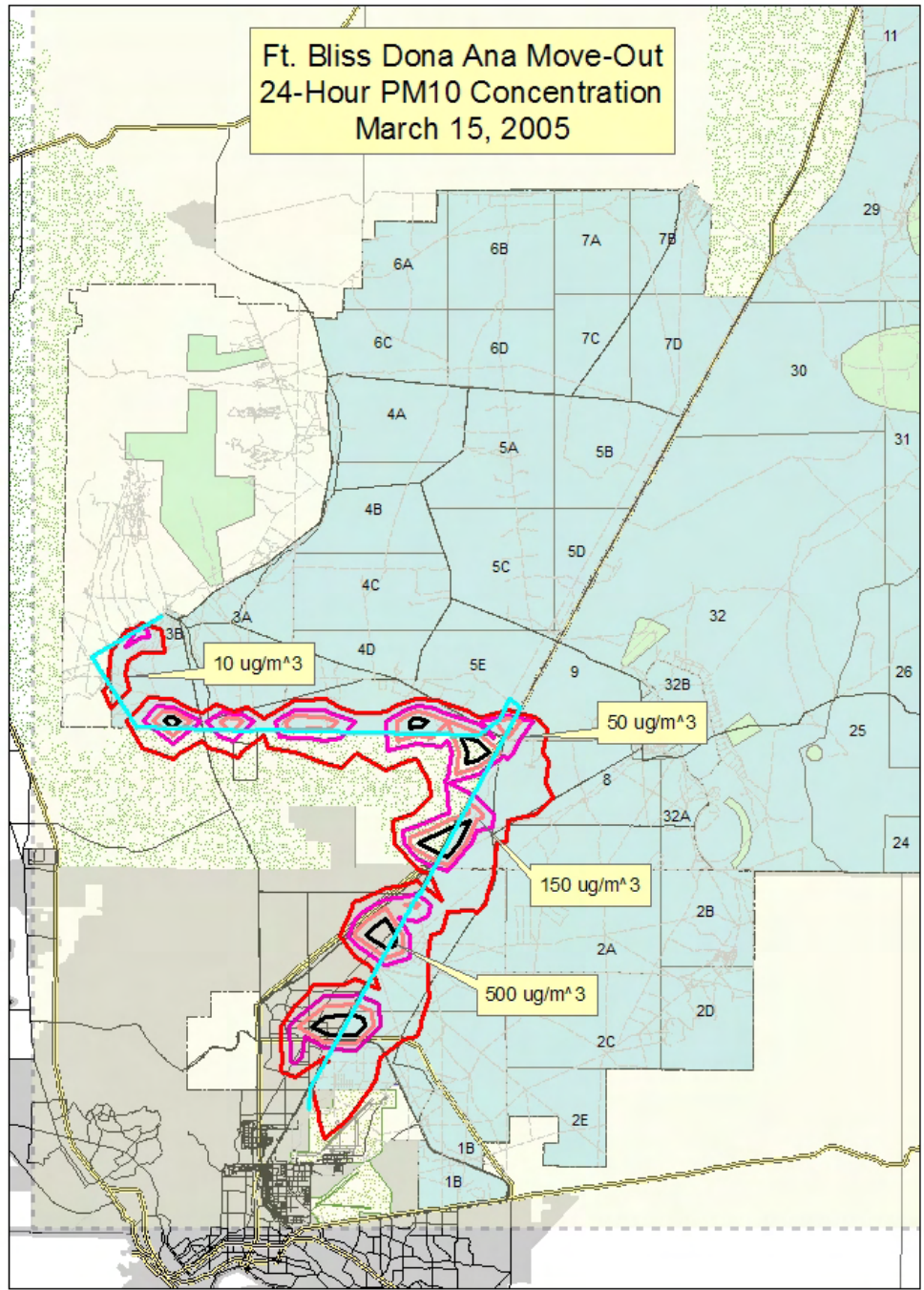
Move-Out Dona Ana Range Camp

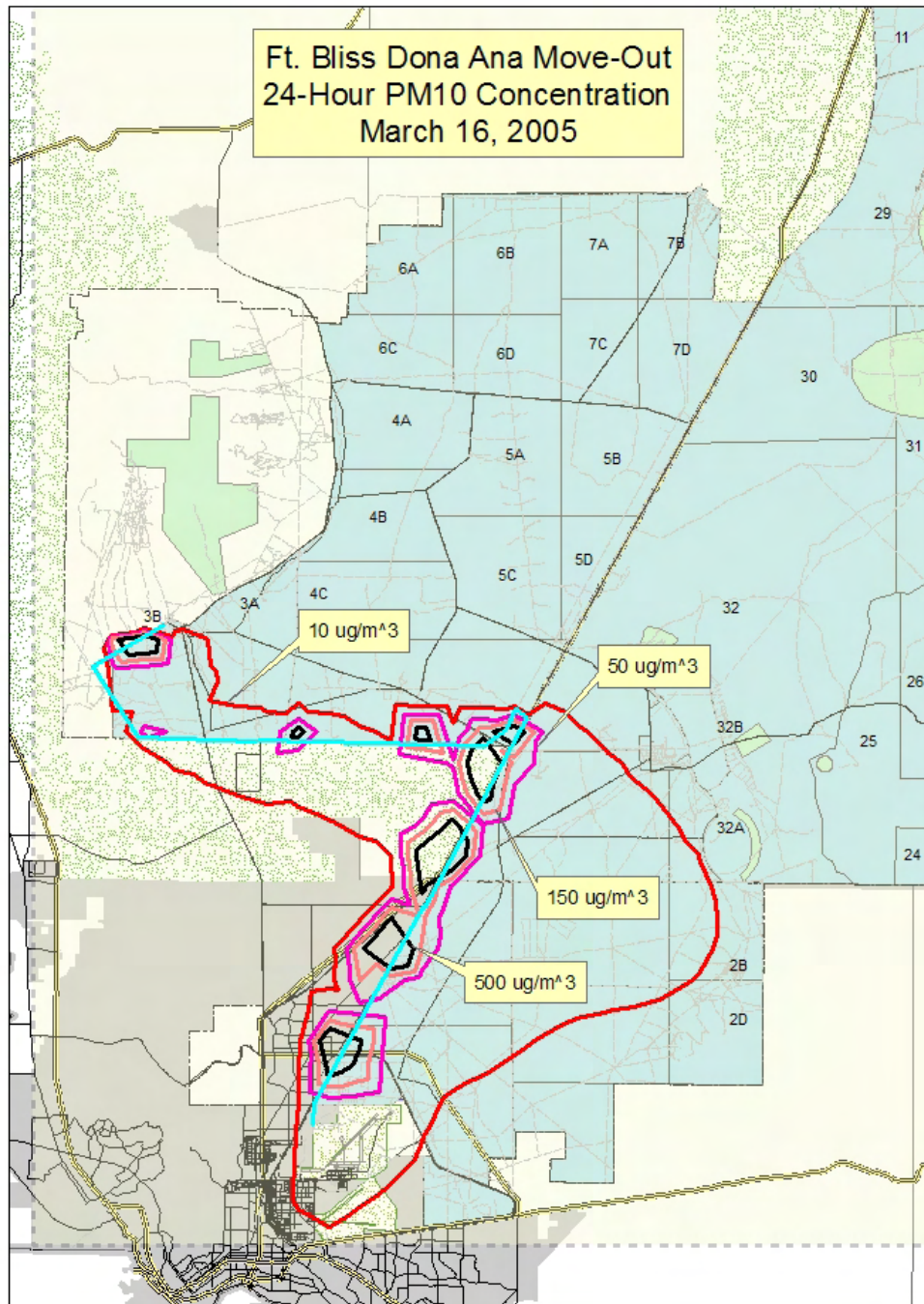
- All vehicles associated with the HBCT travel.
- Move-out route is divided into four segments: “a,” “b,” “c,” and “d” (see Figure 4.1).
- First vehicle leaves Biggs Army Airfield (start of segment “a”) at 0600 MST, reaching the start of segment “b” at 0700 MST, the start of segment “c” at 0800 MST, and the start of segment “d” at 0900 MST.
- Each segment of the move-out route has vehicles on it for a total of 9 hours.
- Mean speed for each type of vehicle is 16 kilometers per hour (9.9 miles per hour) along segment “a,” 17 kilometers per hour (10.6 miles per hour) along segments “b” and “c,” and 19 kilometers per hour (11.8 miles per hour) along segment “d.”
- Vehicle types are uniformly mixed throughout the convoy.

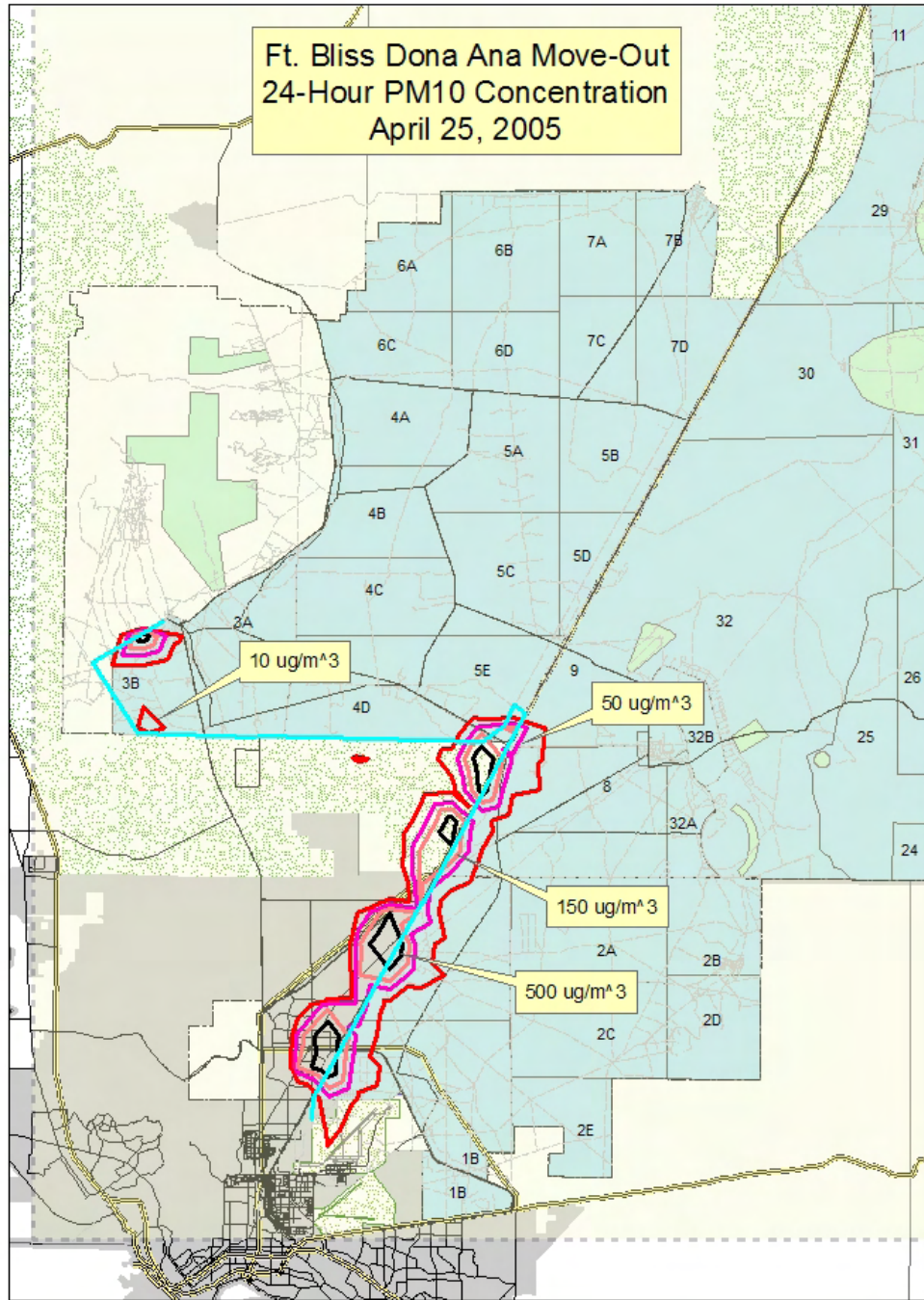


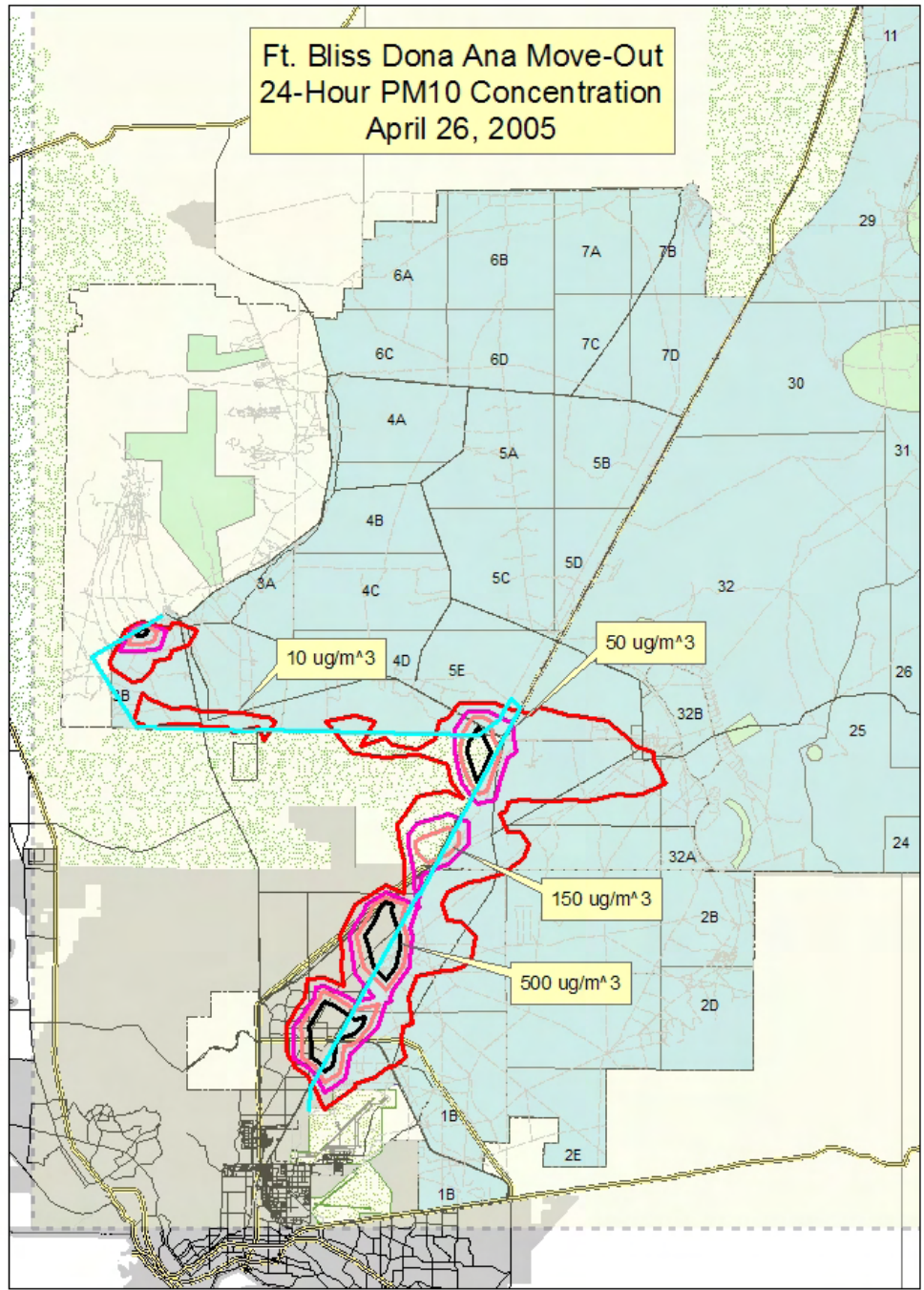


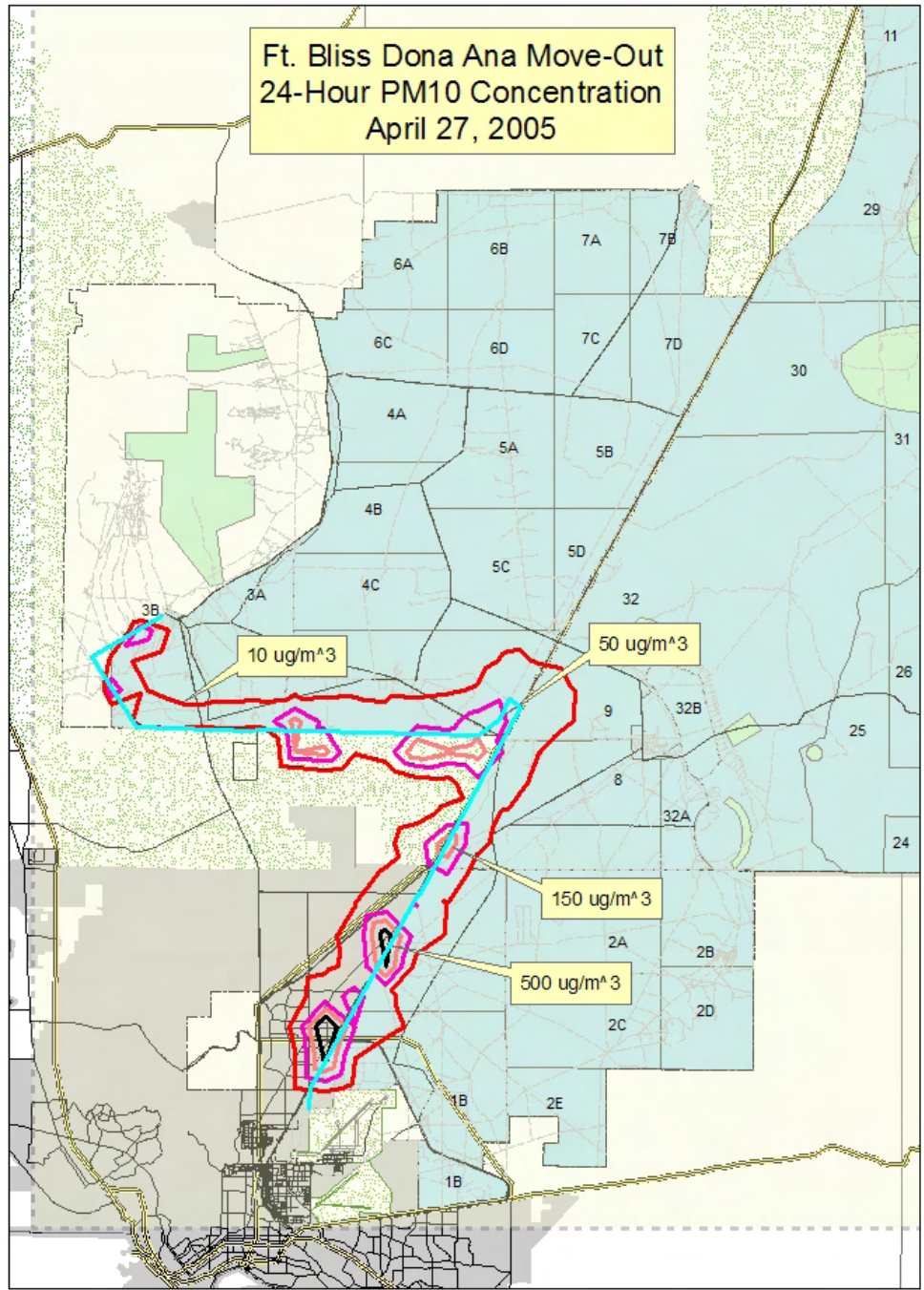


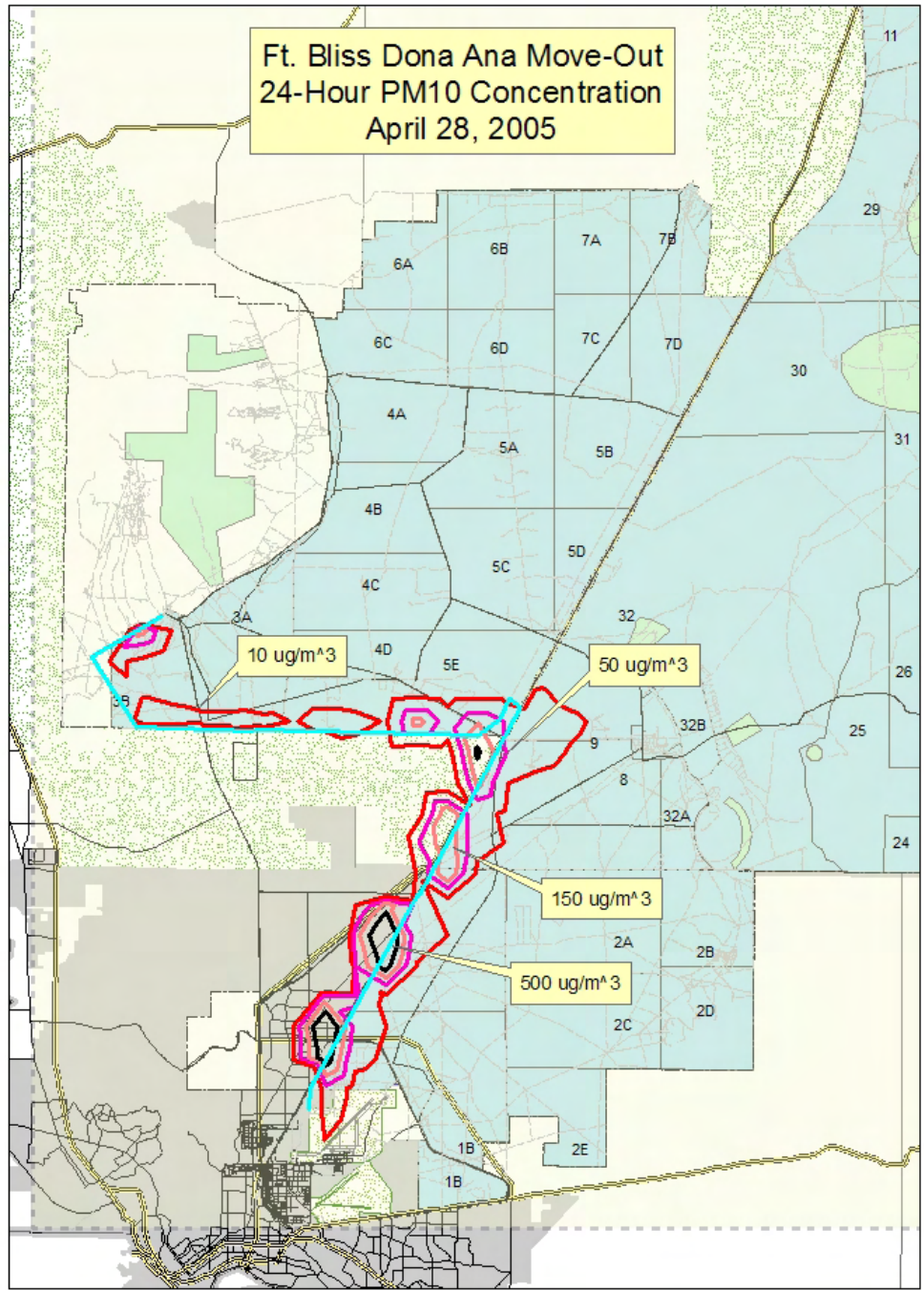


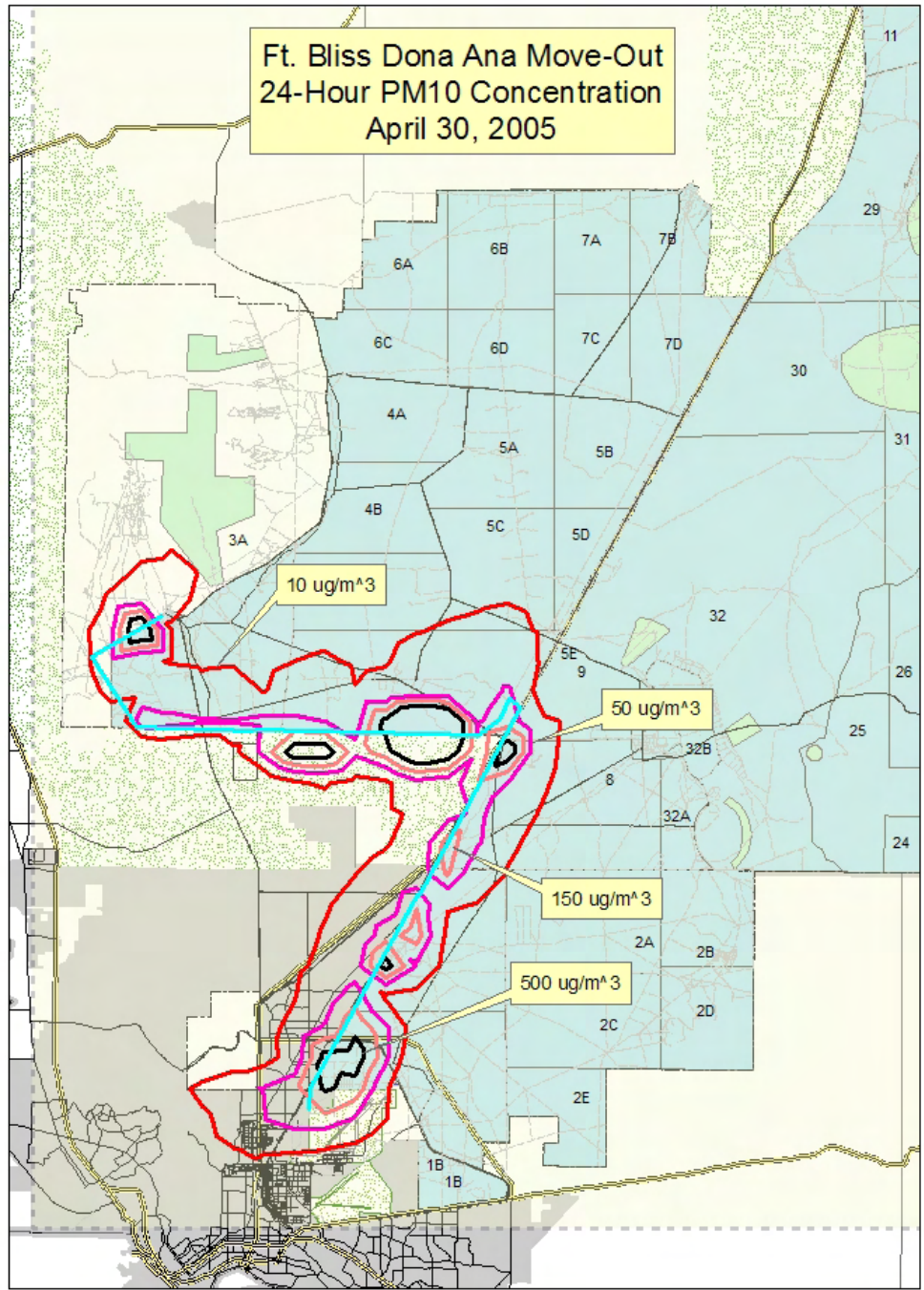


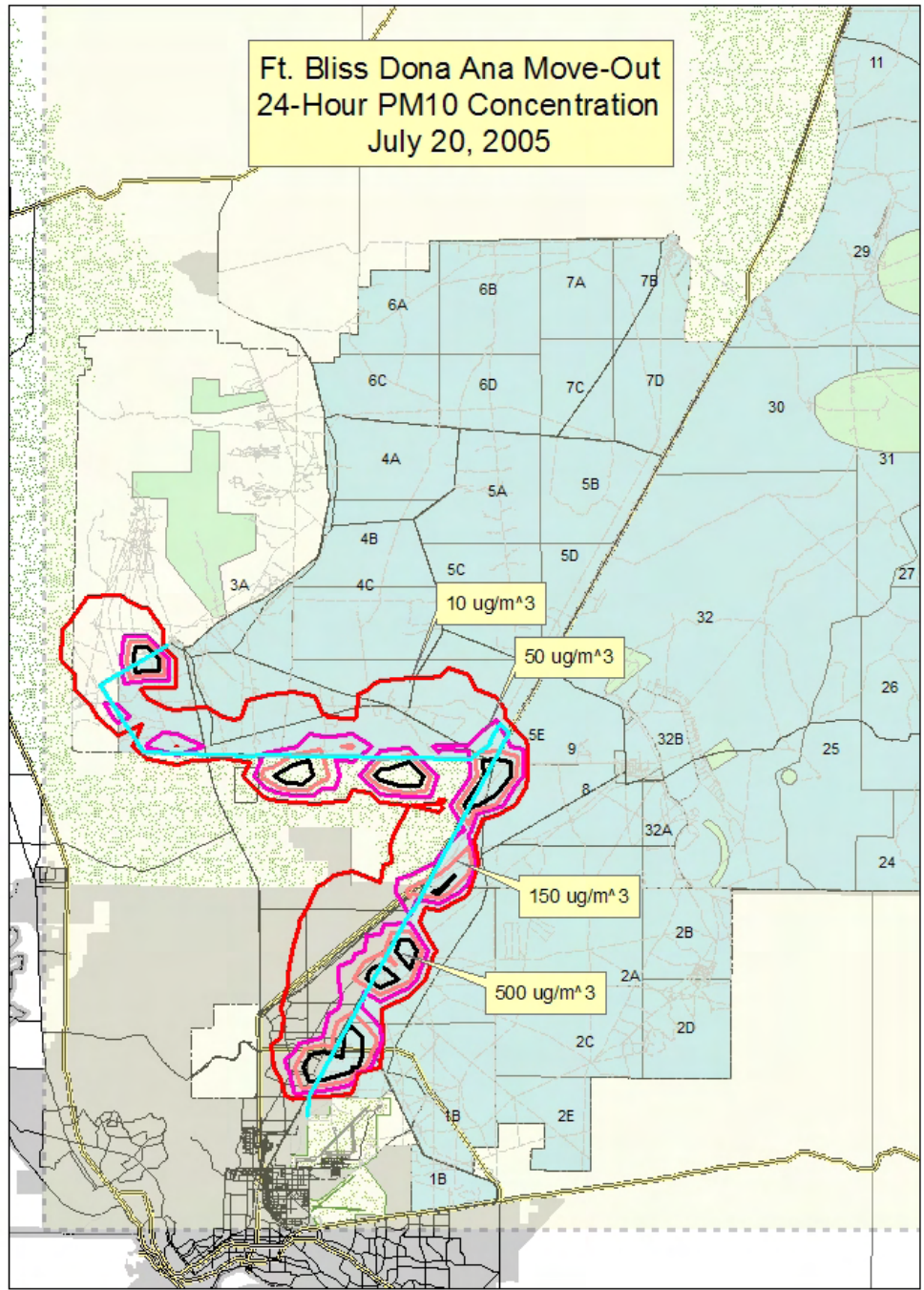


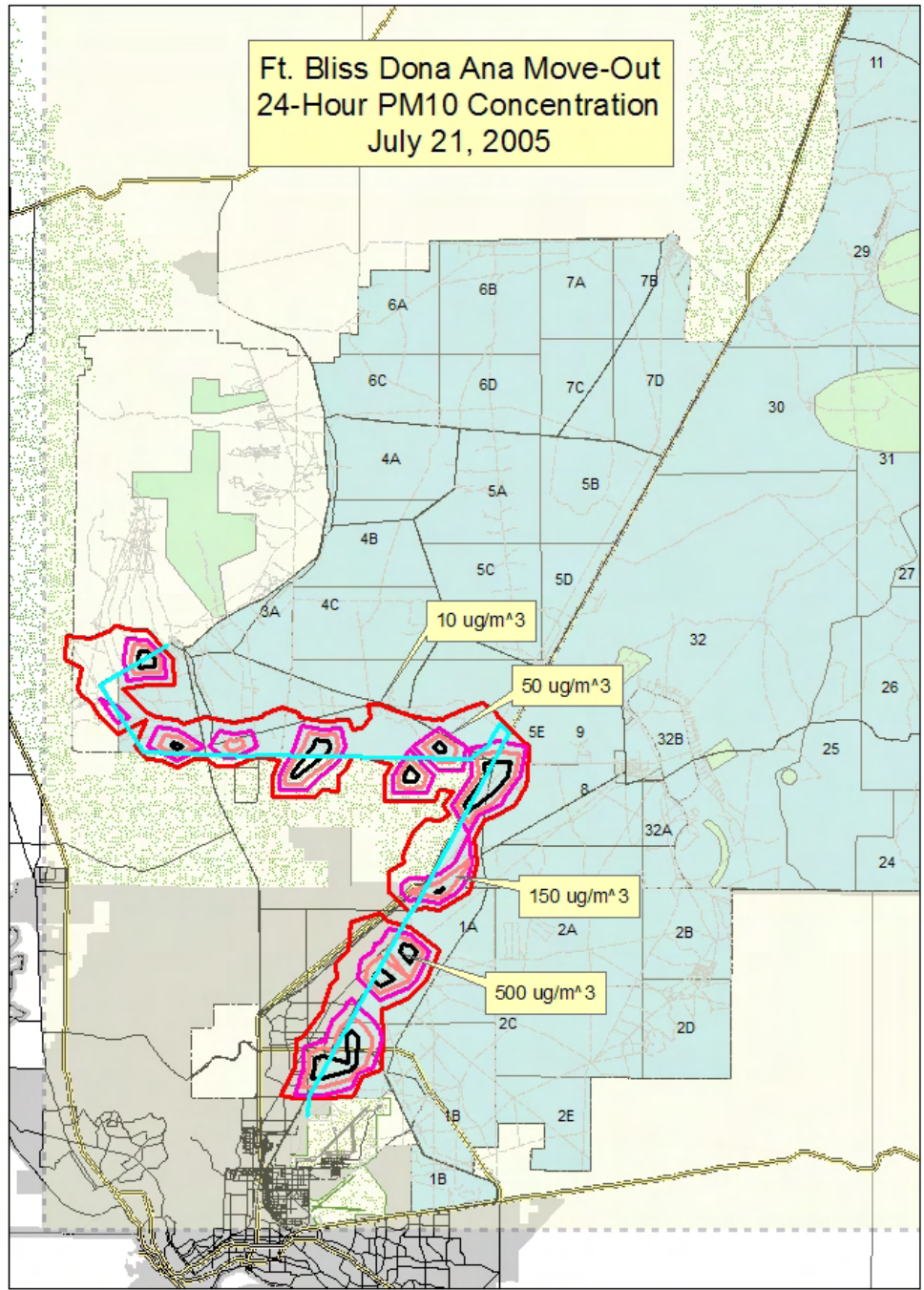


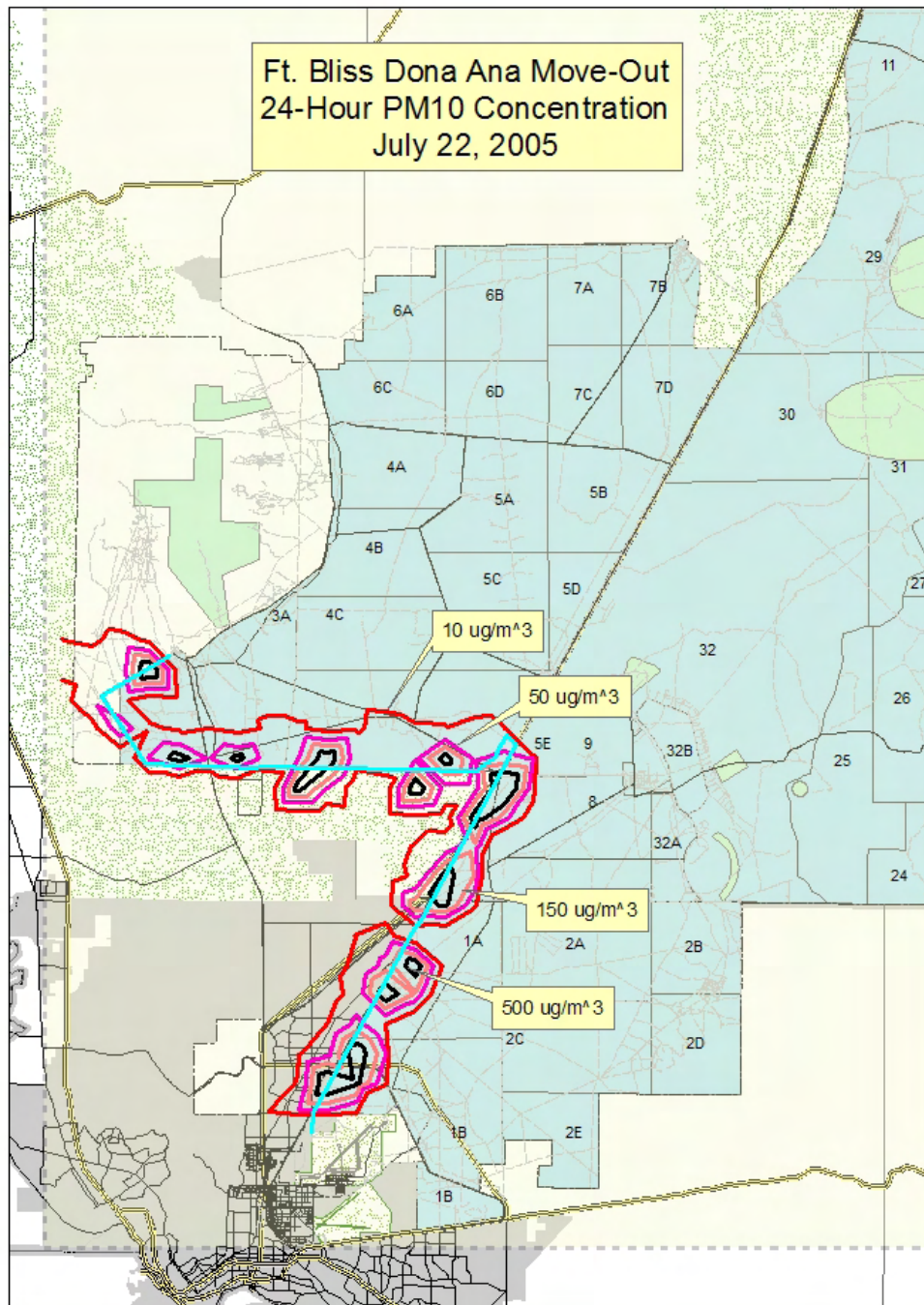


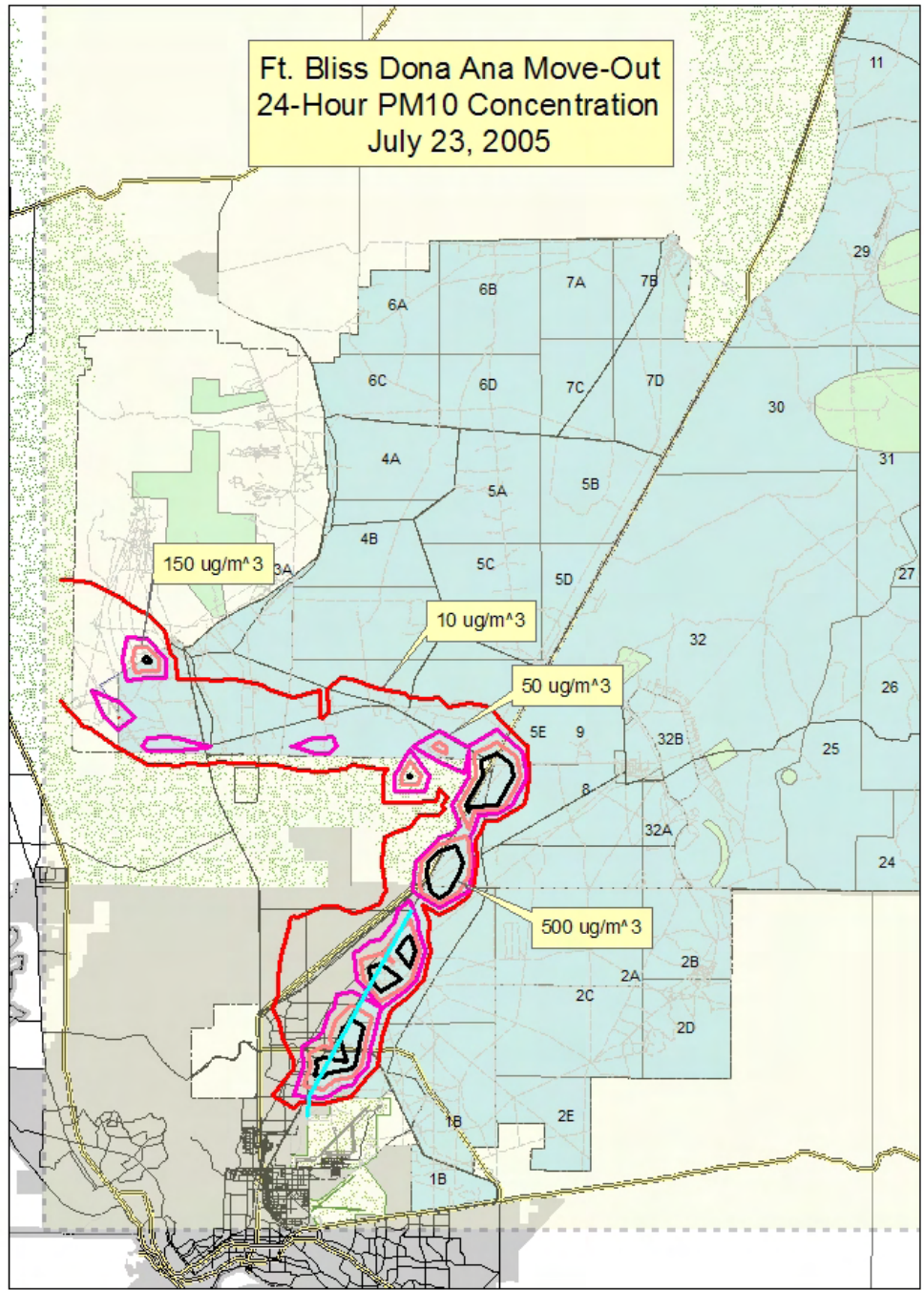


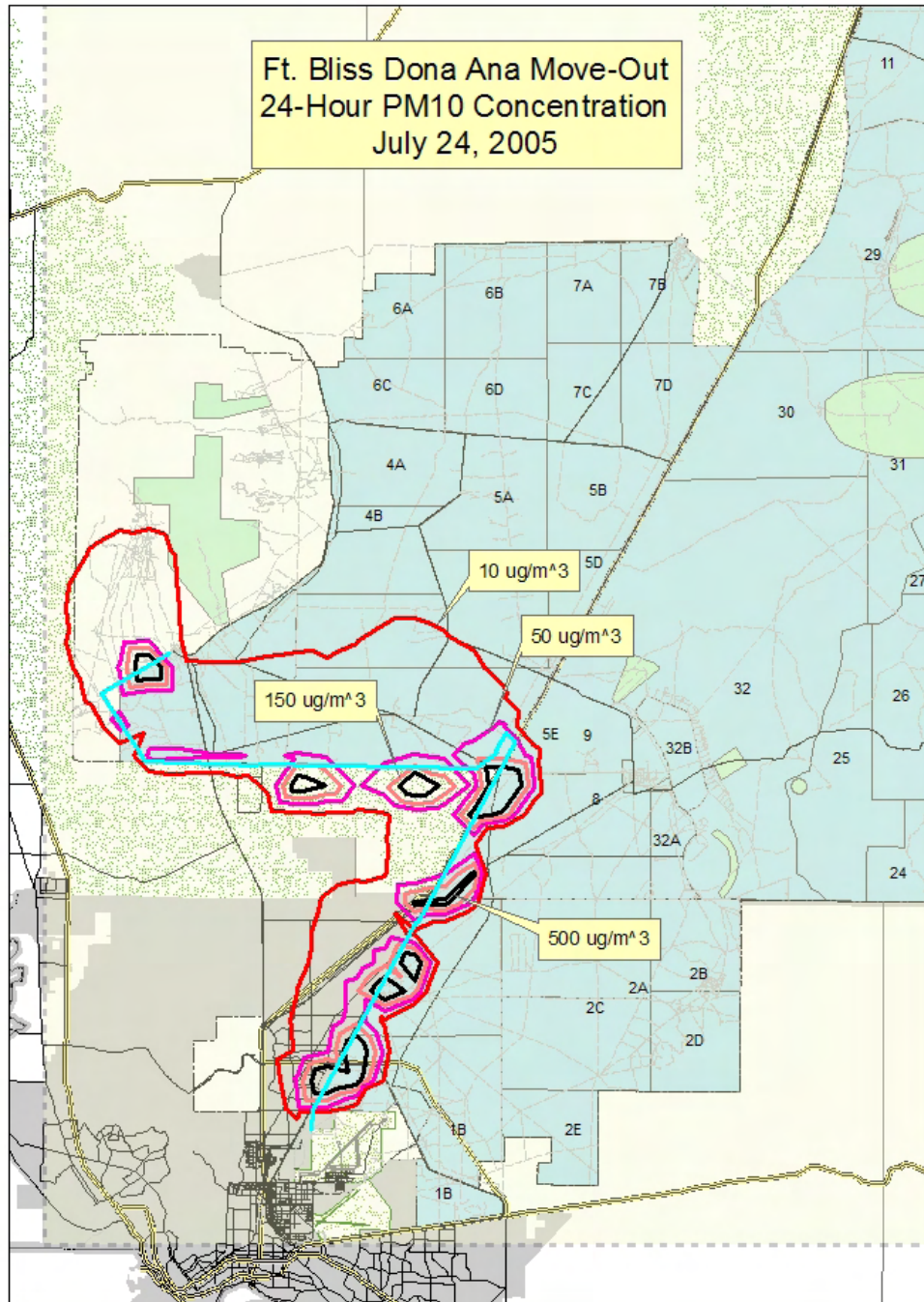


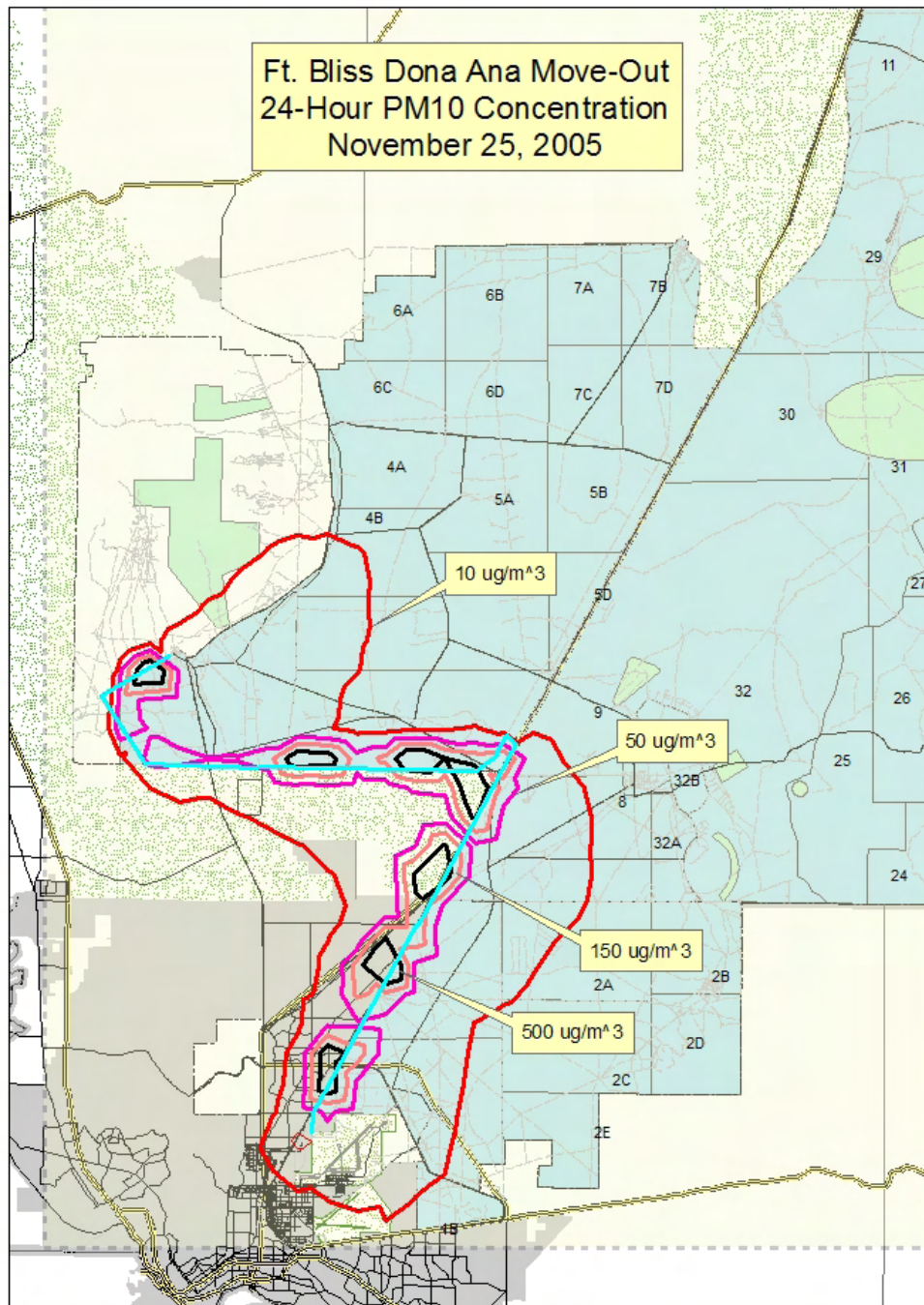


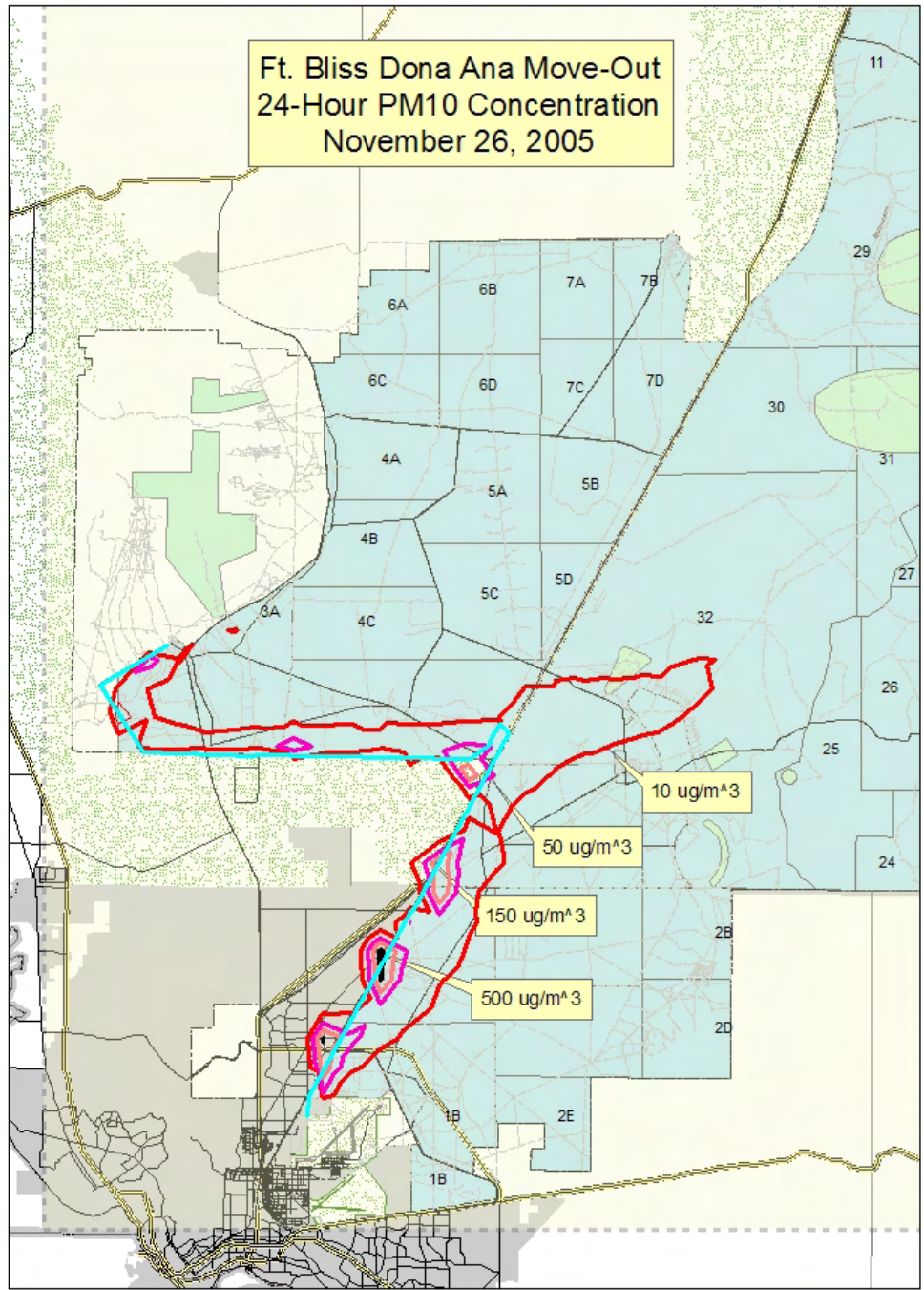


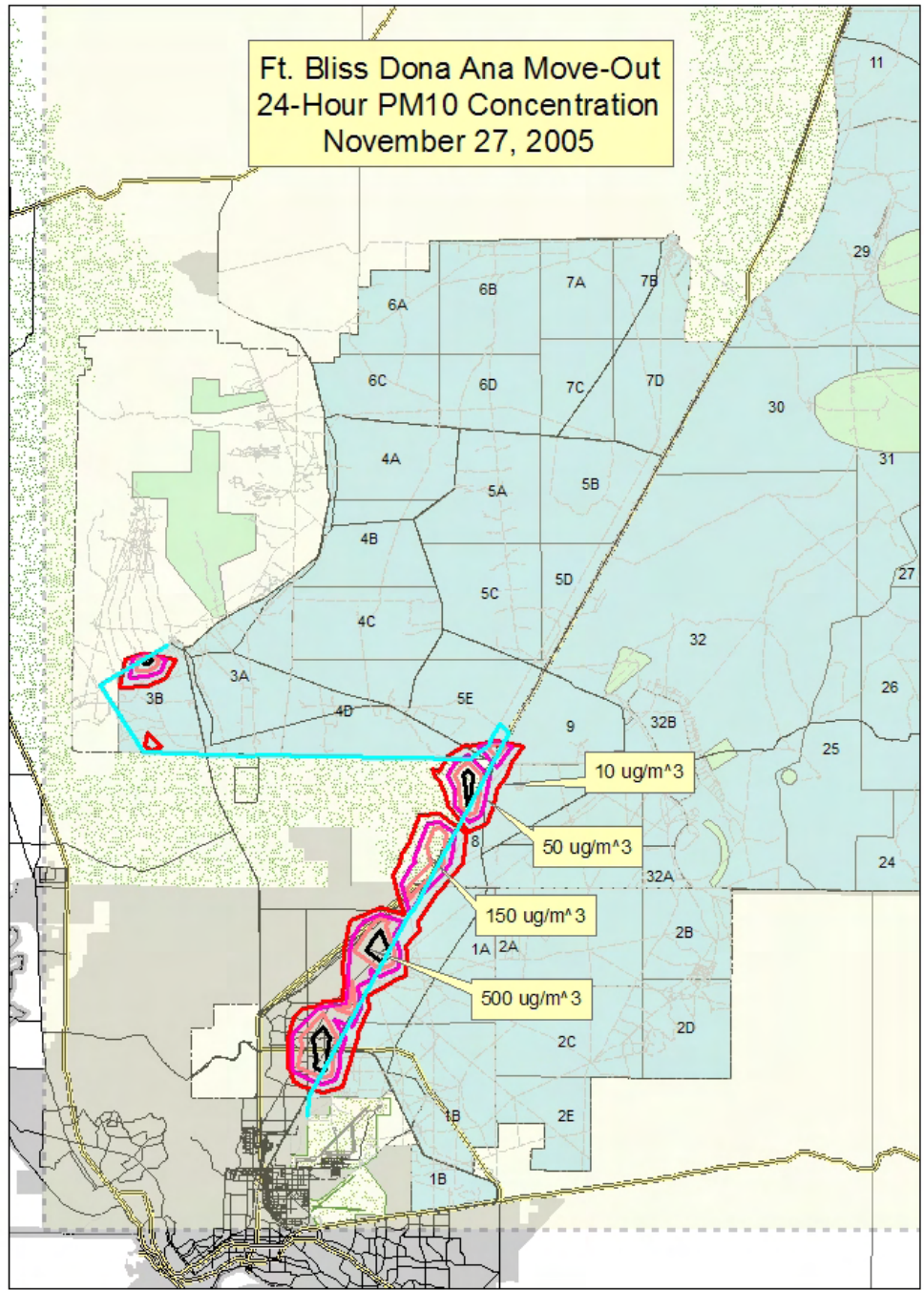


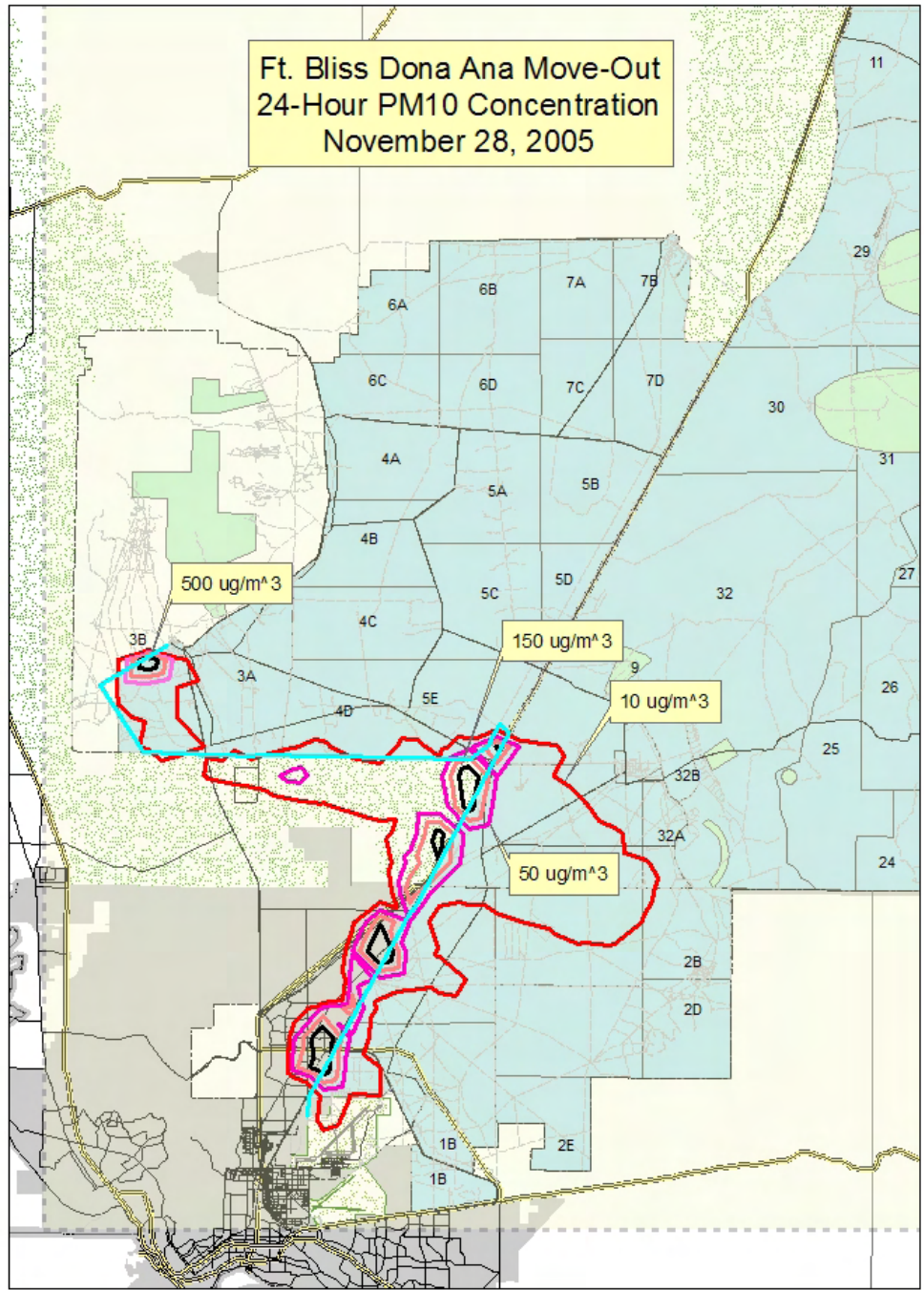


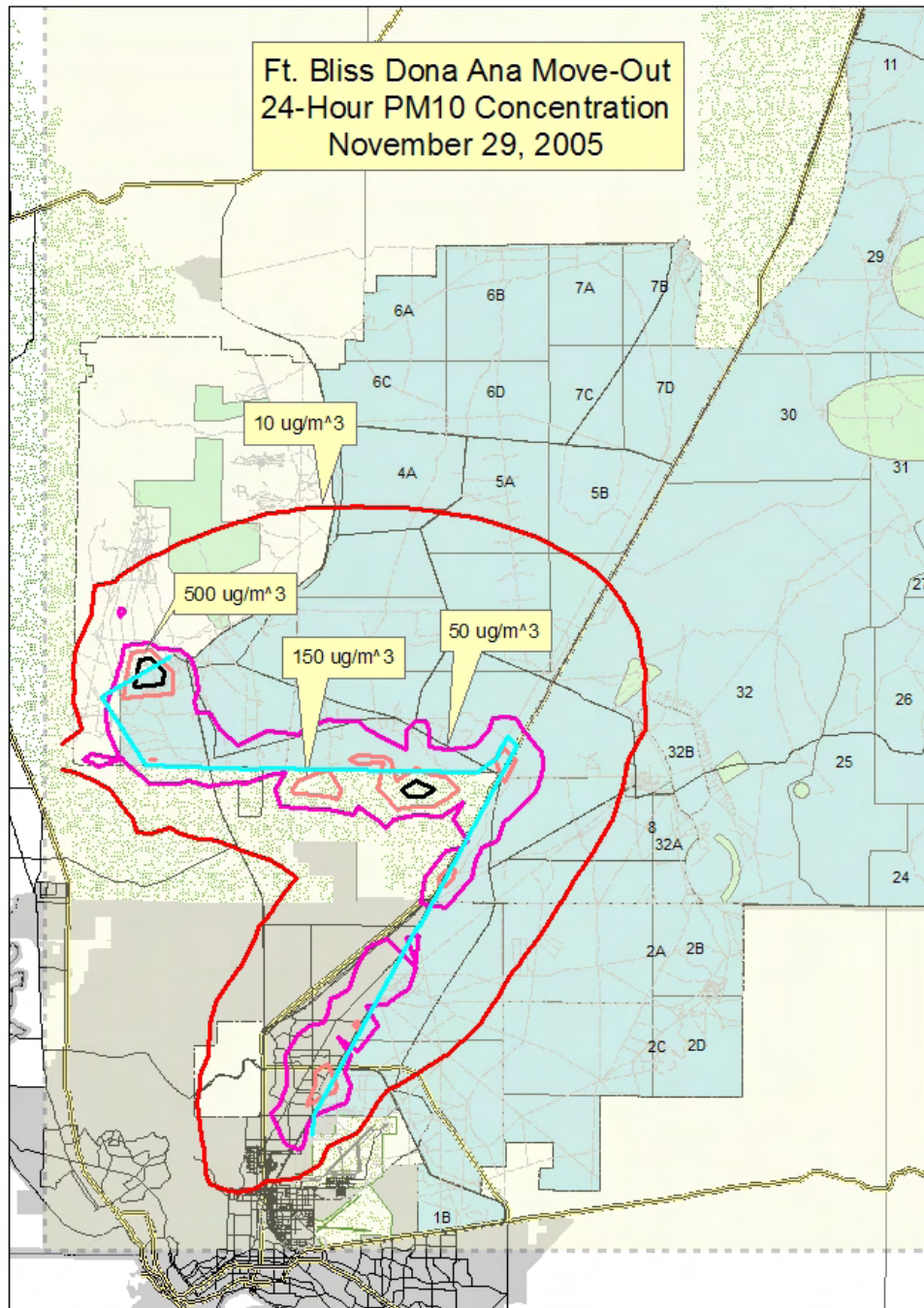












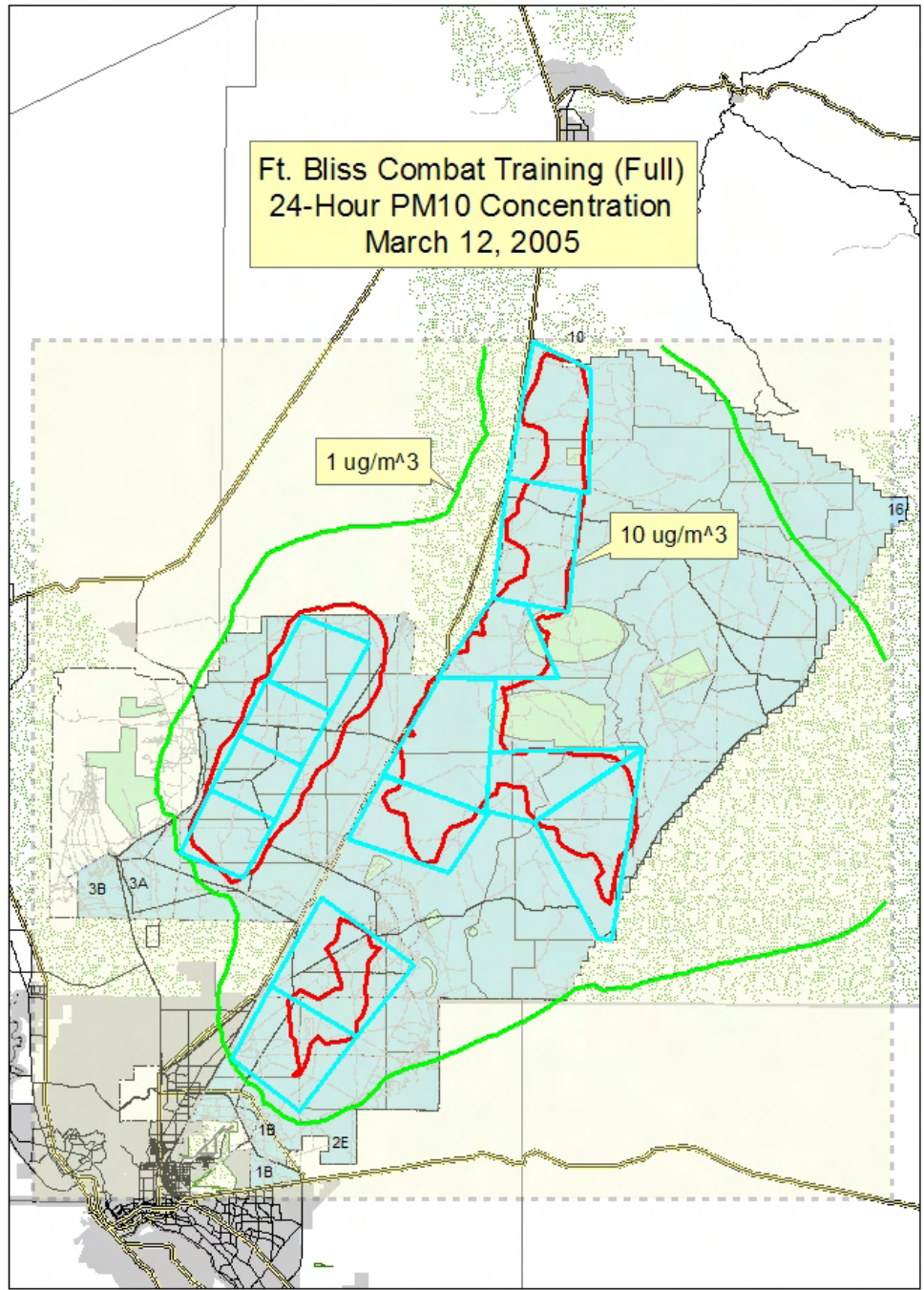
Appendix F

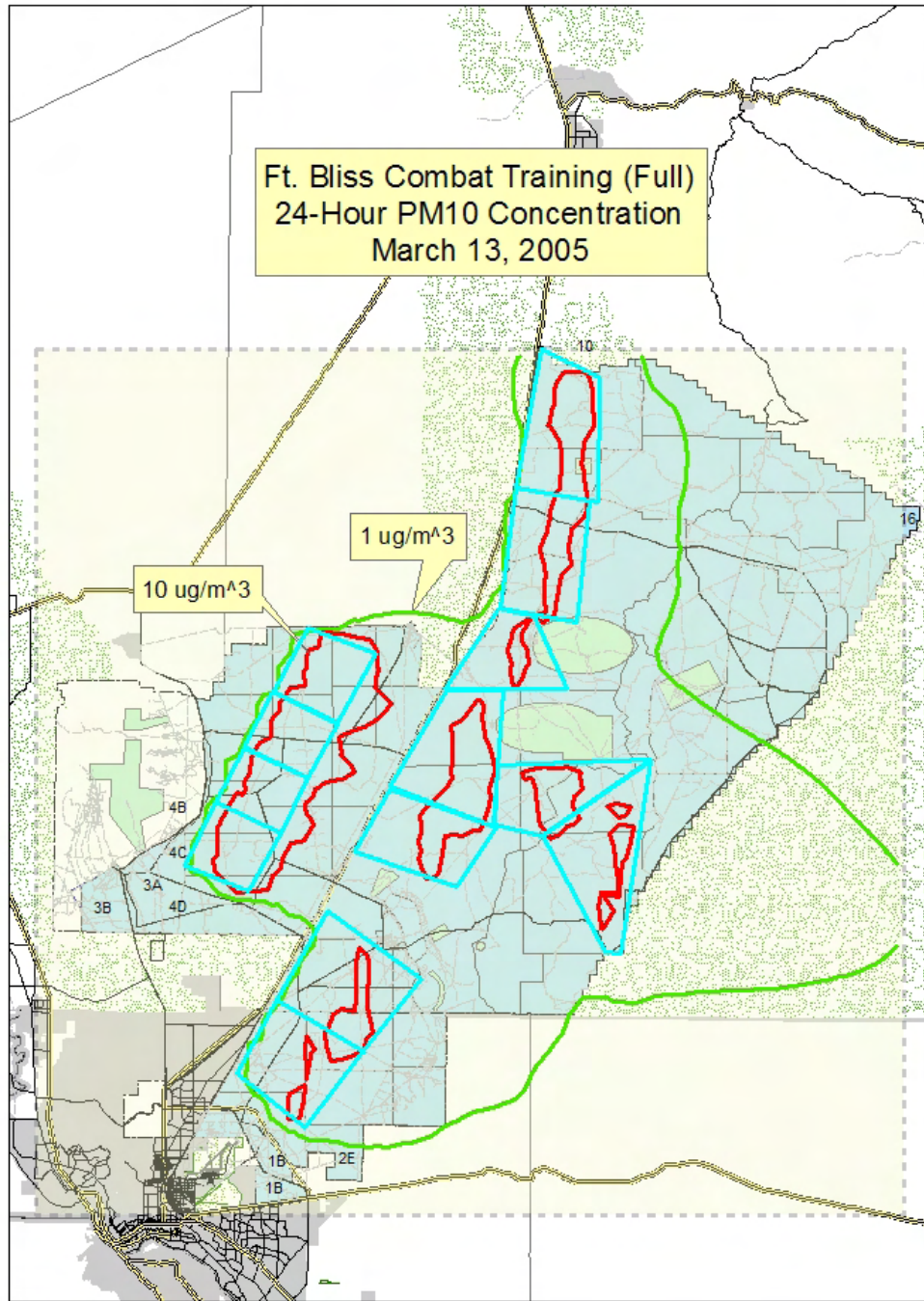
Simulated 24-h-Average PM₁₀ Concentrations for Combat Training

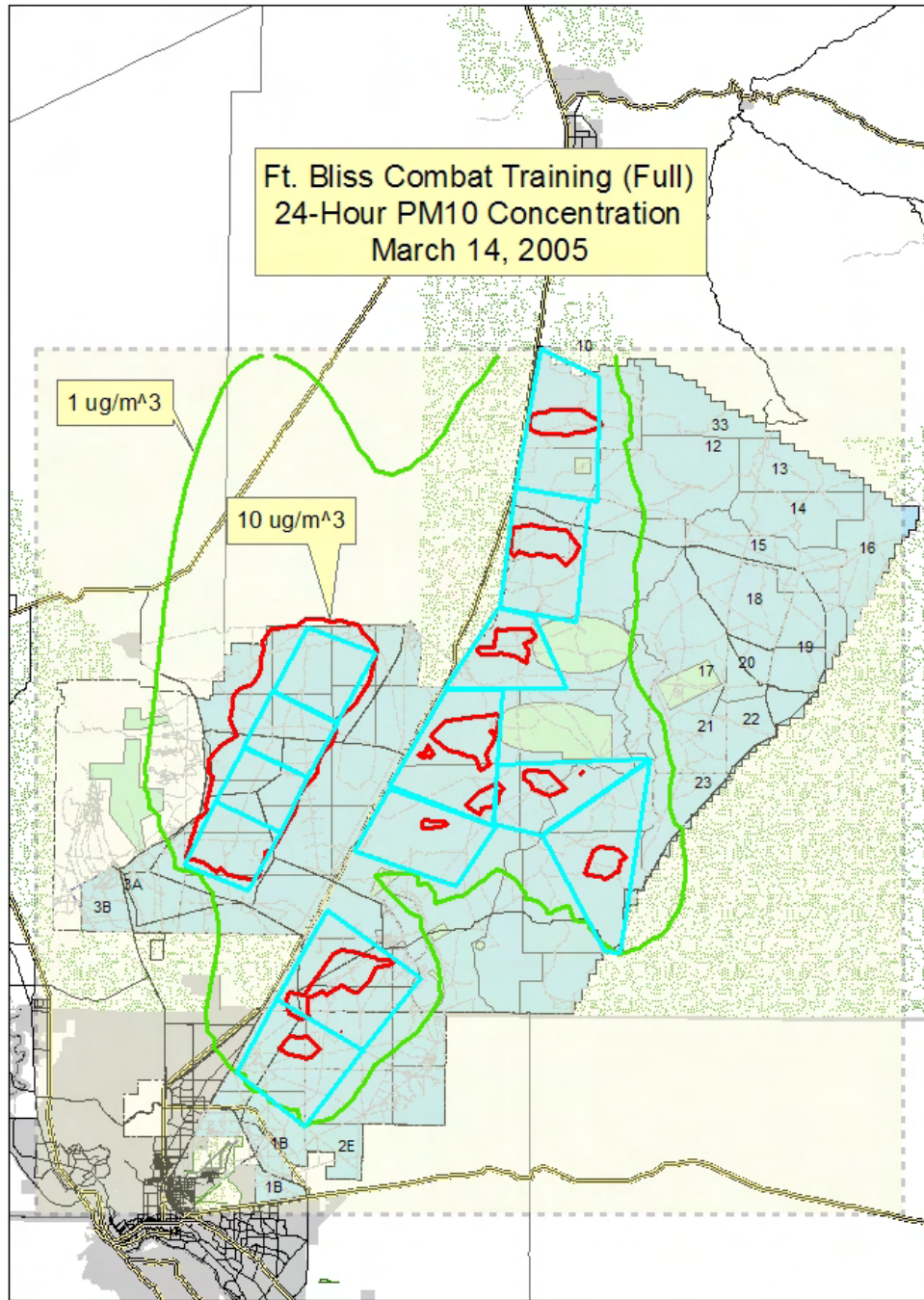
Appendix F: Simulated 24-h-Average PM₁₀ Concentrations for Combat Training

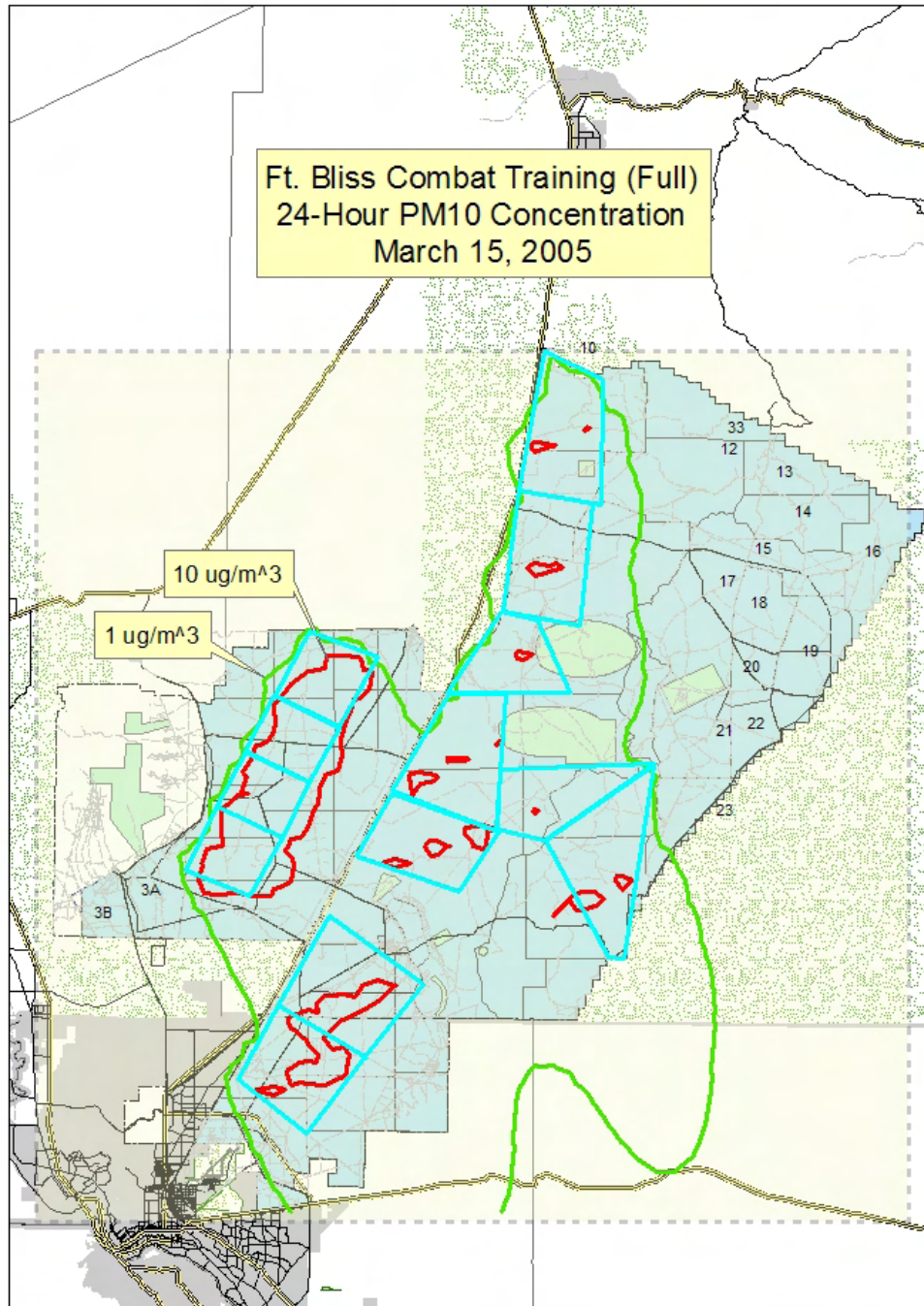
Contour maps of 24-hour-average PM₁₀ concentrations contributed from combat training activities to air quality in and around Fort Bliss are given for the 21 simulated days (March 12–16, April 25–30, July 20–24, and November 25–29, 2005). The combat training scenario consists of training activities occurring concurrently in the Dona Ana 1 maneuver area, the McGregor maneuver area and the South Training maneuver area. Combat training scenario assumptions for DUSTAN simulations are summarized below.

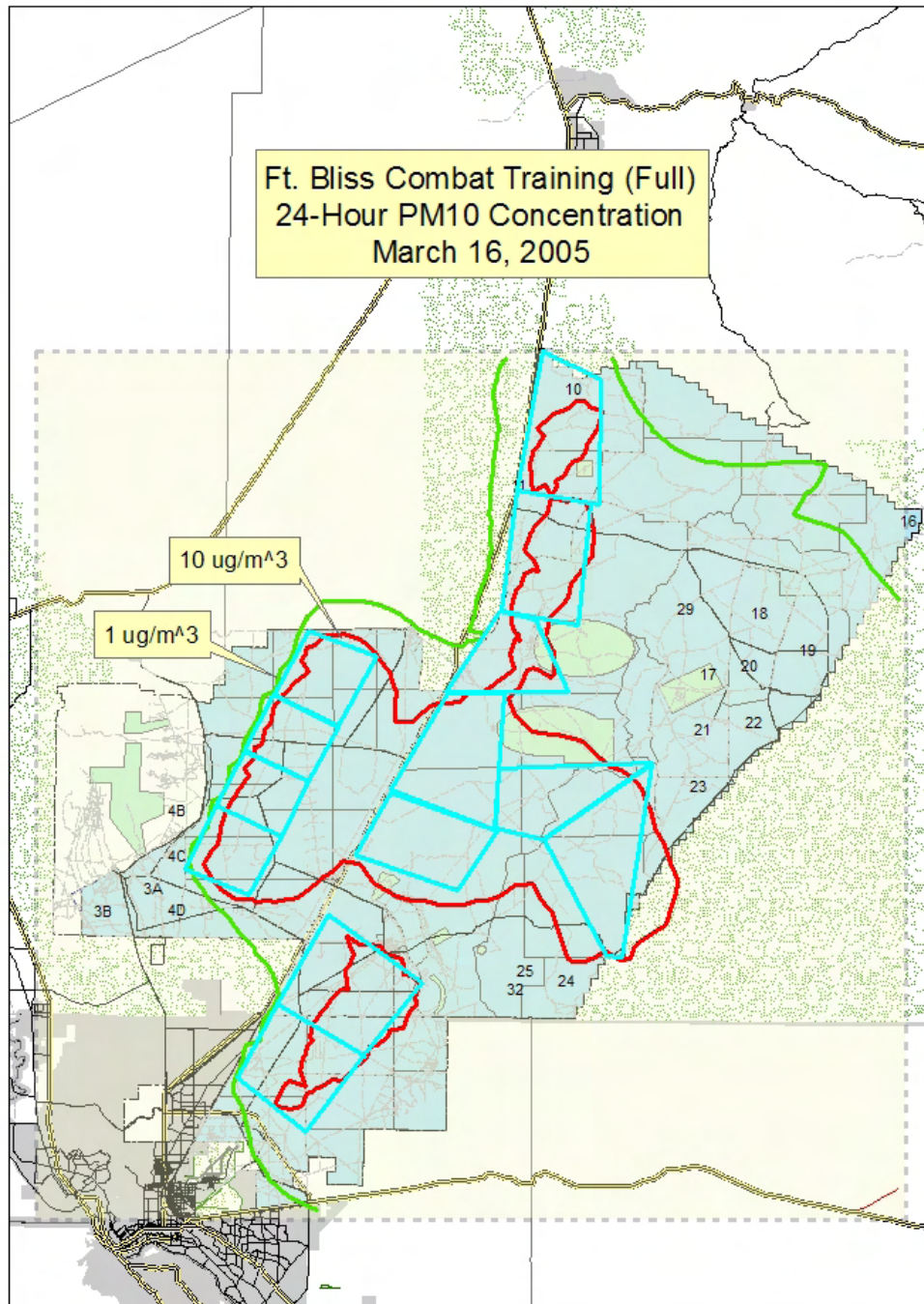
- All vehicles associated with one HBCT are located in the region labeled “Combat Training Dona Ana 1” in Figure 4.4.
- All vehicles associated with one HBCT are located in the region labeled “Combat Training McGregor” in Figure 4.4.
- Vehicles associated with one-third of a HBCT (i.e., one battalion) are located in the region labeled “Combat Training South” in Figure 4.4.
- Within each training area and sub-area, uniform distributions of vehicle type and vehicle numbers exist.
- Vehicles are already located in the training areas when activities commence (i.e., no travel to training areas from the McGregor or Dona Ana Range Camps).
- All combat training begins at 0700 MST.
- Vehicle movement occurs uniformly over a 10-hour period.
- The total distance traveled by each wheeled vehicle over the course of a training day is 32 km, or approximately 20 miles.
- The total distance traveled by each tracked vehicle over the course of a training day is 21 km, or approximately 13 miles.
- When moving, all vehicles travel at a speed of 40 km per hour.

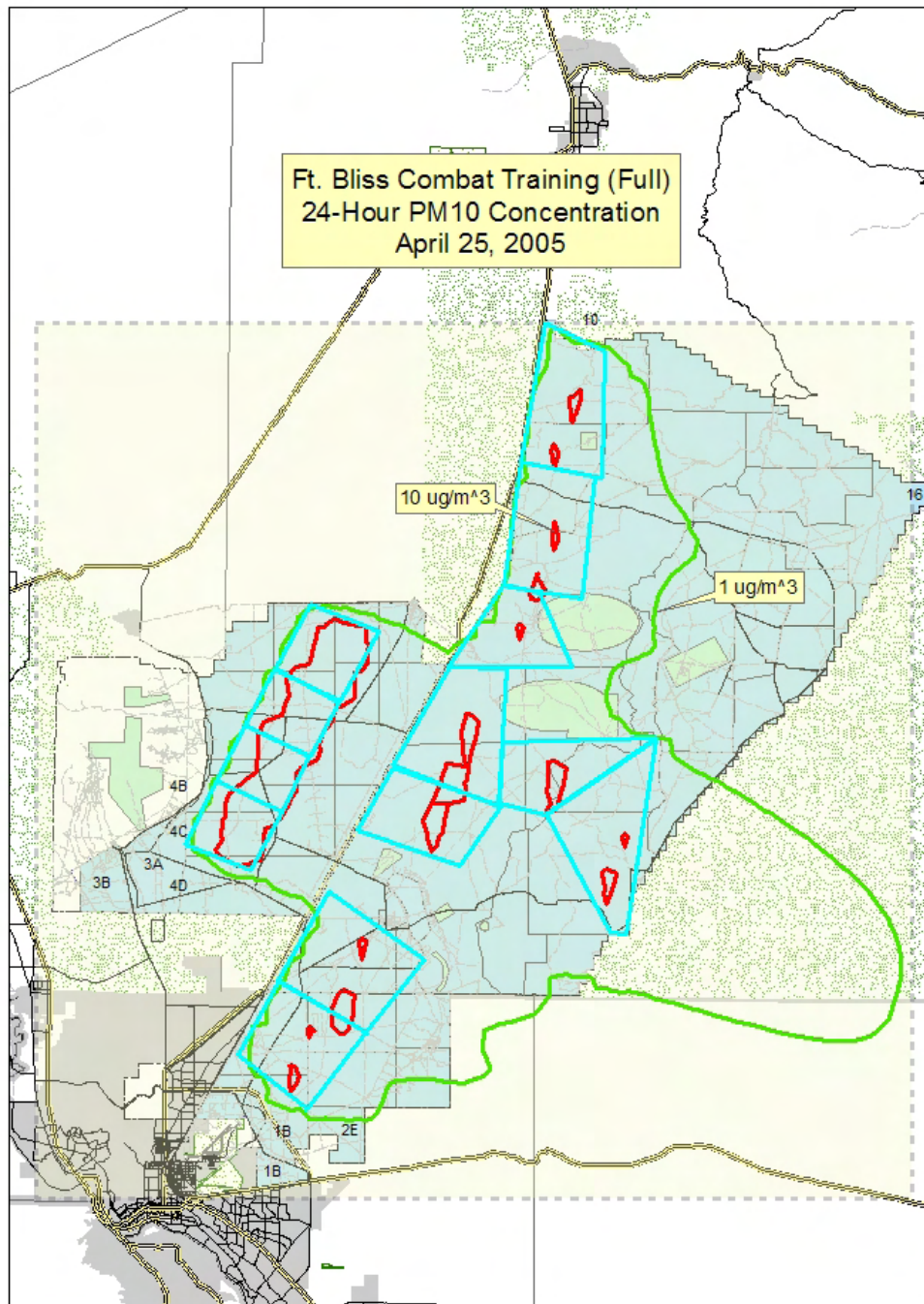


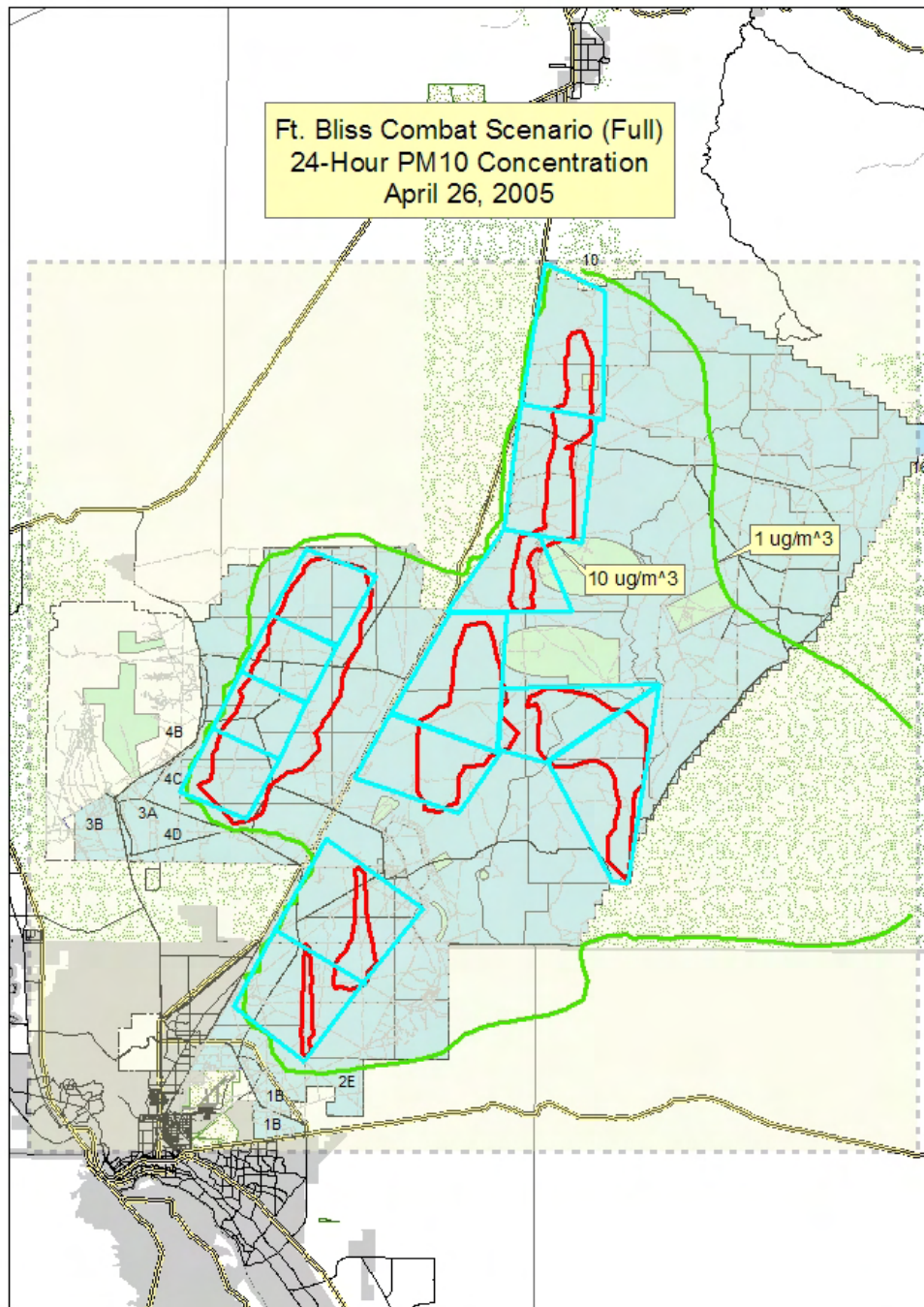


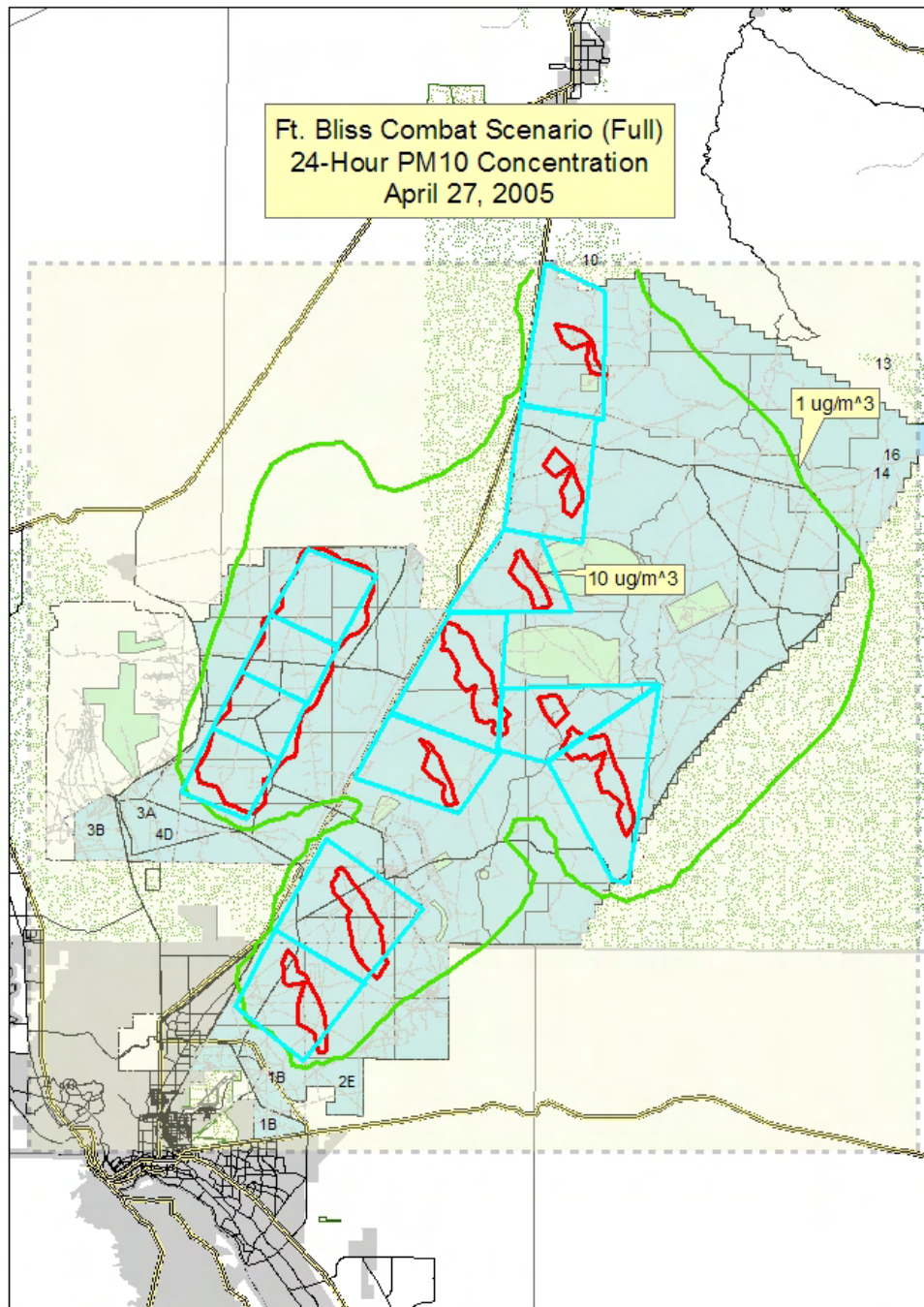


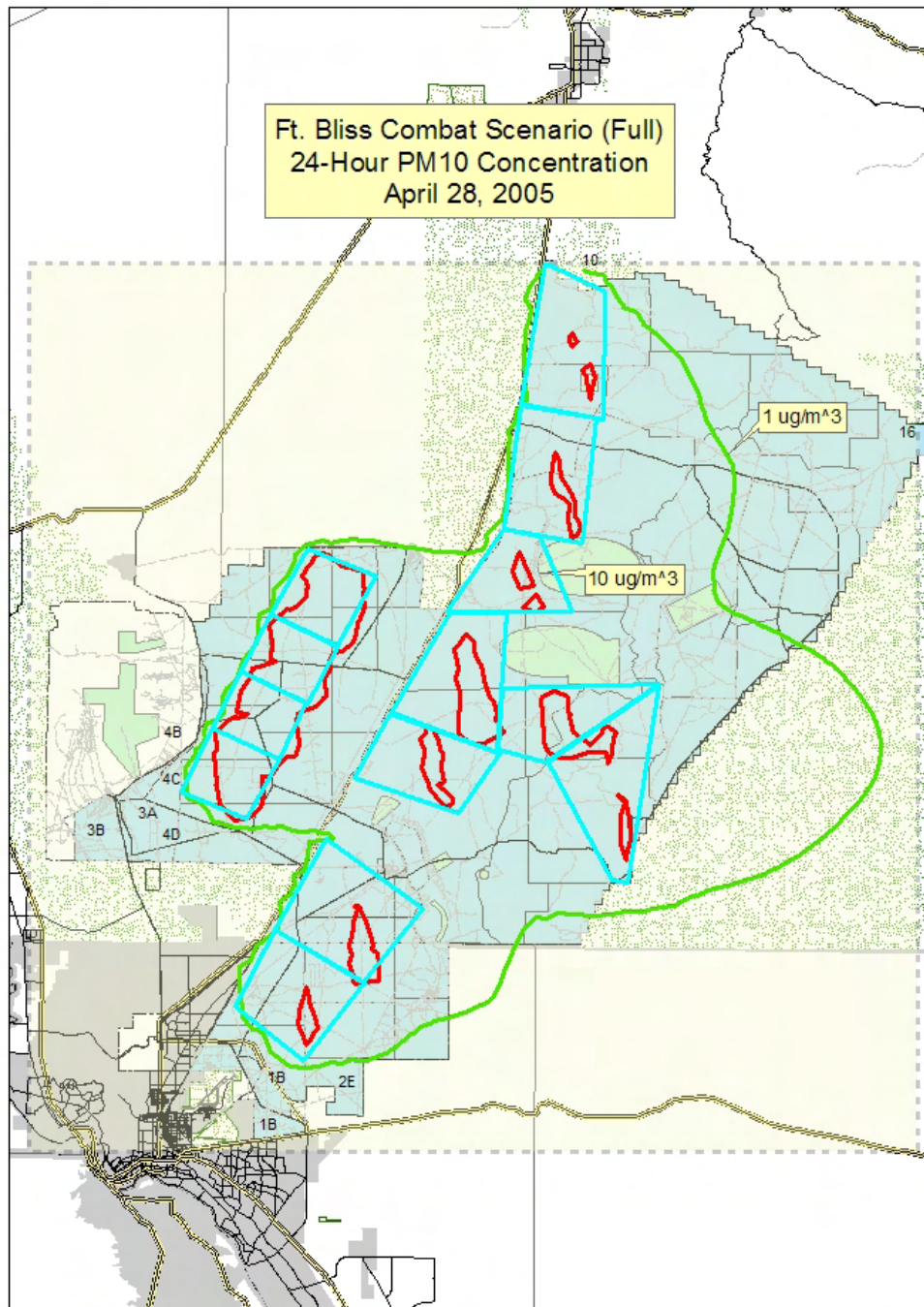


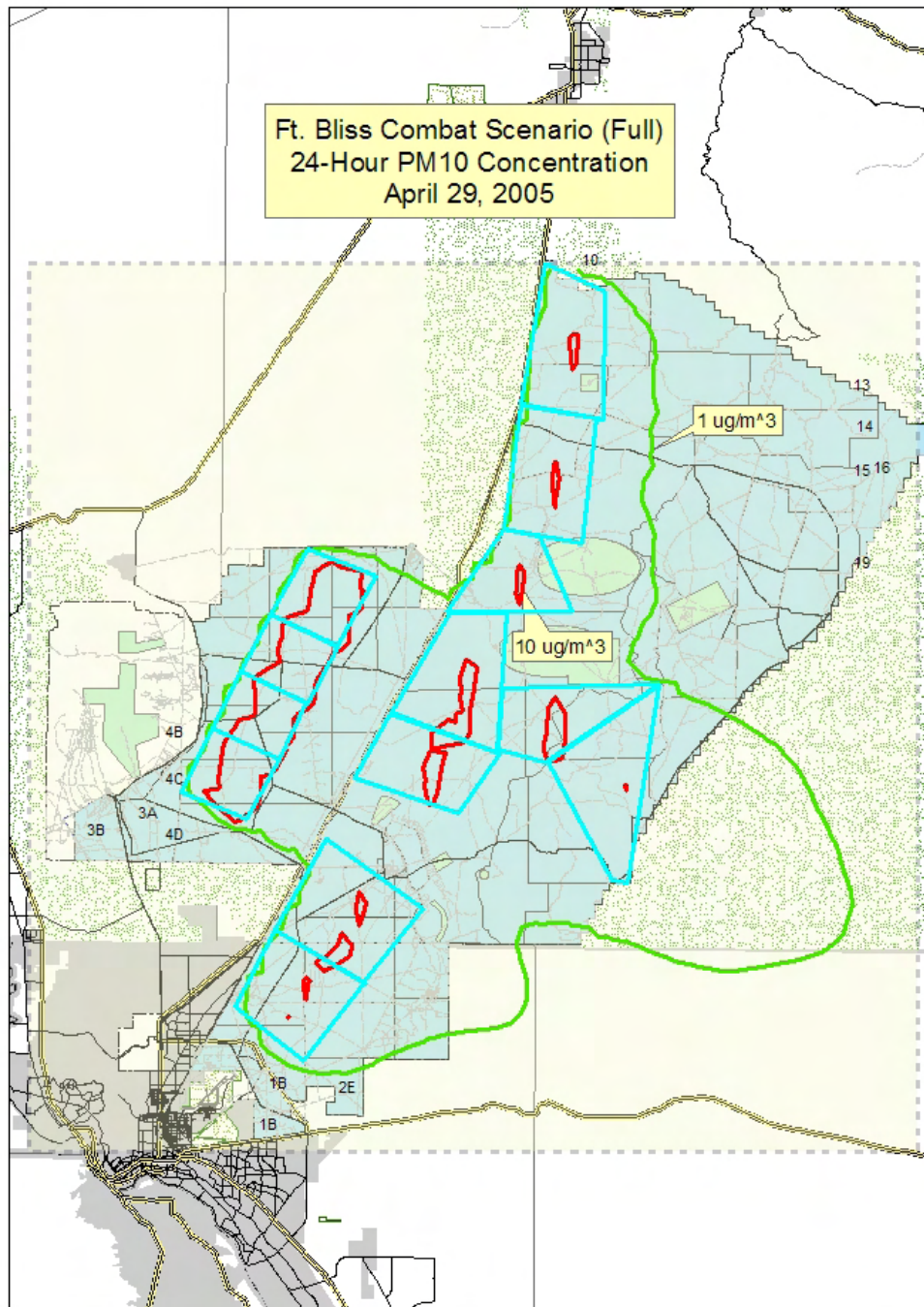


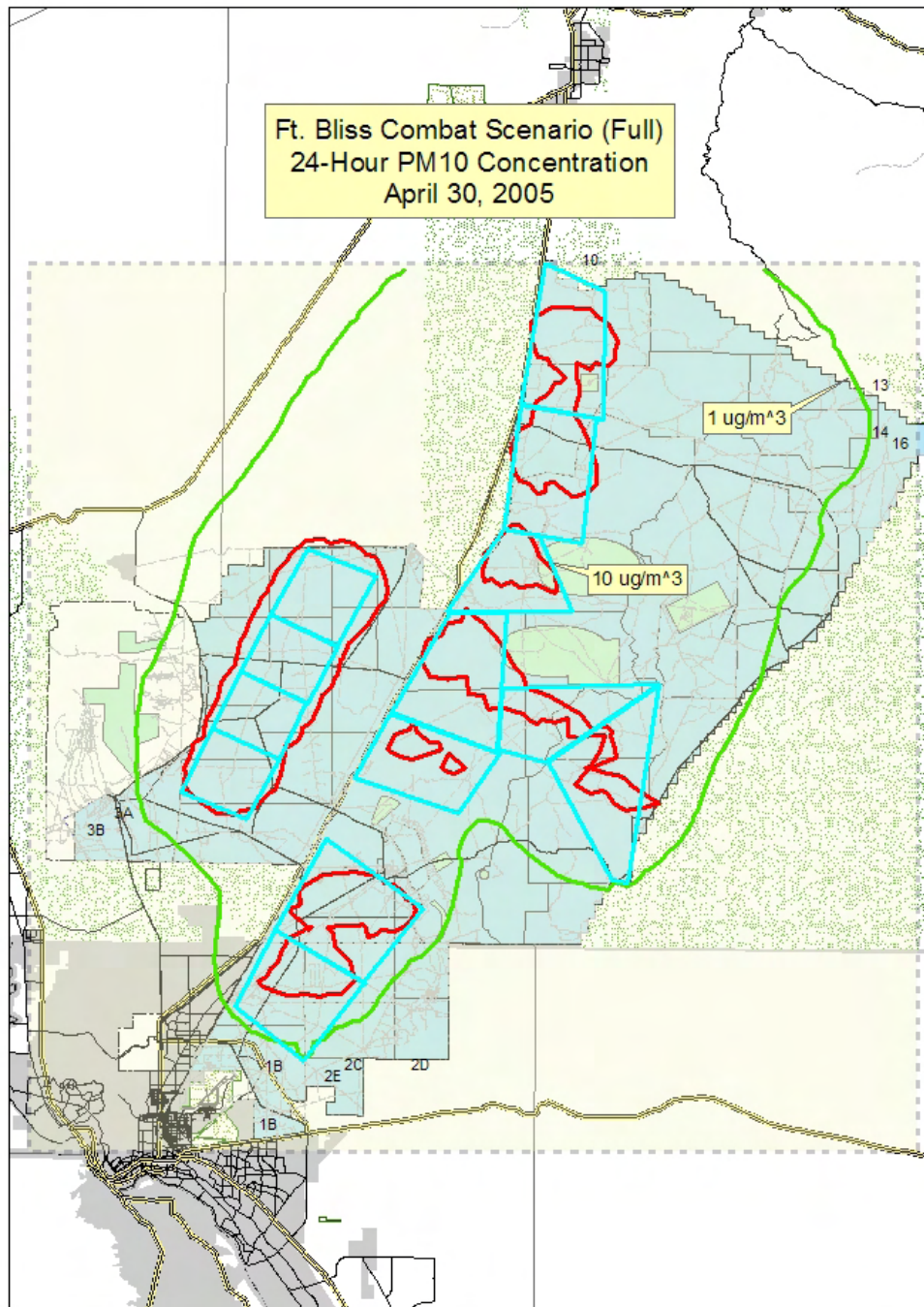


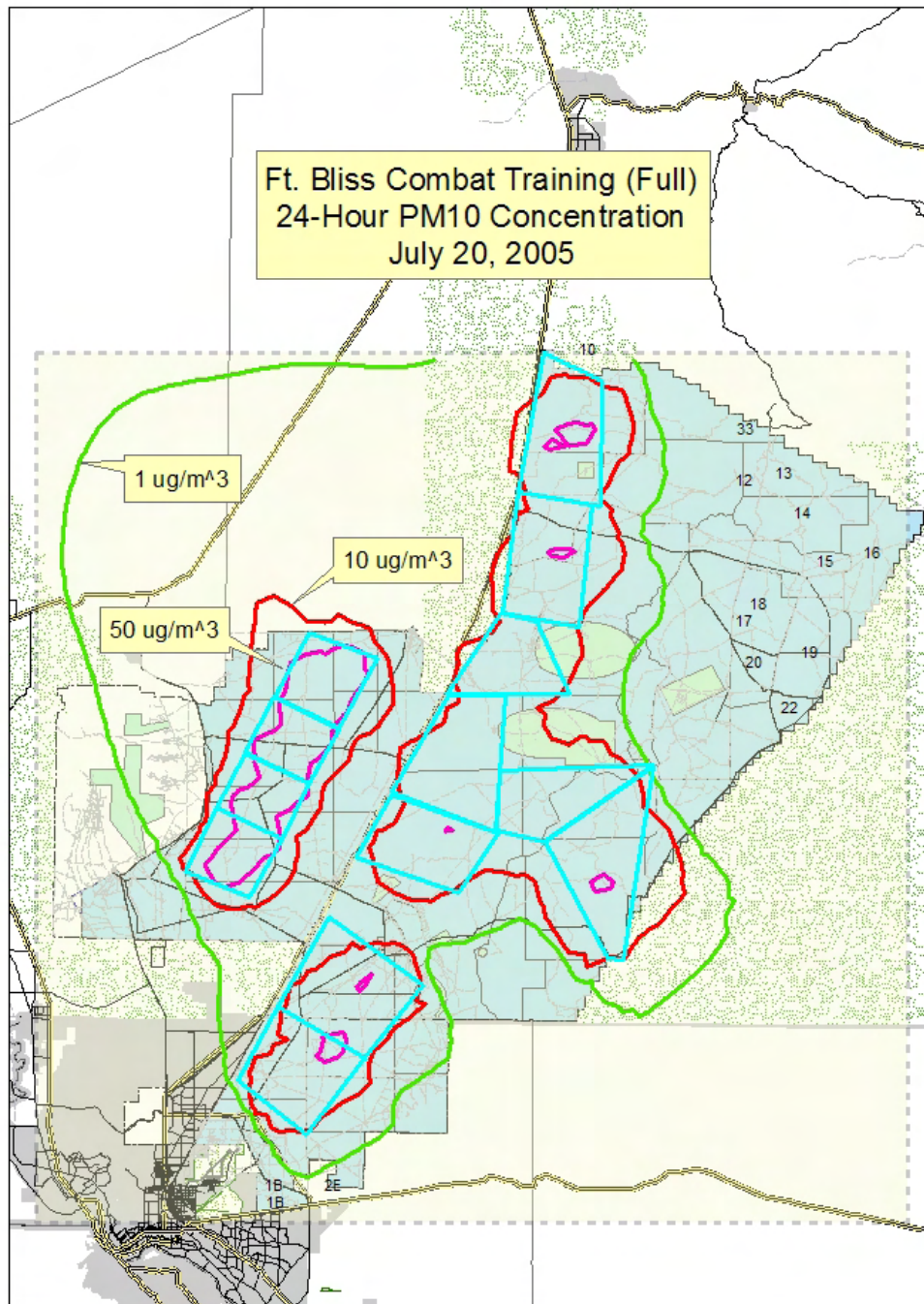


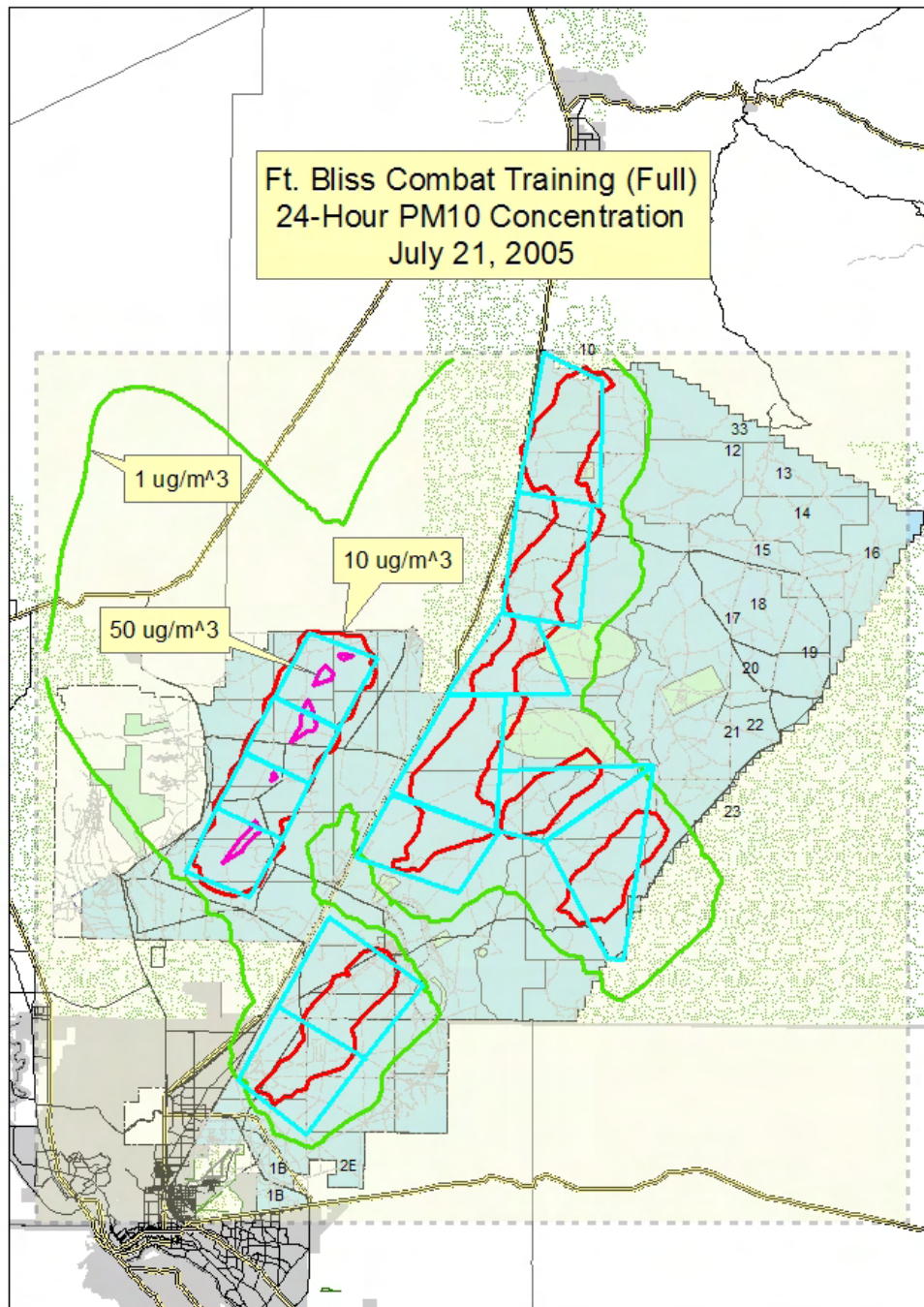


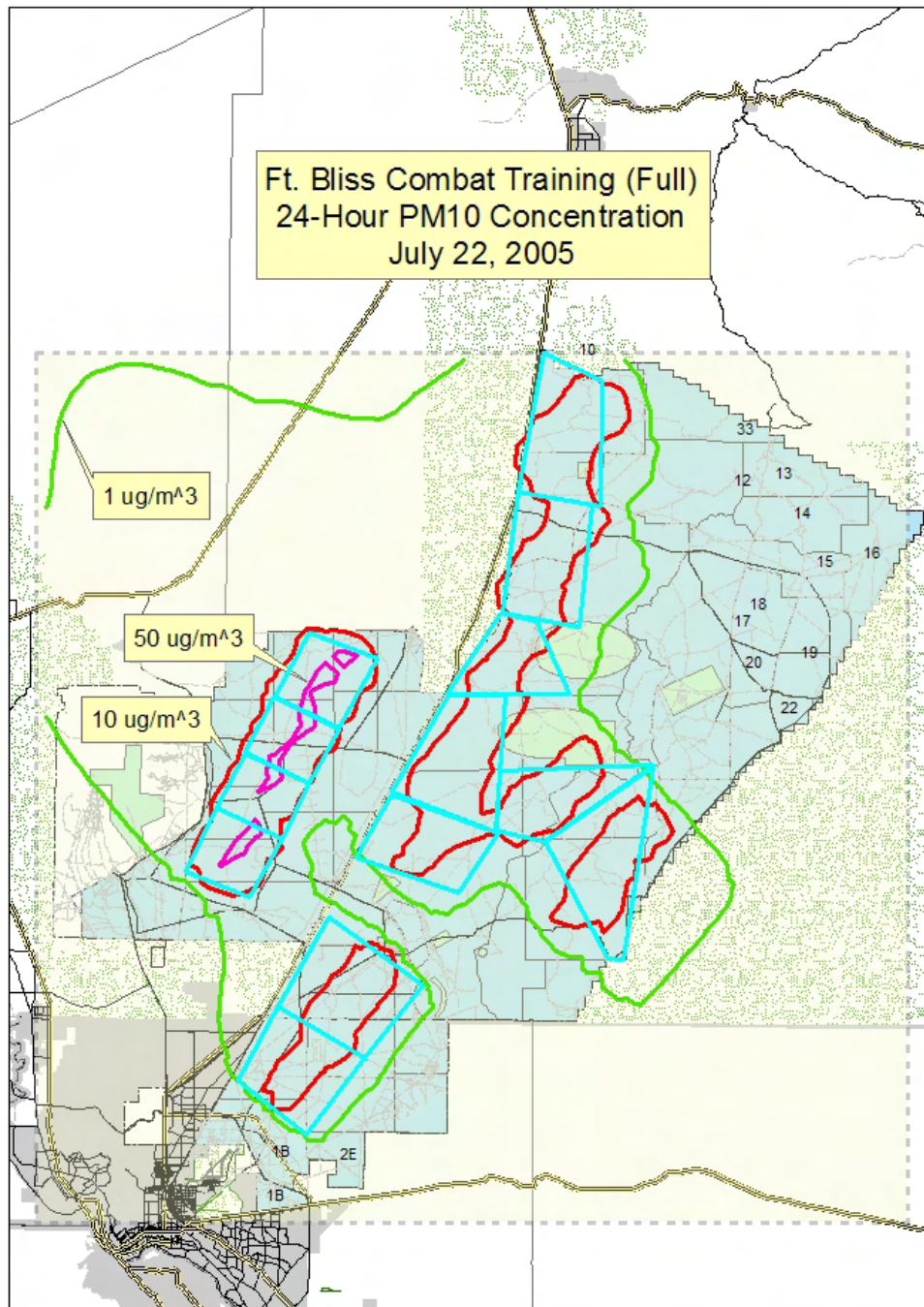


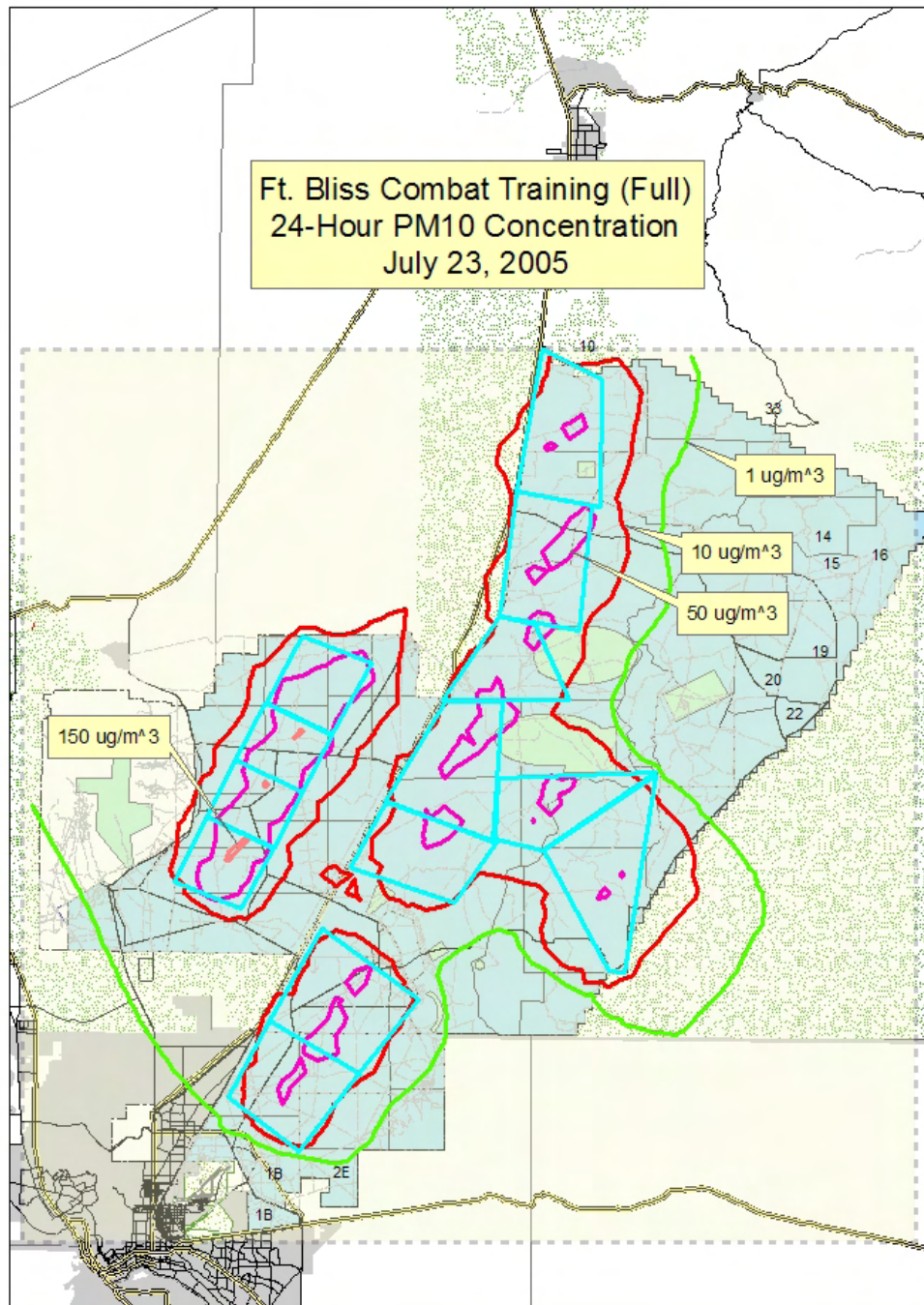


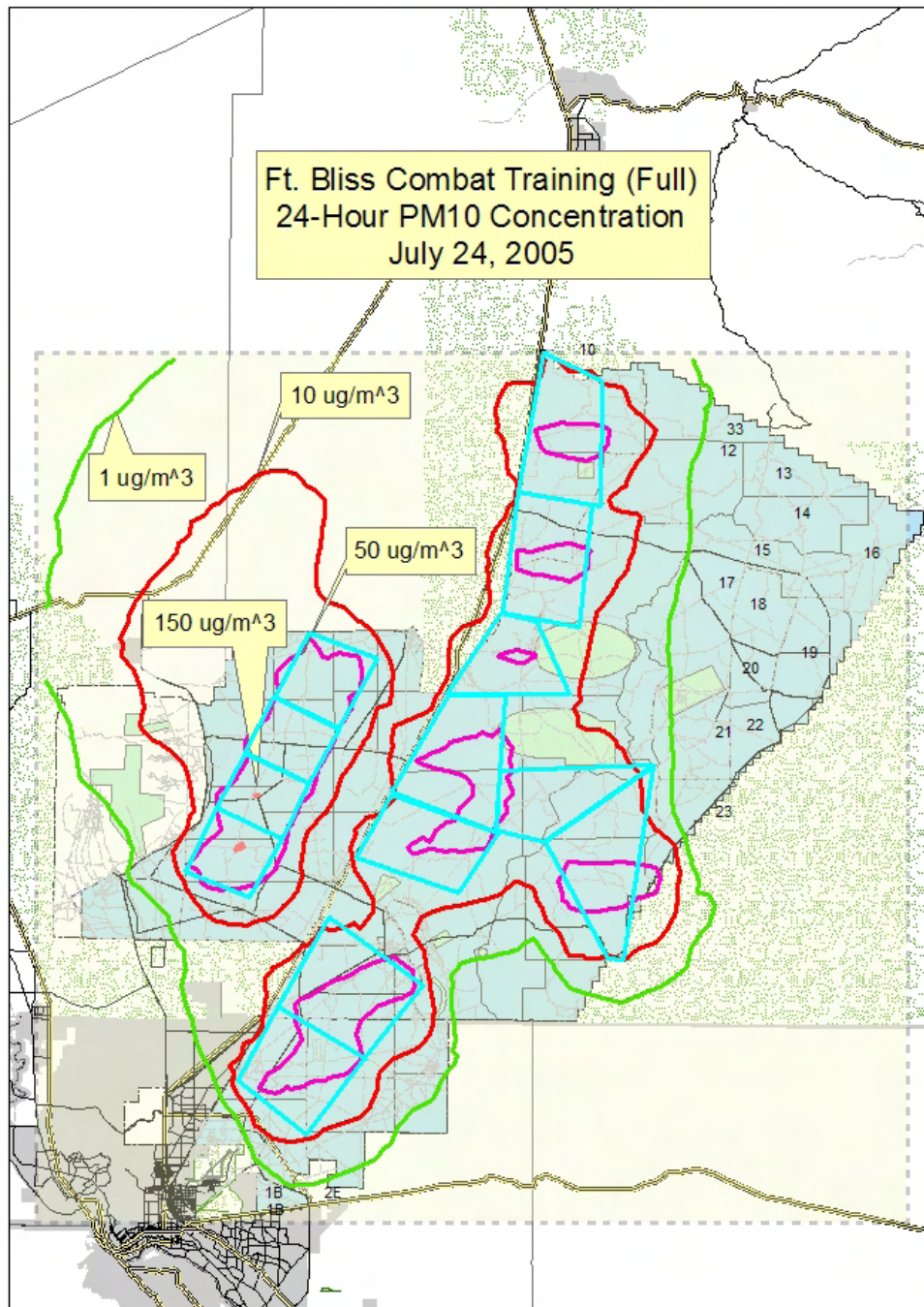


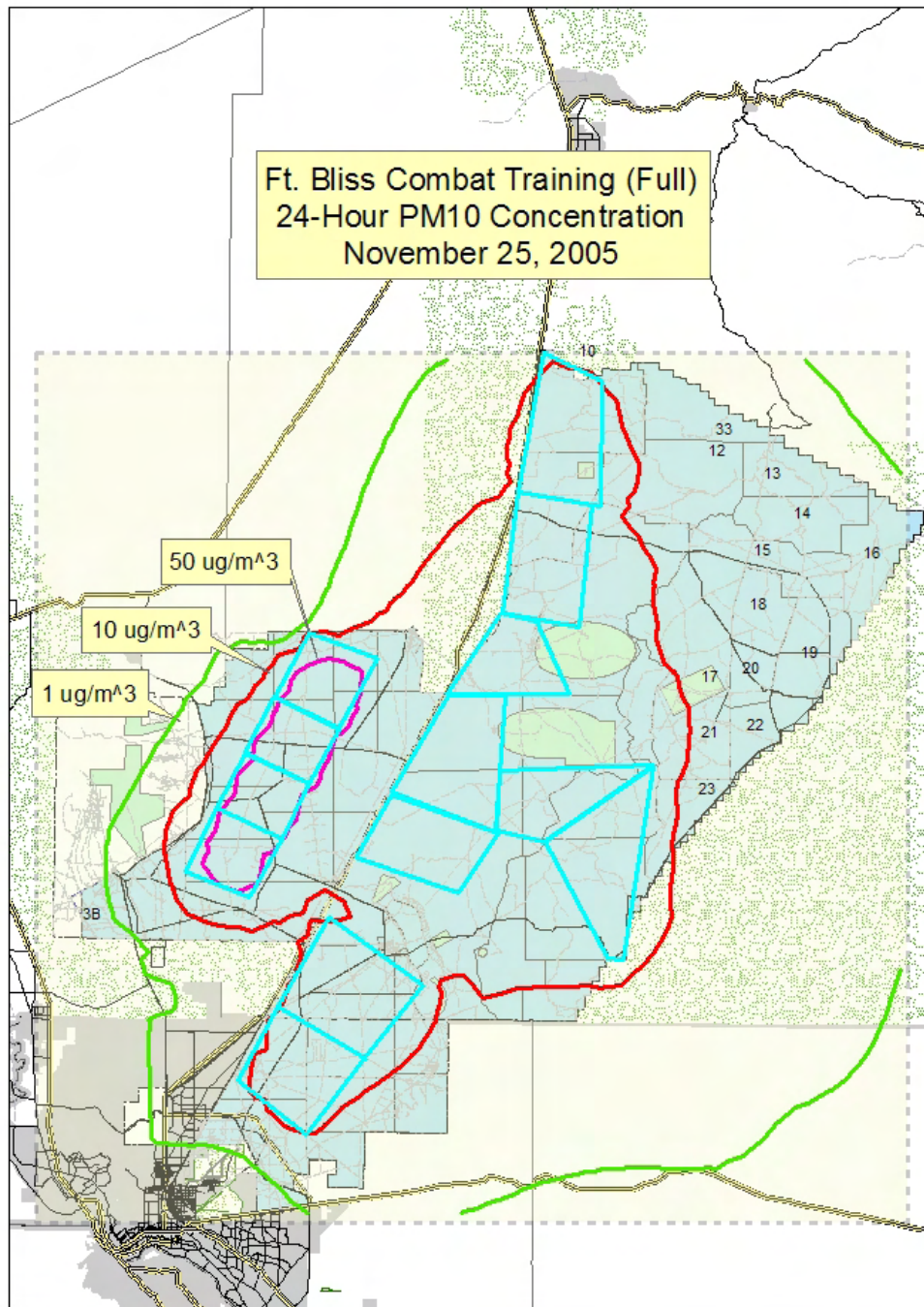


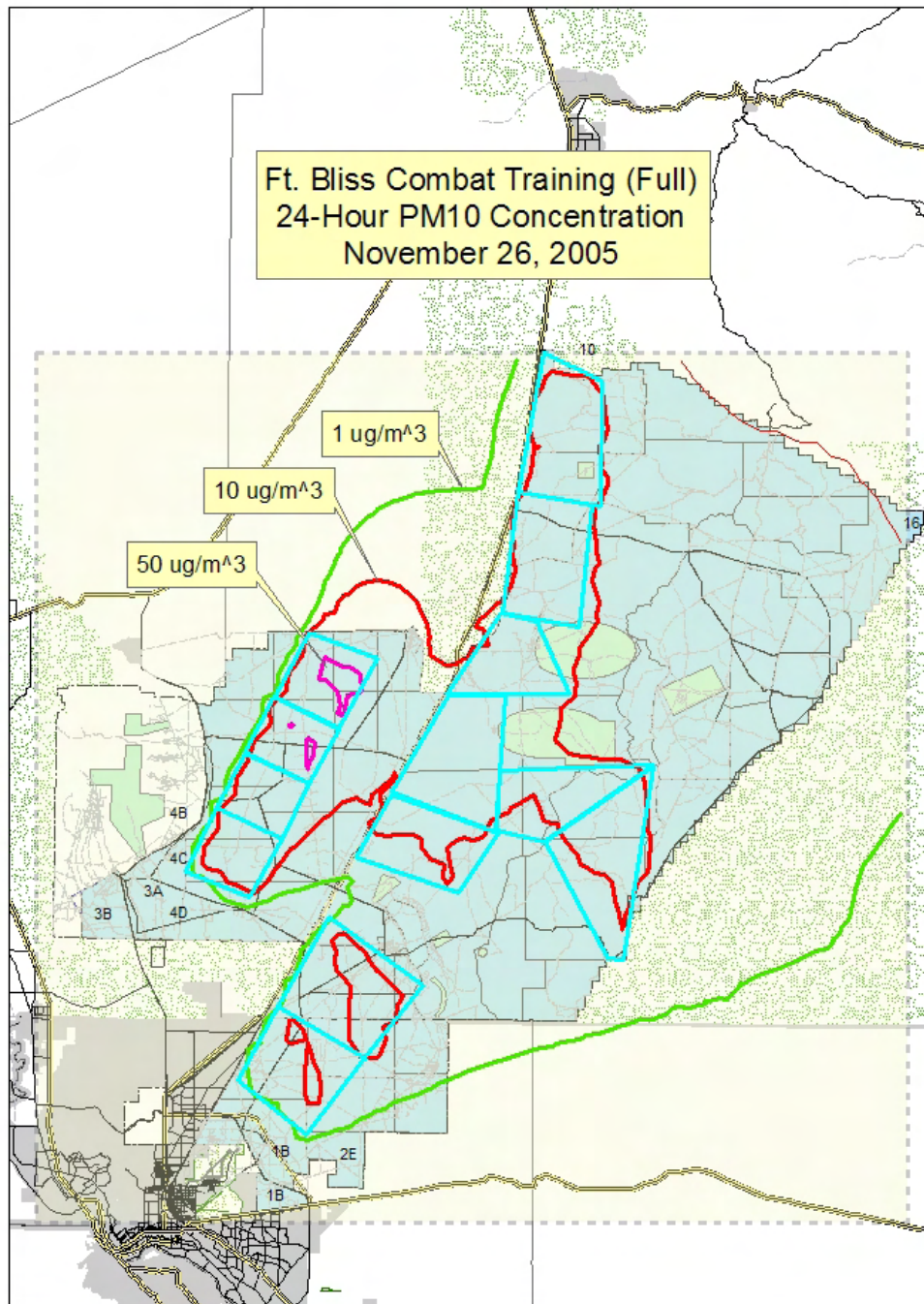


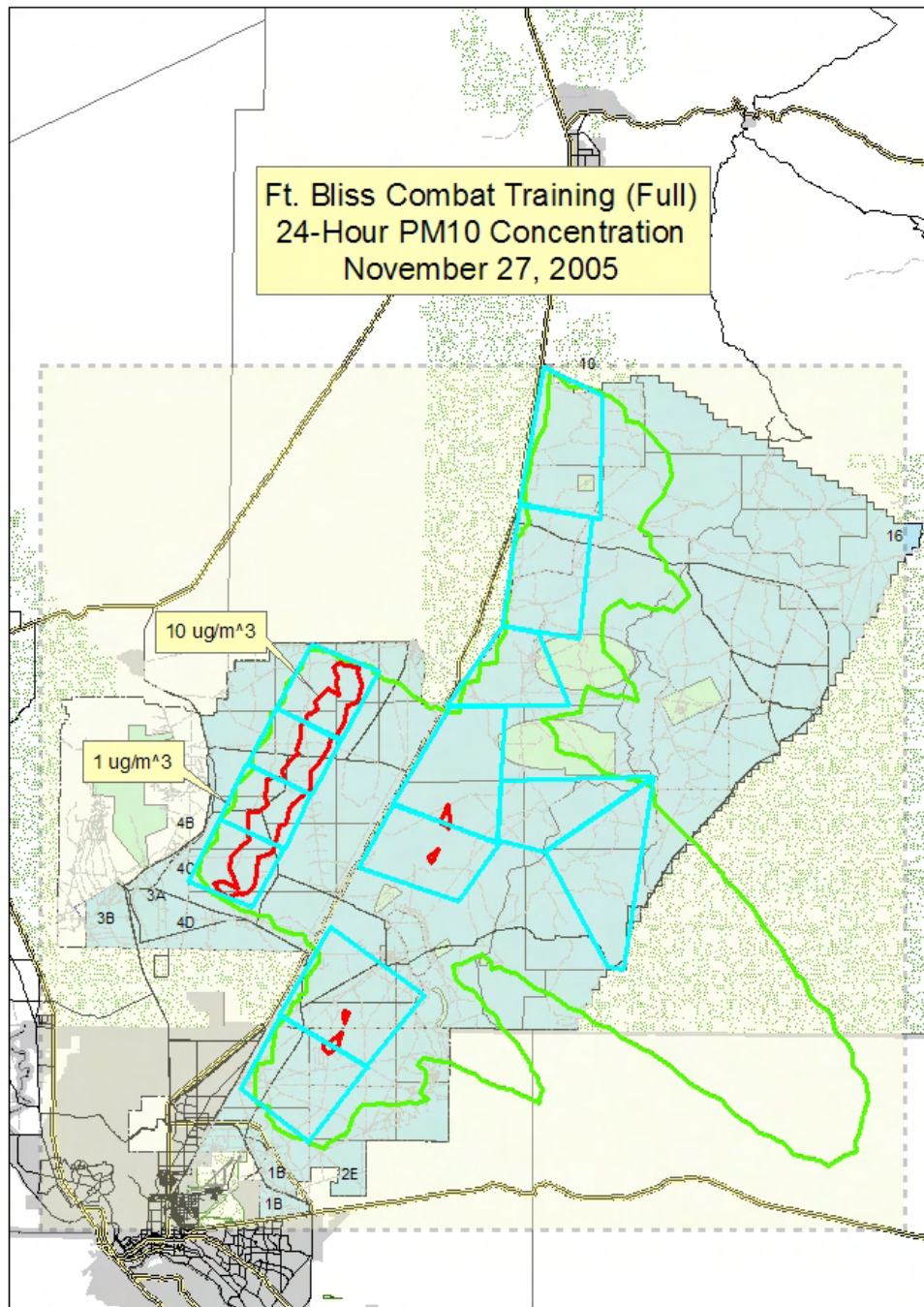


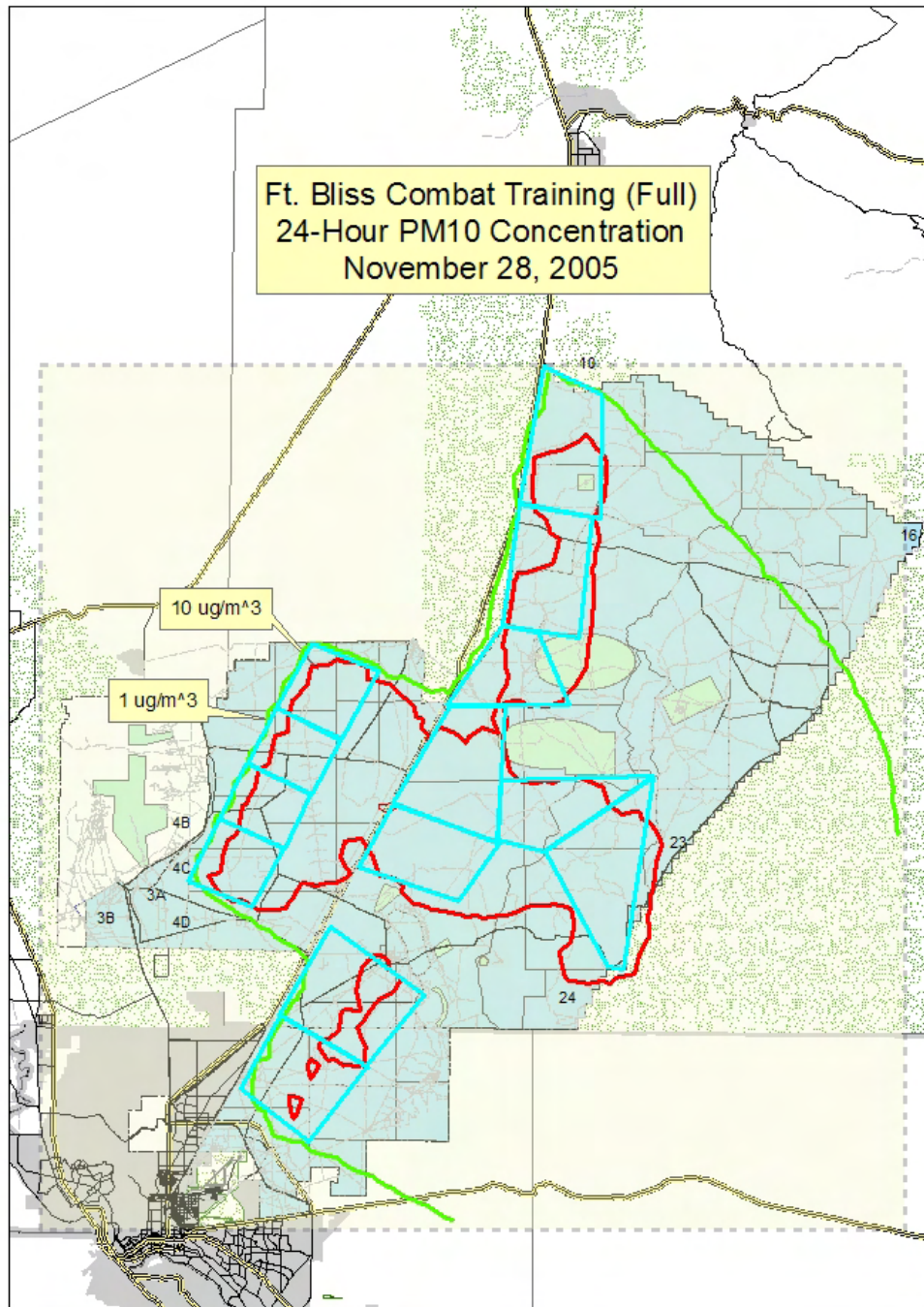


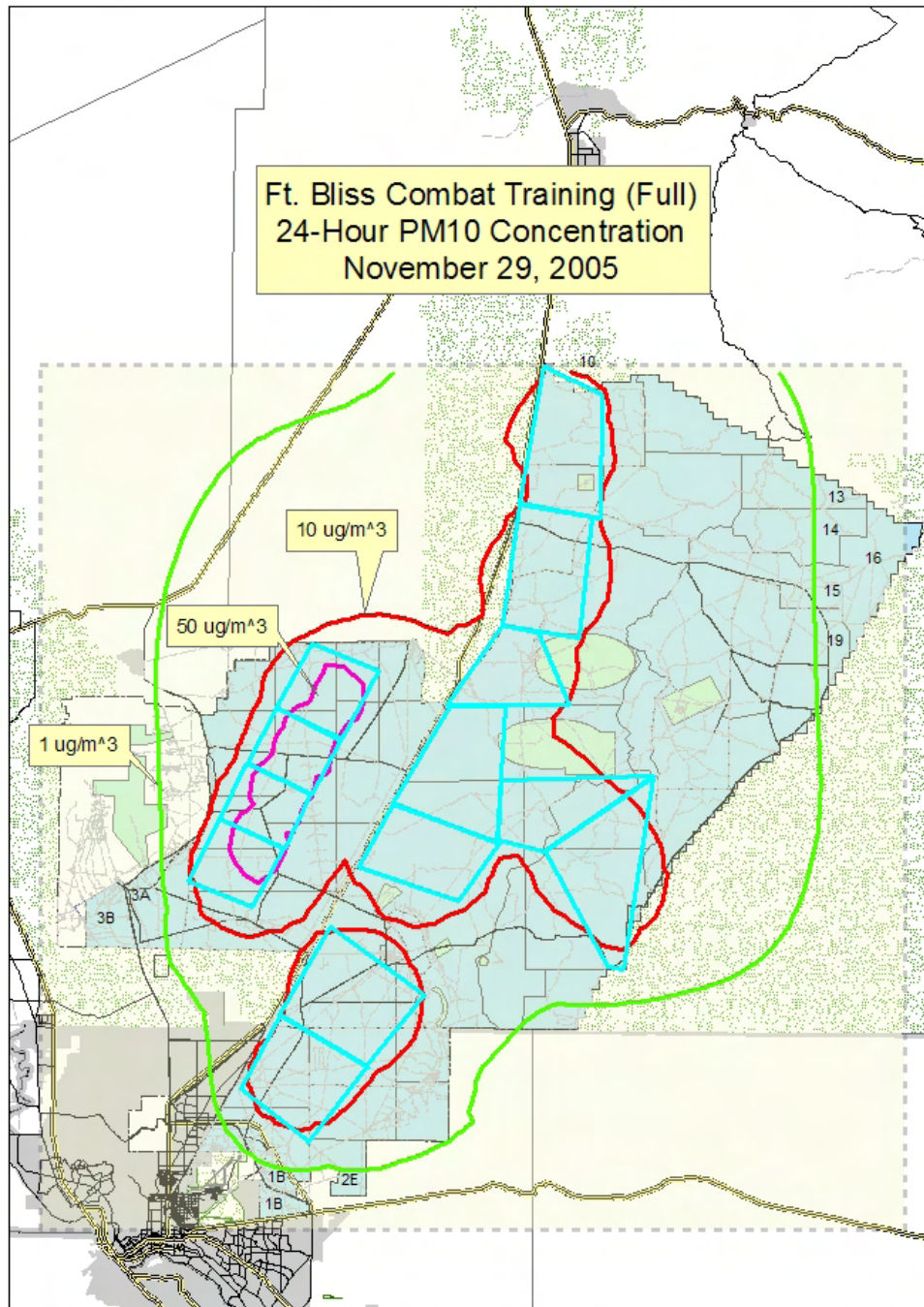










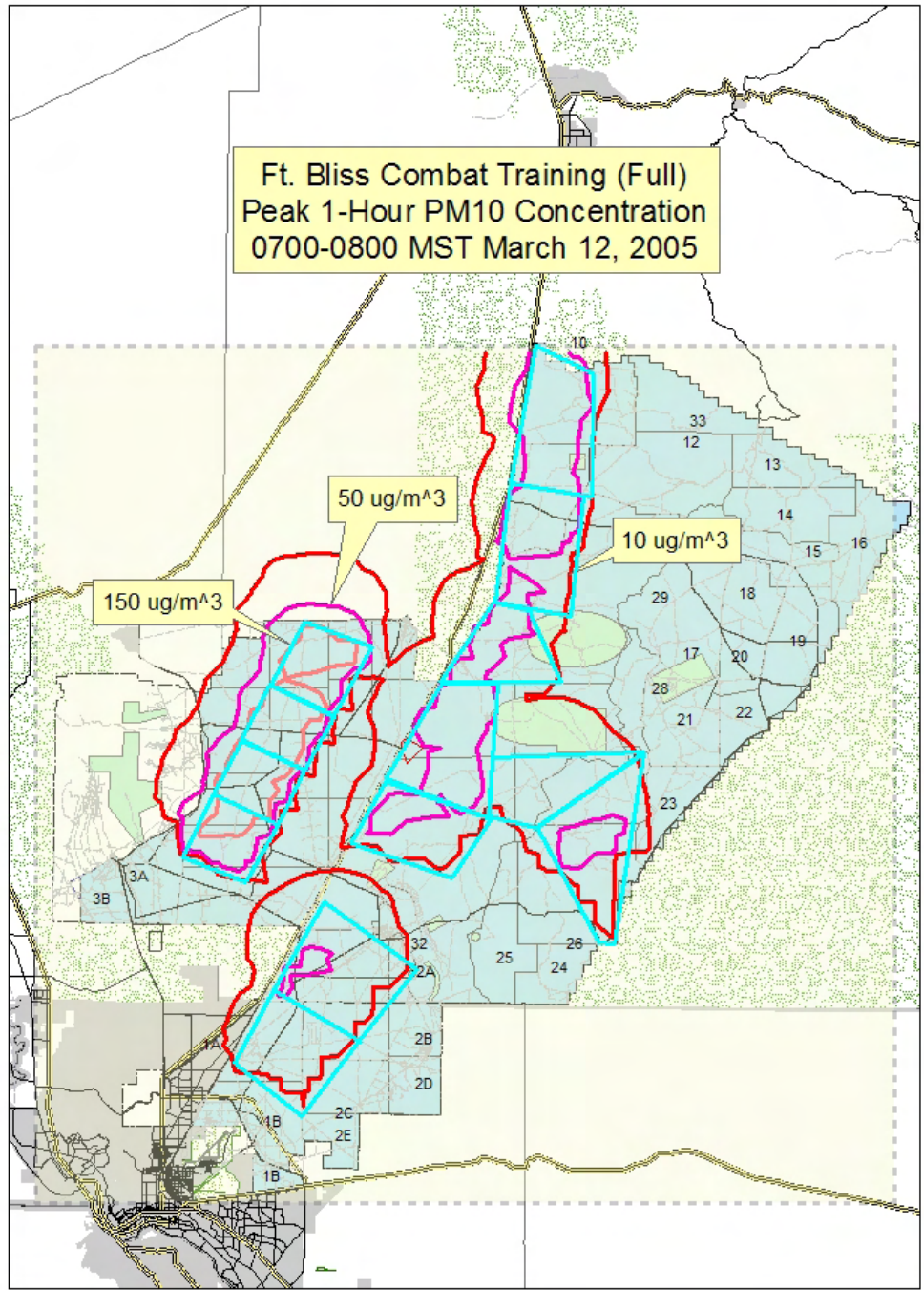


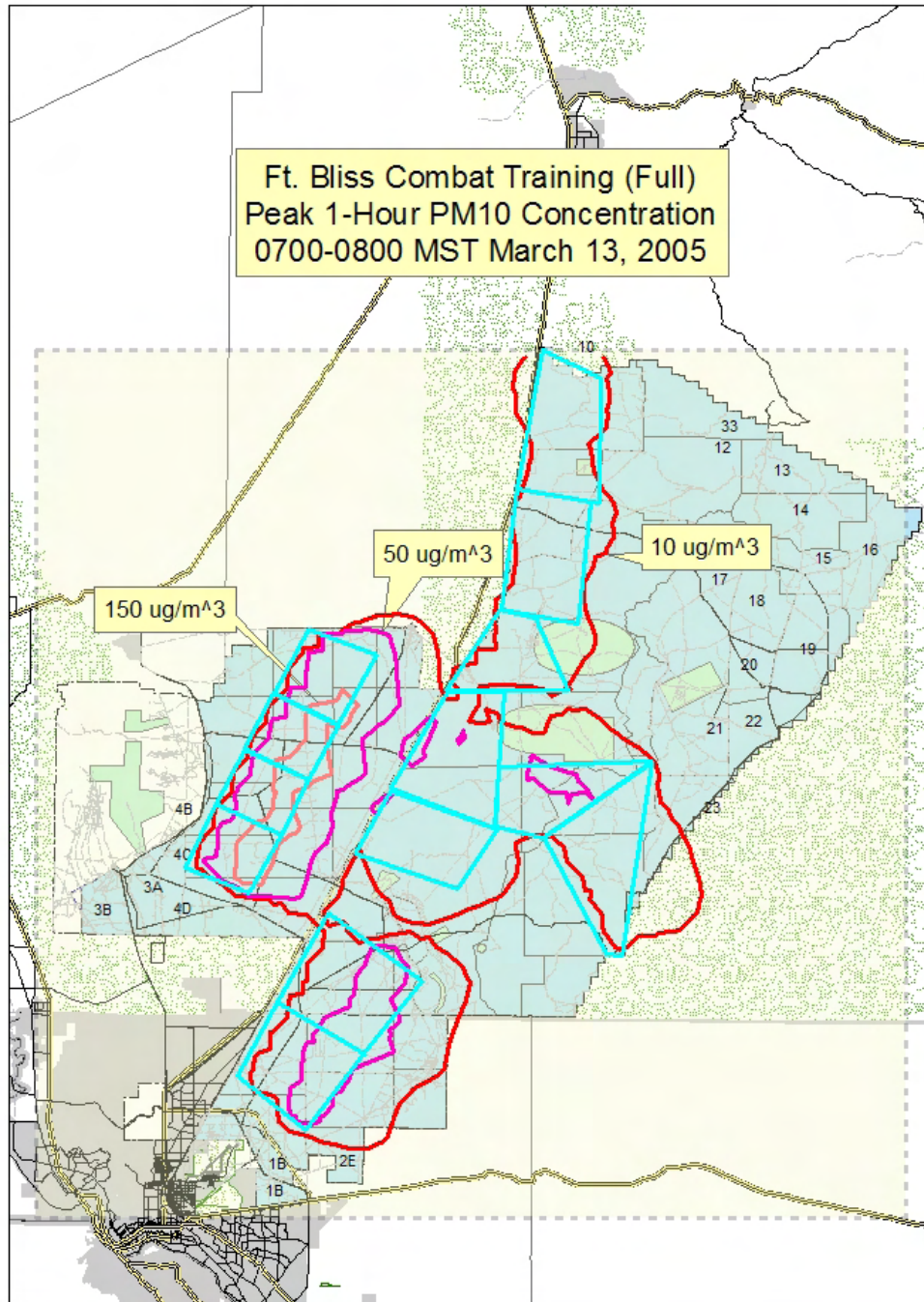
Appendix G

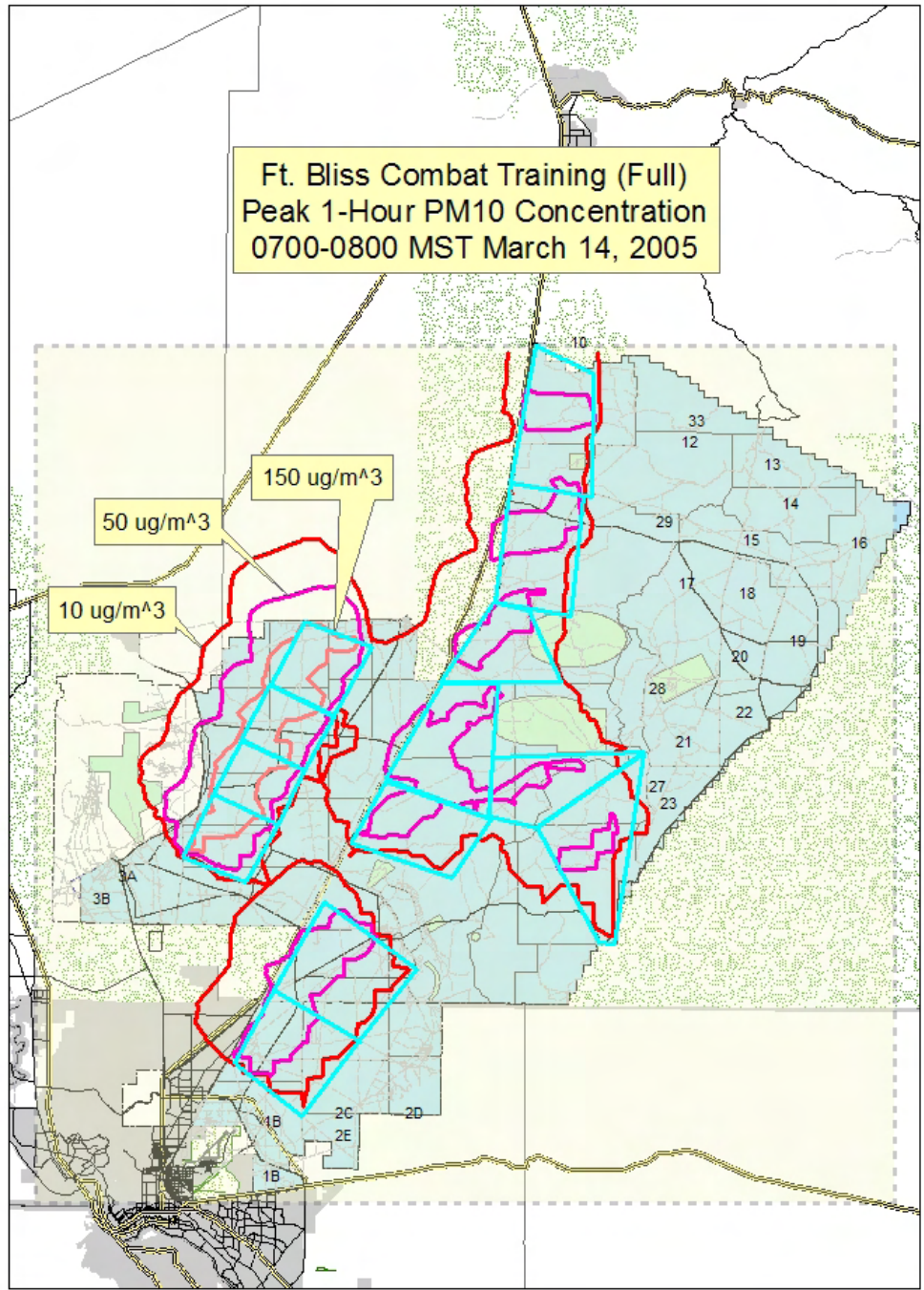
Simulated Peak 1-h-Average PM₁₀ Concentrations for Combat Training

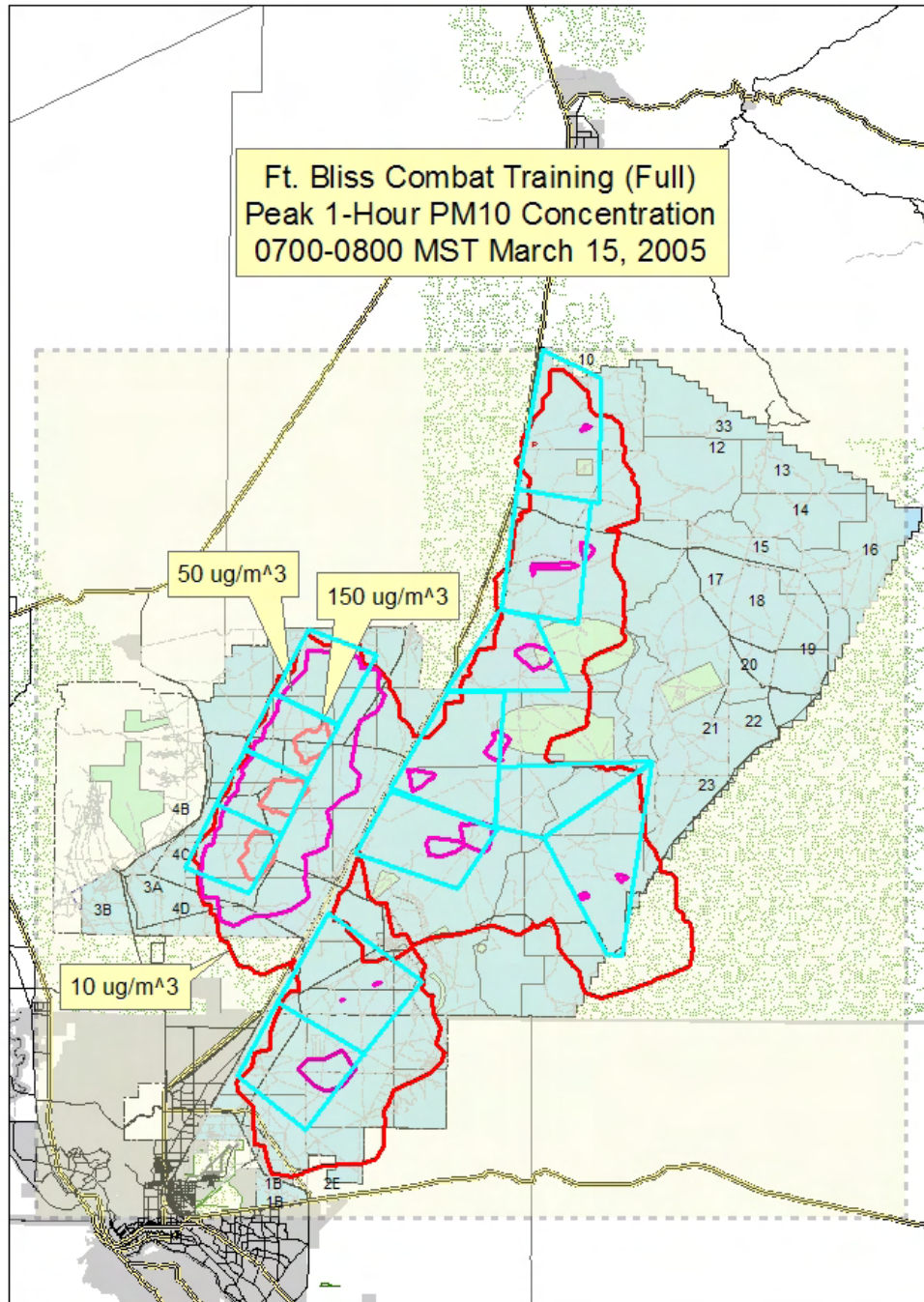
Appendix G: Simulated Peak 1-h-Average PM₁₀ Concentrations for Combat Training

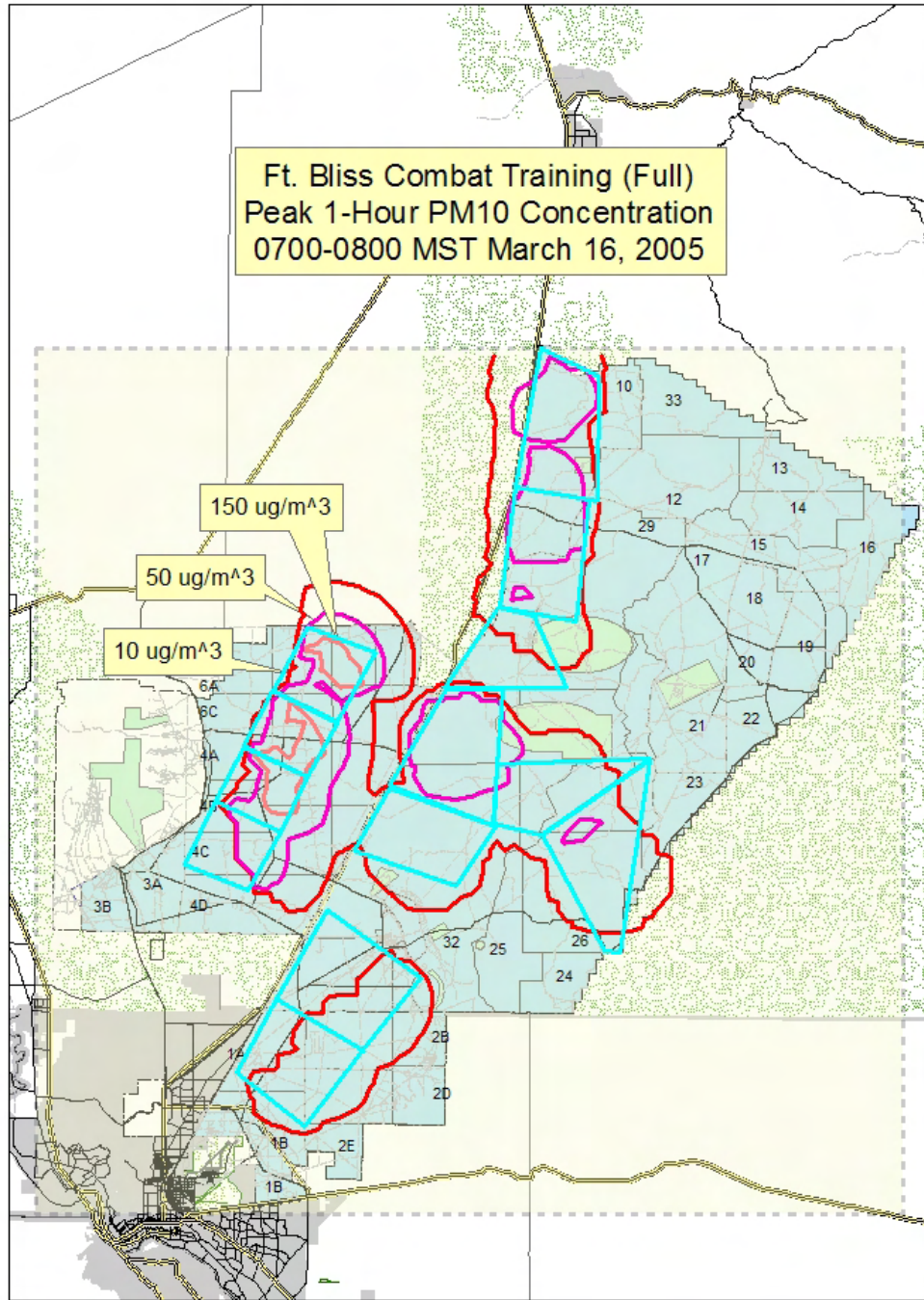
Contour maps of peak 1-hour-average PM₁₀ concentrations contributed from combat training activities to air quality in and around Fort Bliss are given for the 21 simulated days (March 12–16, April 25–30, July 20–24, and November 25–29, 2005). Each figure is for the hour of each day with the peak 1-hour-average concentration. The combat training scenario consists of training activities occurring concurrently in the Dona Ana 1 maneuver area, the McGregor maneuver area, and the South Training maneuver area.

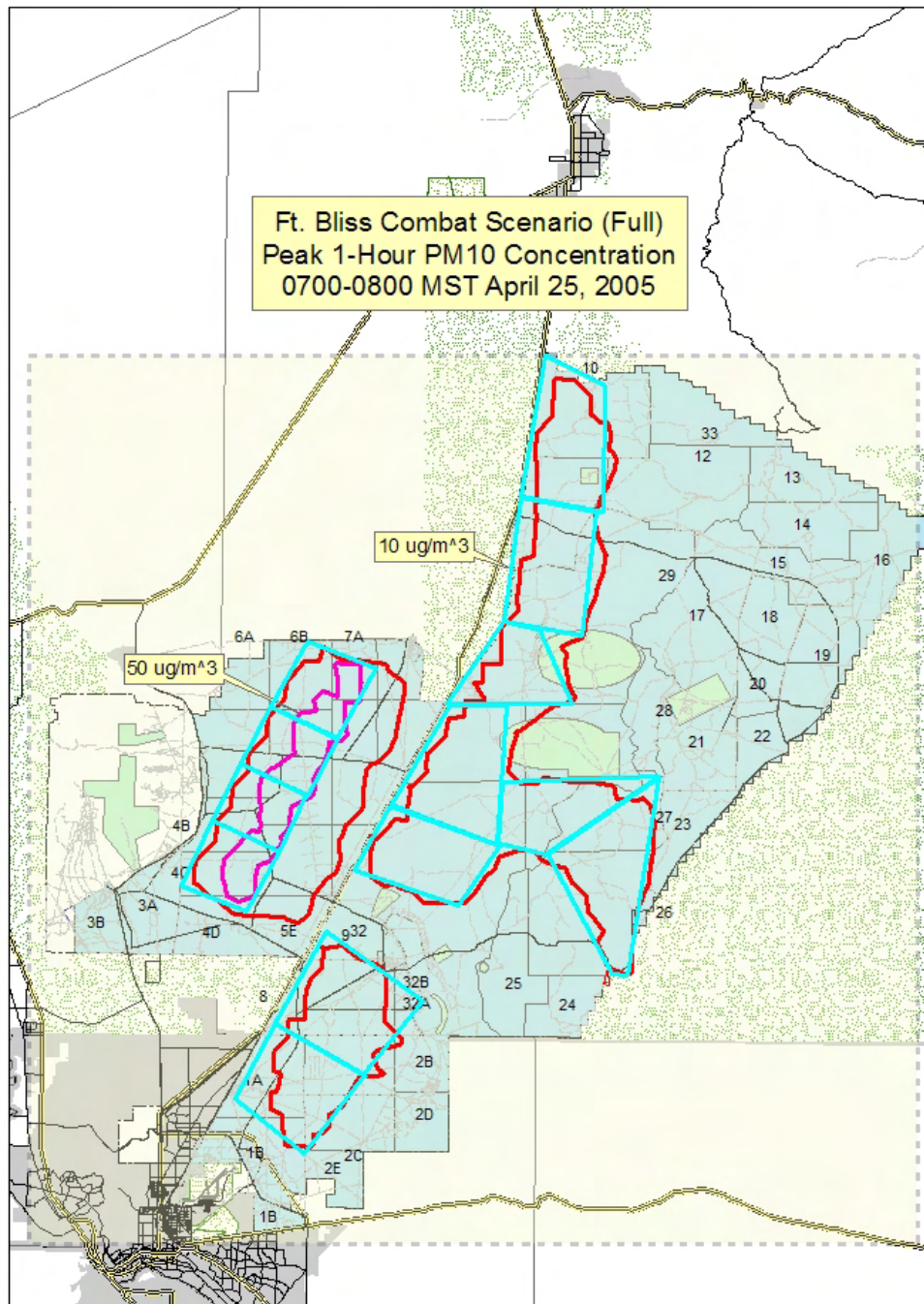


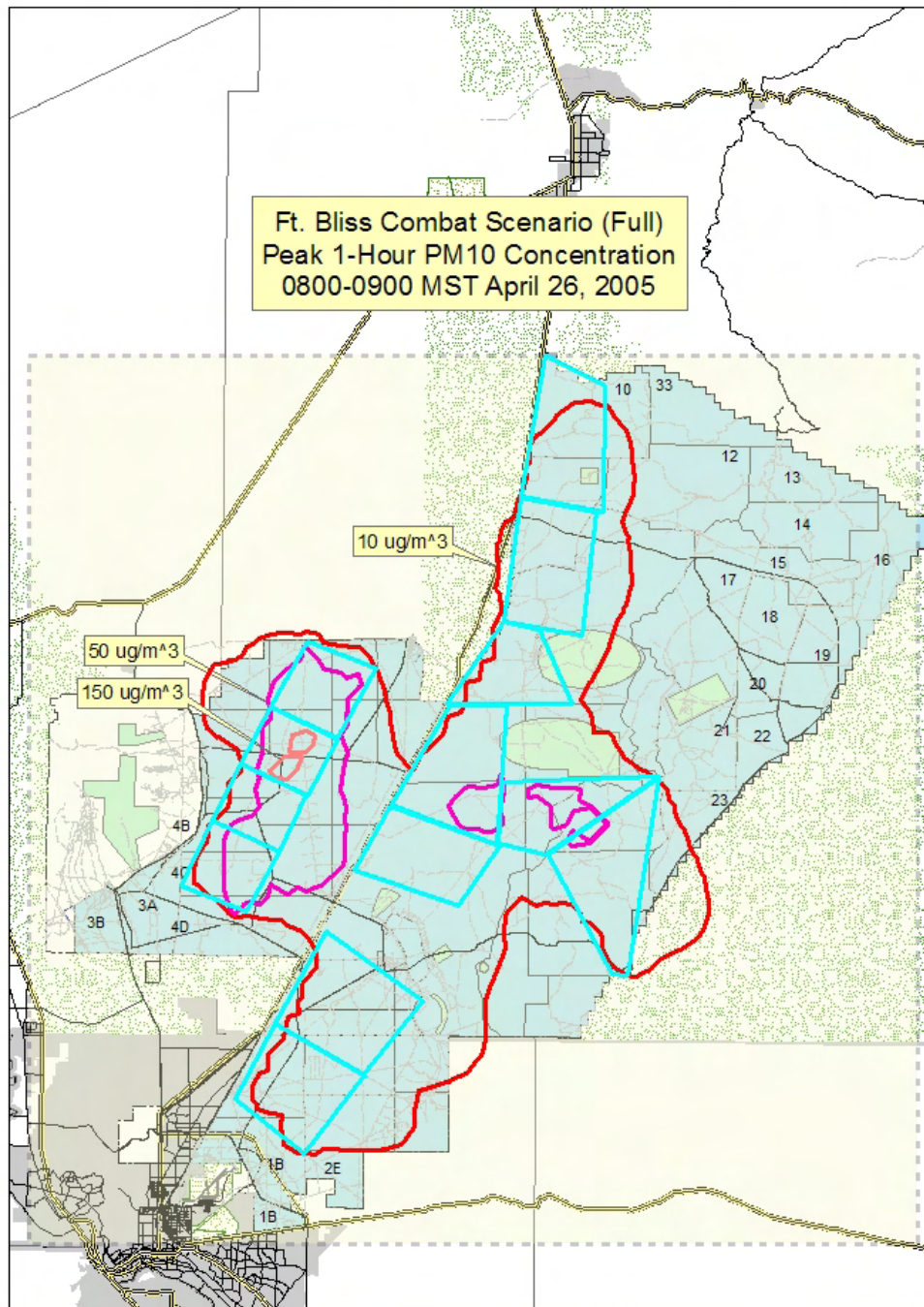


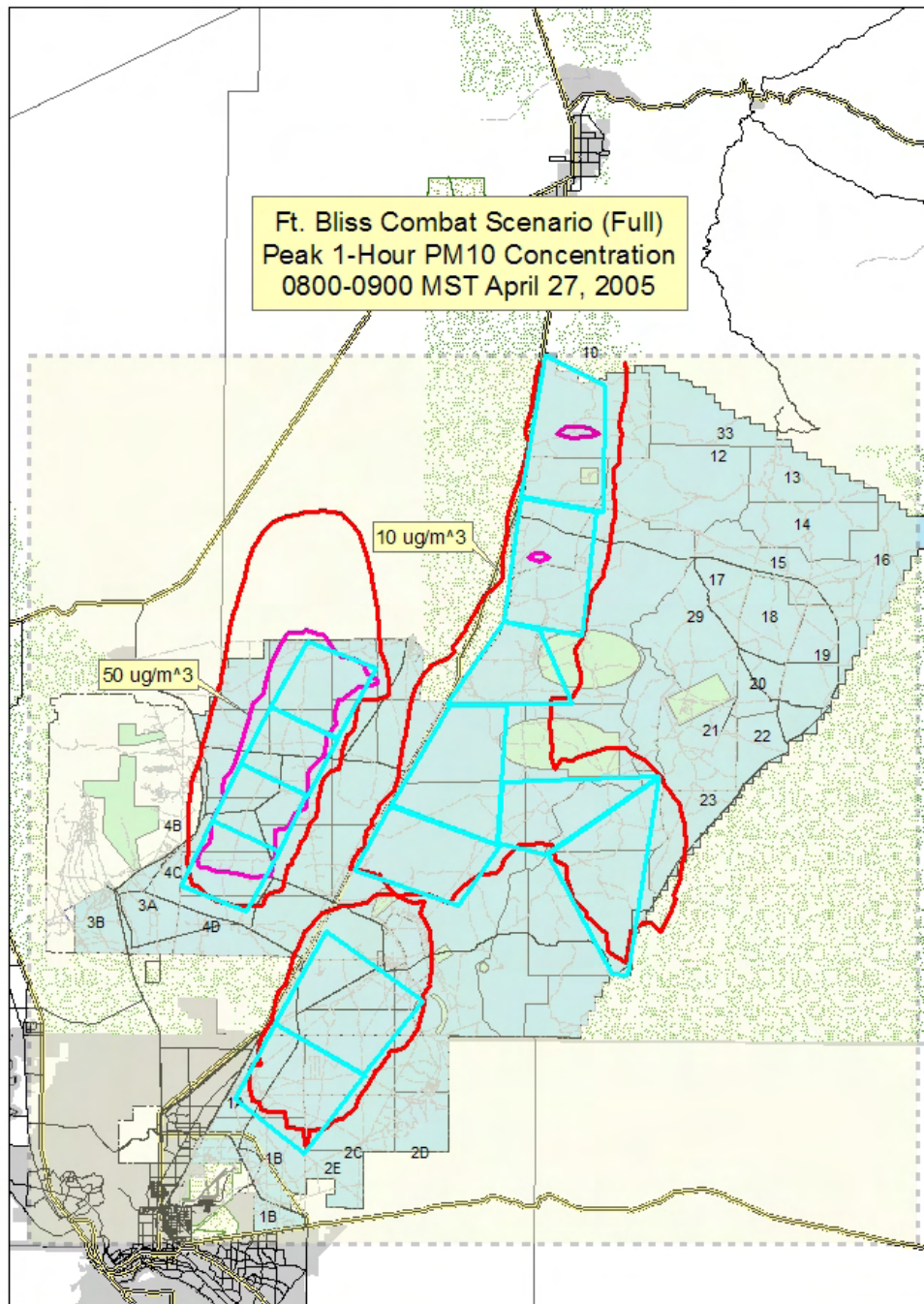


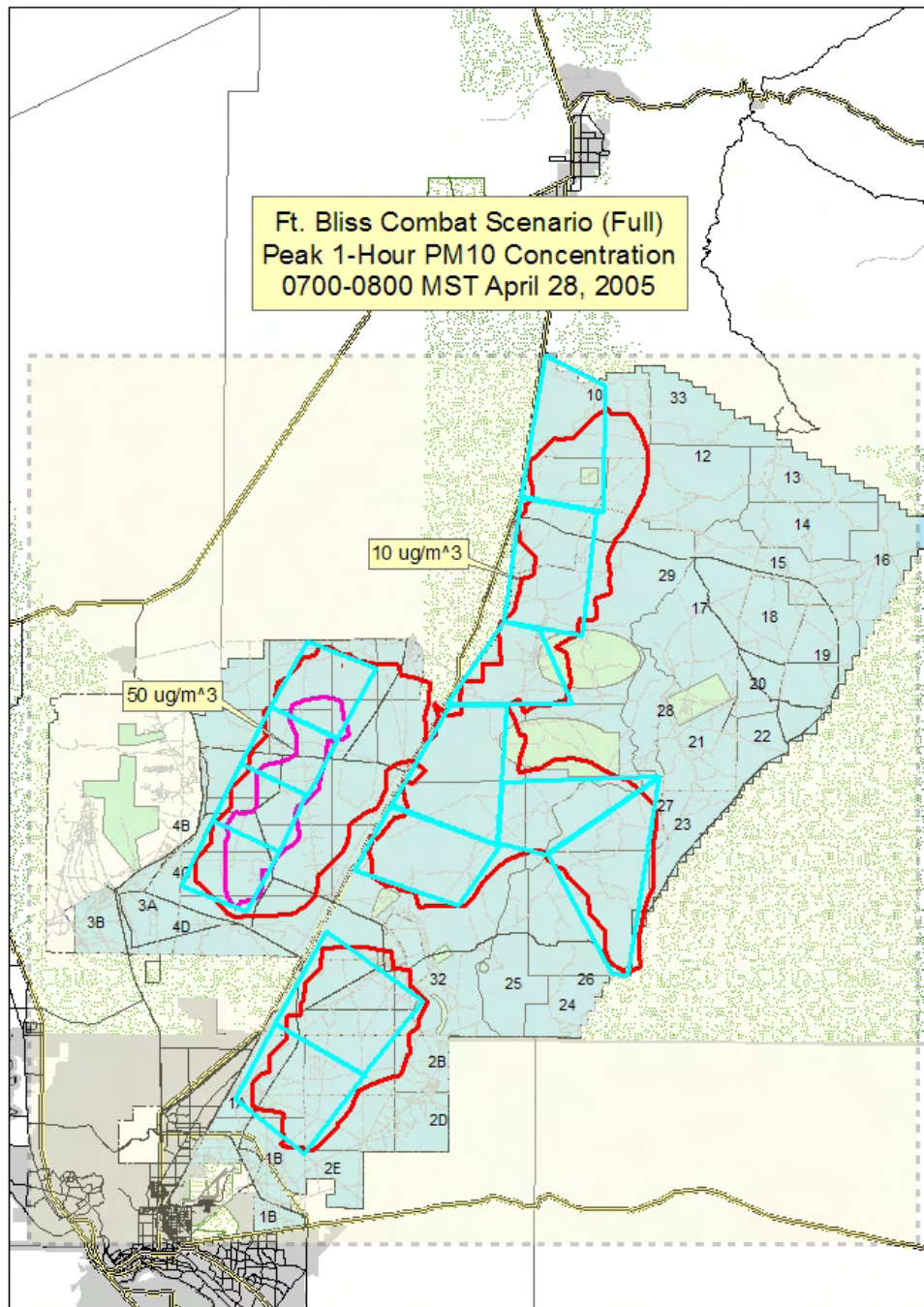


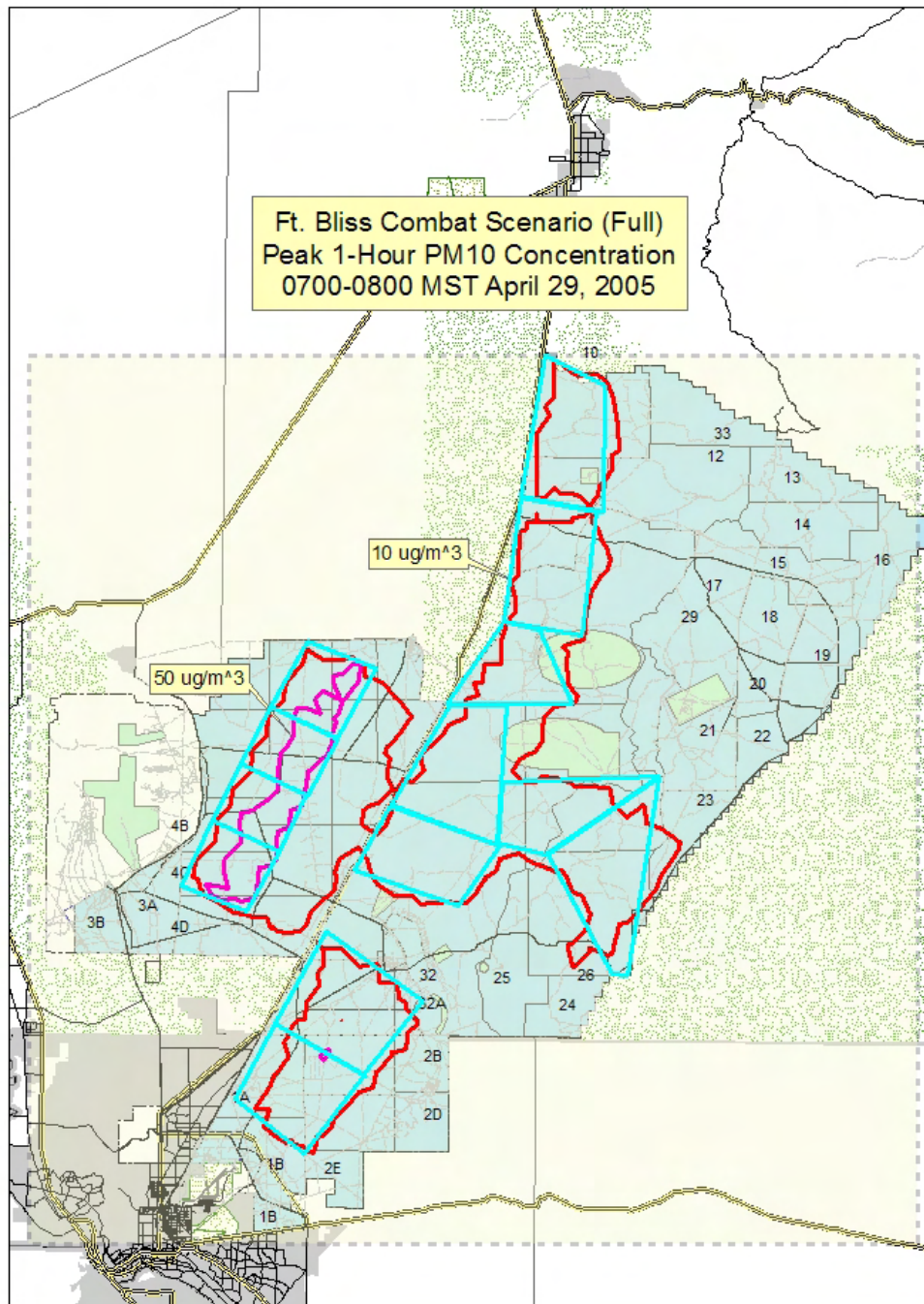


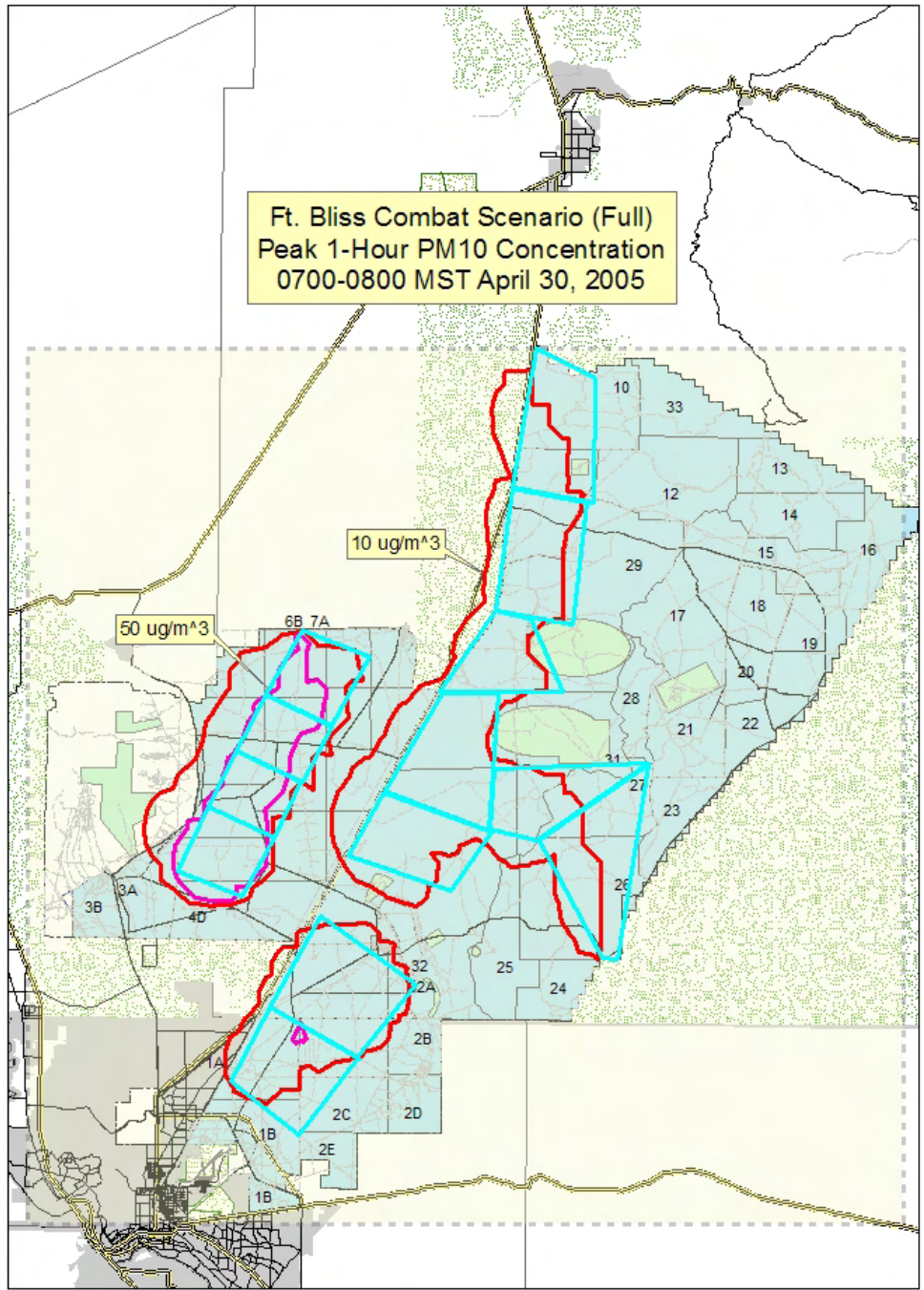


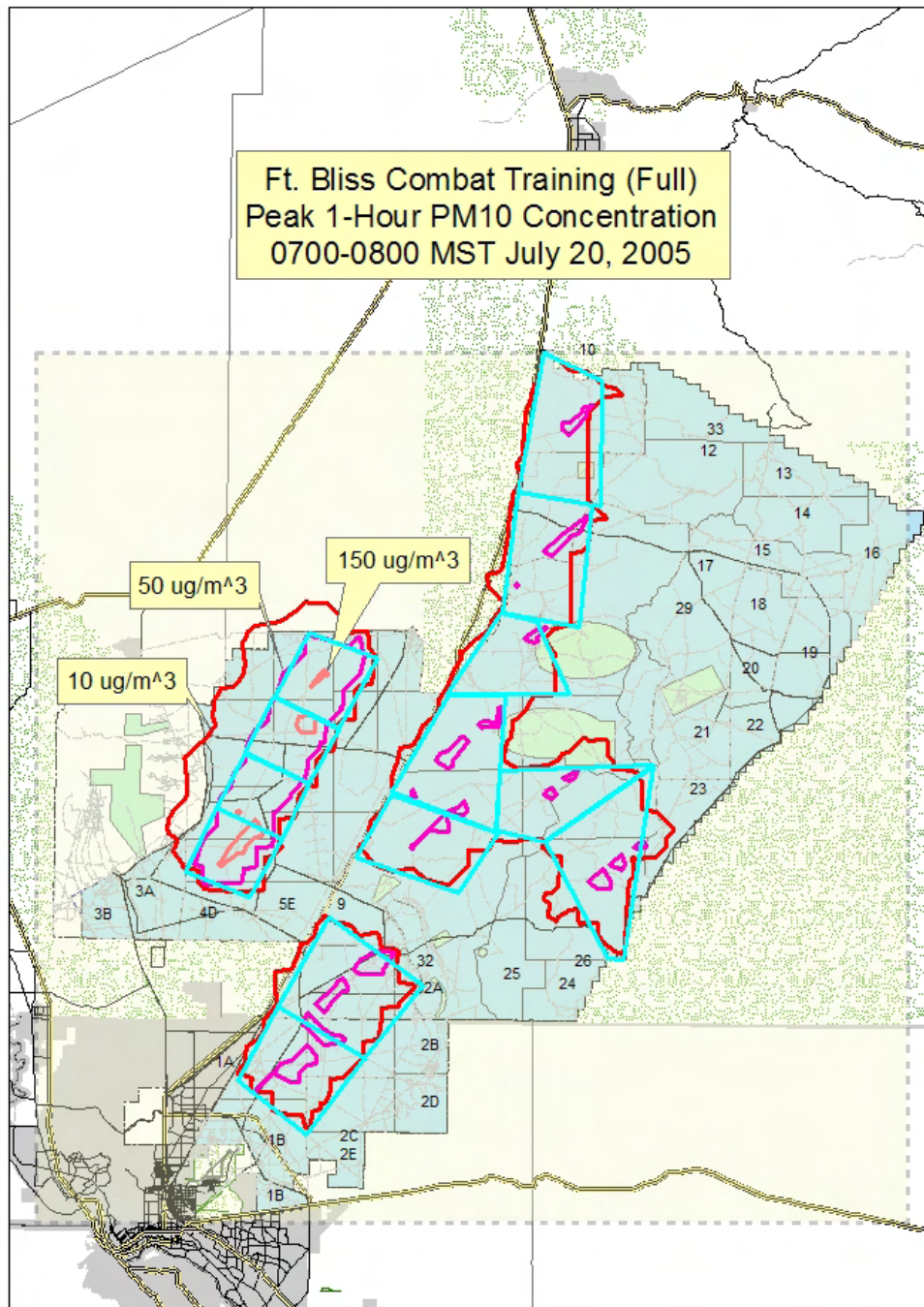


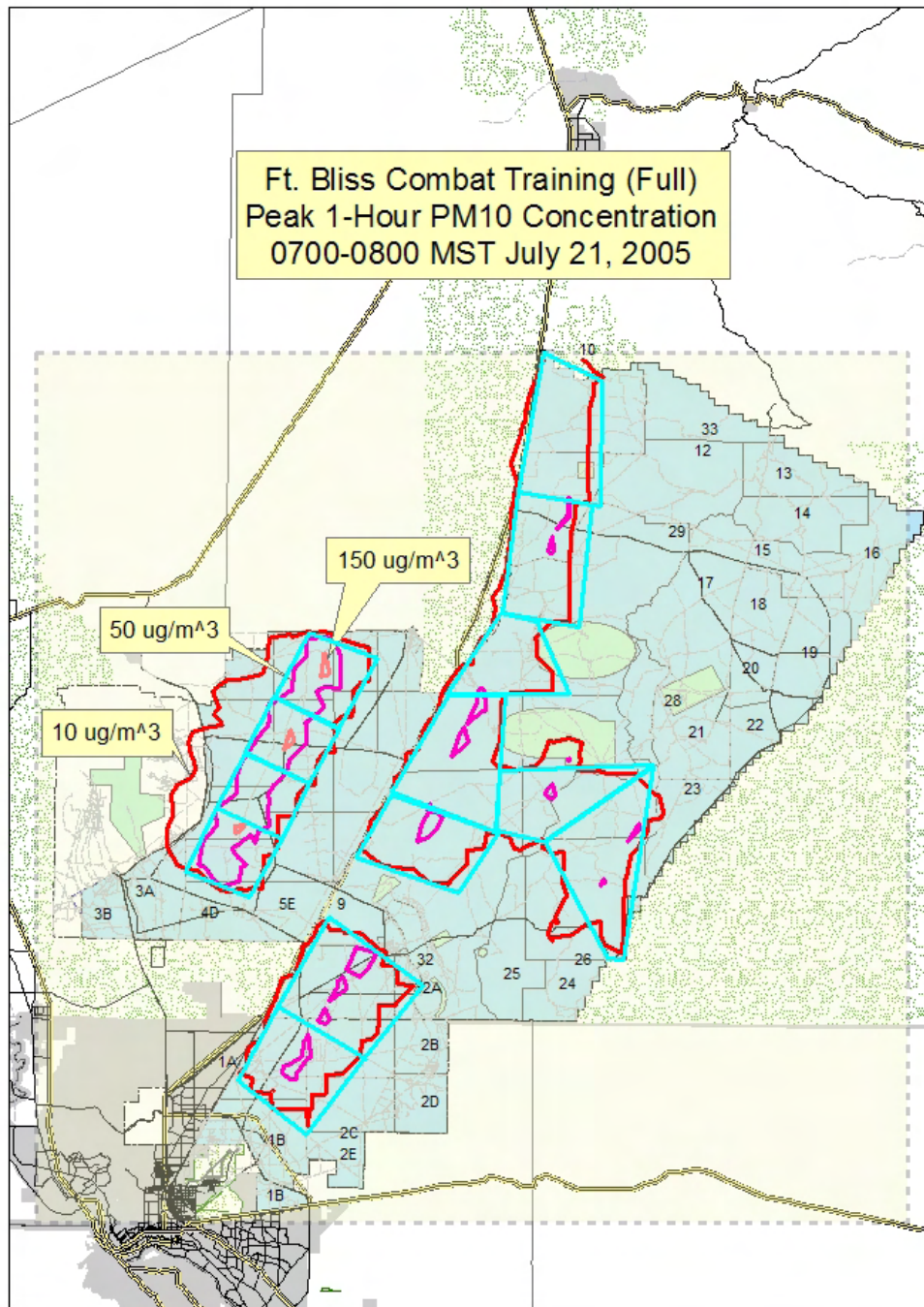


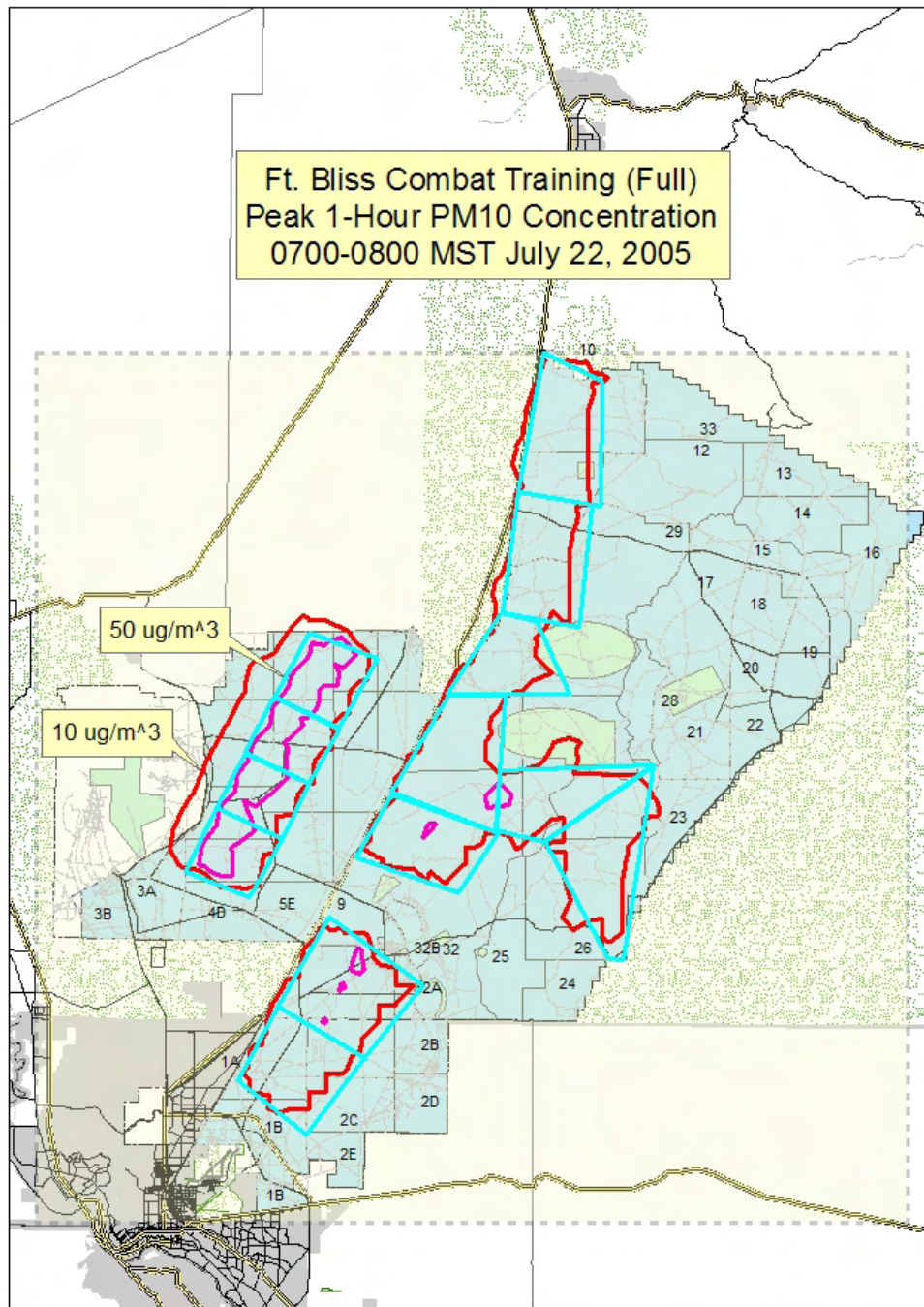


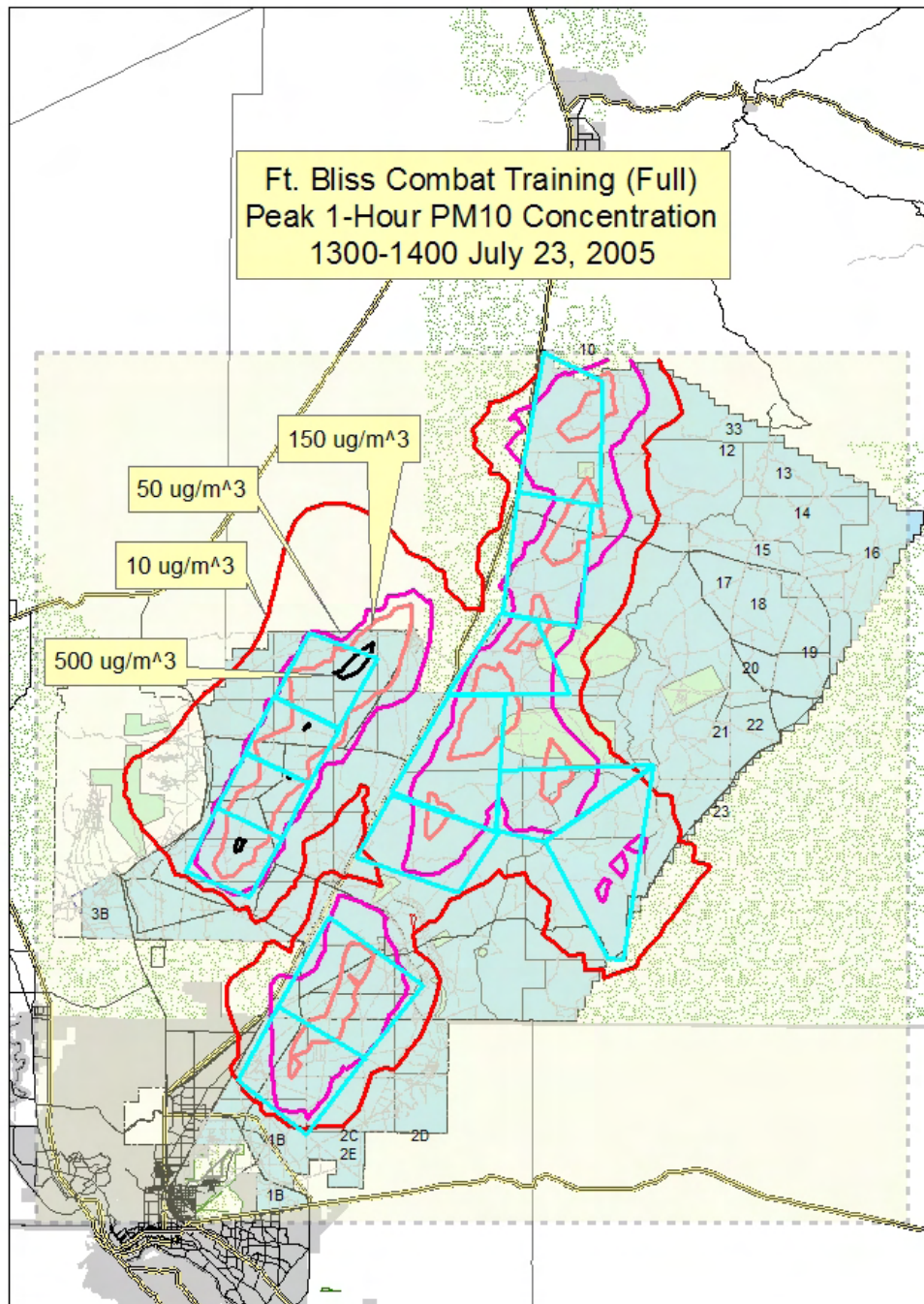


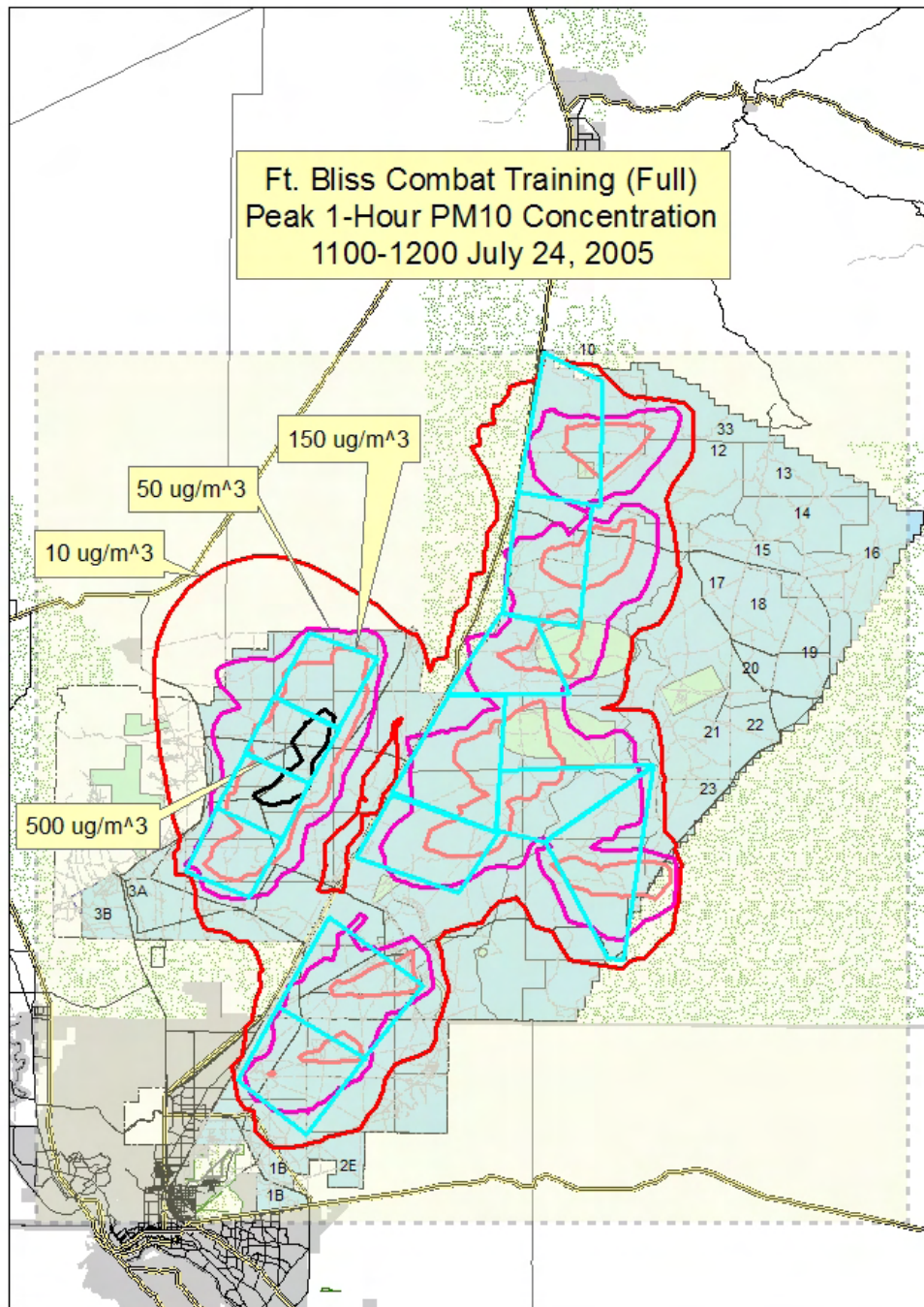


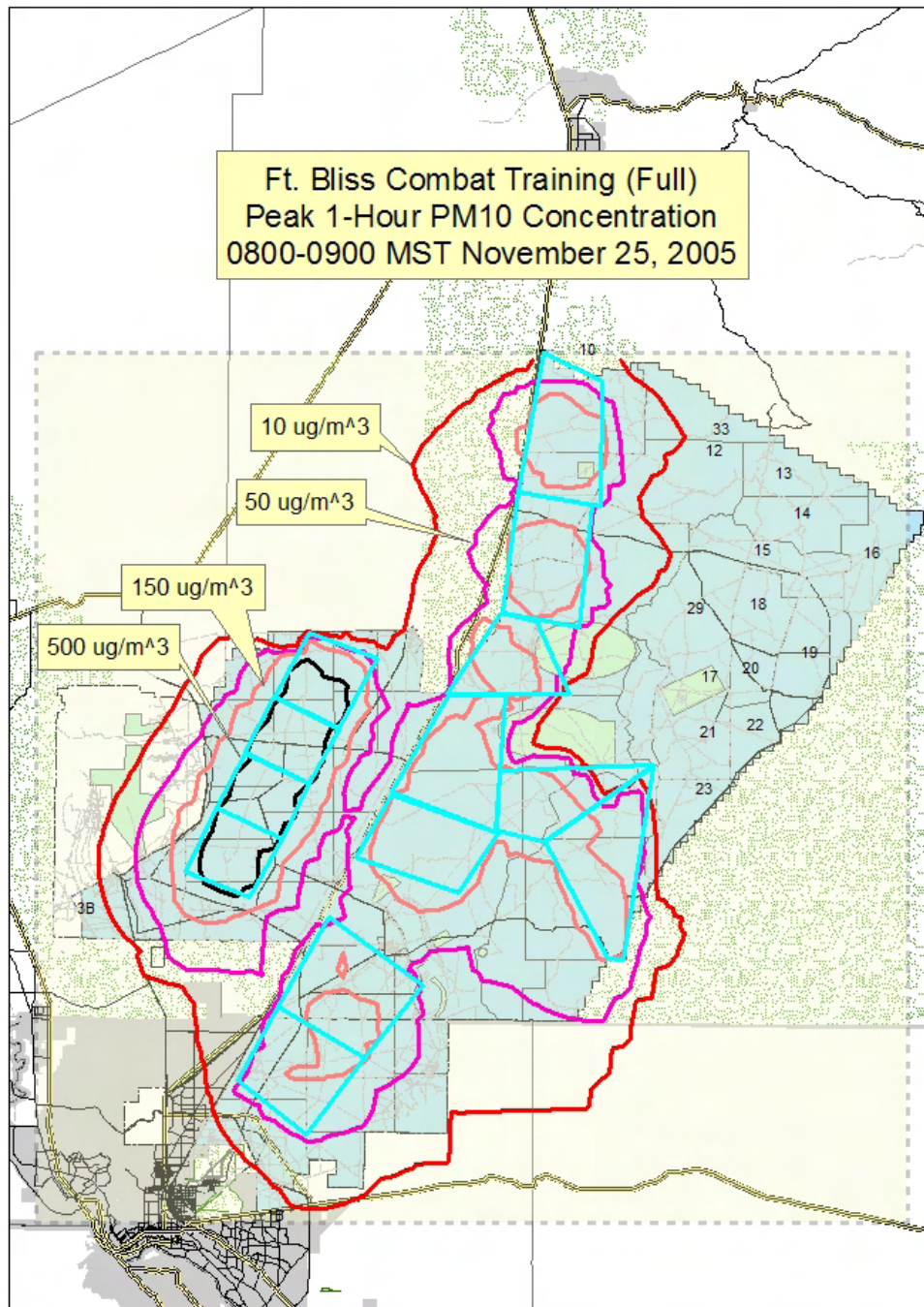


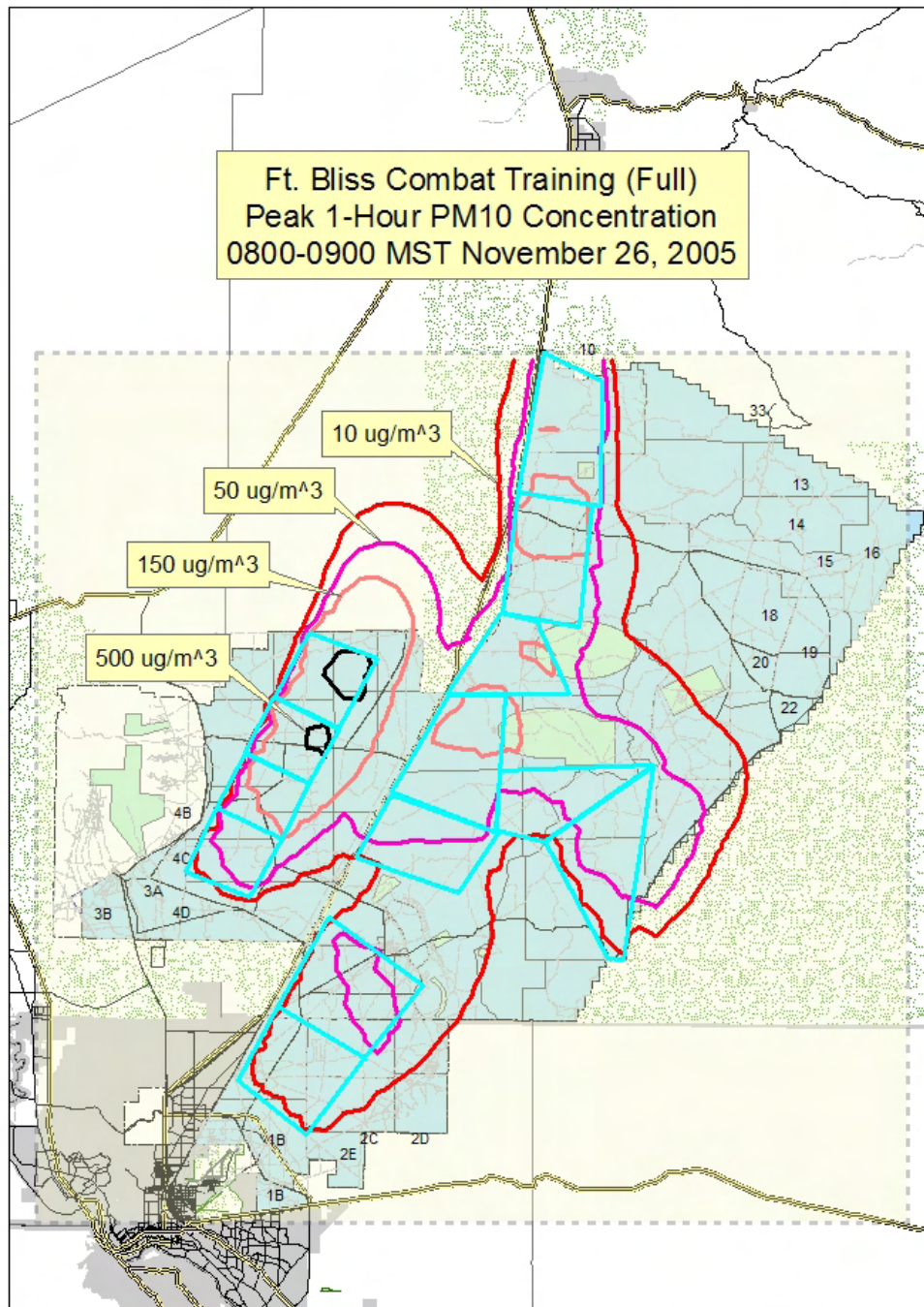


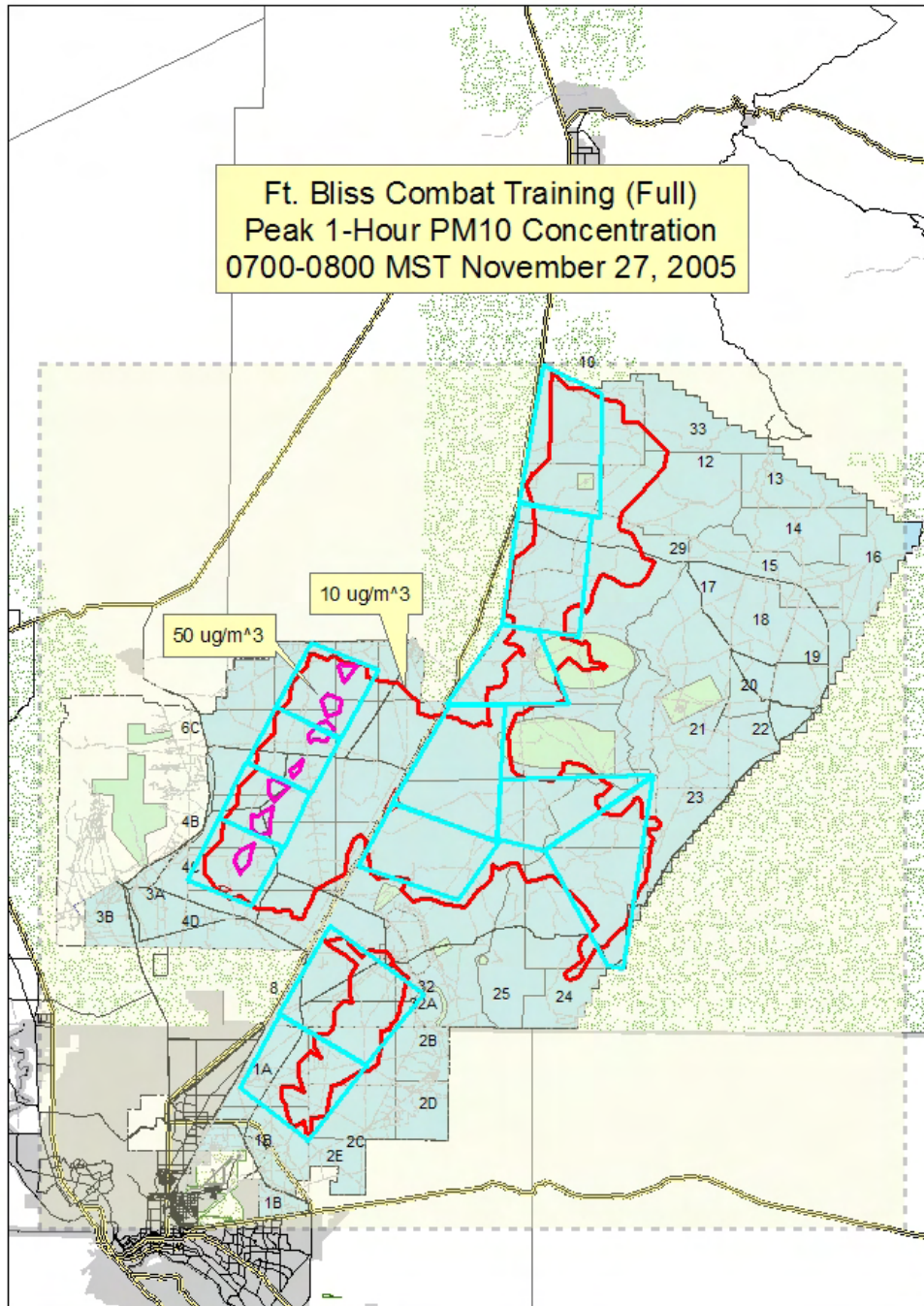


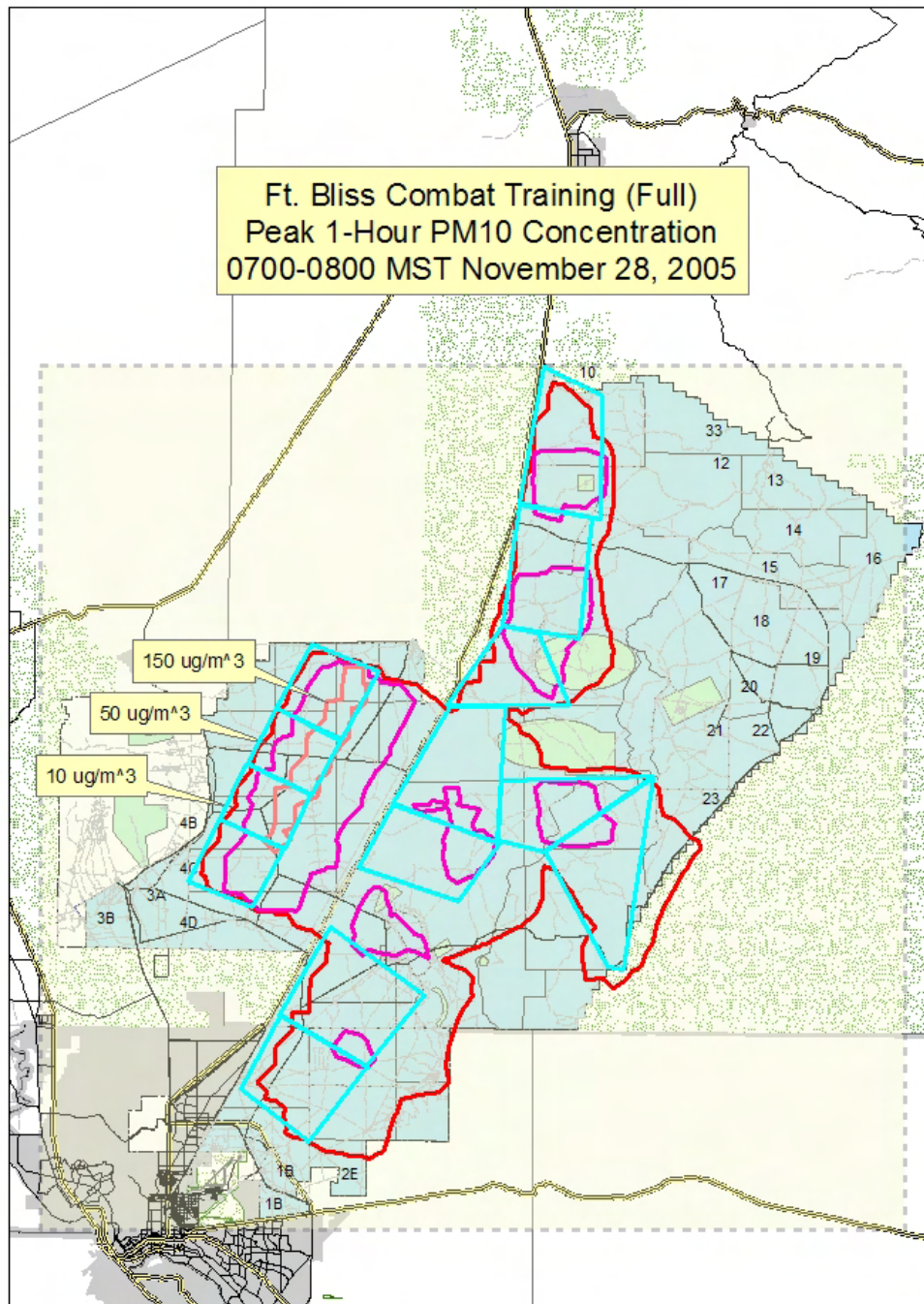


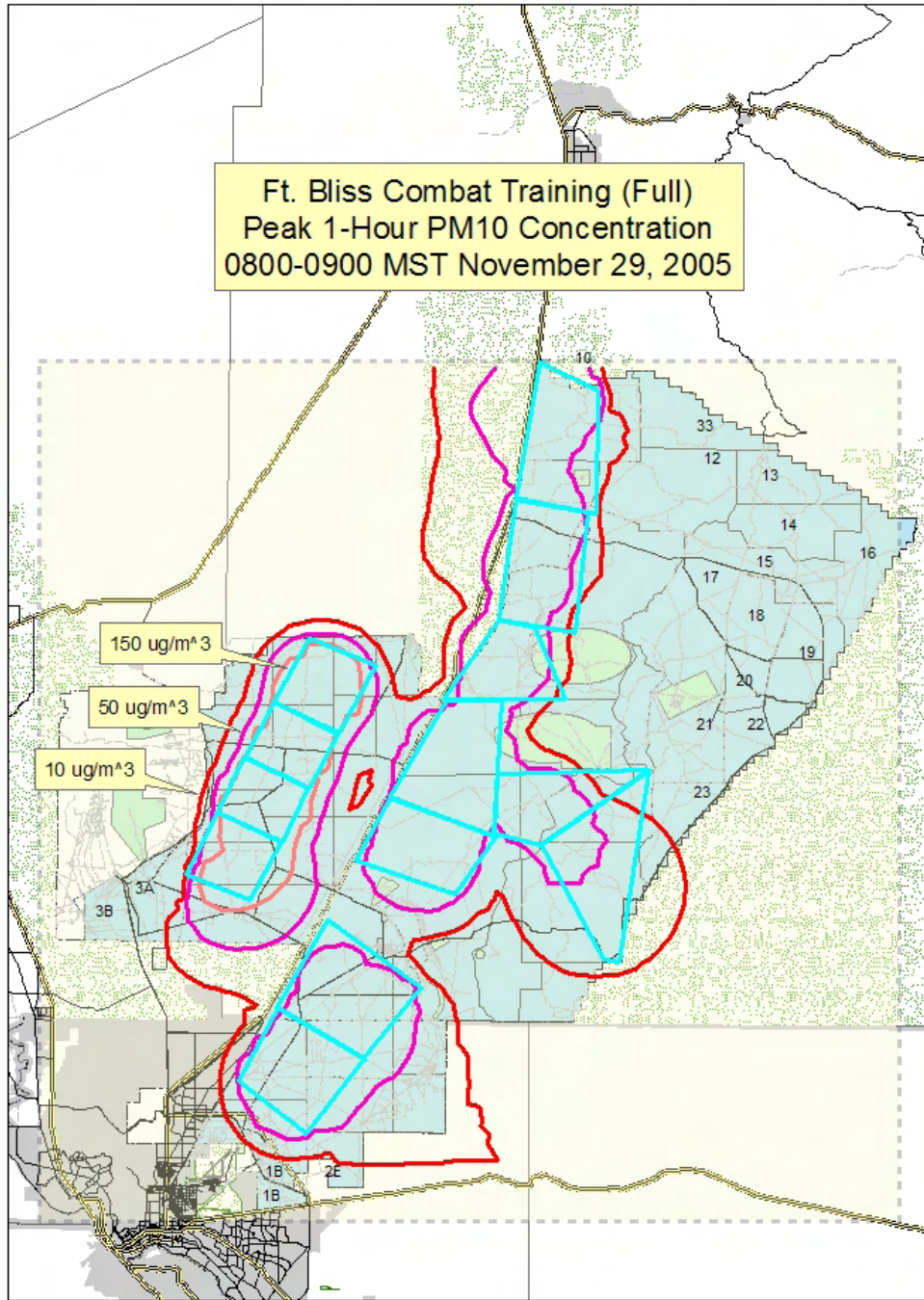










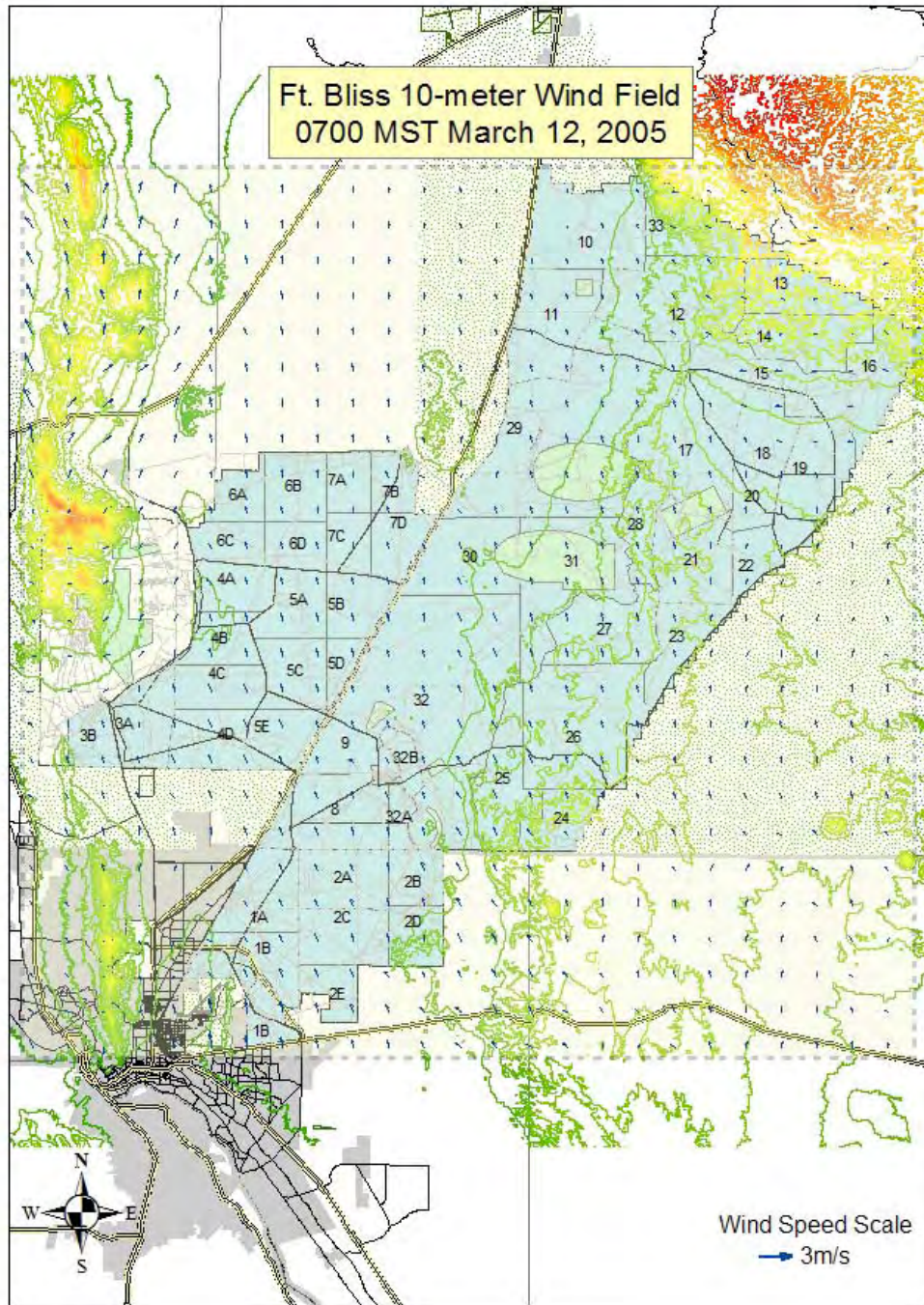


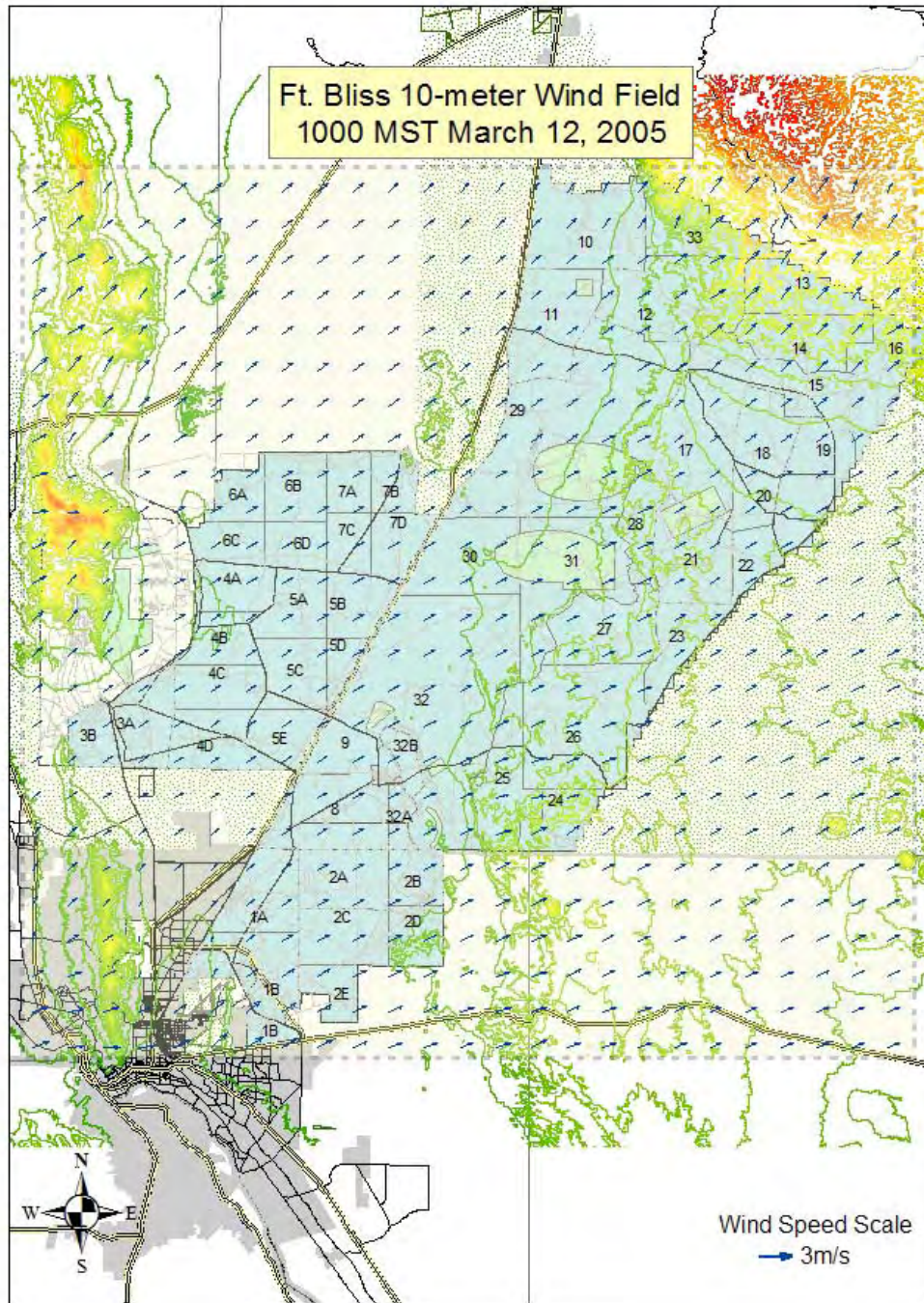
Appendix H

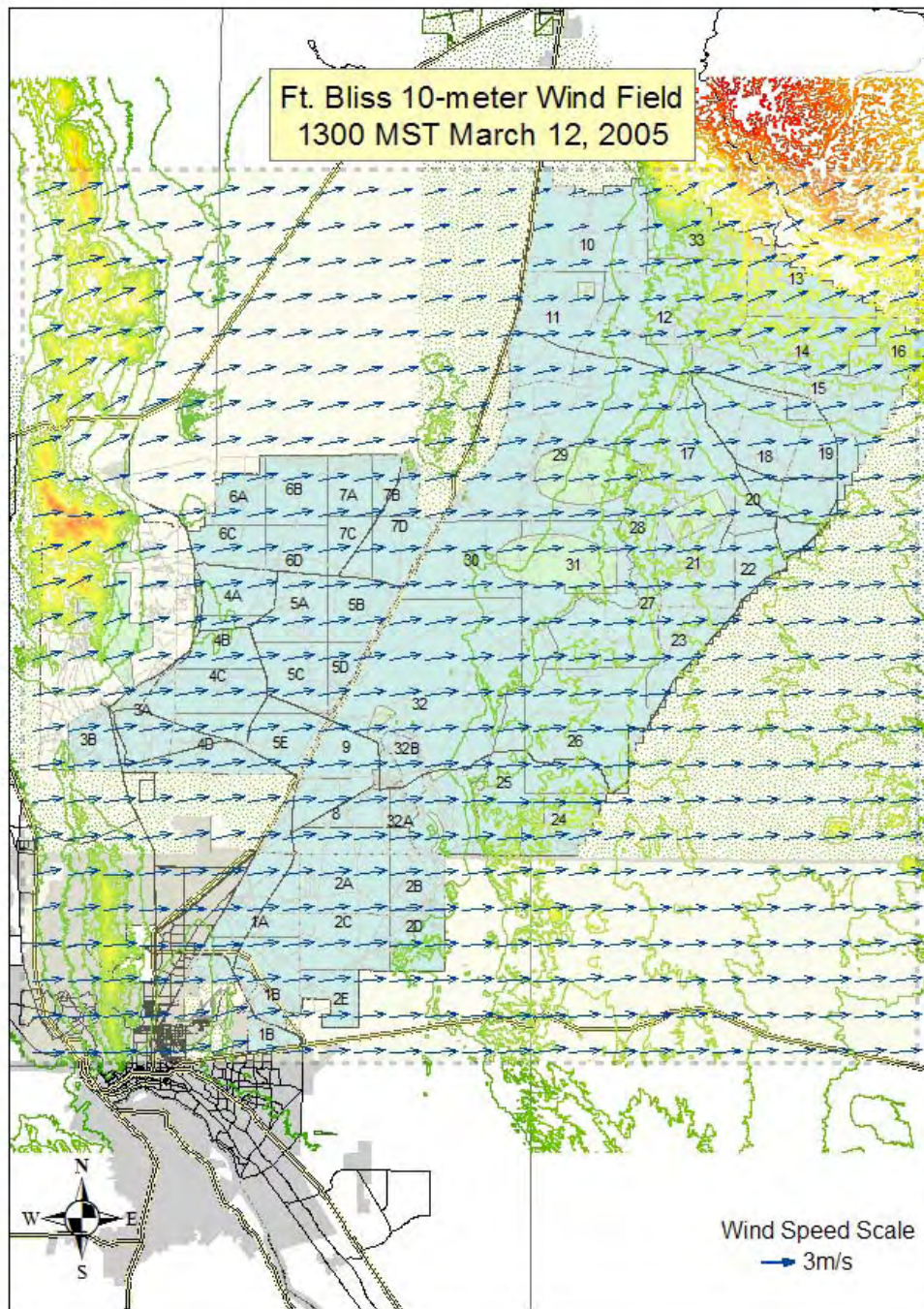
DUSTRAN 10-m-Above-Ground Wind Fields for March 12–16, 2005

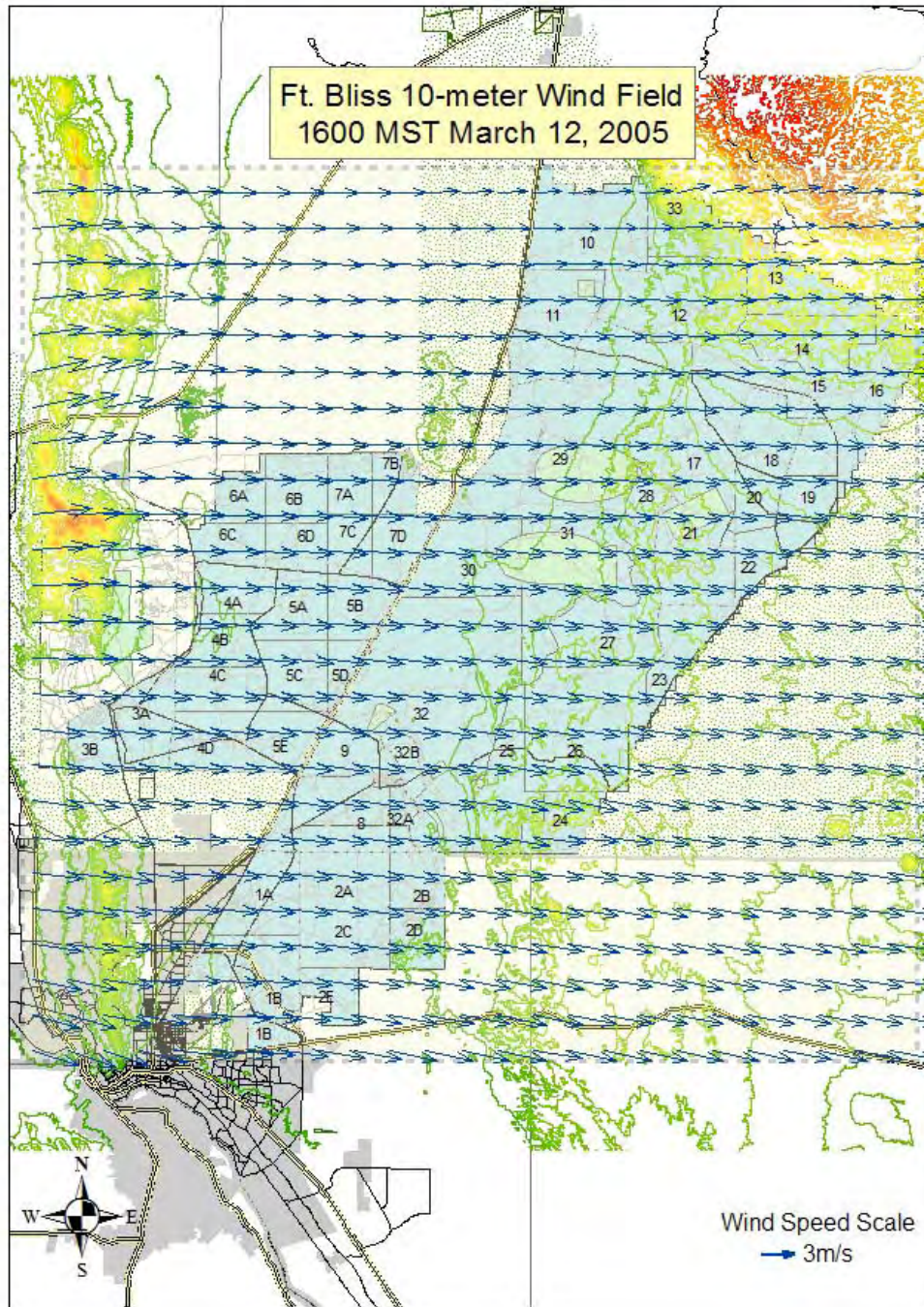
Appendix H: DUSTRAN 10-m-Above-Ground Wind Fields for March 12–16, 2005

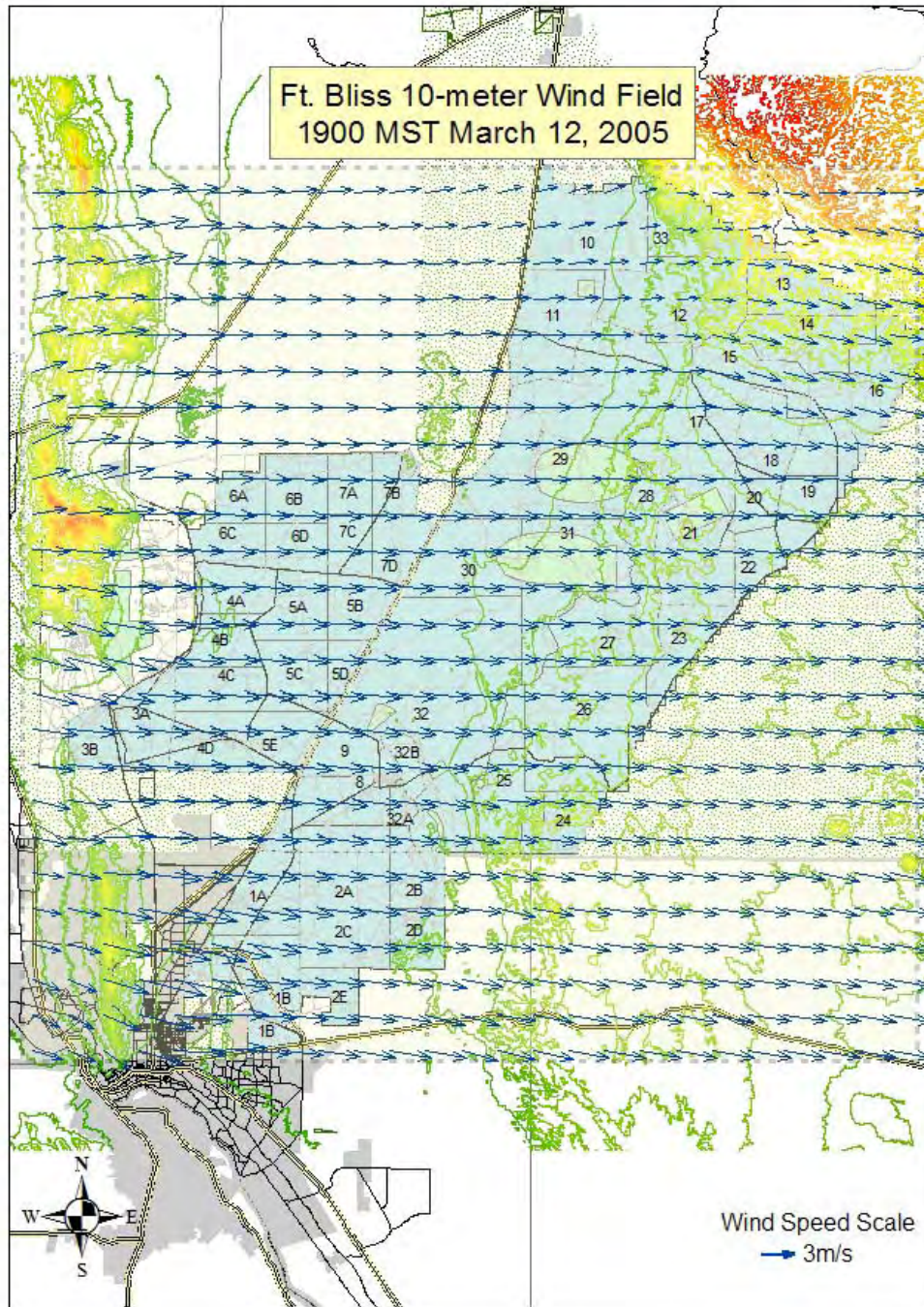
This appendix contains 25 screen captures of the 10-m above-ground wind fields predicted by the CALMET model within DUSTRAN. Wind fields are shown at 0700, 1000, 1300, 1600, and 1900 MST for the 5 days included in the current simulations (March 12 through 16, 2005). Header captions within each figure indicate the day and time represented by a given plot. The arrow on each vector indicates wind direction while the scaling of vector length indicates wind speed. A reference vector whose length represents a wind speed of 3 m/s is shown on each plot.

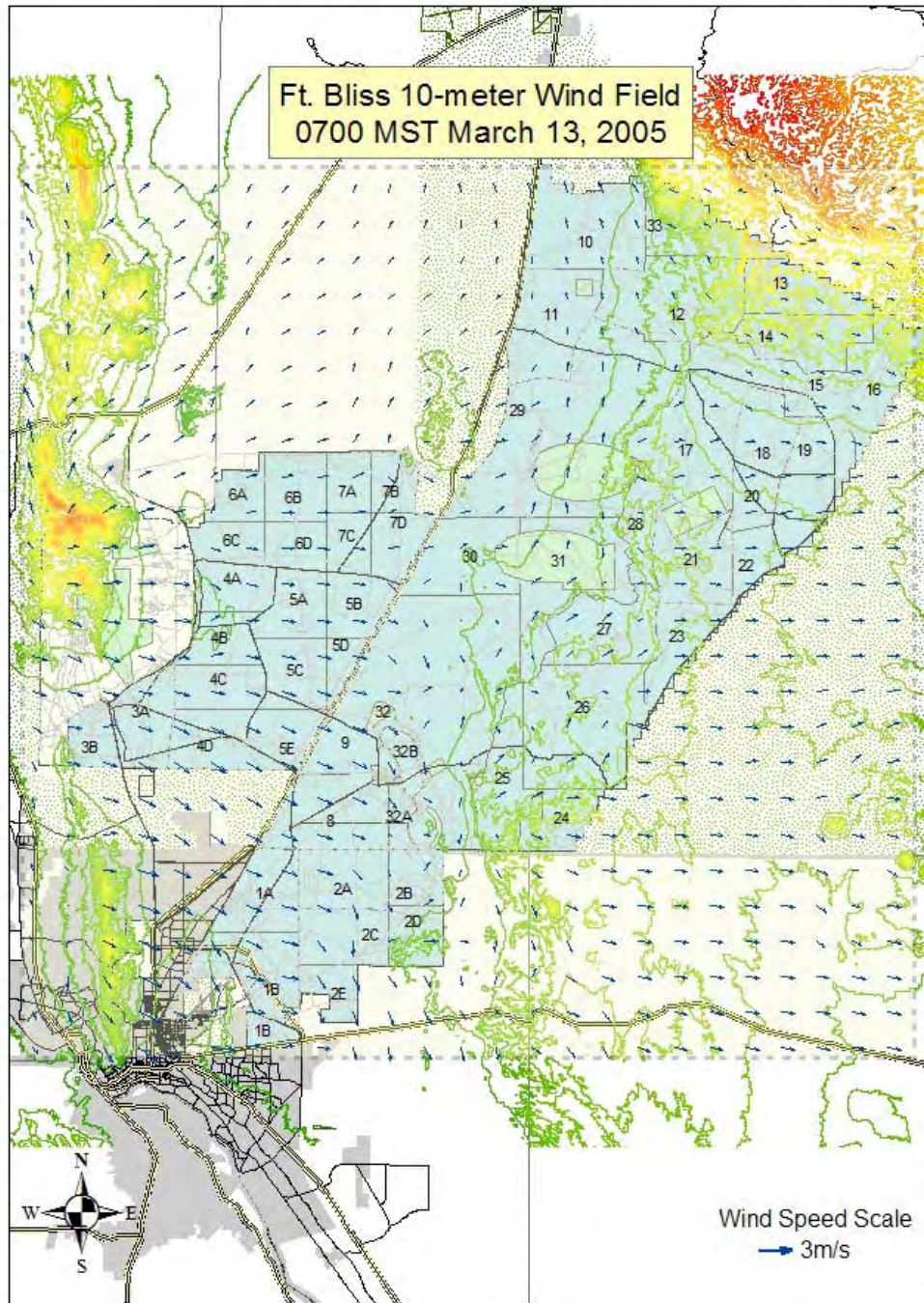


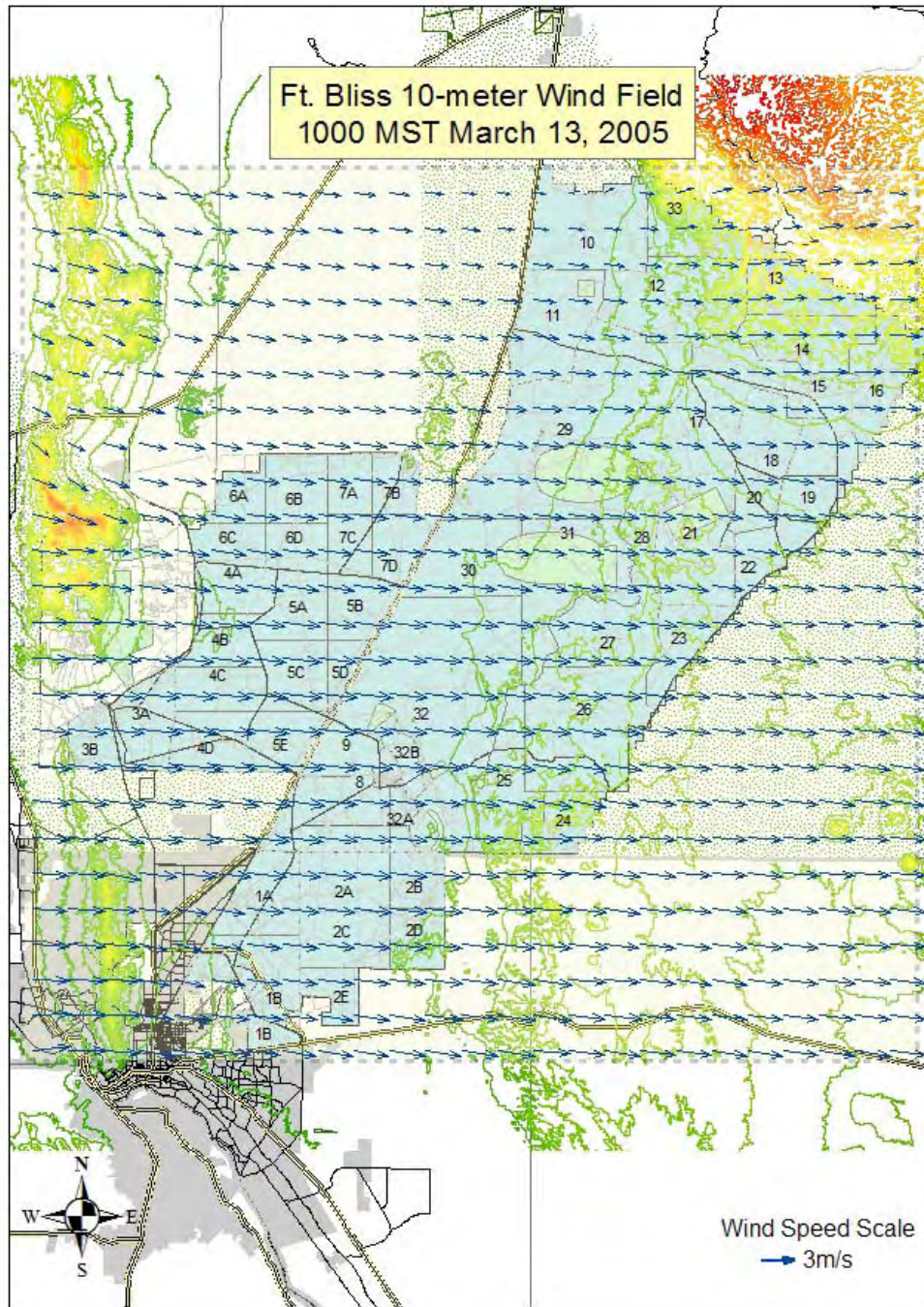


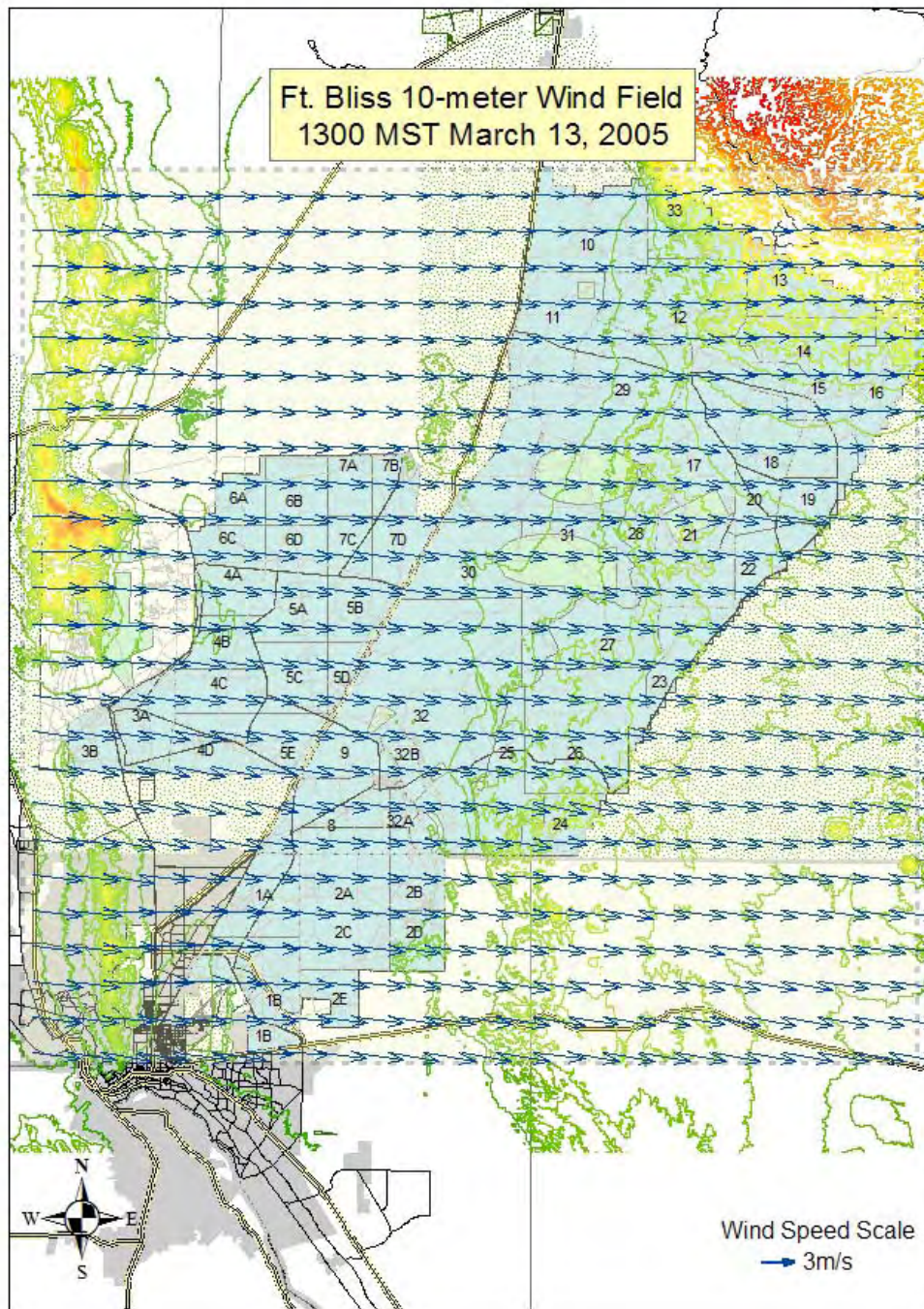


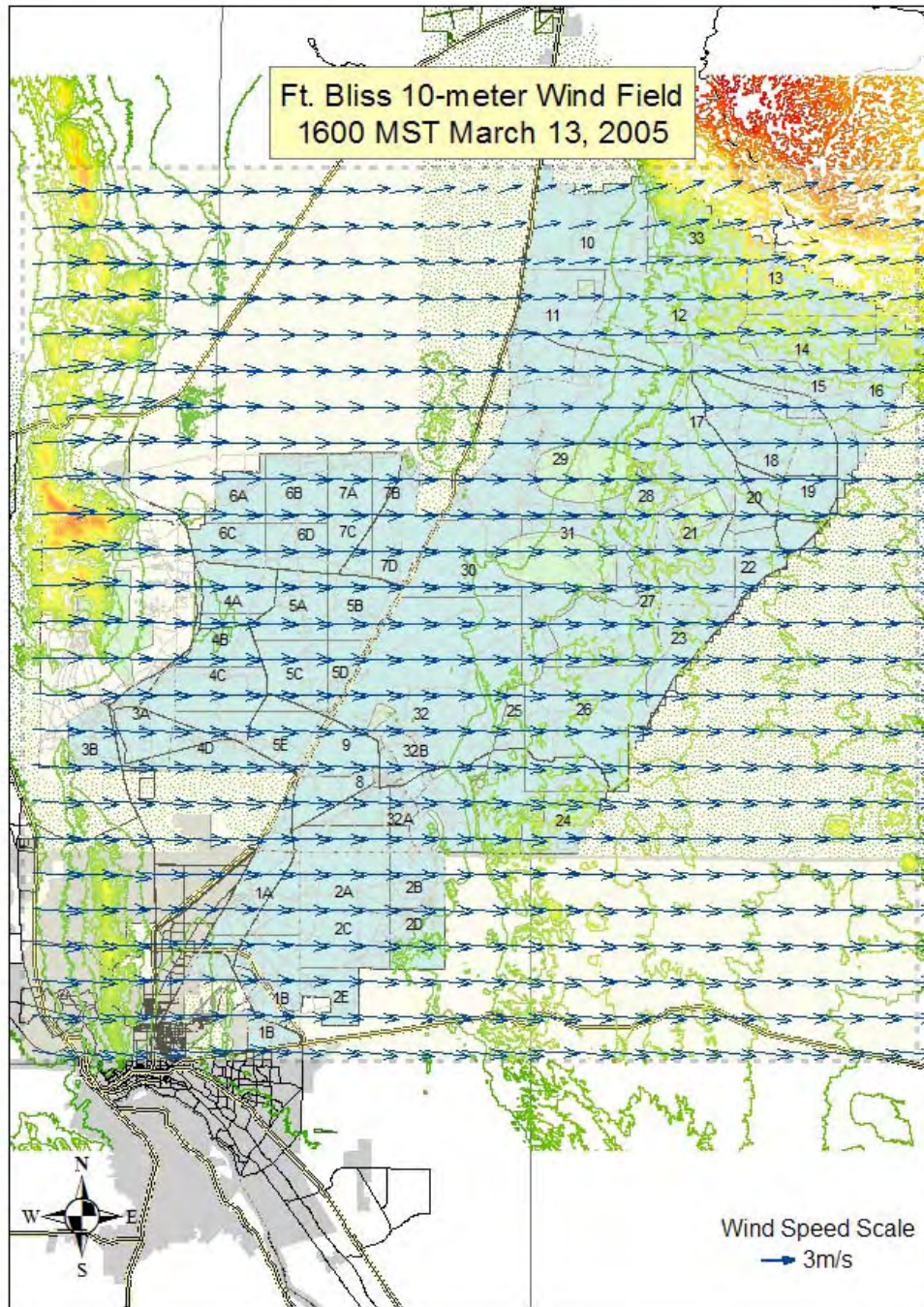


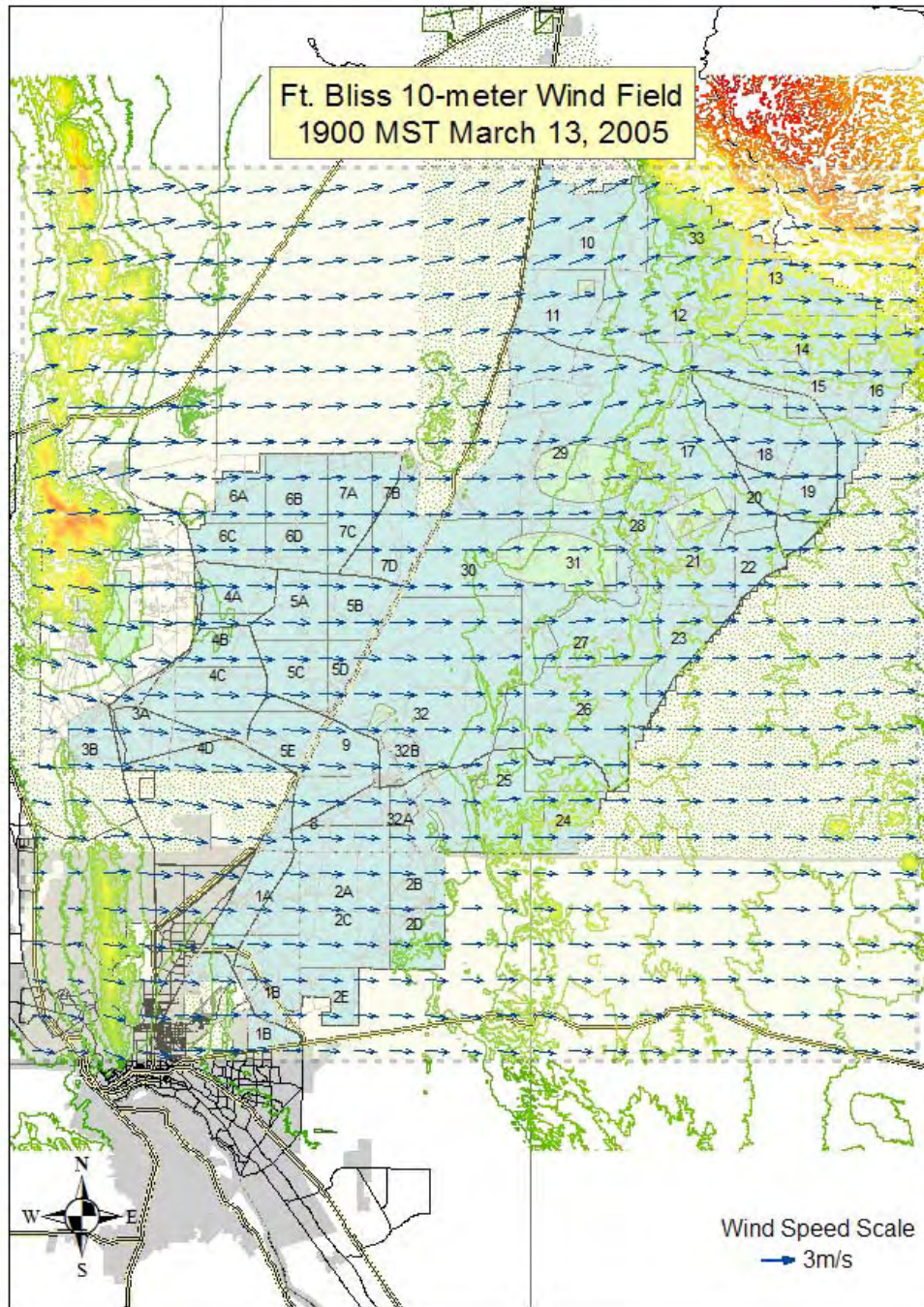


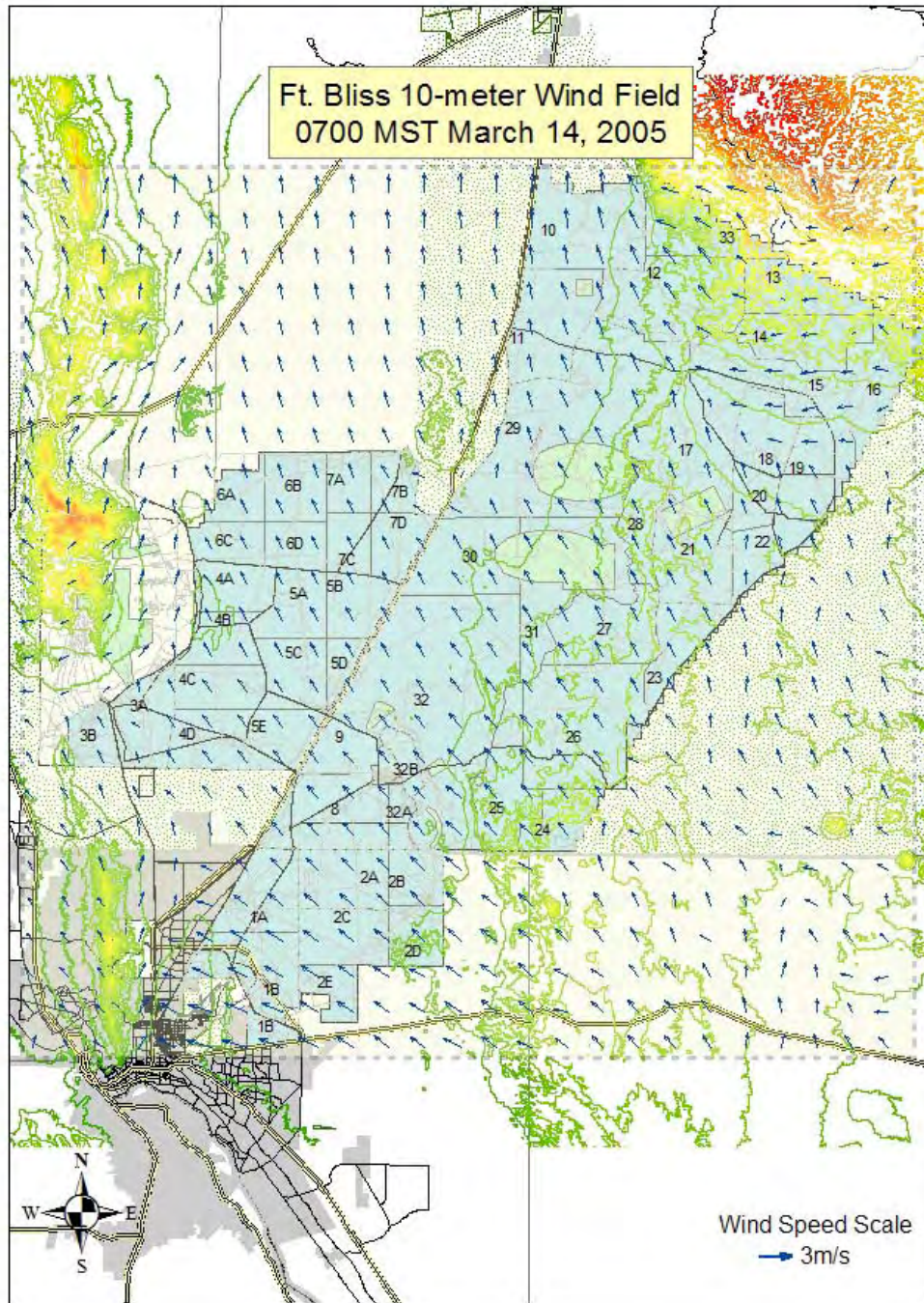


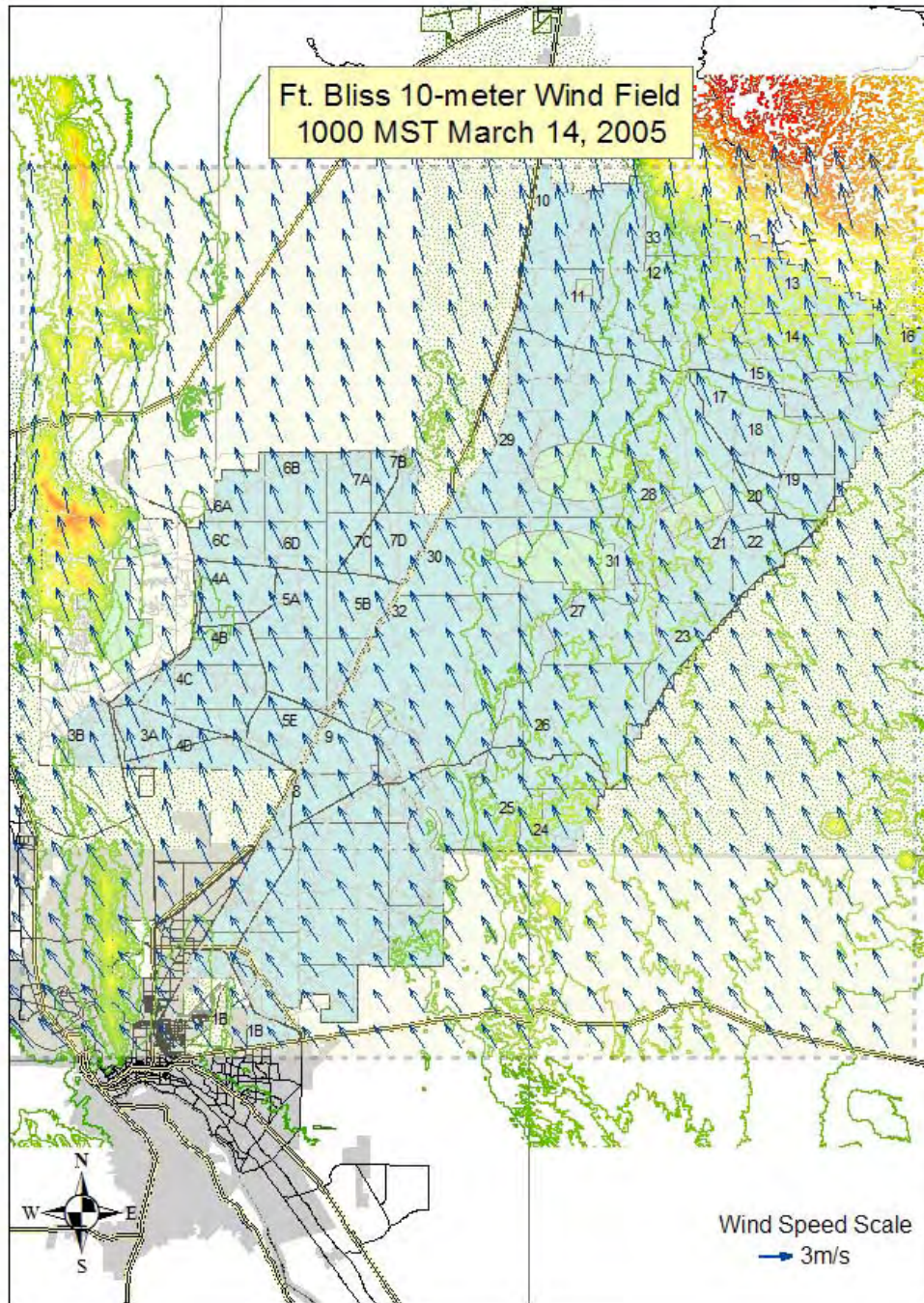


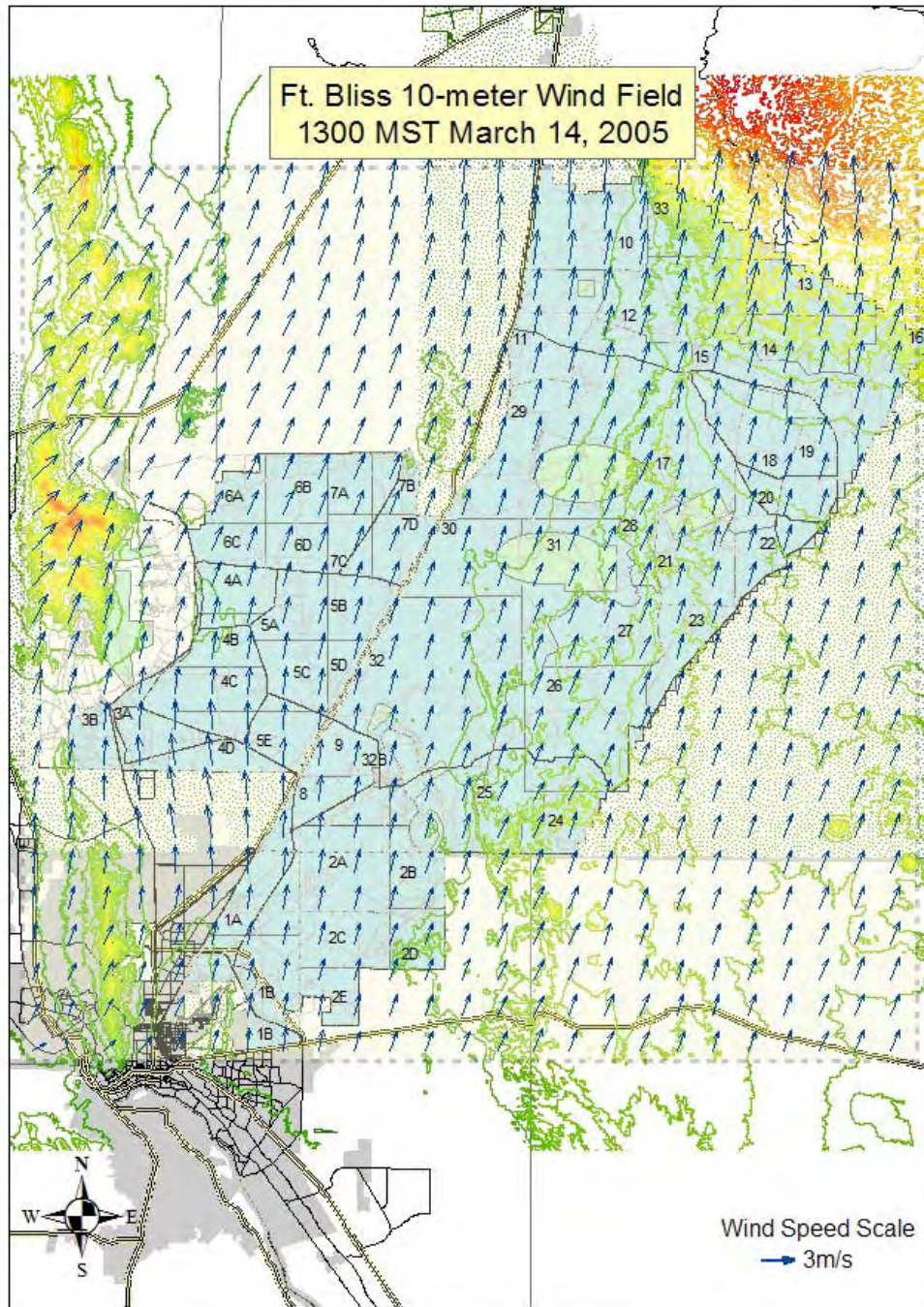


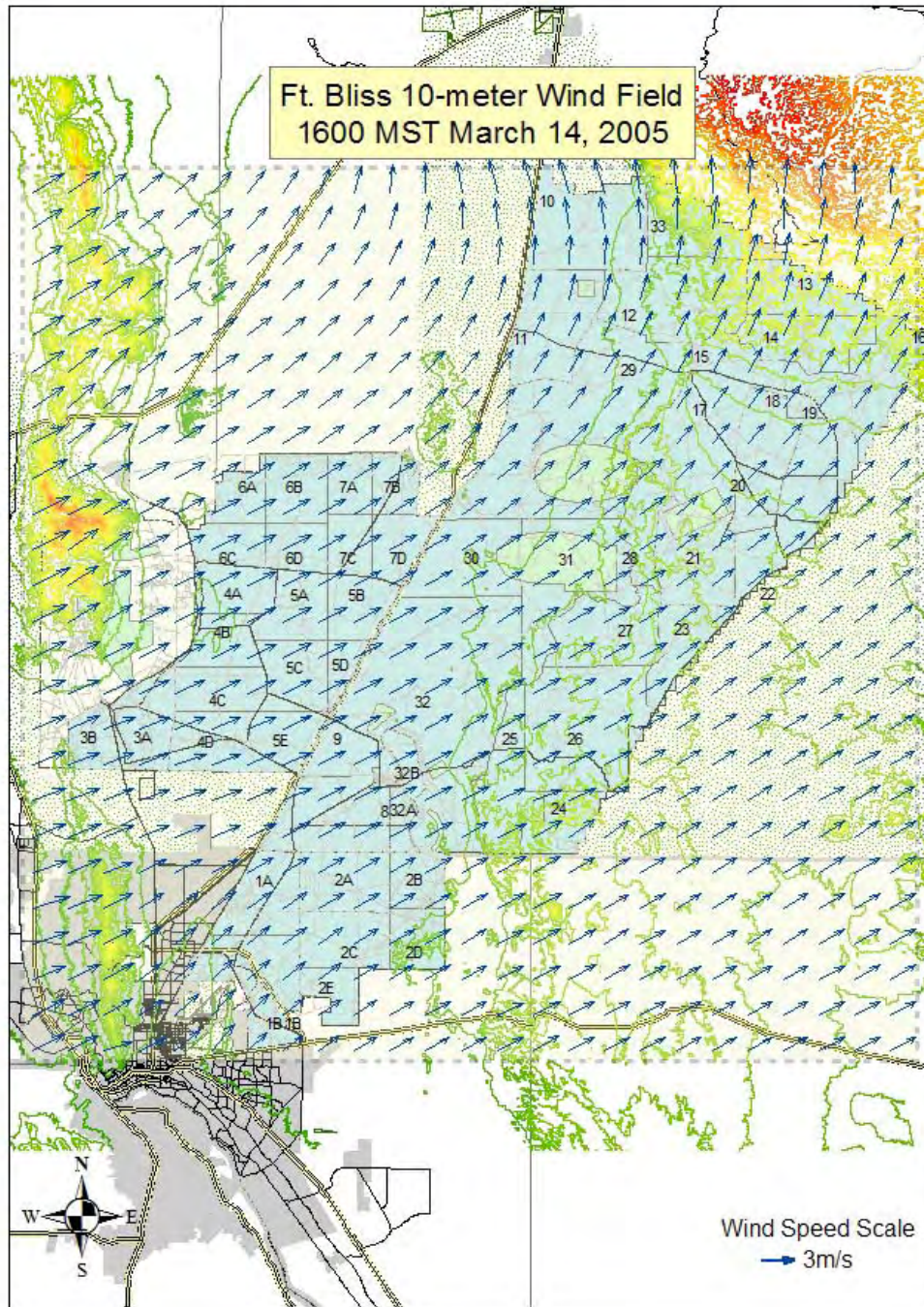


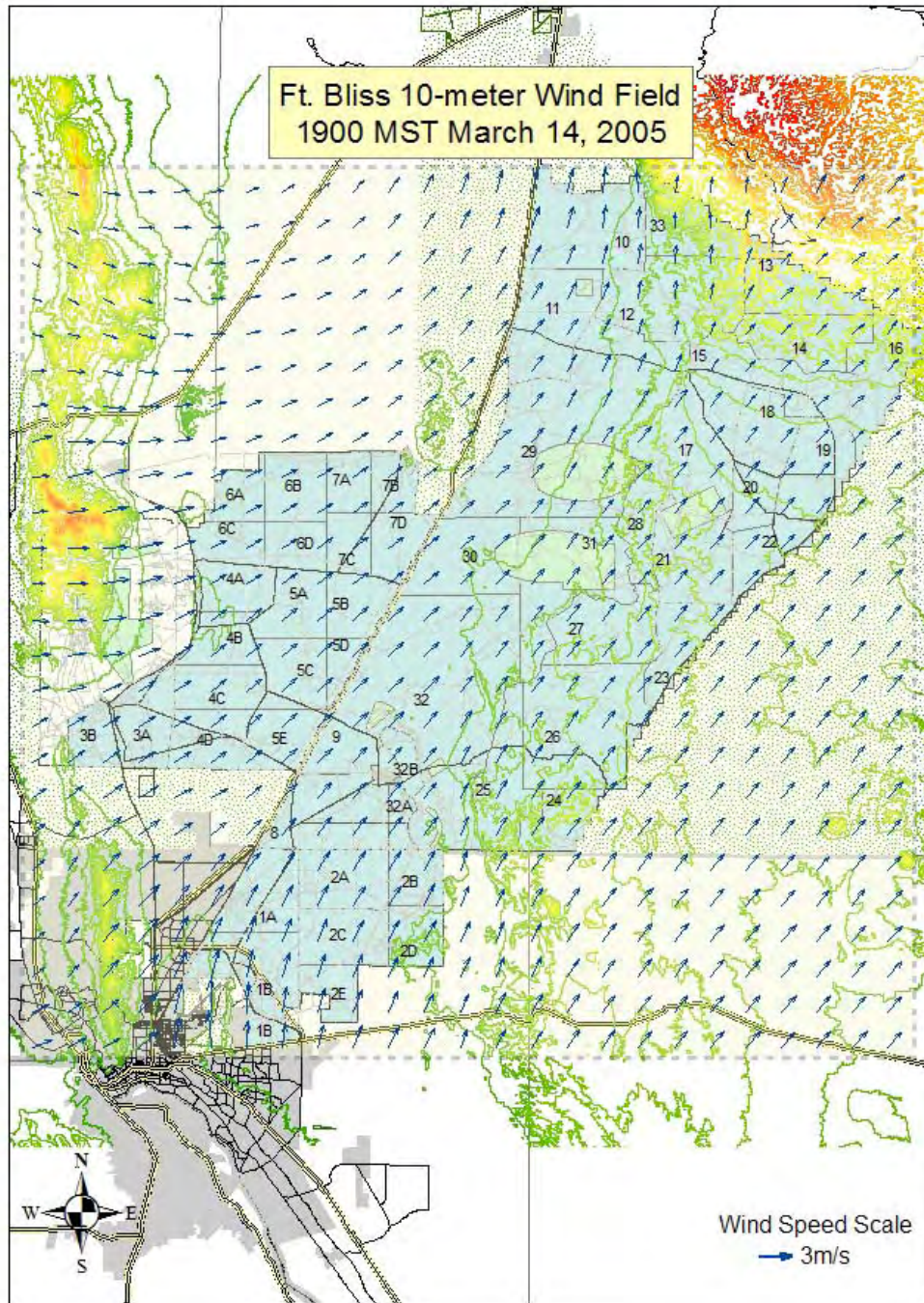


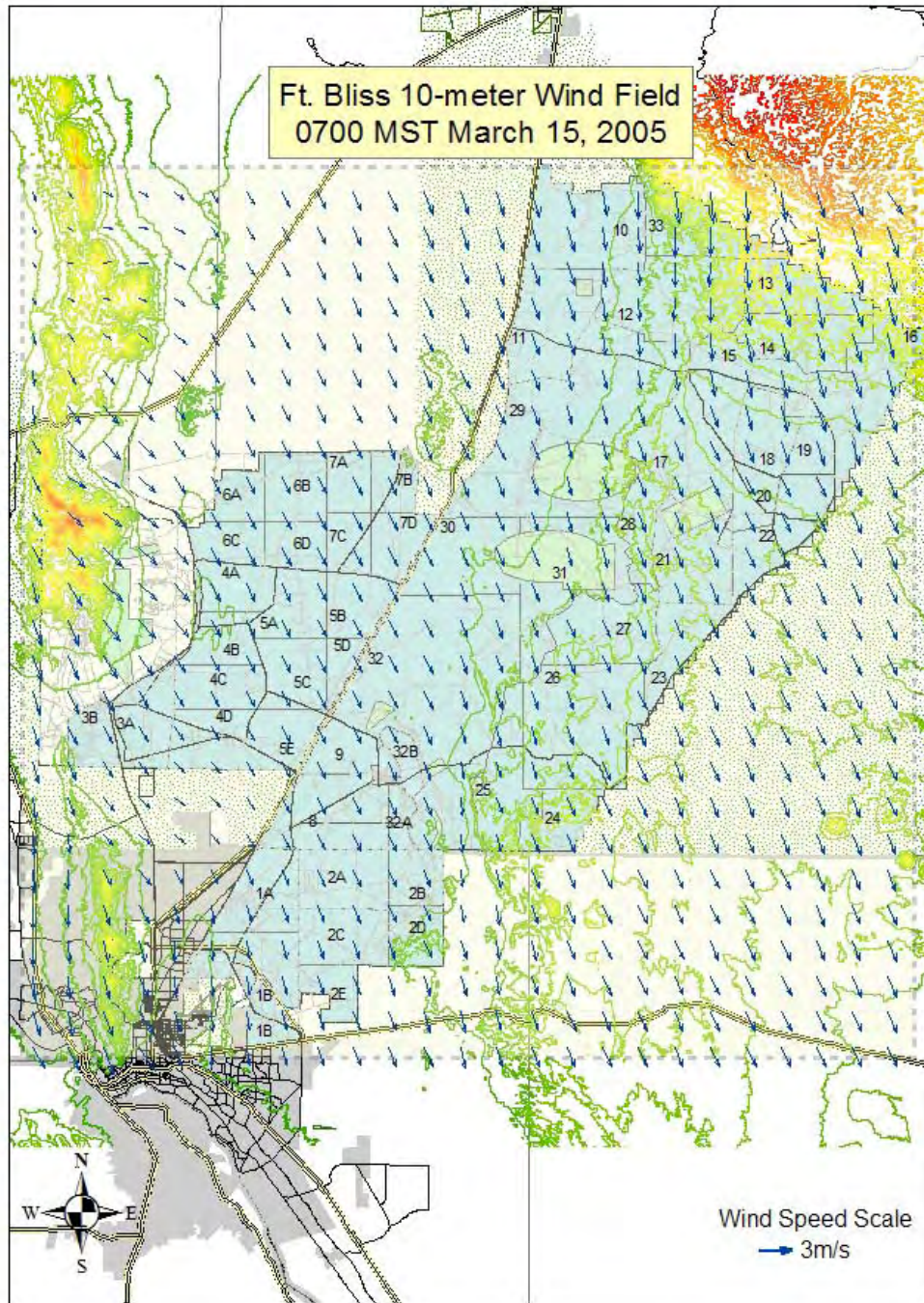


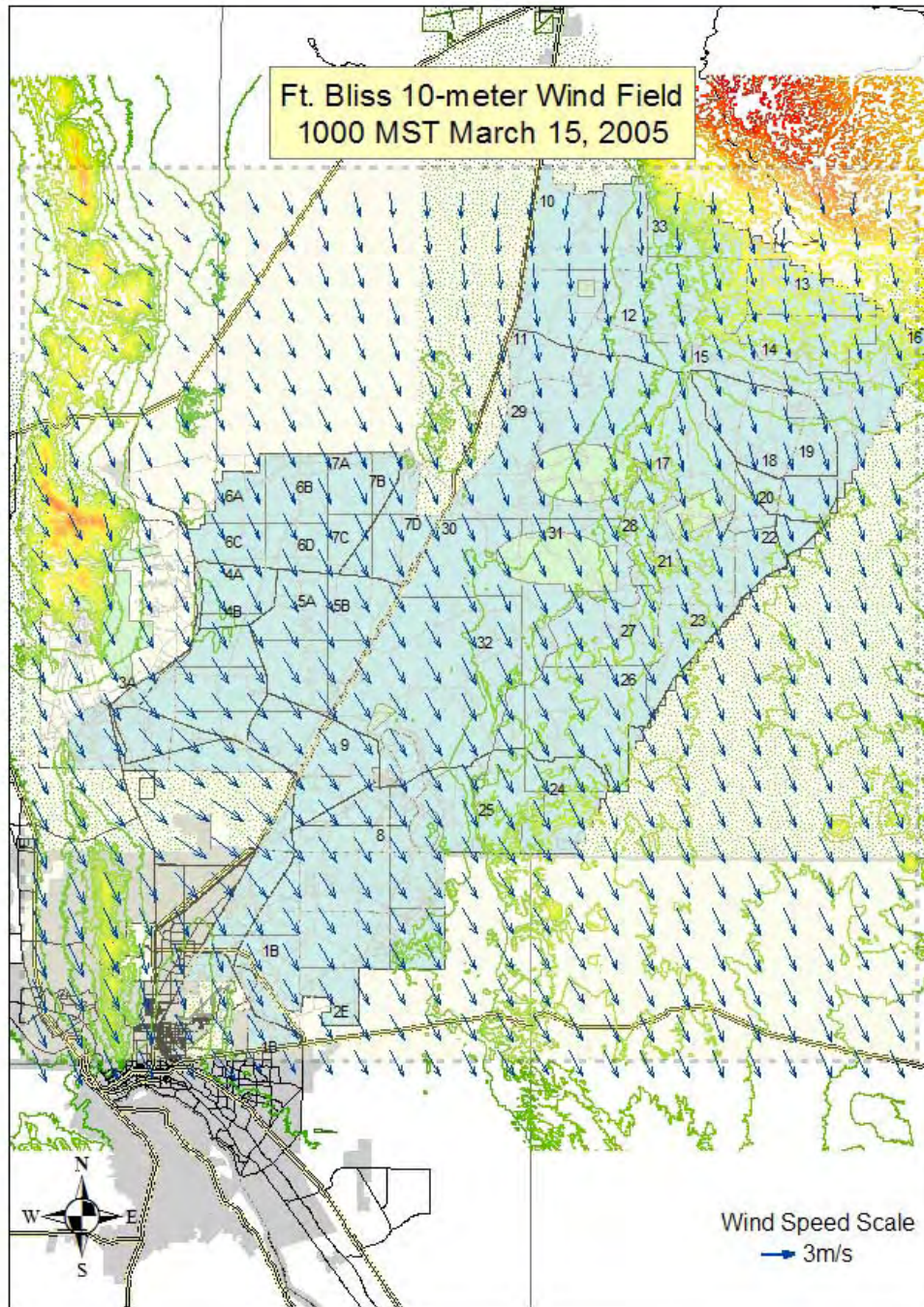


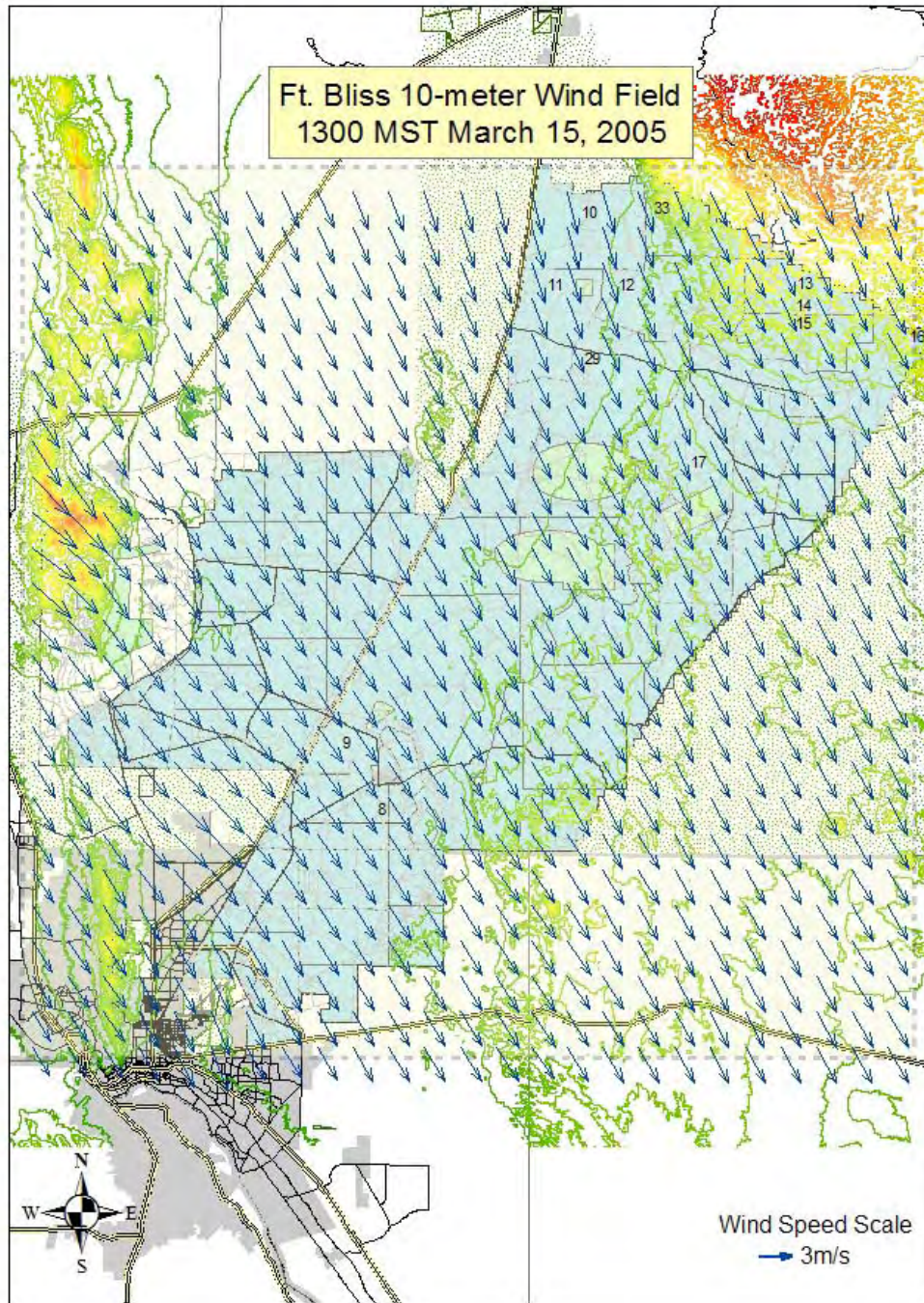


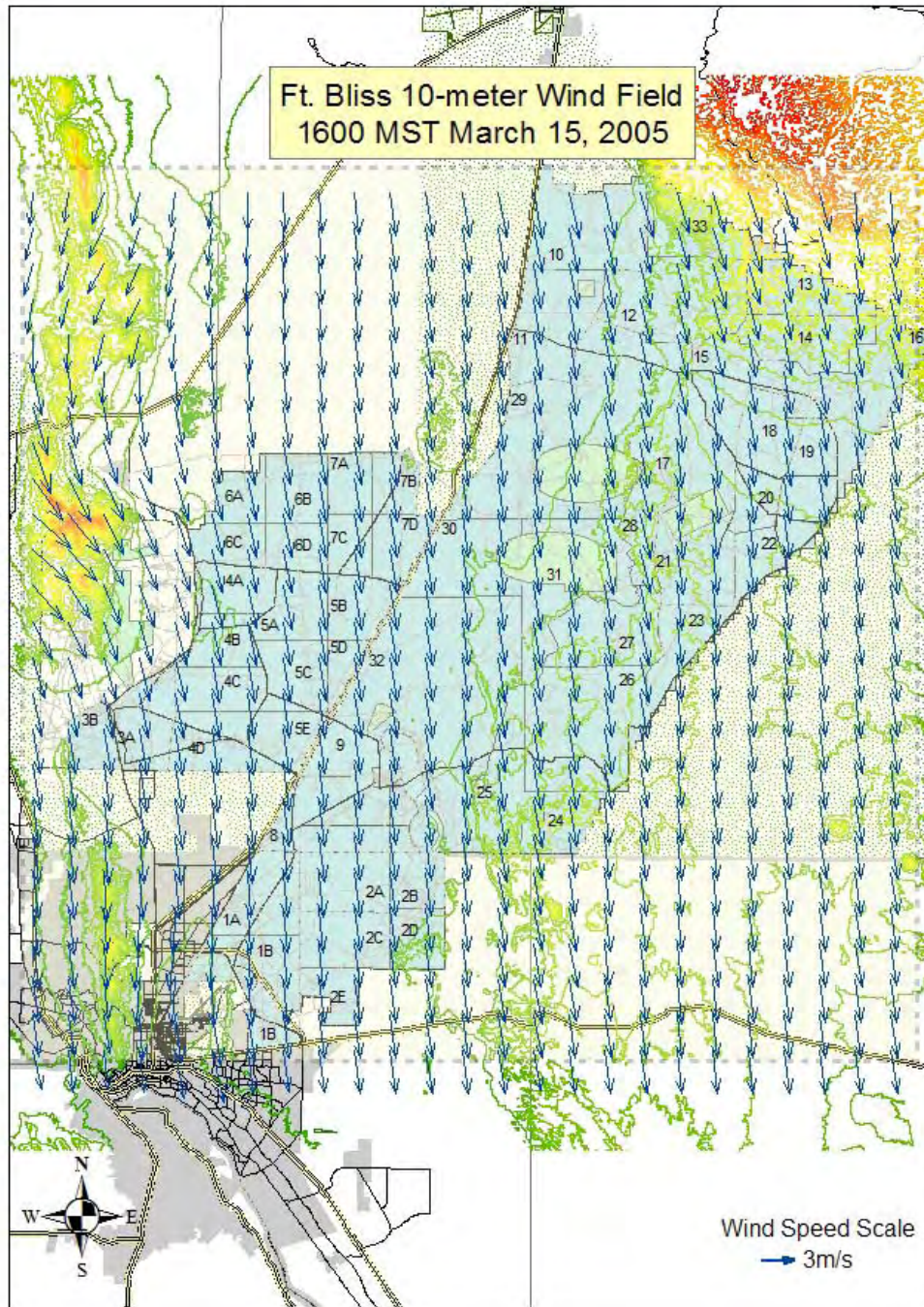


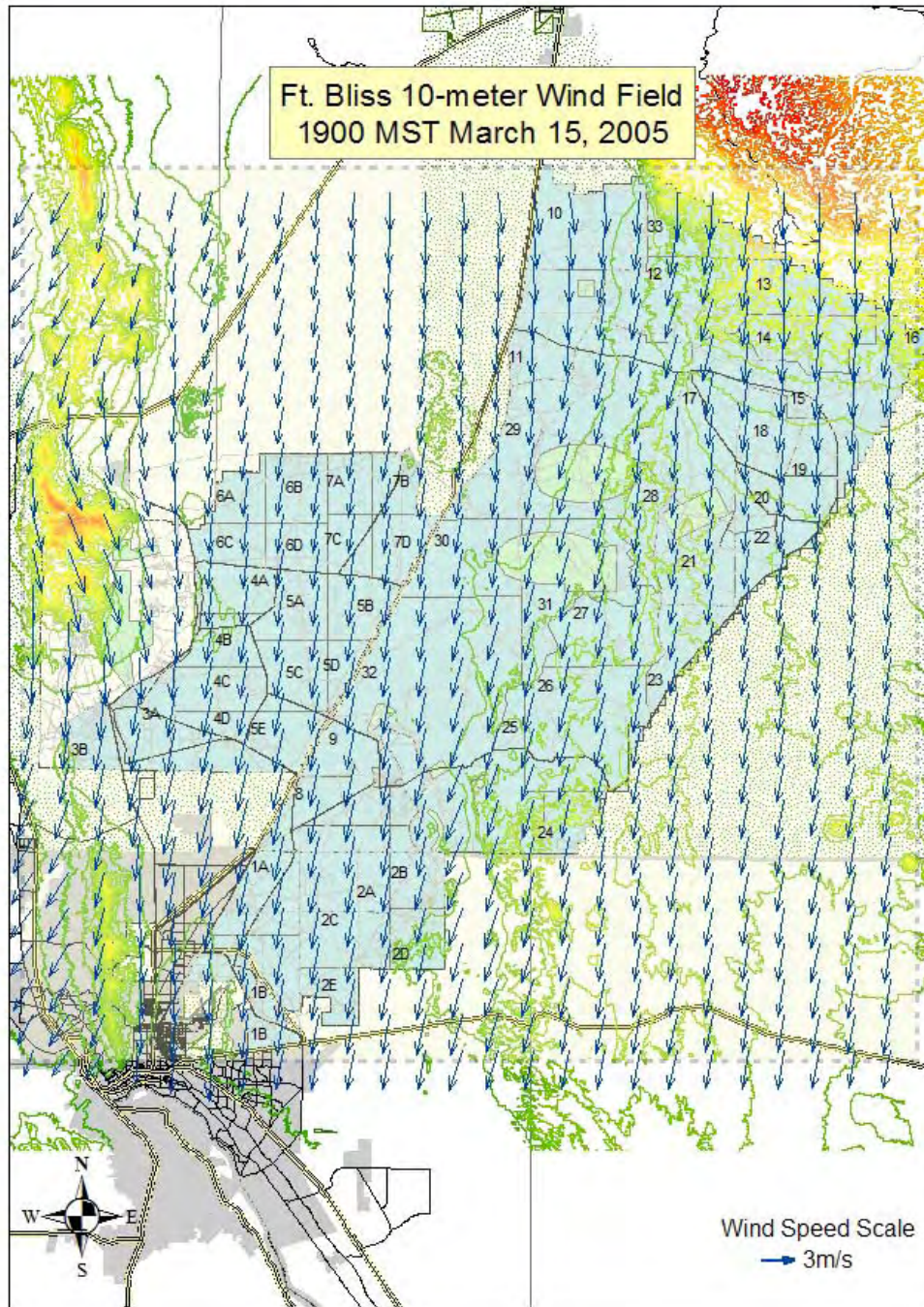


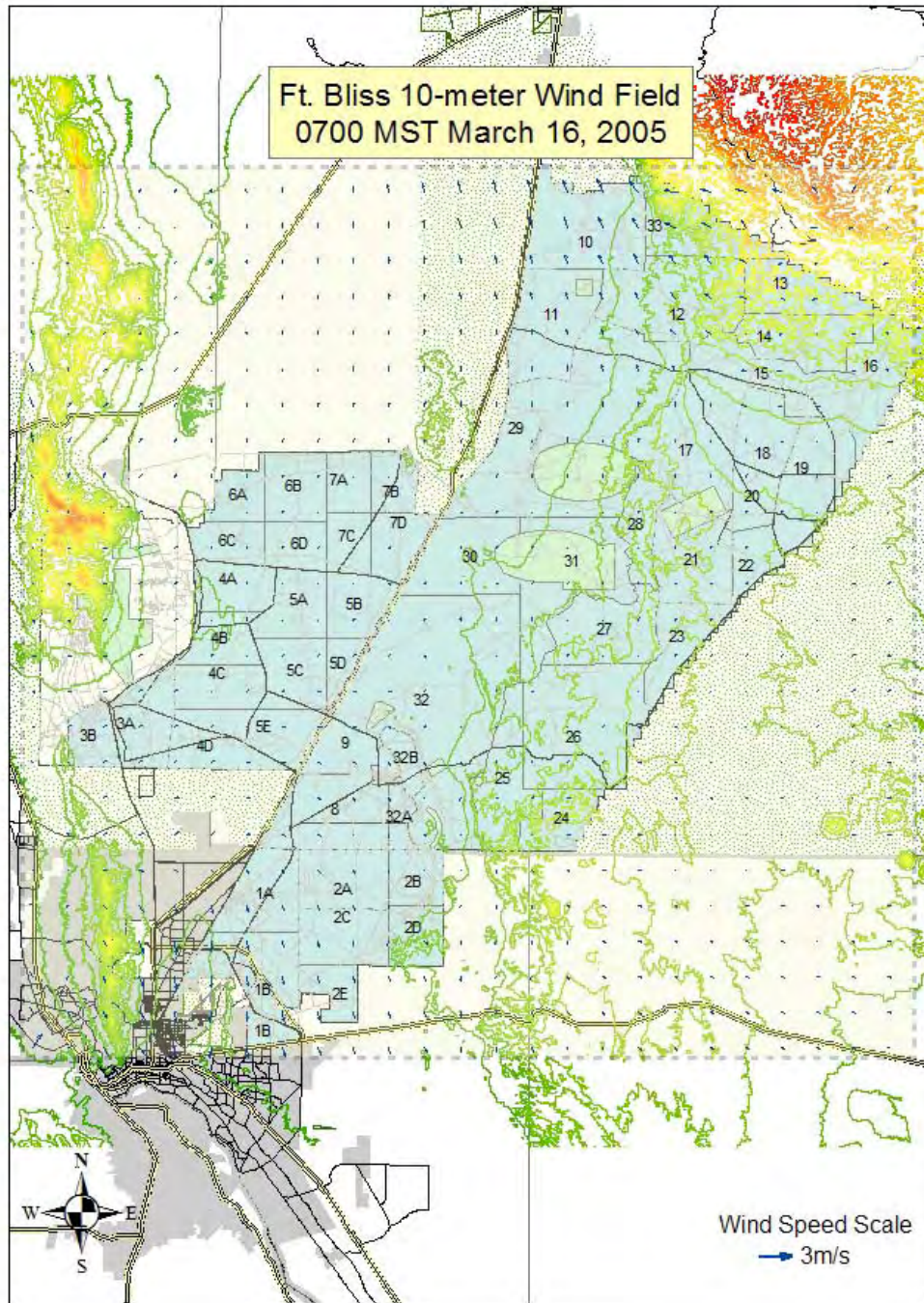


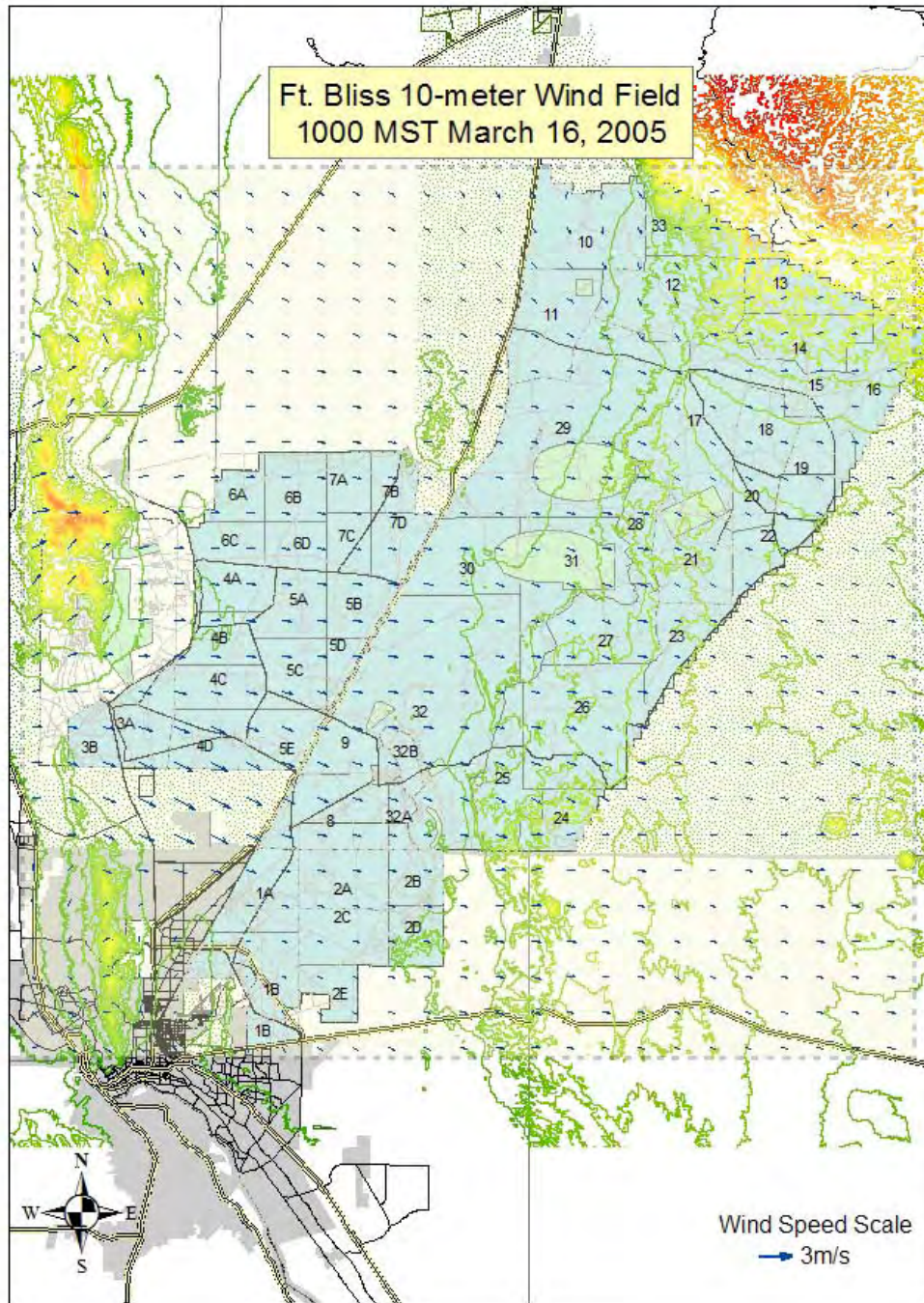


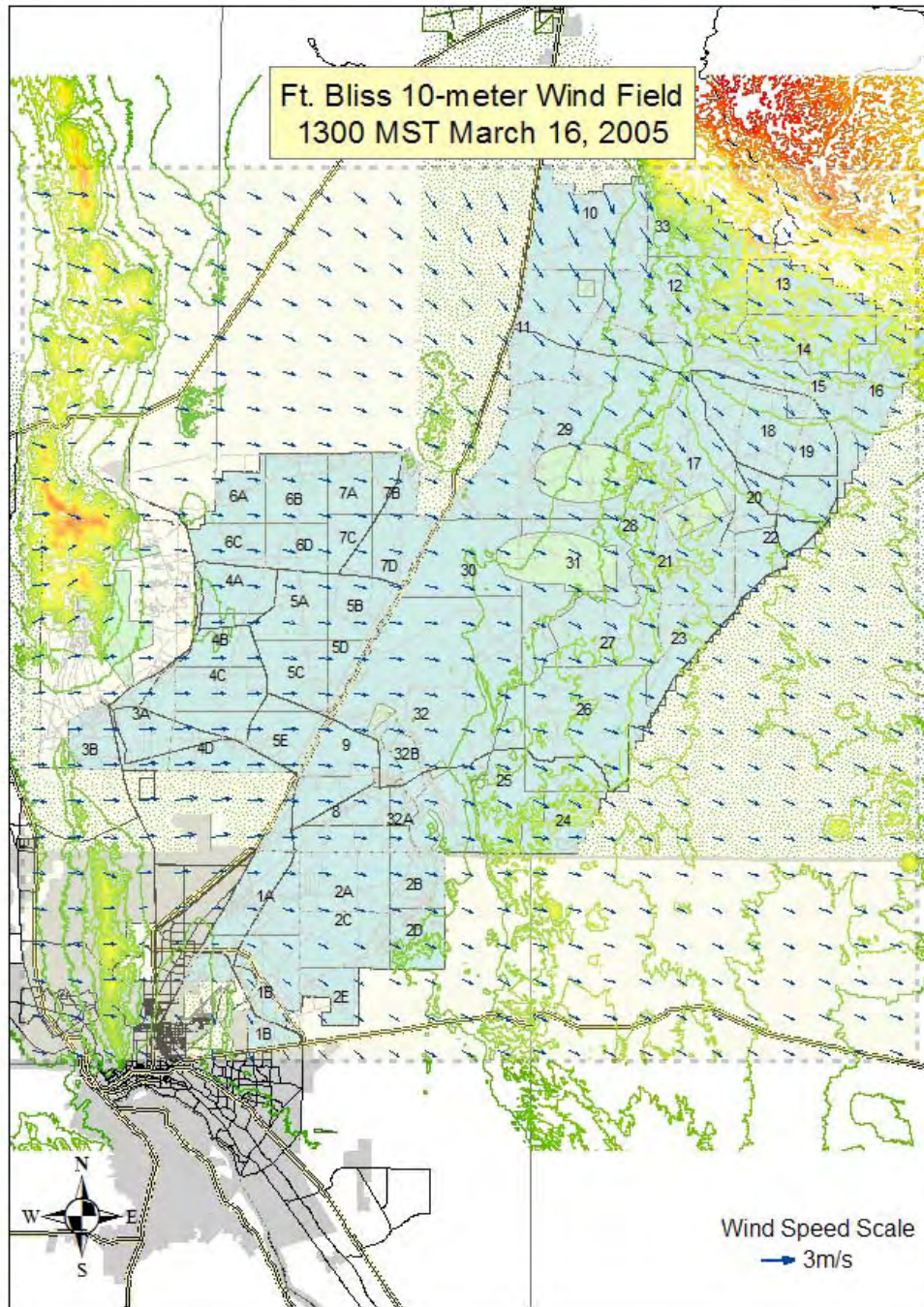


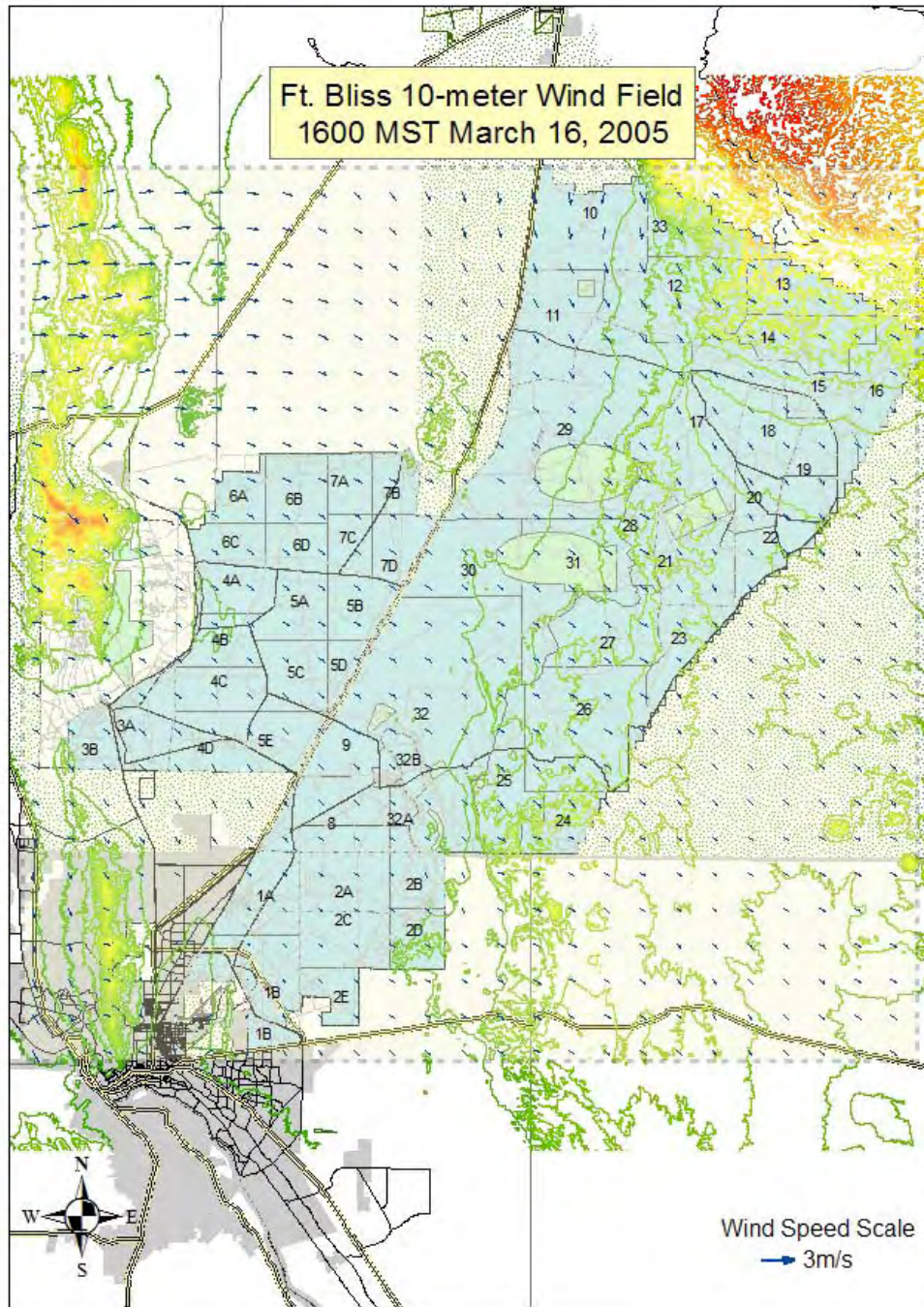


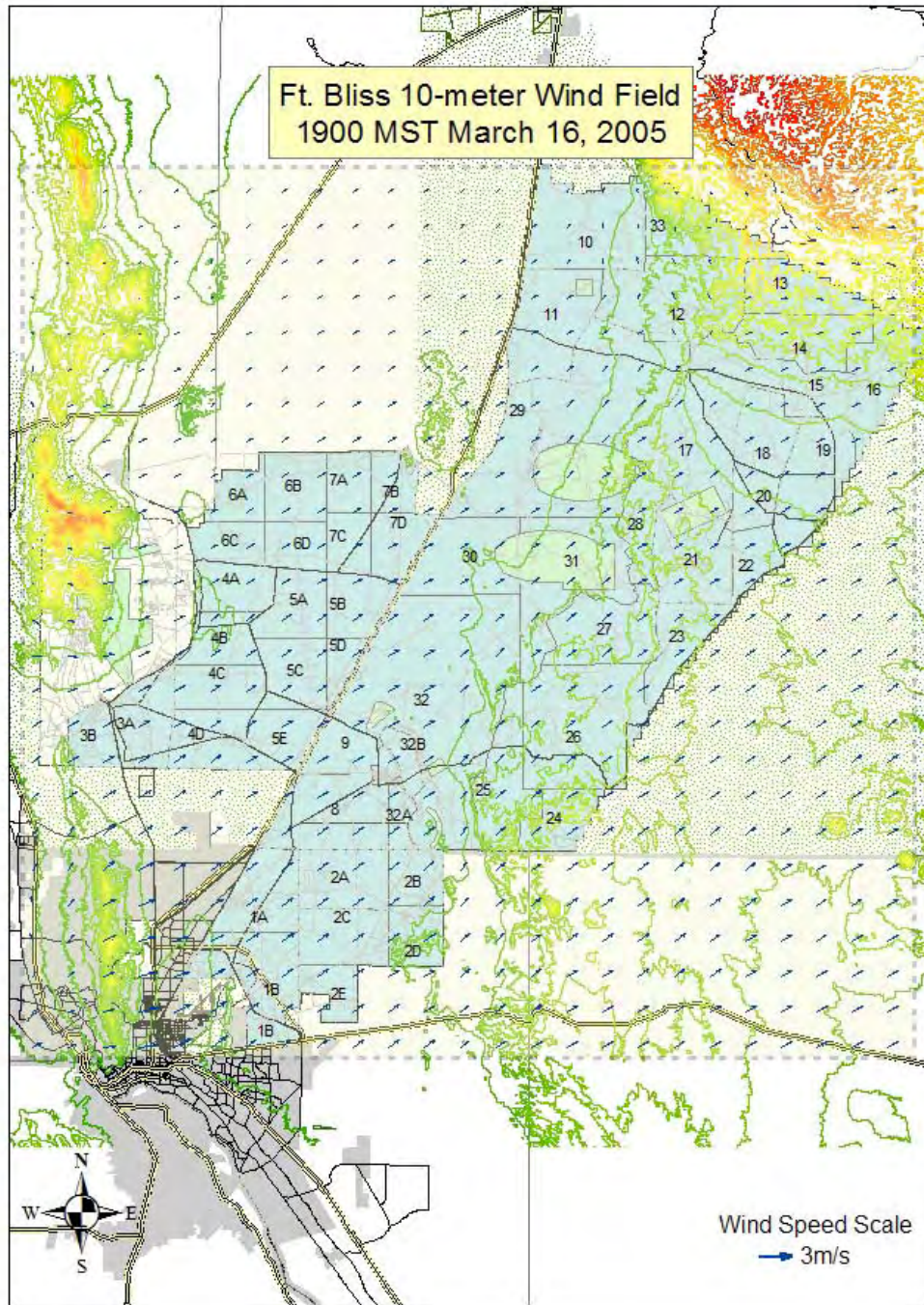










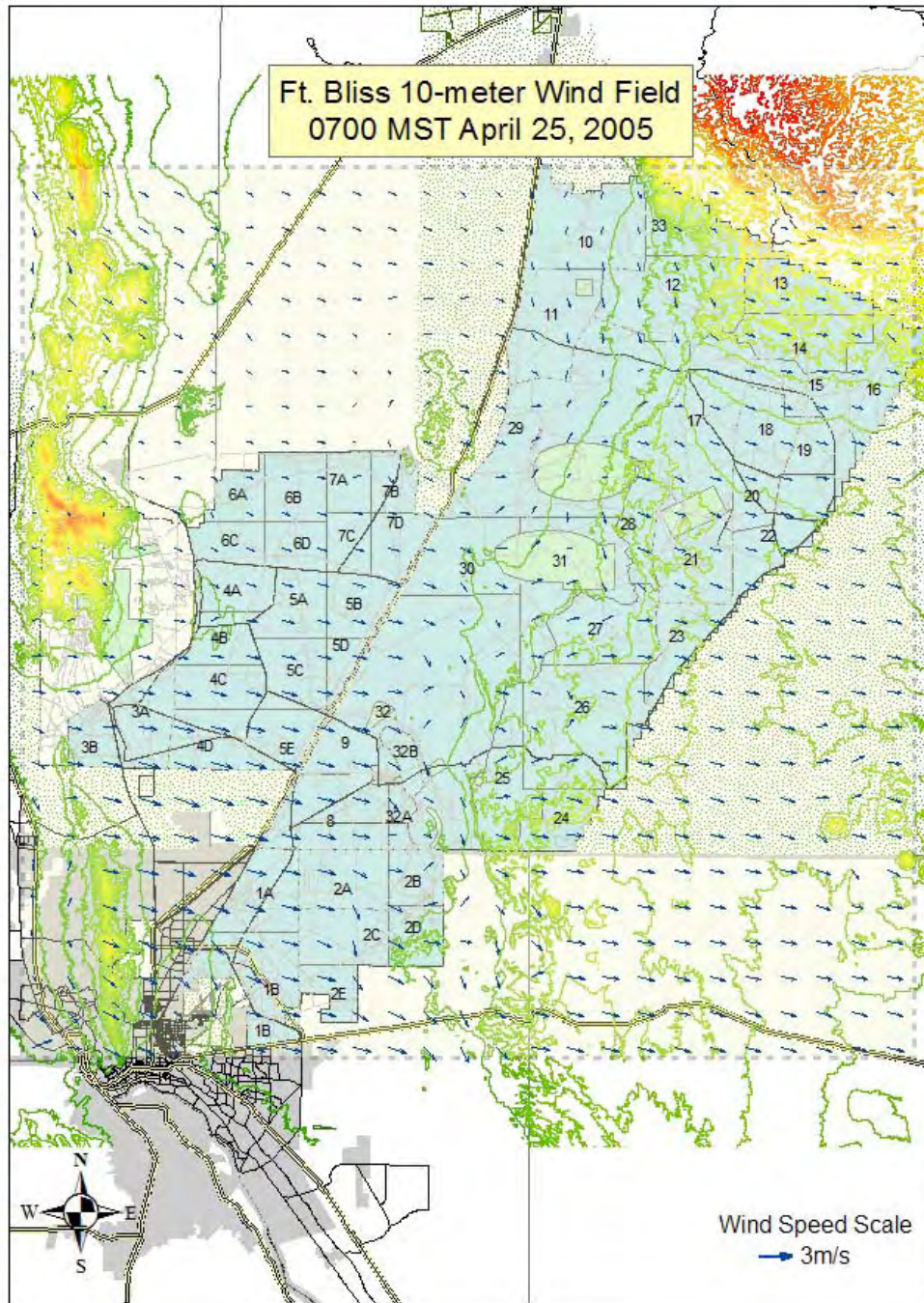


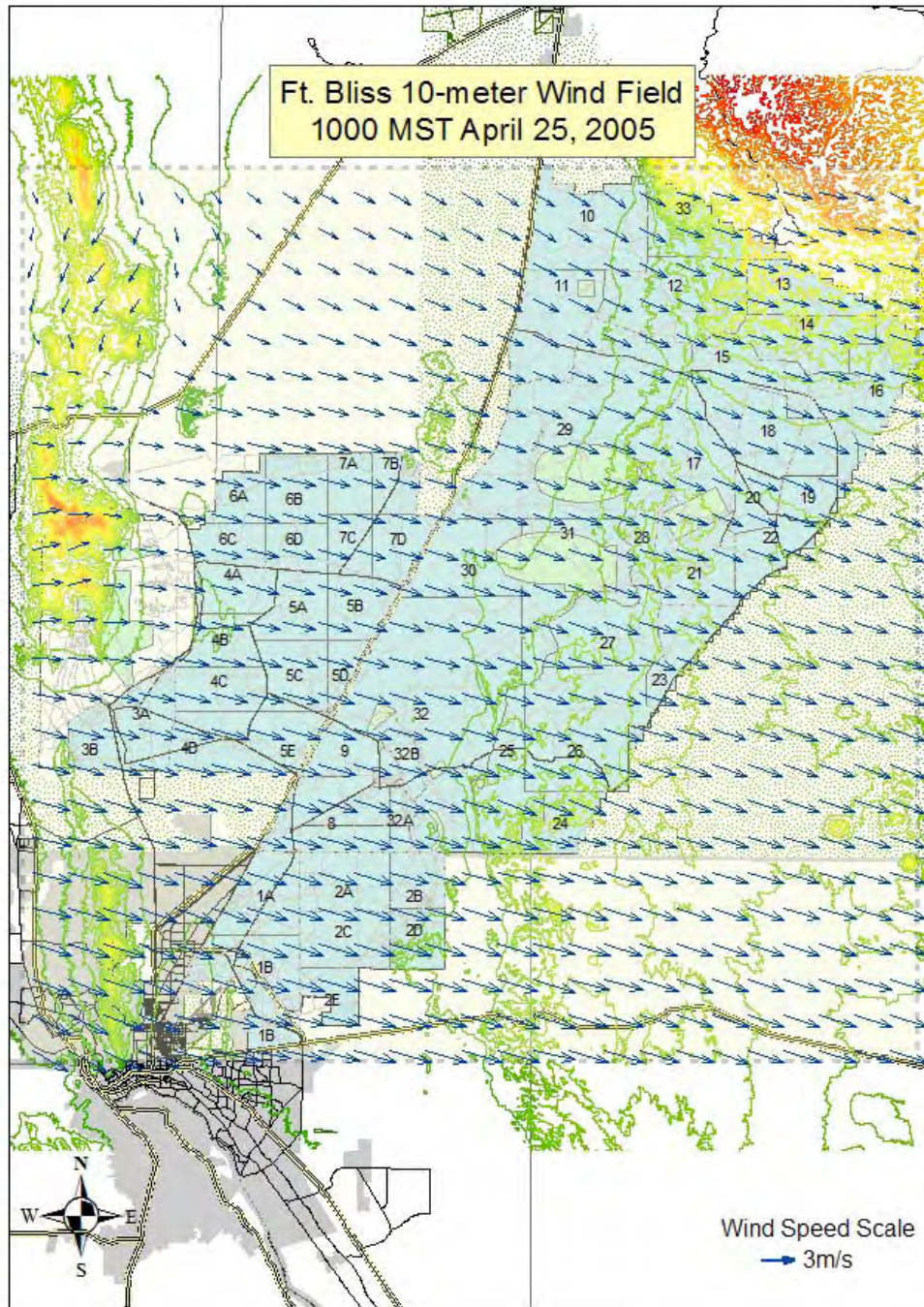
Appendix I

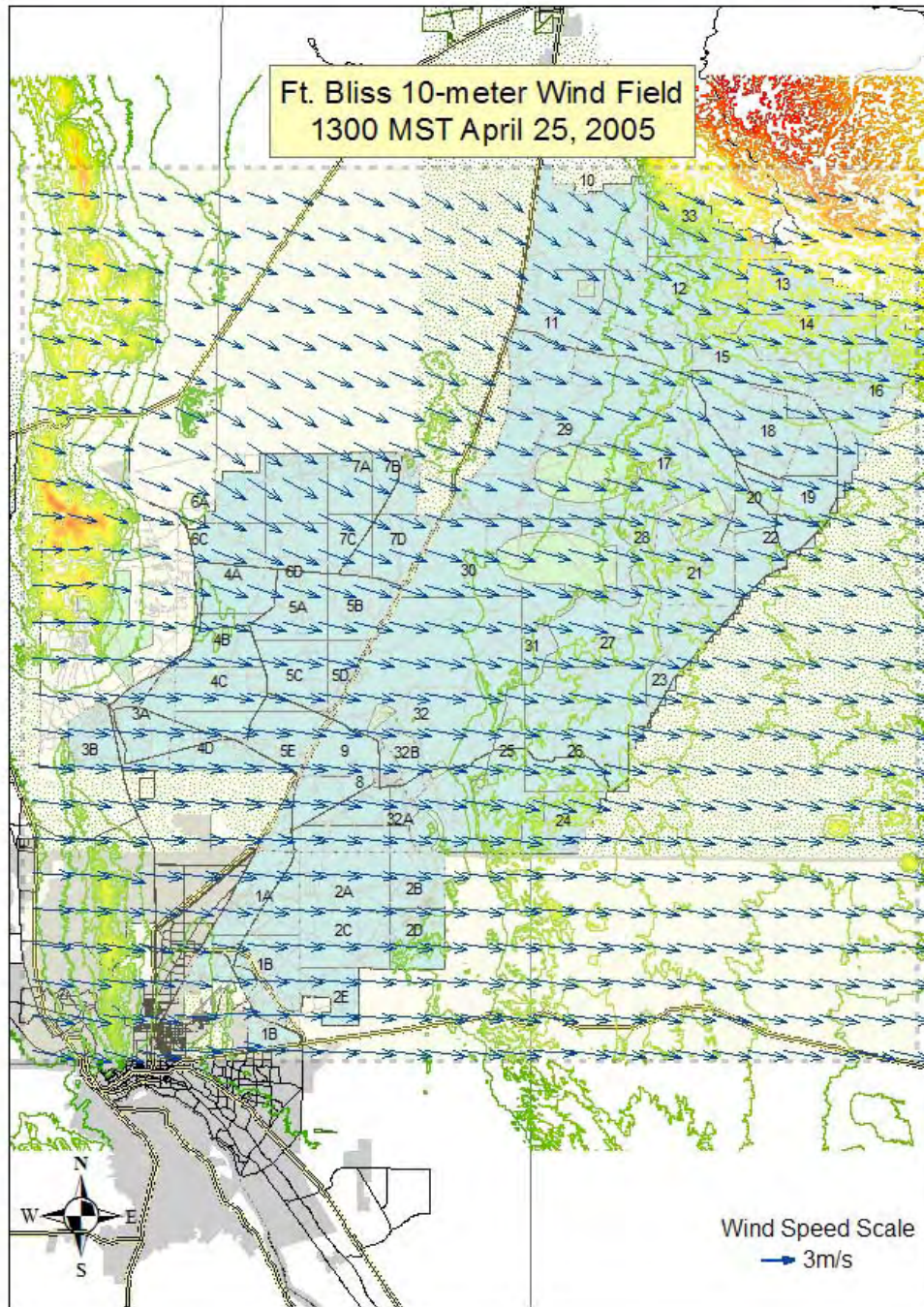
DUSTRAN 10-m-Above-Ground Wind Fields for April 25–30, 2005

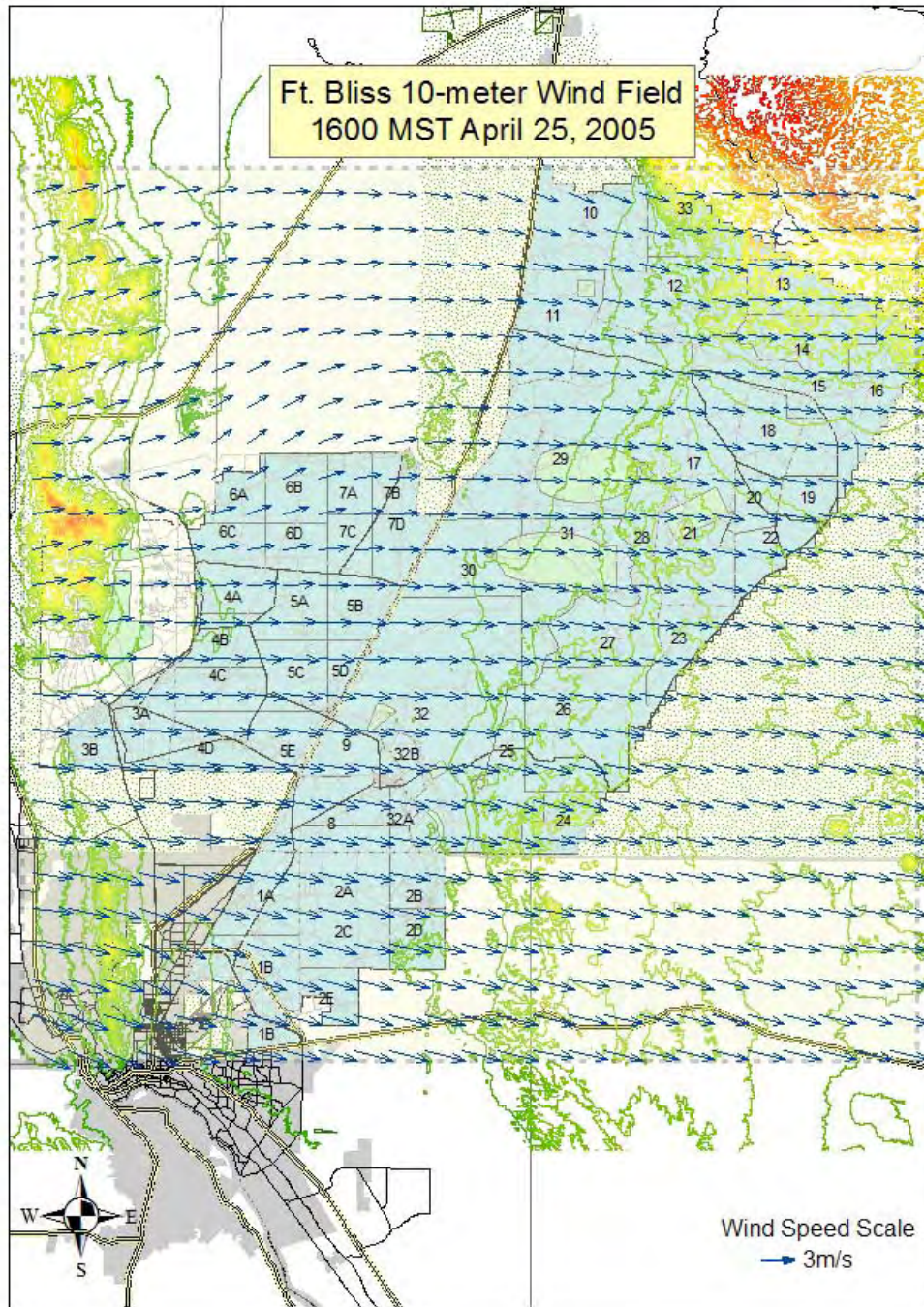
Appendix I: DUSTRAN 10-m-Above-Ground Wind Fields for April 25–30, 2005

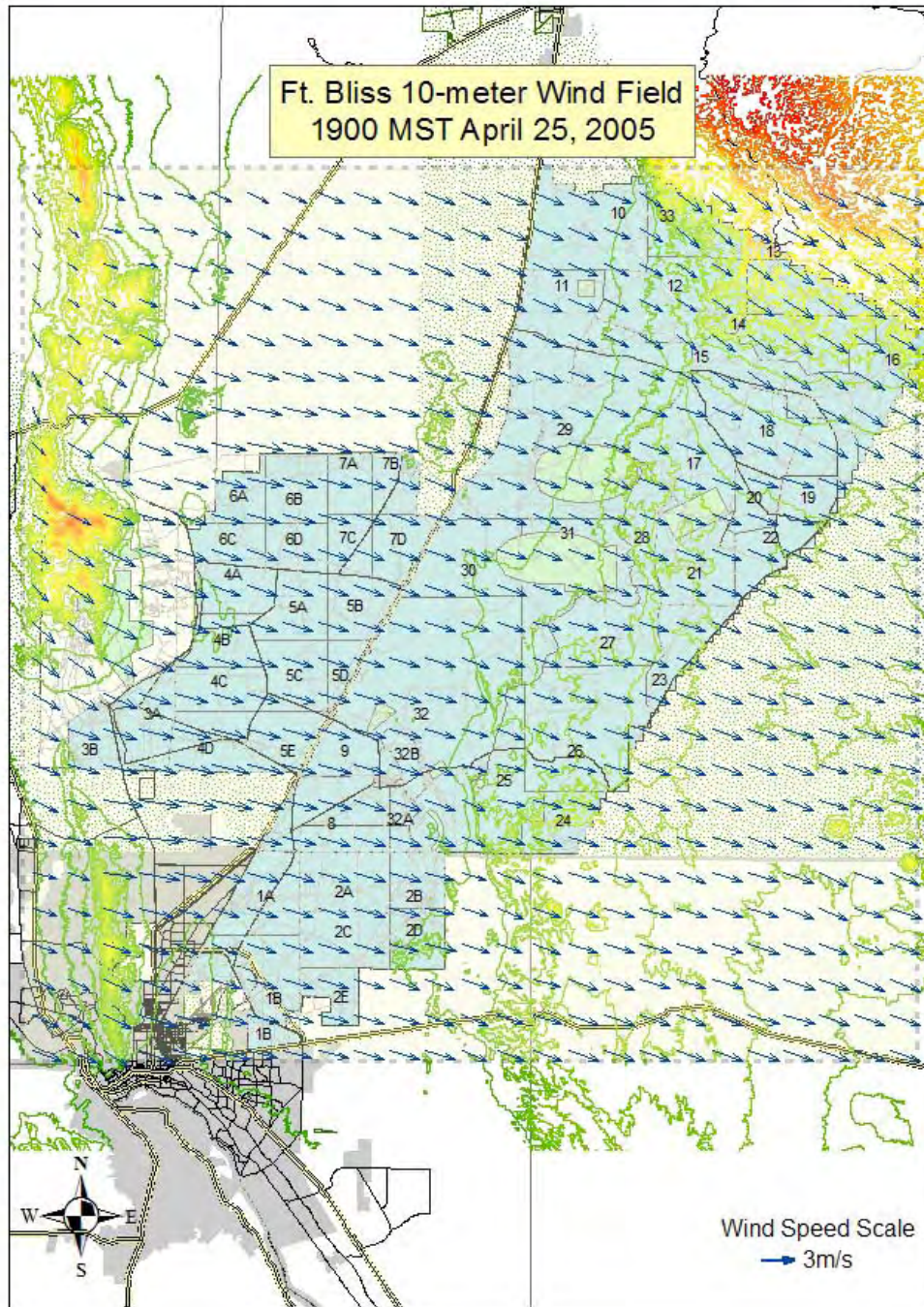
This appendix contains 30 screen captures of the 10-m above ground wind fields predicted by the CALMET module within DUSTRAN. Wind fields are shown at 0700, 1000, 1300, 1600, and 1900 MST for the 6 days included in the current simulations (April 25 through 30, 2005). Header captions within each figure indicate the day and time represented by a given plot. The arrow on each vector indicates wind direction while the scaling of vector length indicates wind speed. A reference vector whose length represents a wind speed of 3 m/s is shown on each plot.

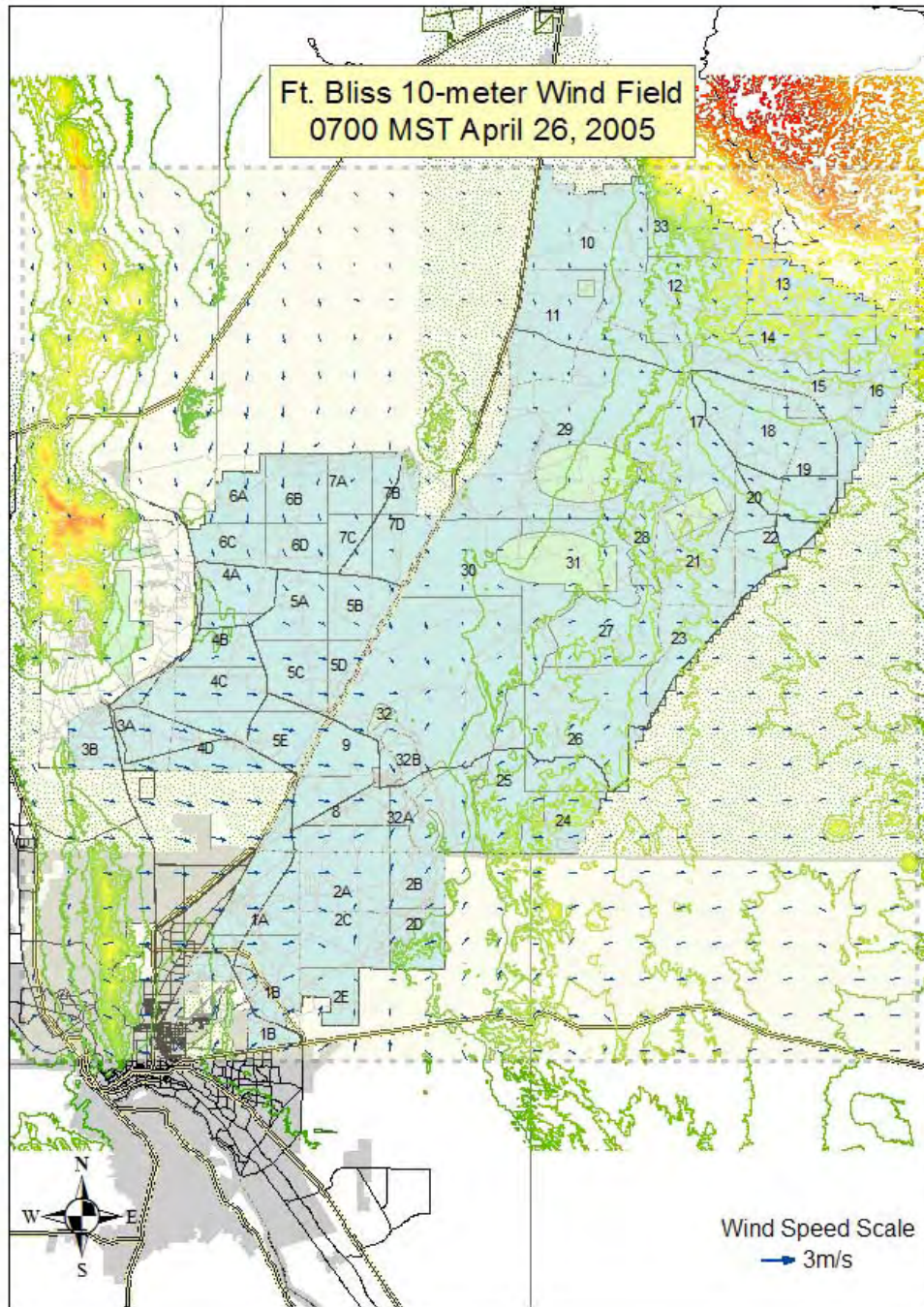


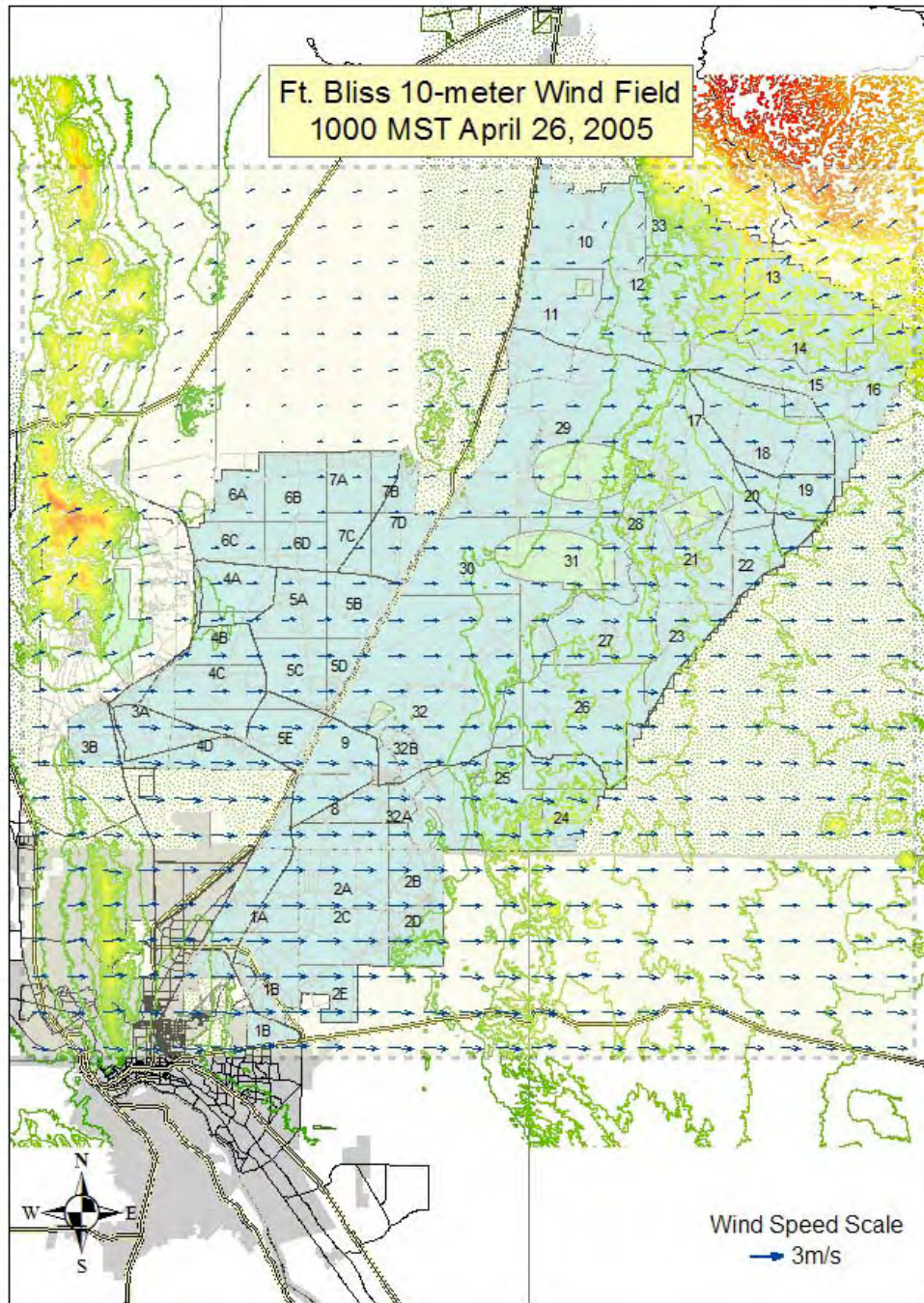


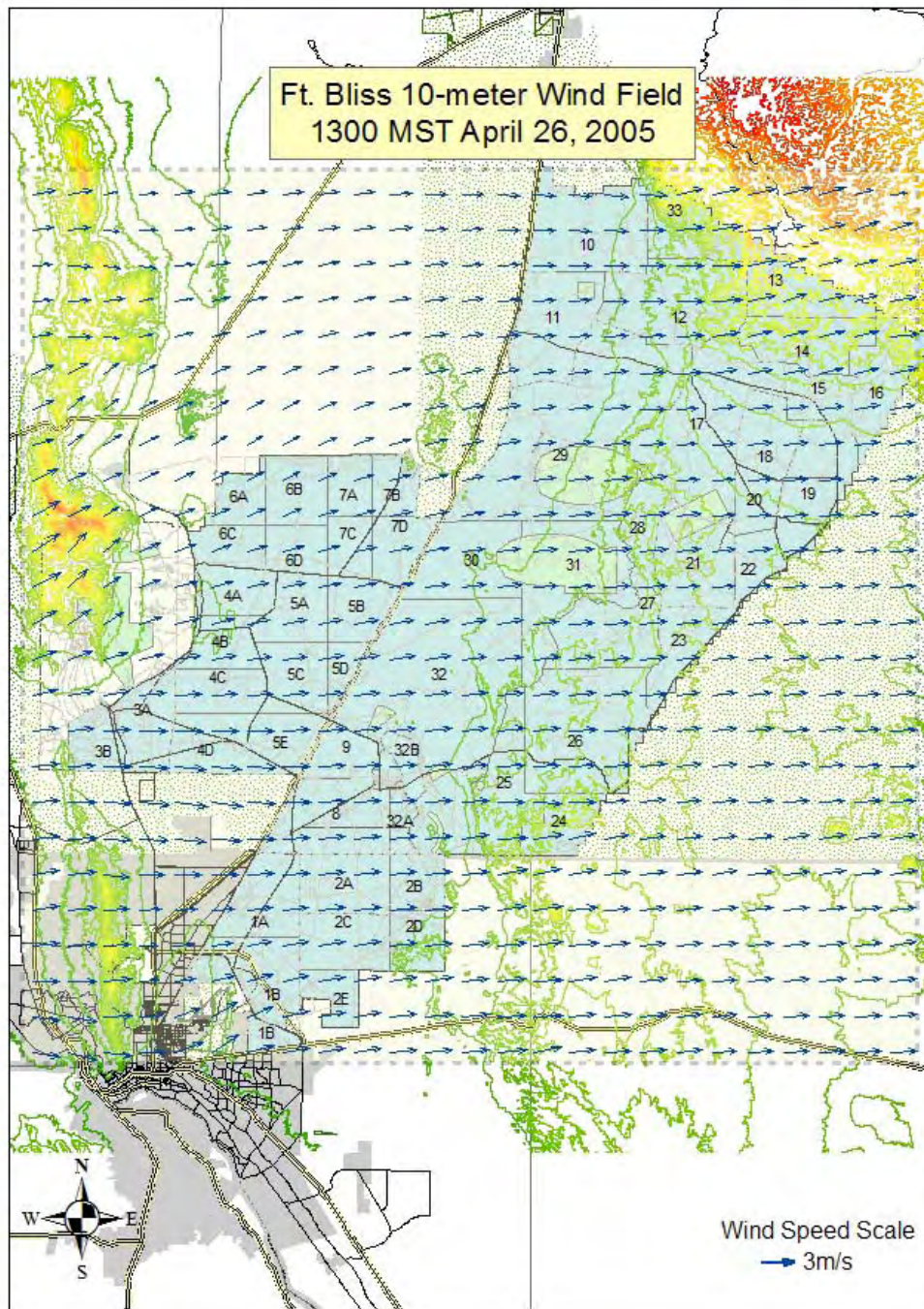


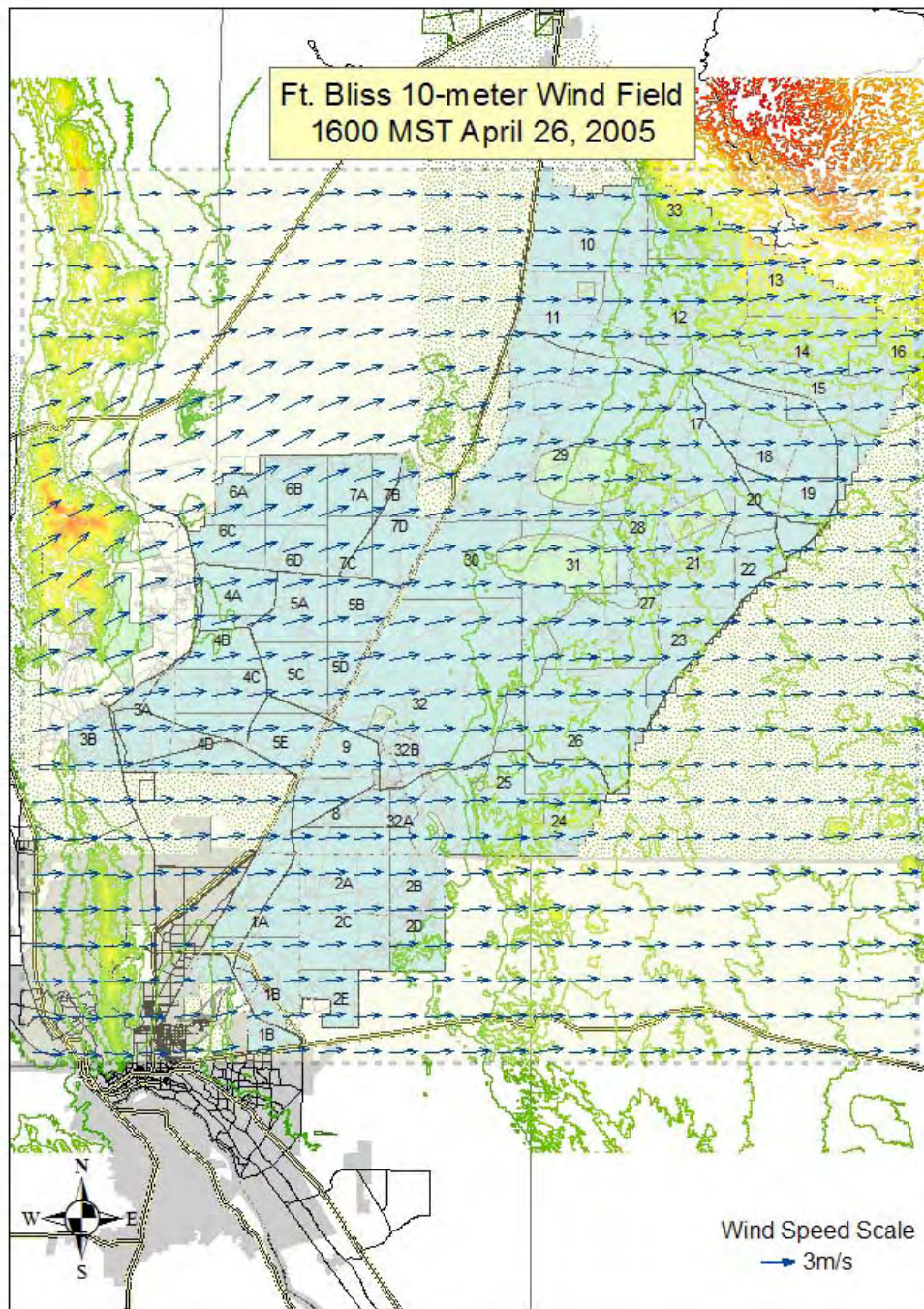


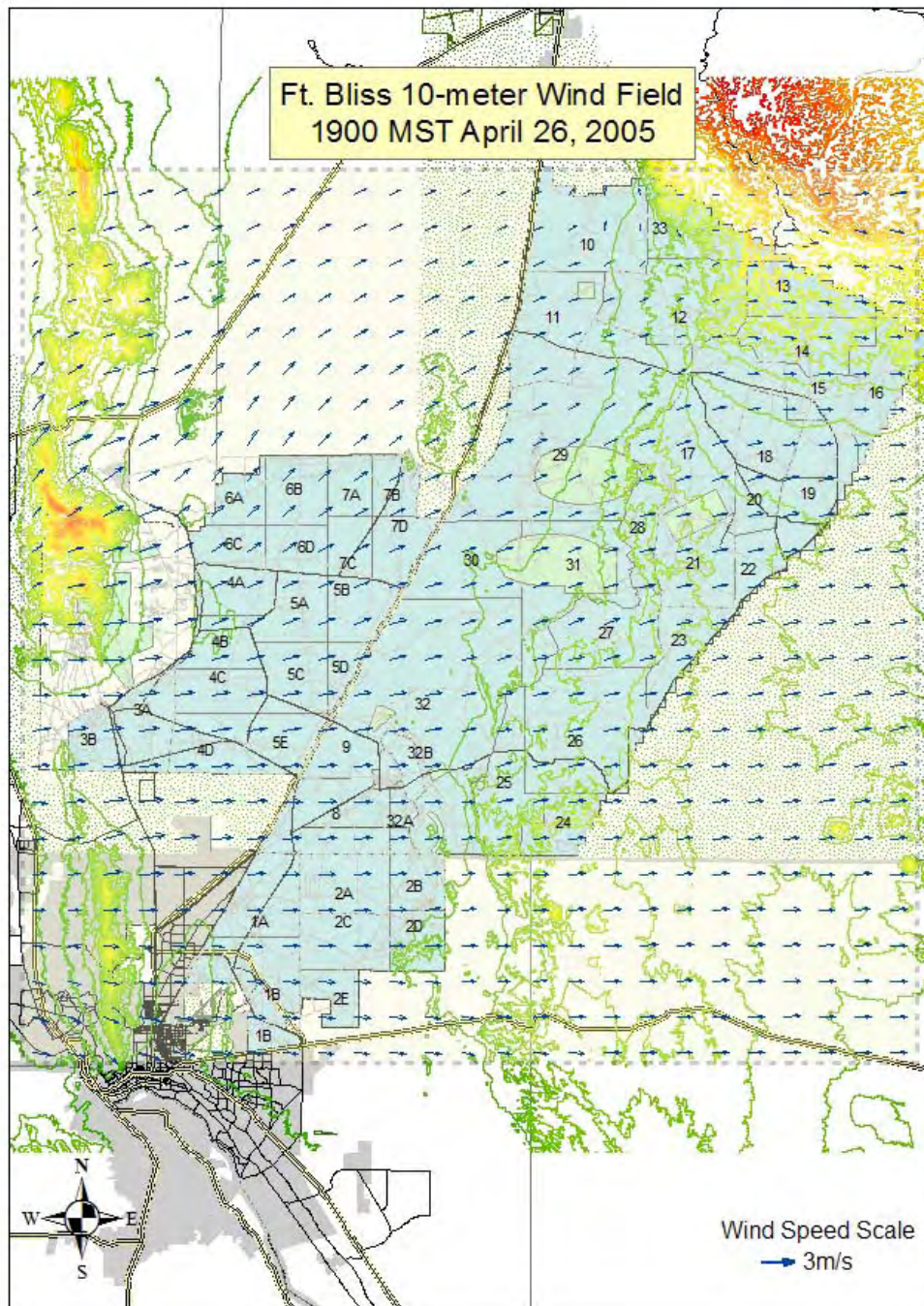


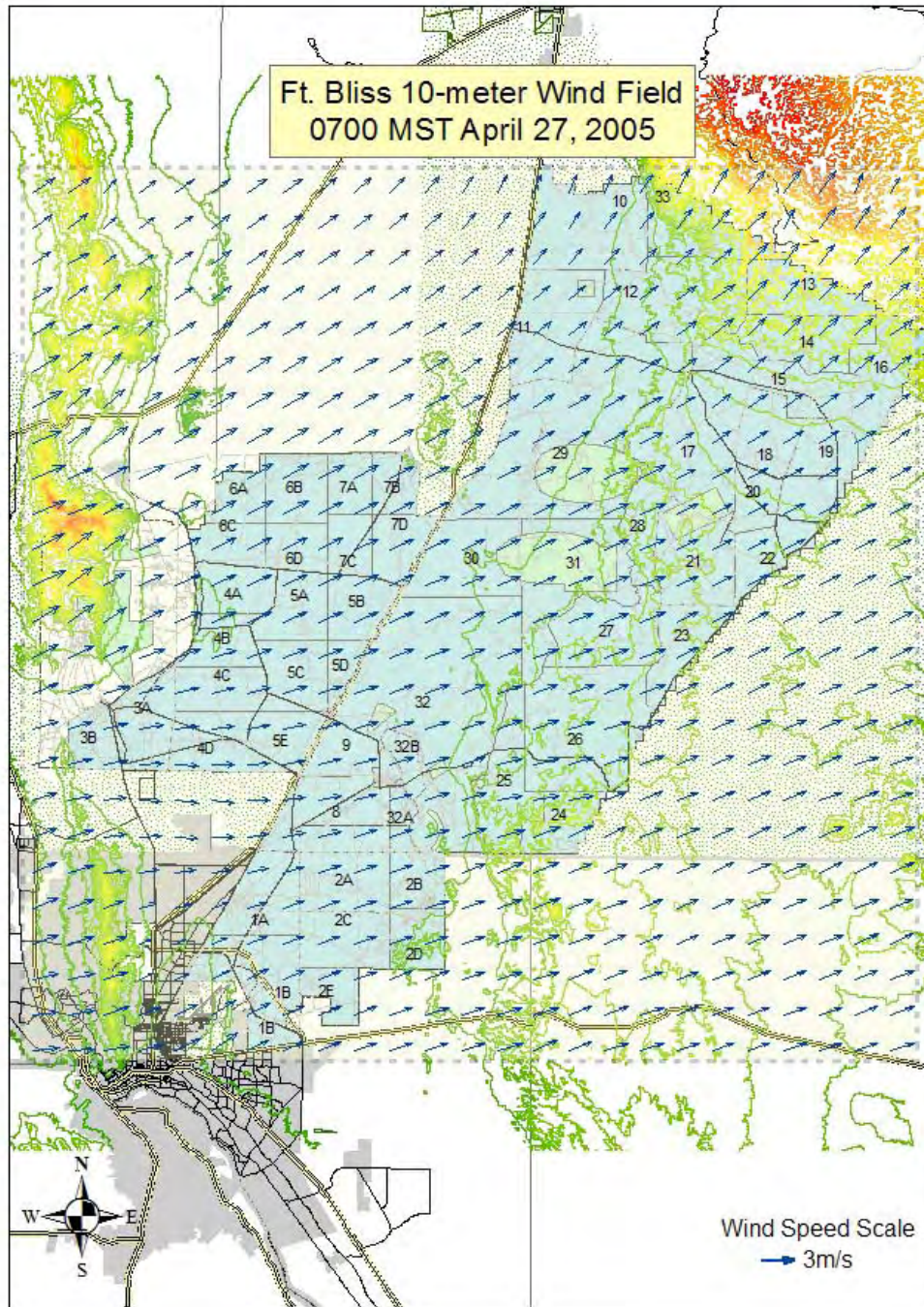


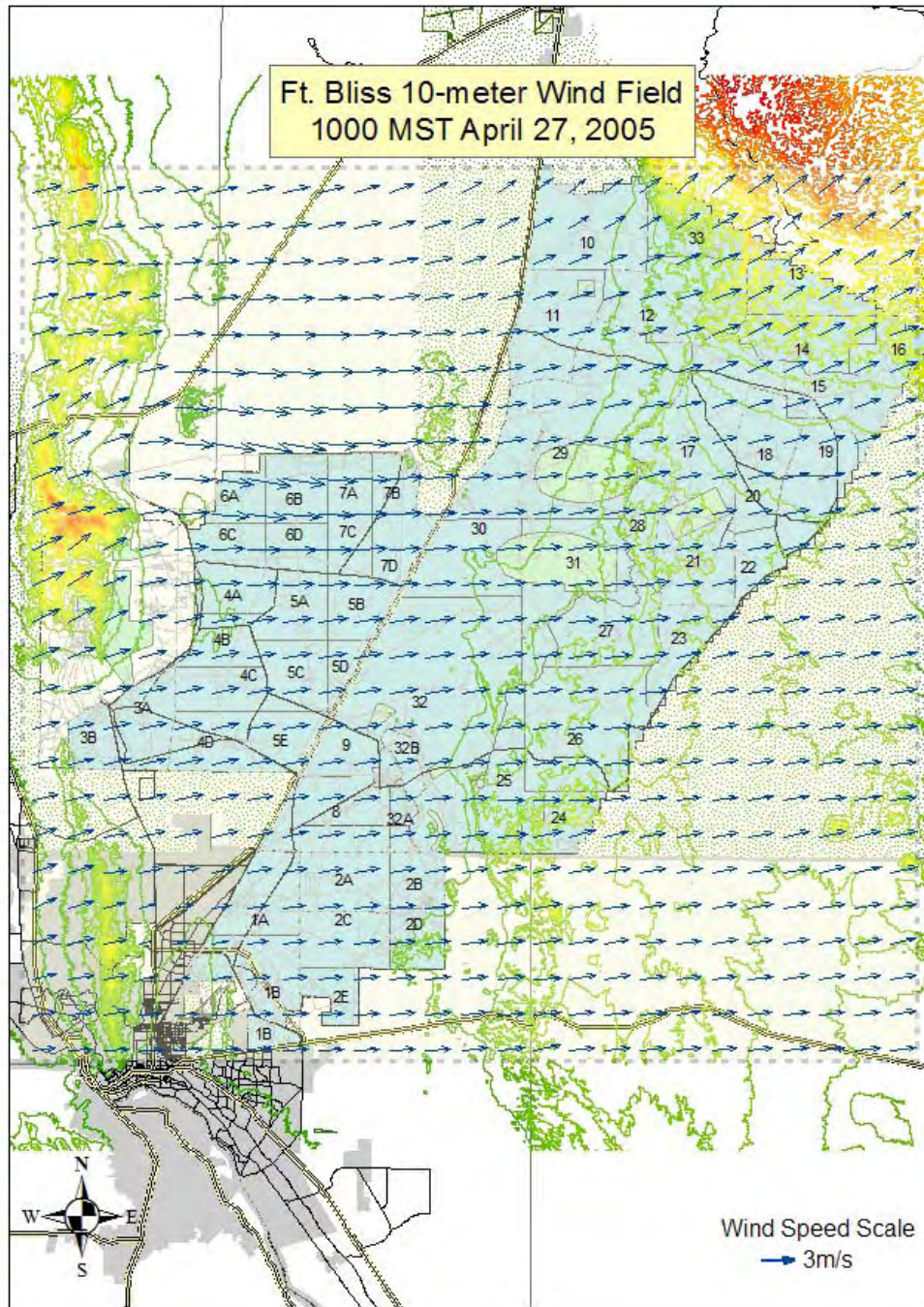


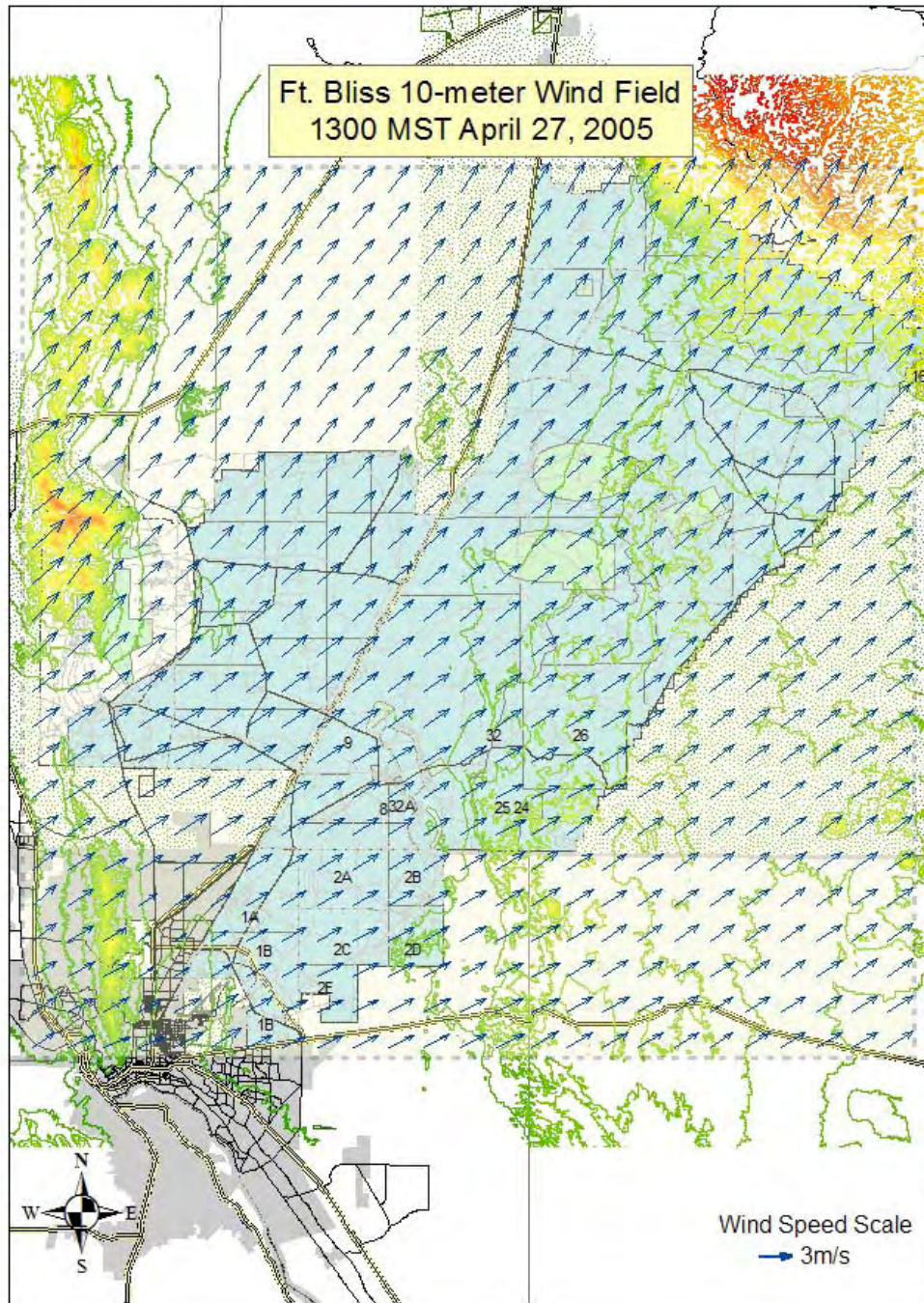


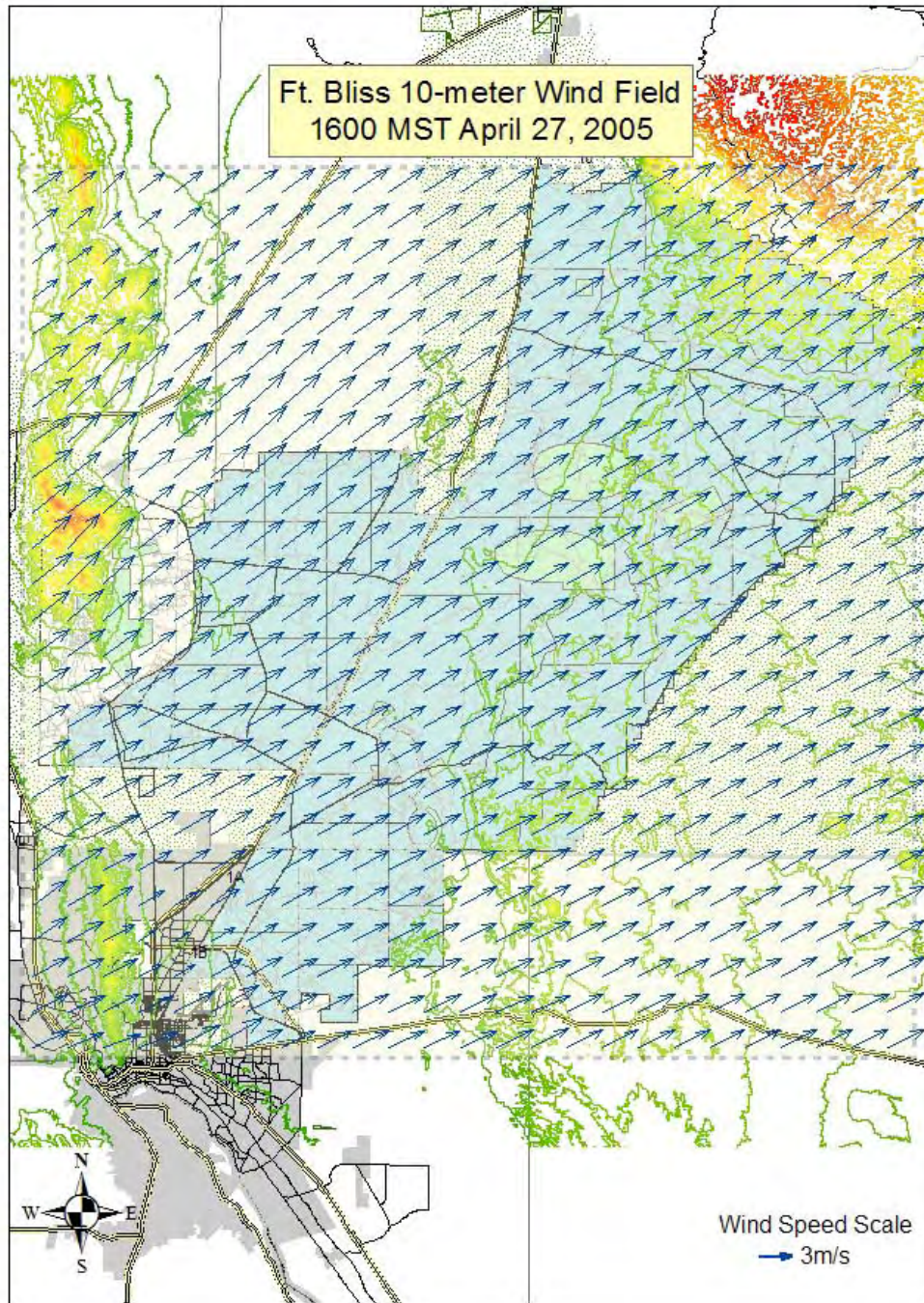


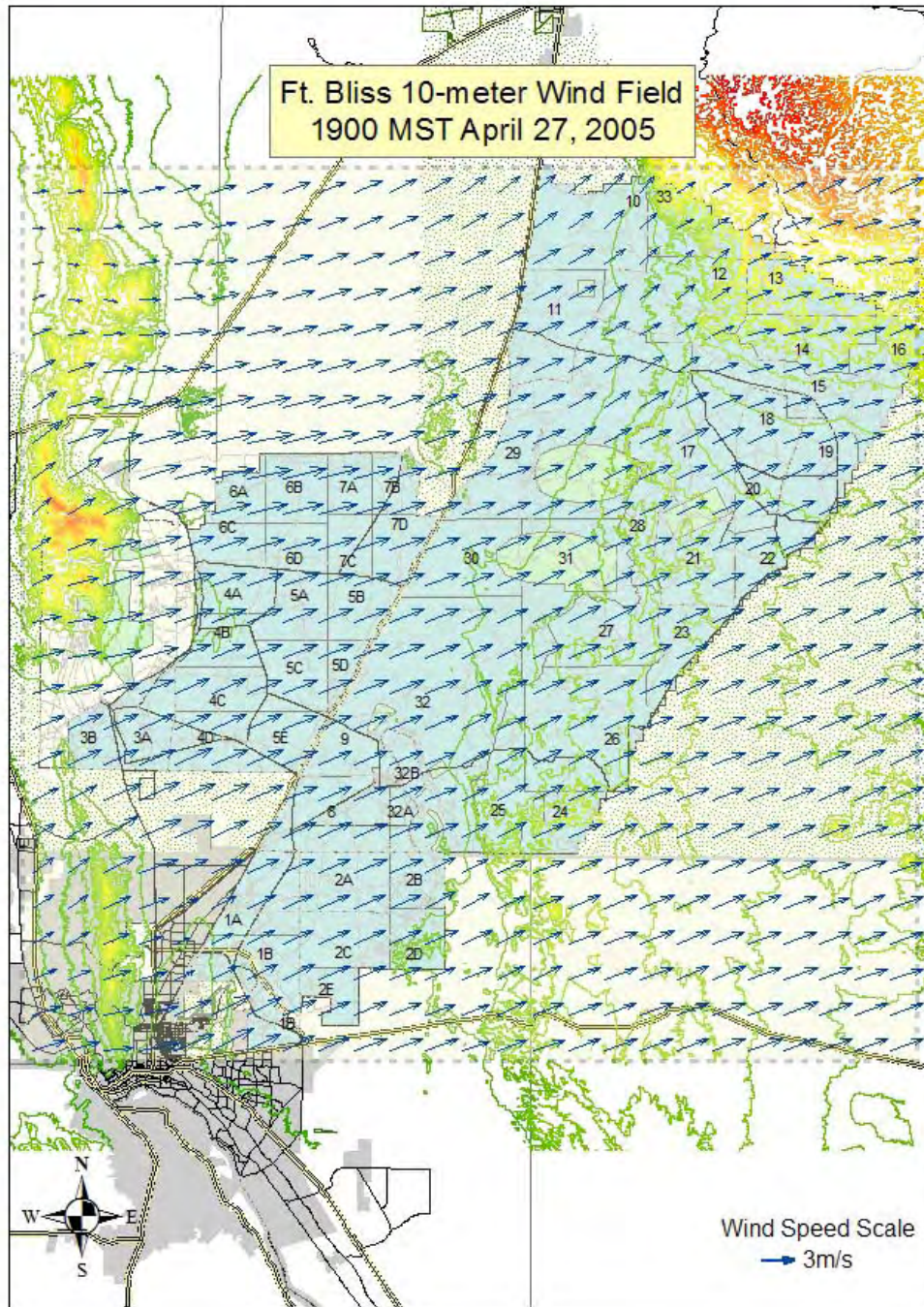


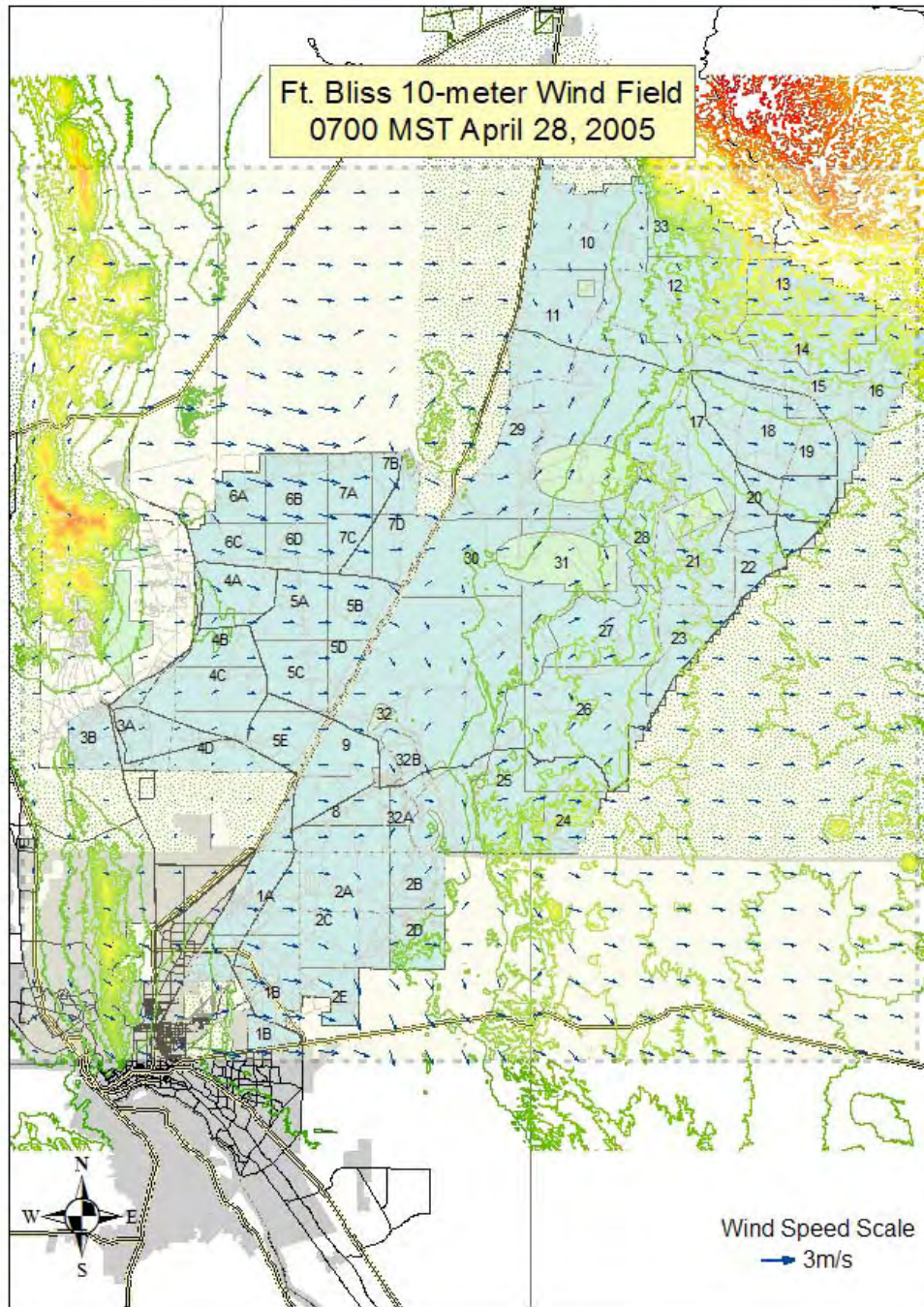


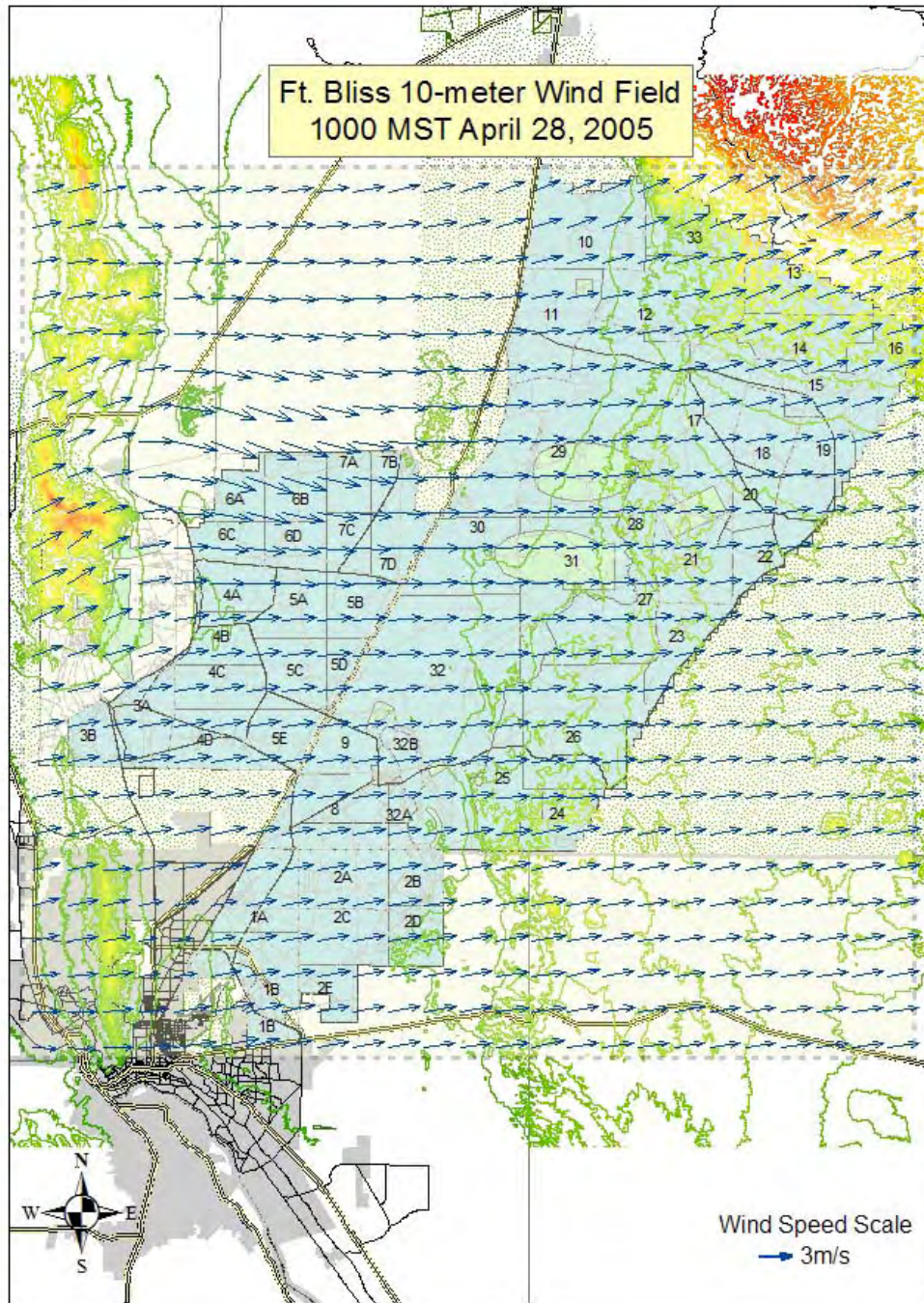


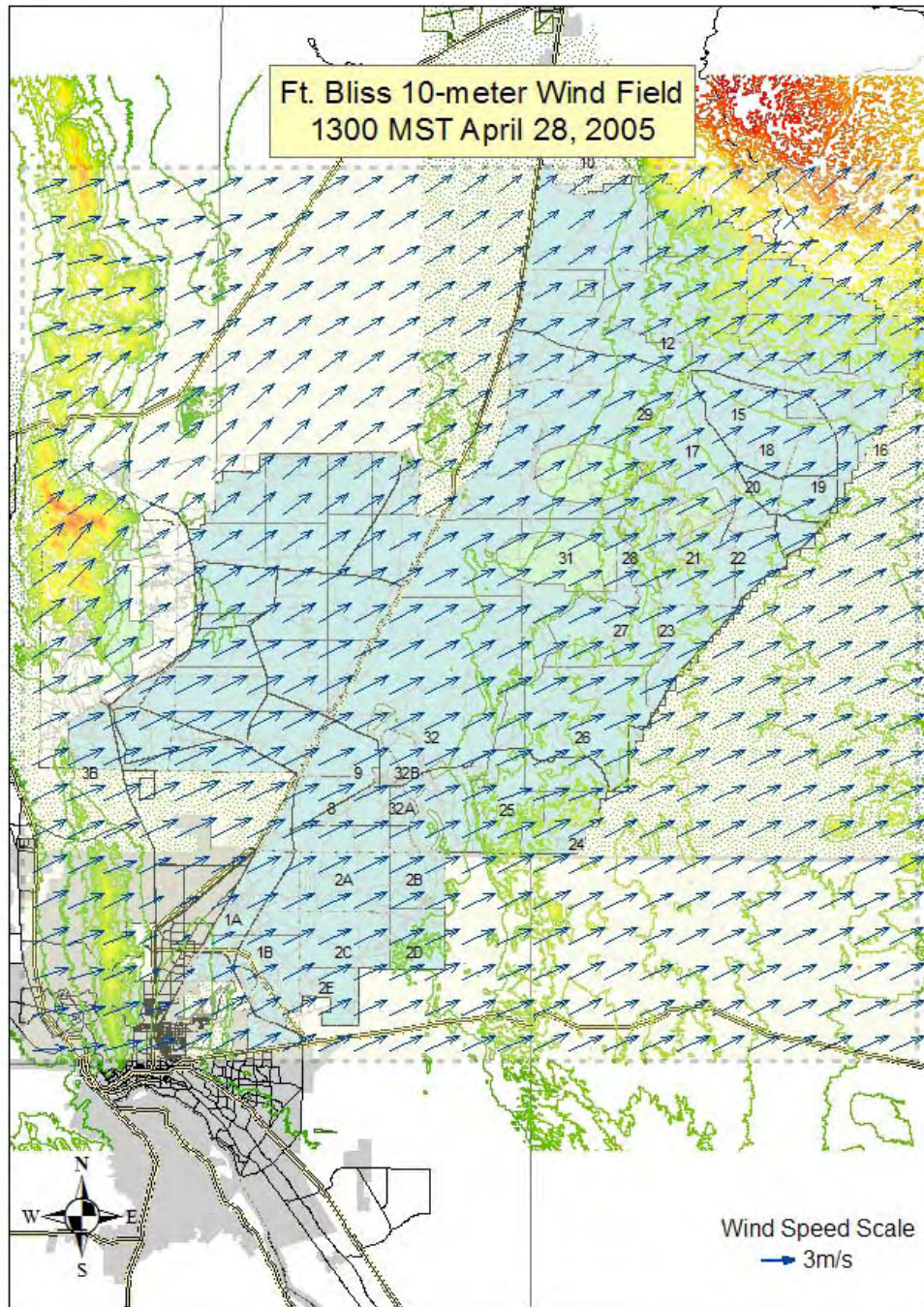


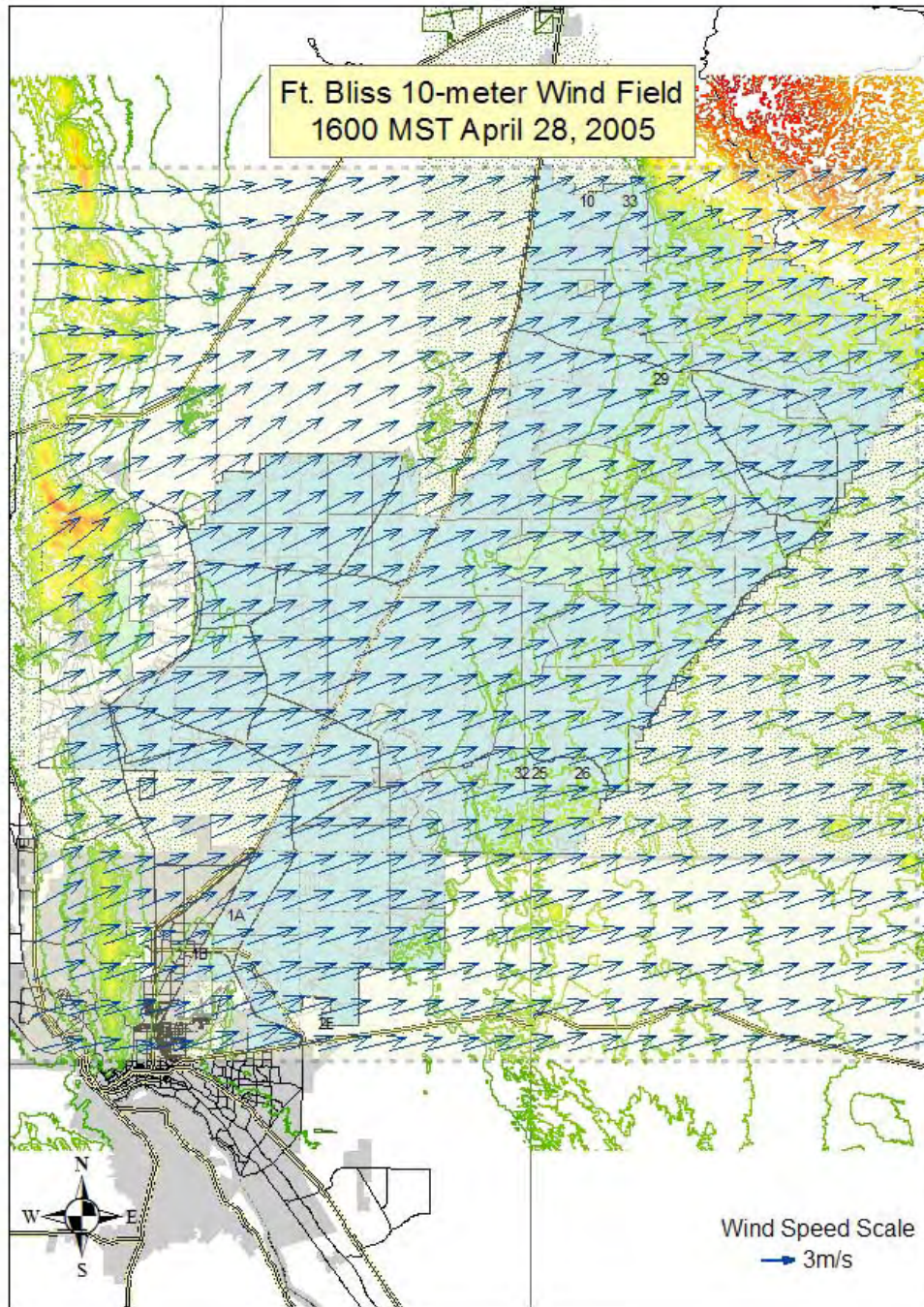


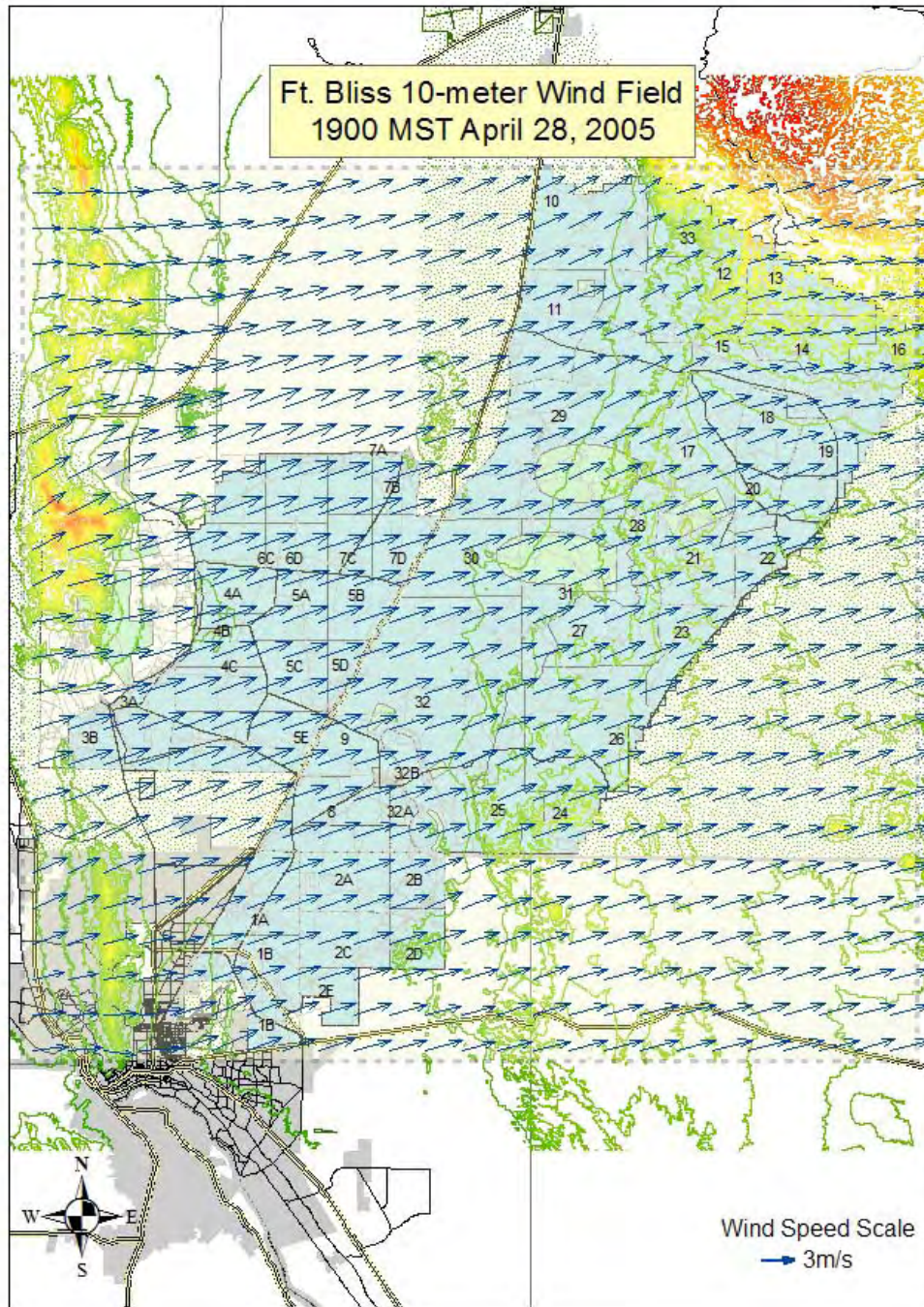


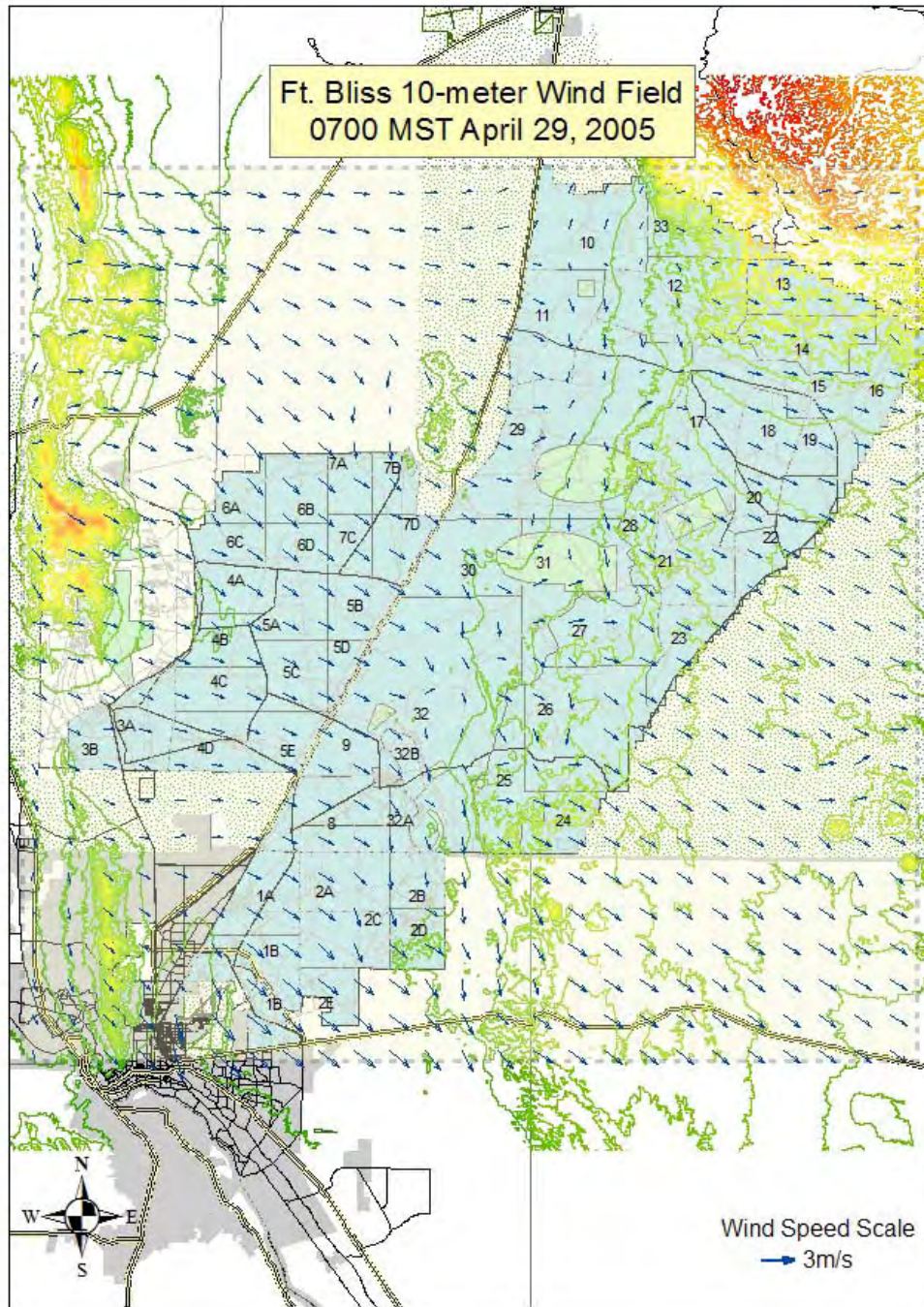


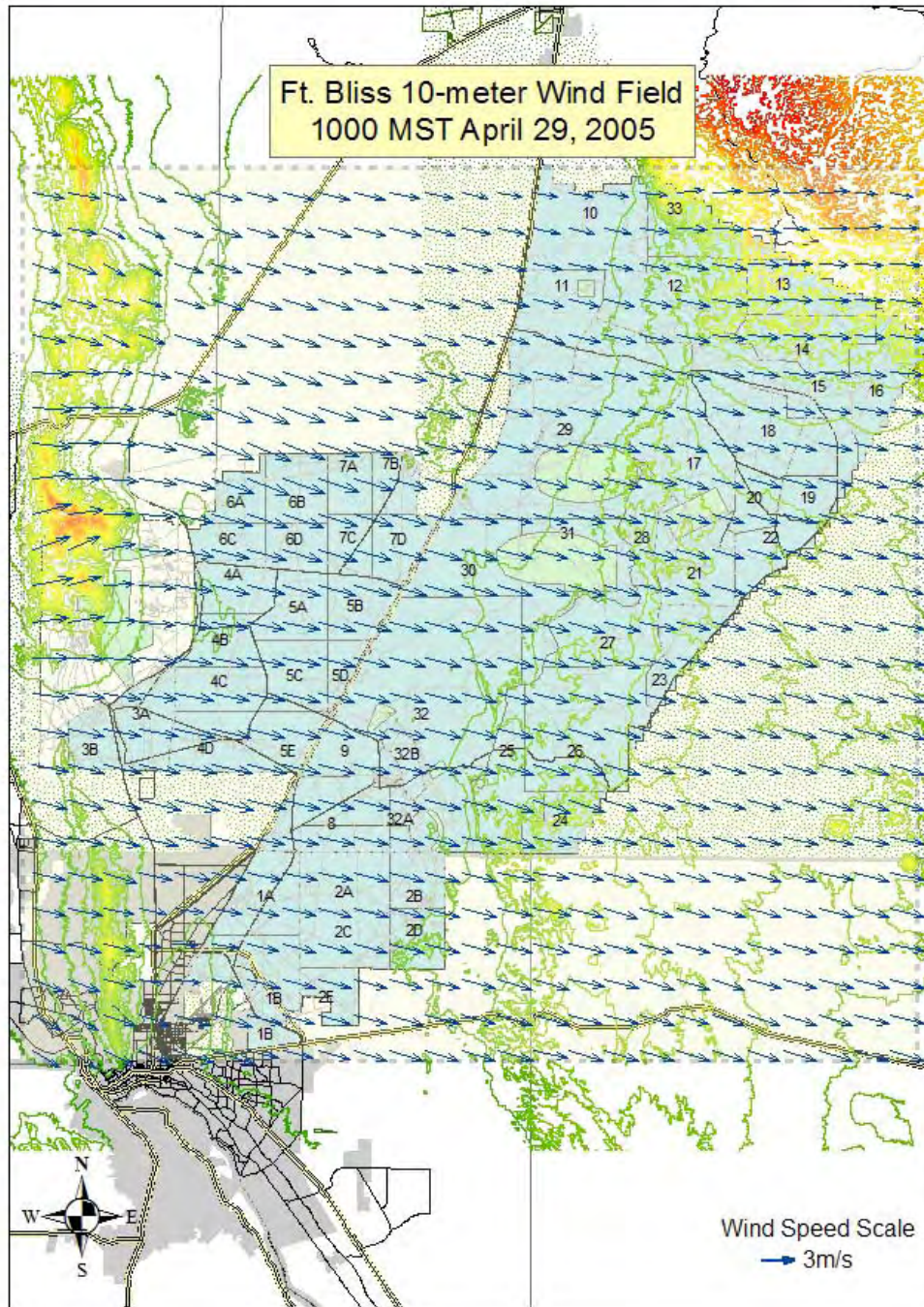


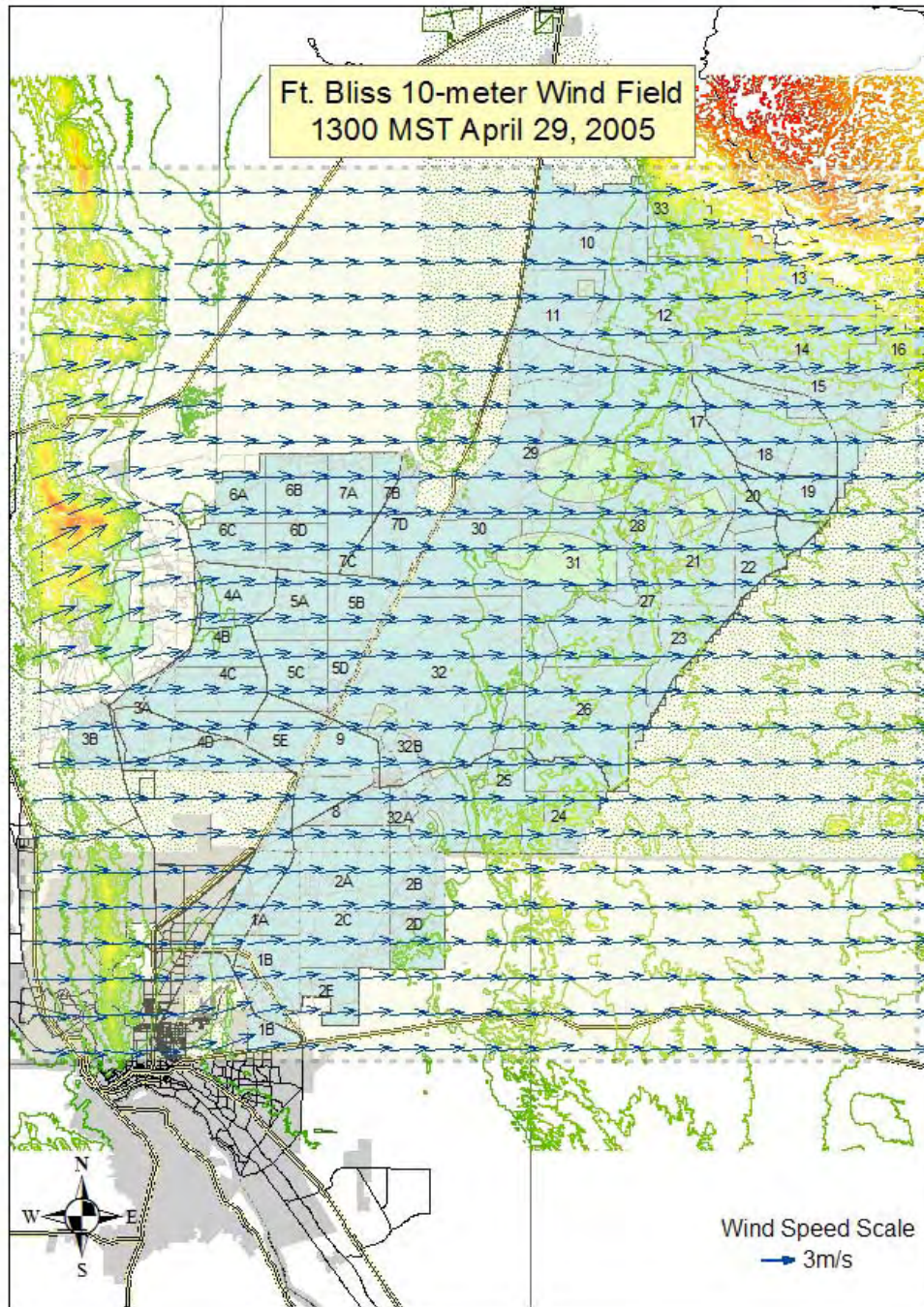


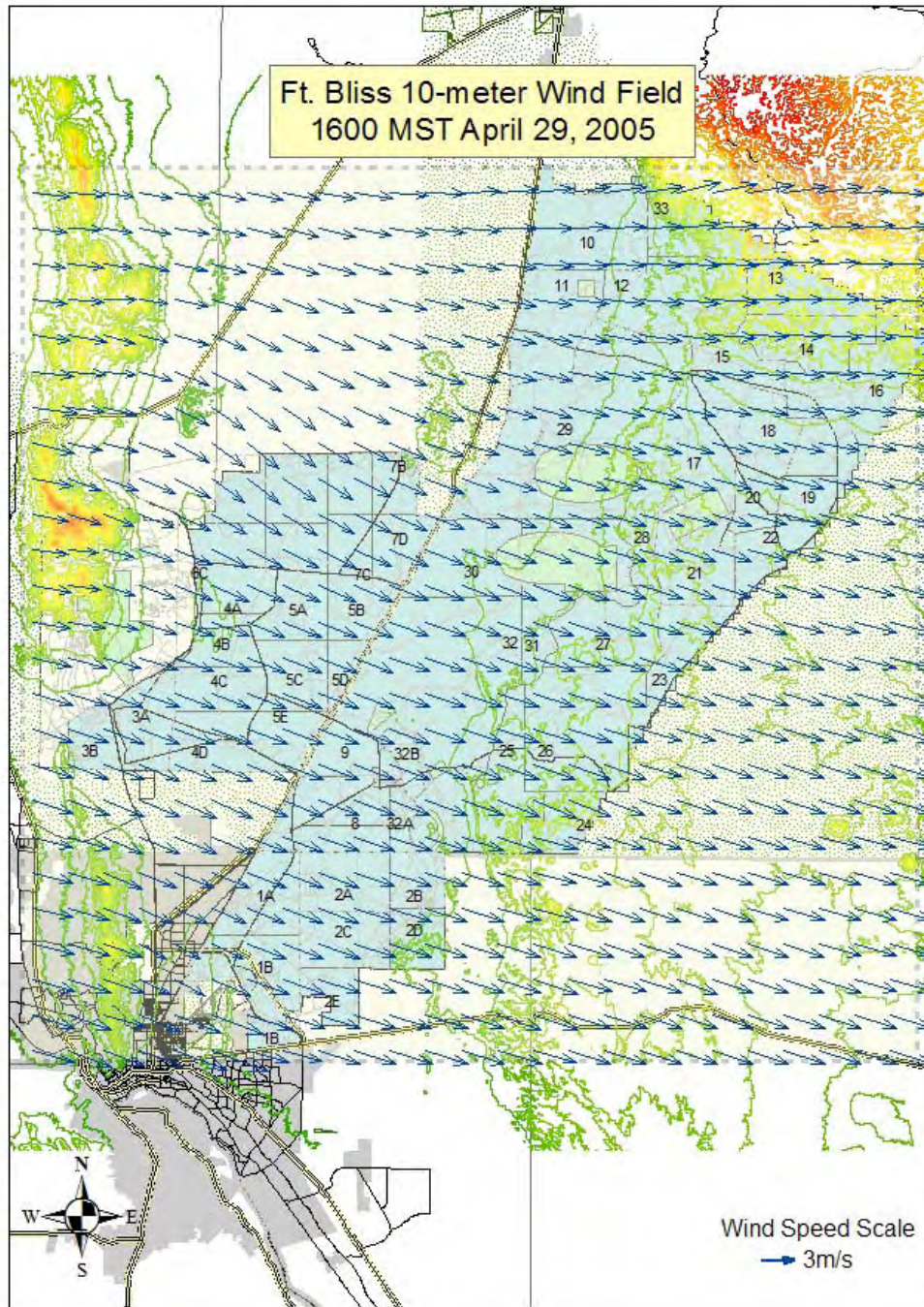


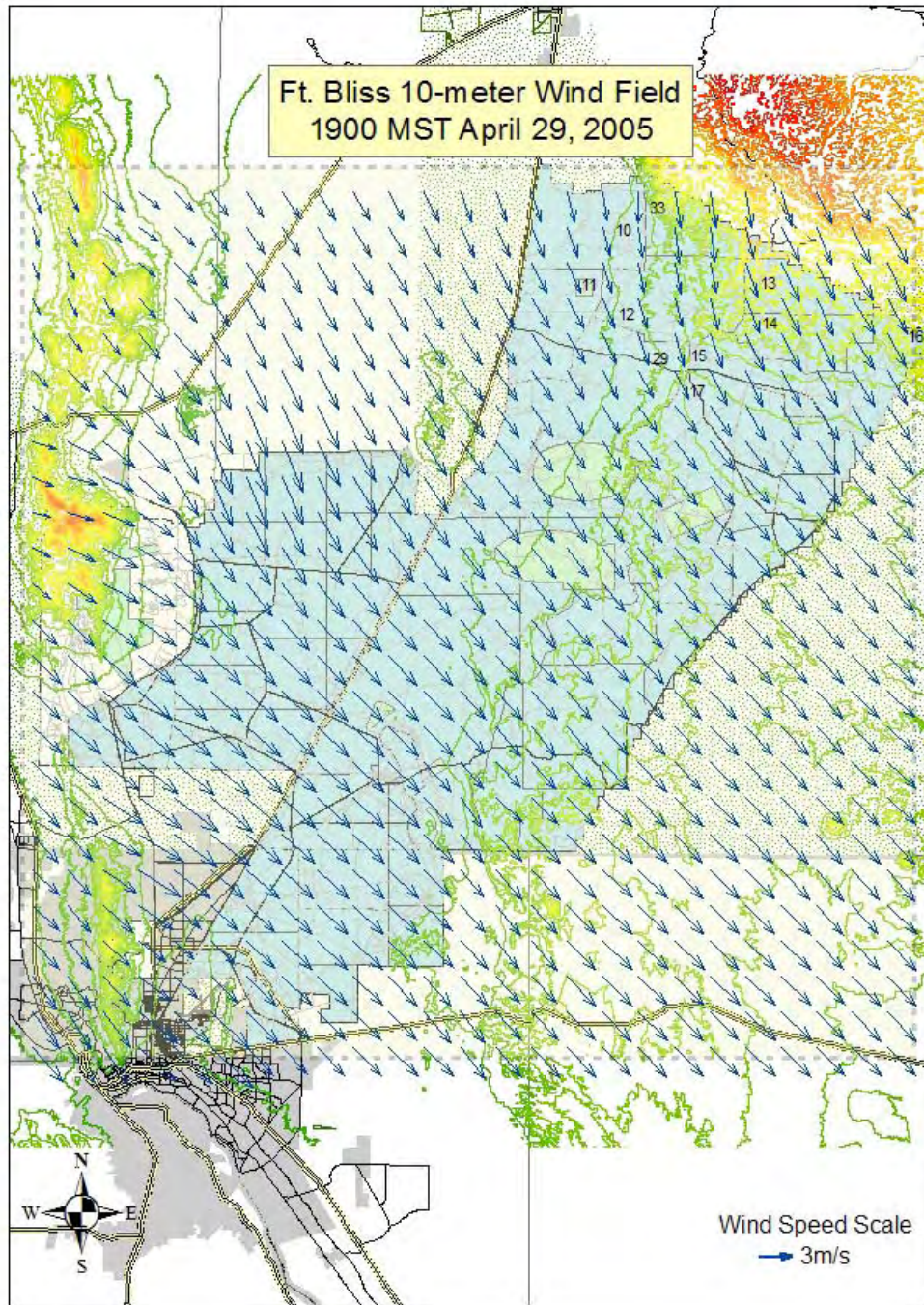


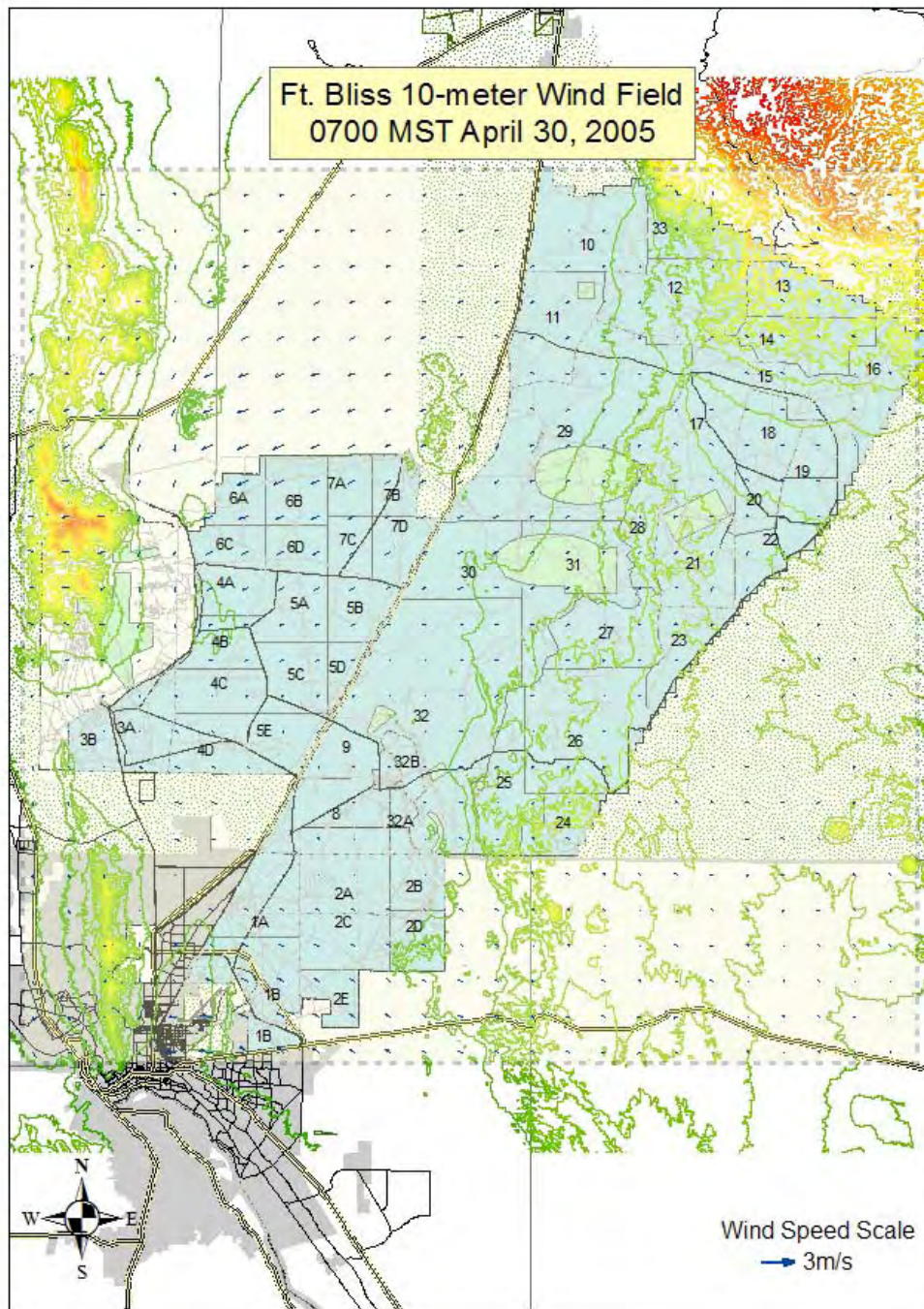


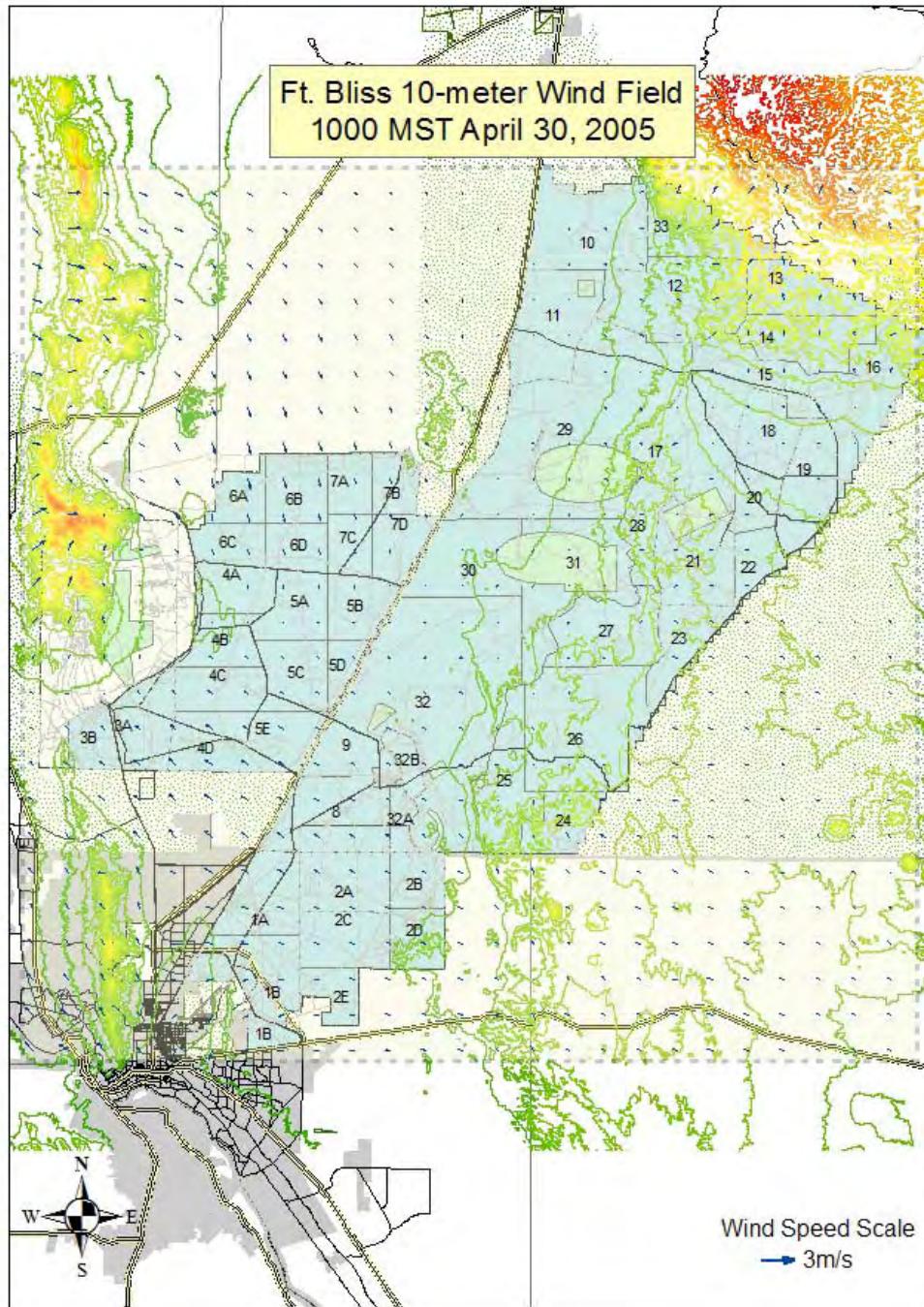


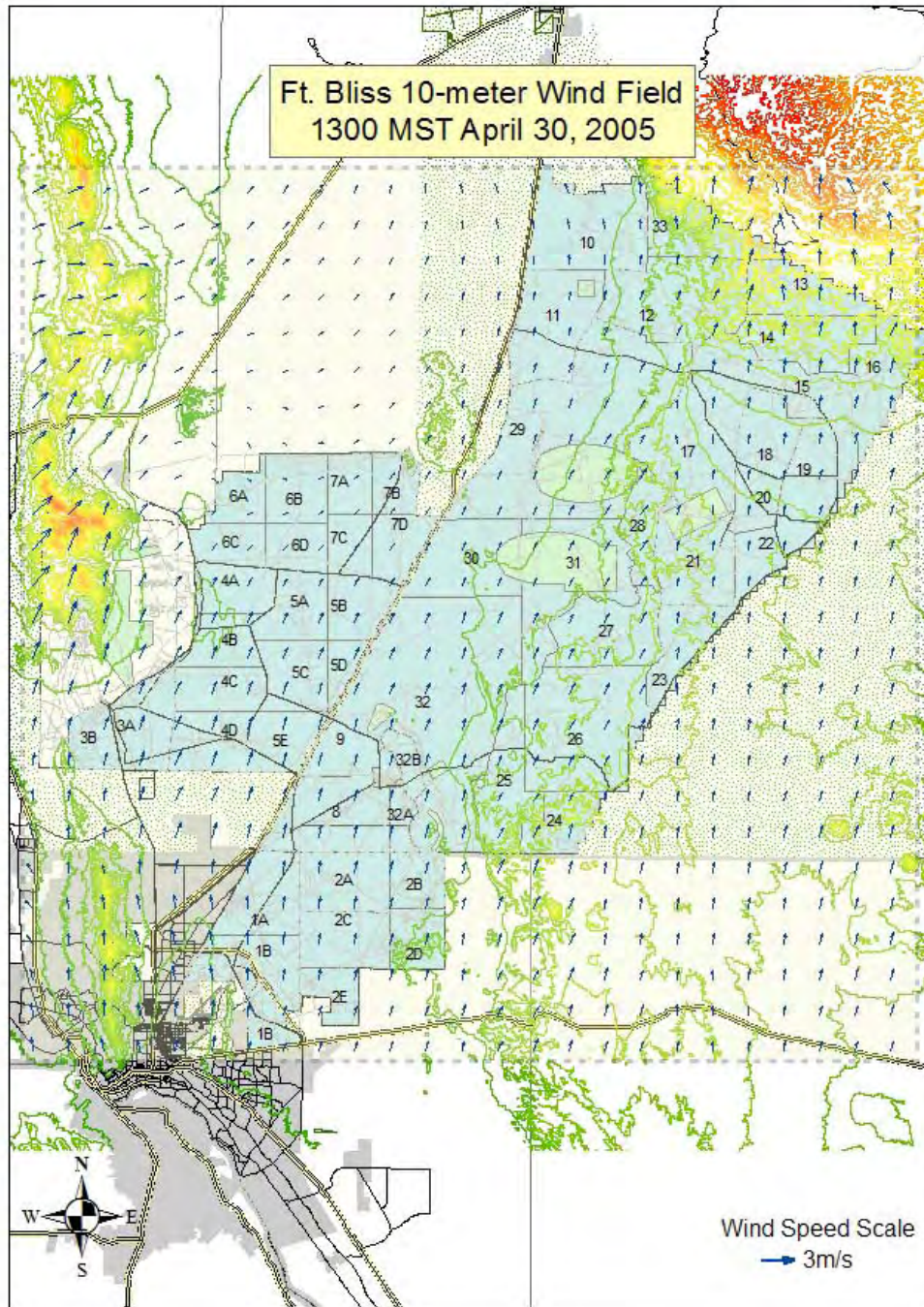


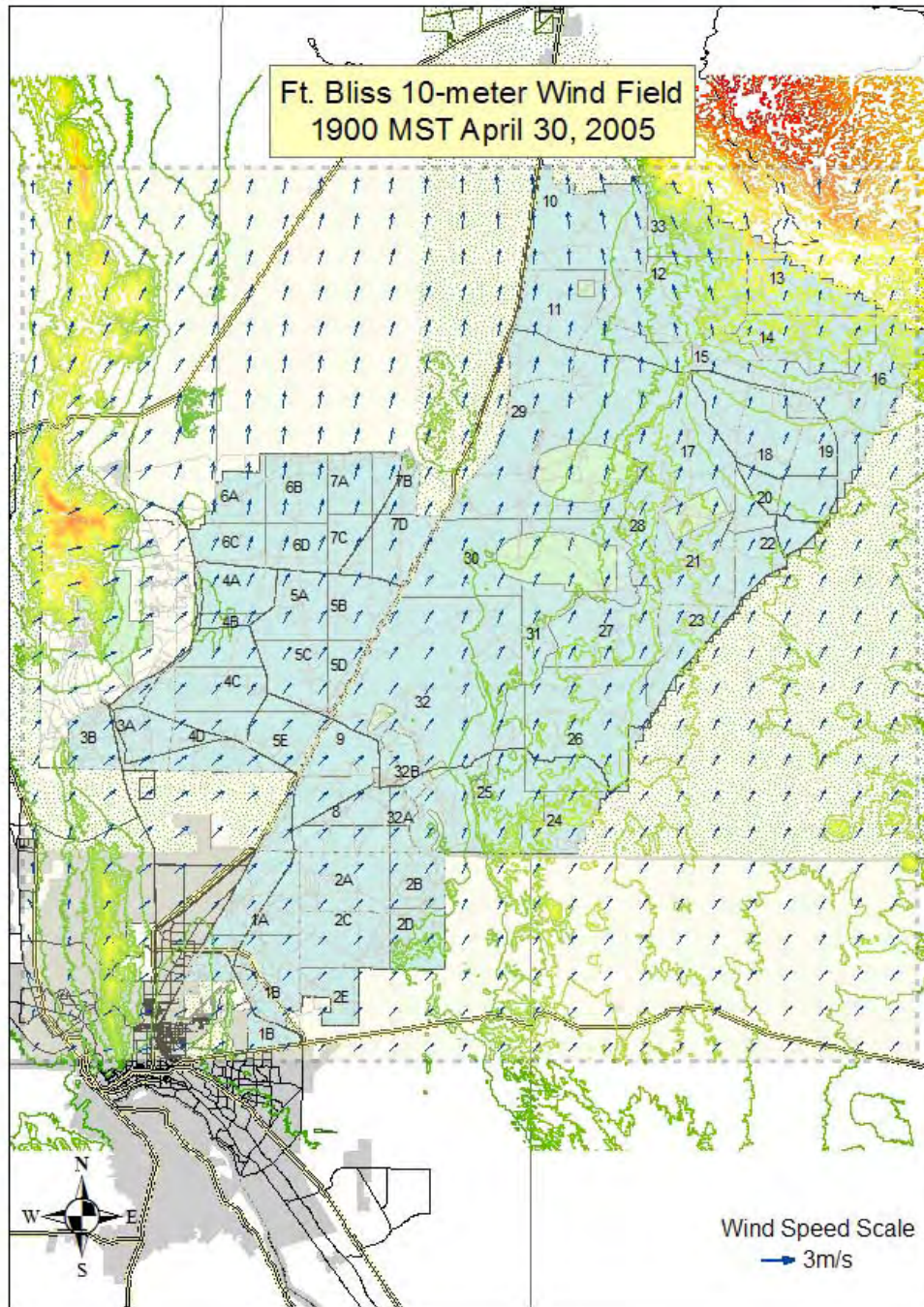










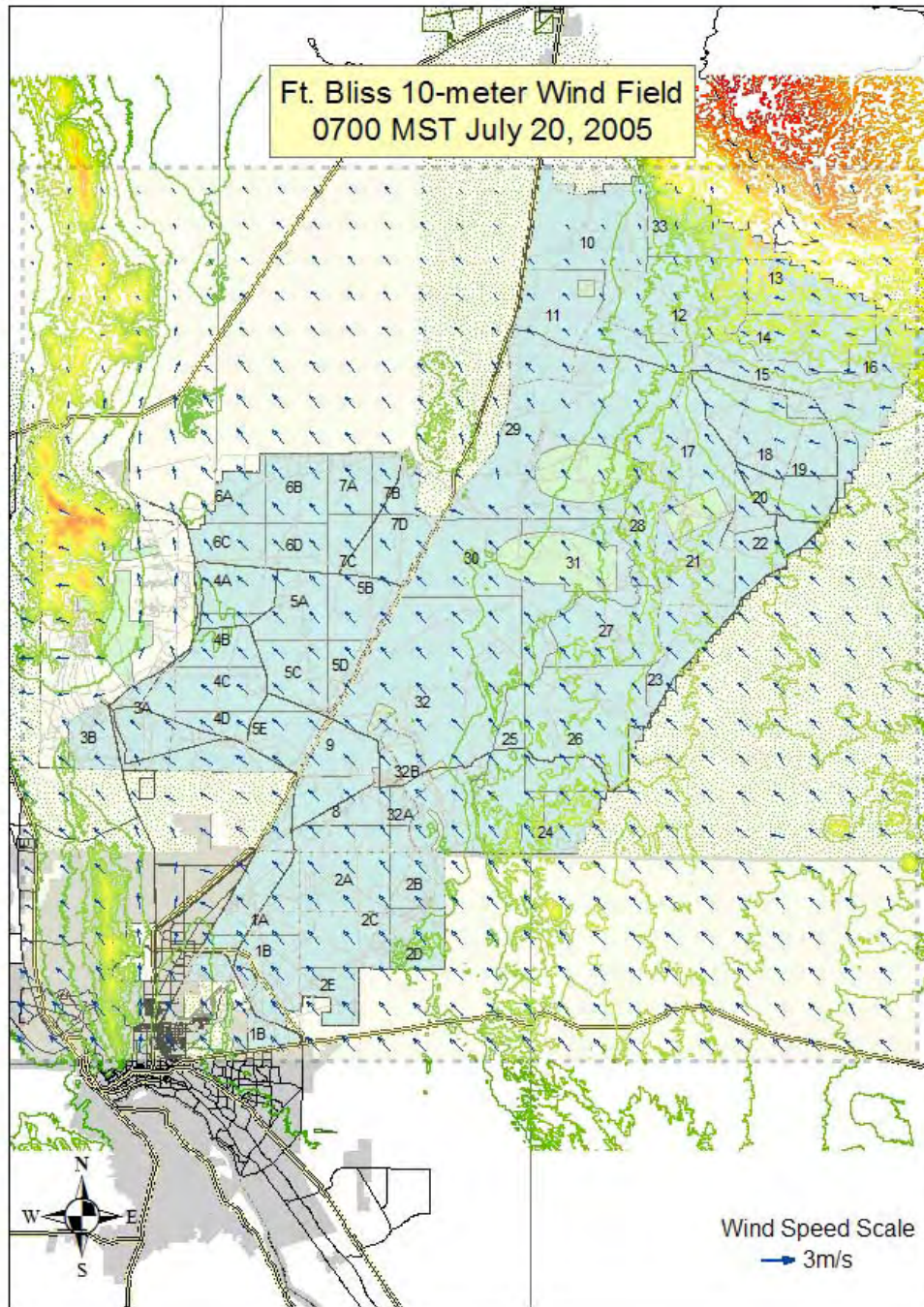


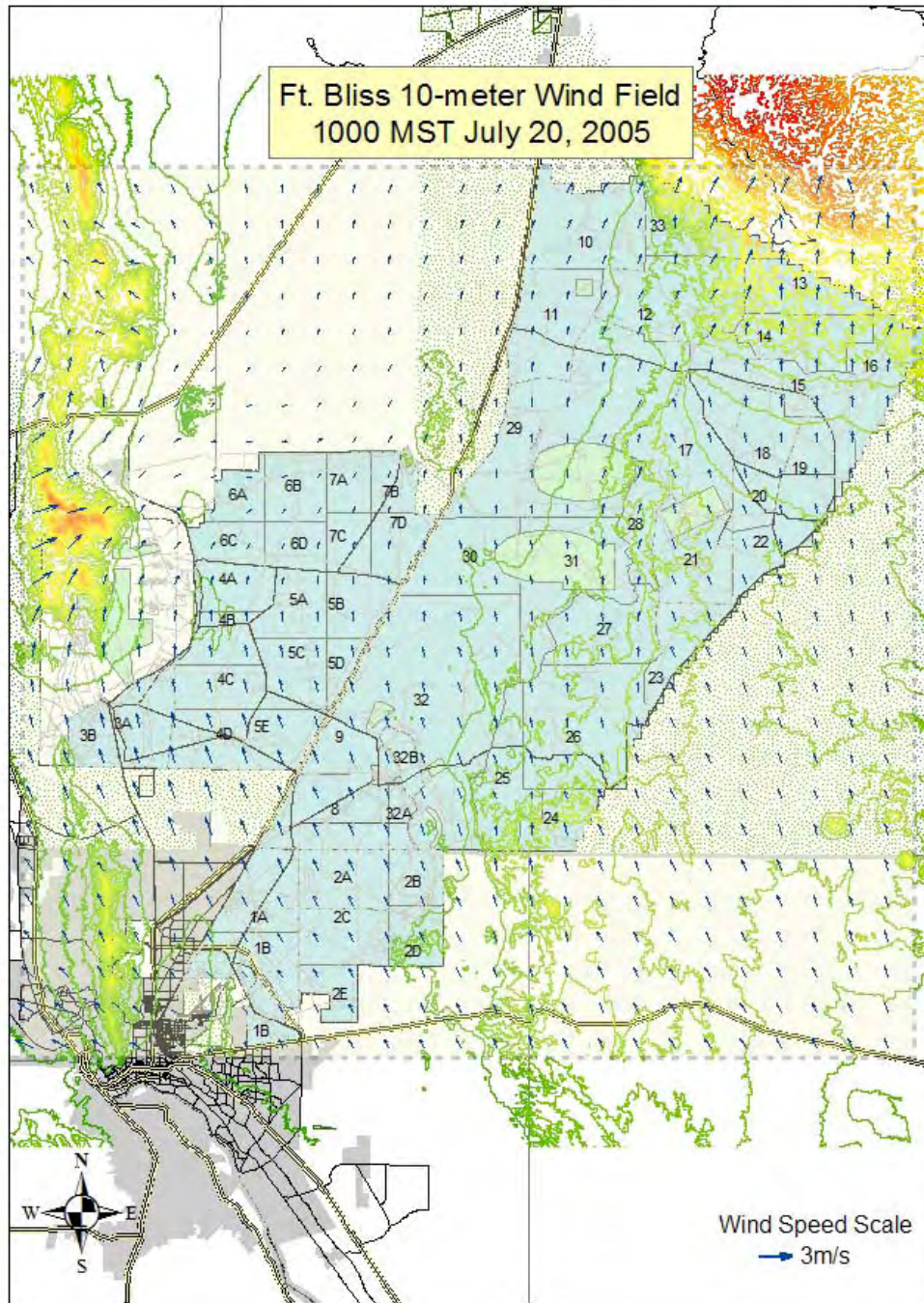
Appendix J

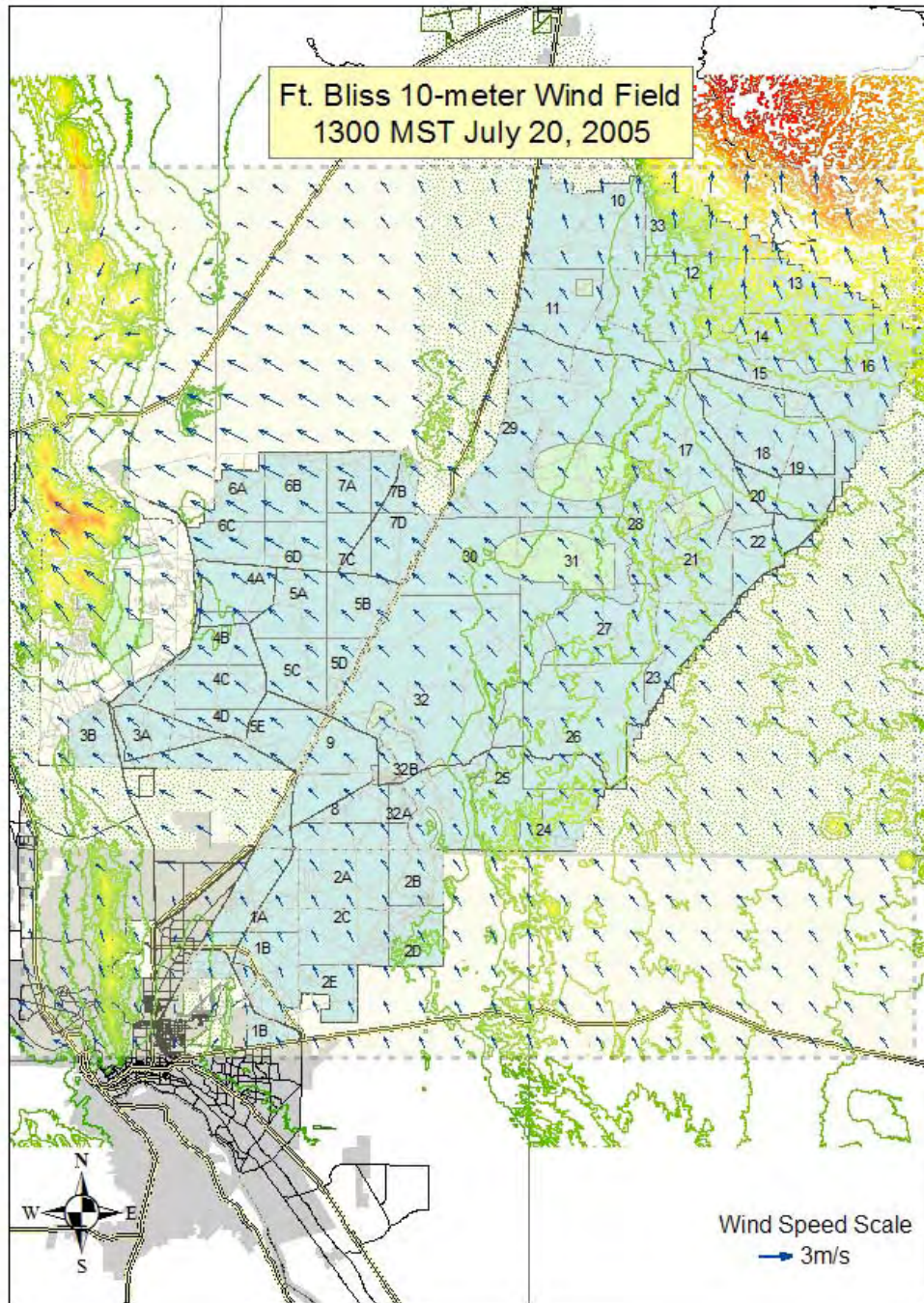
DUSTRAN 10-m-Above-Ground Wind Fields for July 20–24, 2005

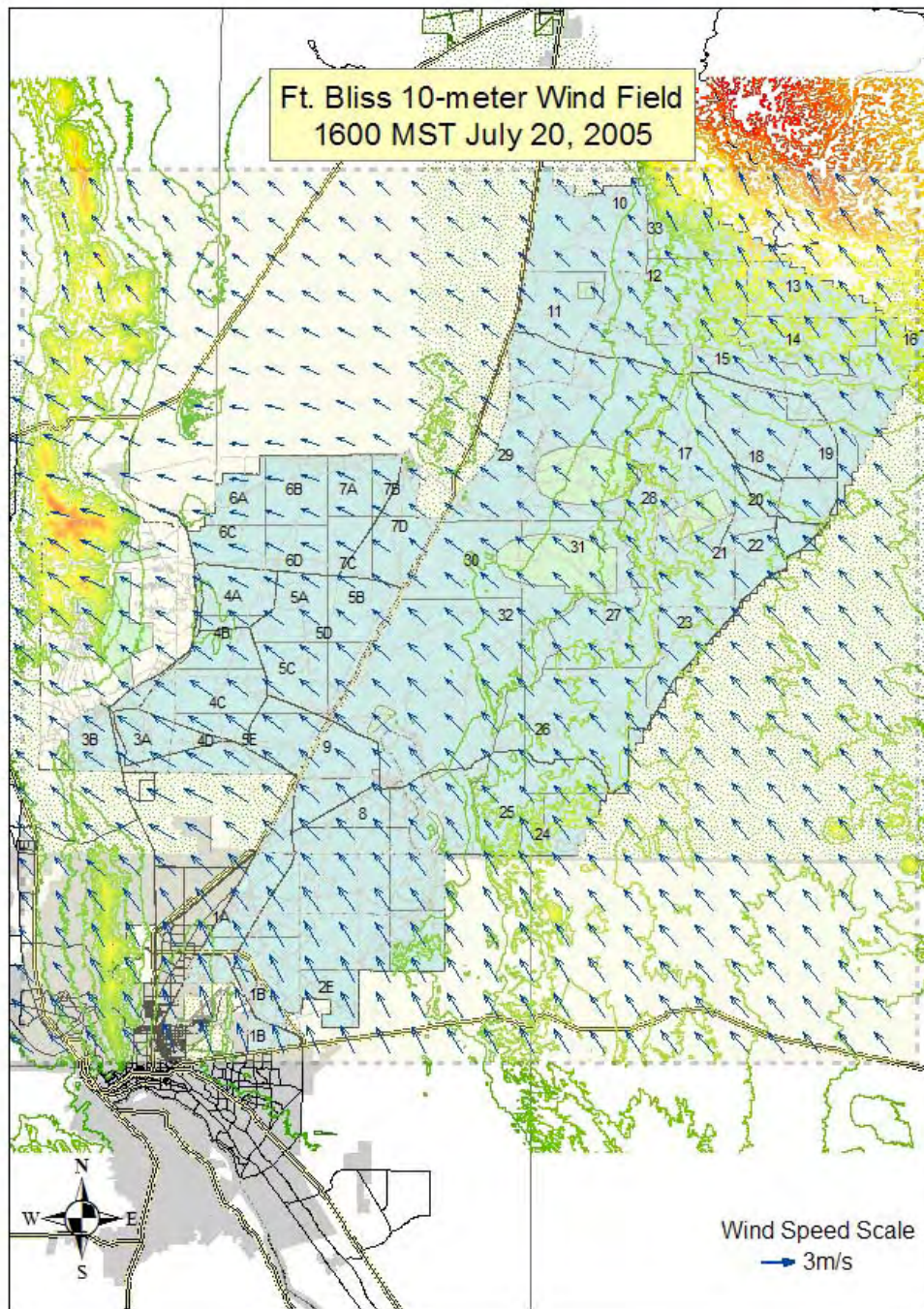
Appendix J: DUSTRAN 10-m-Above-Ground Wind Fields for July 20–24, 2005

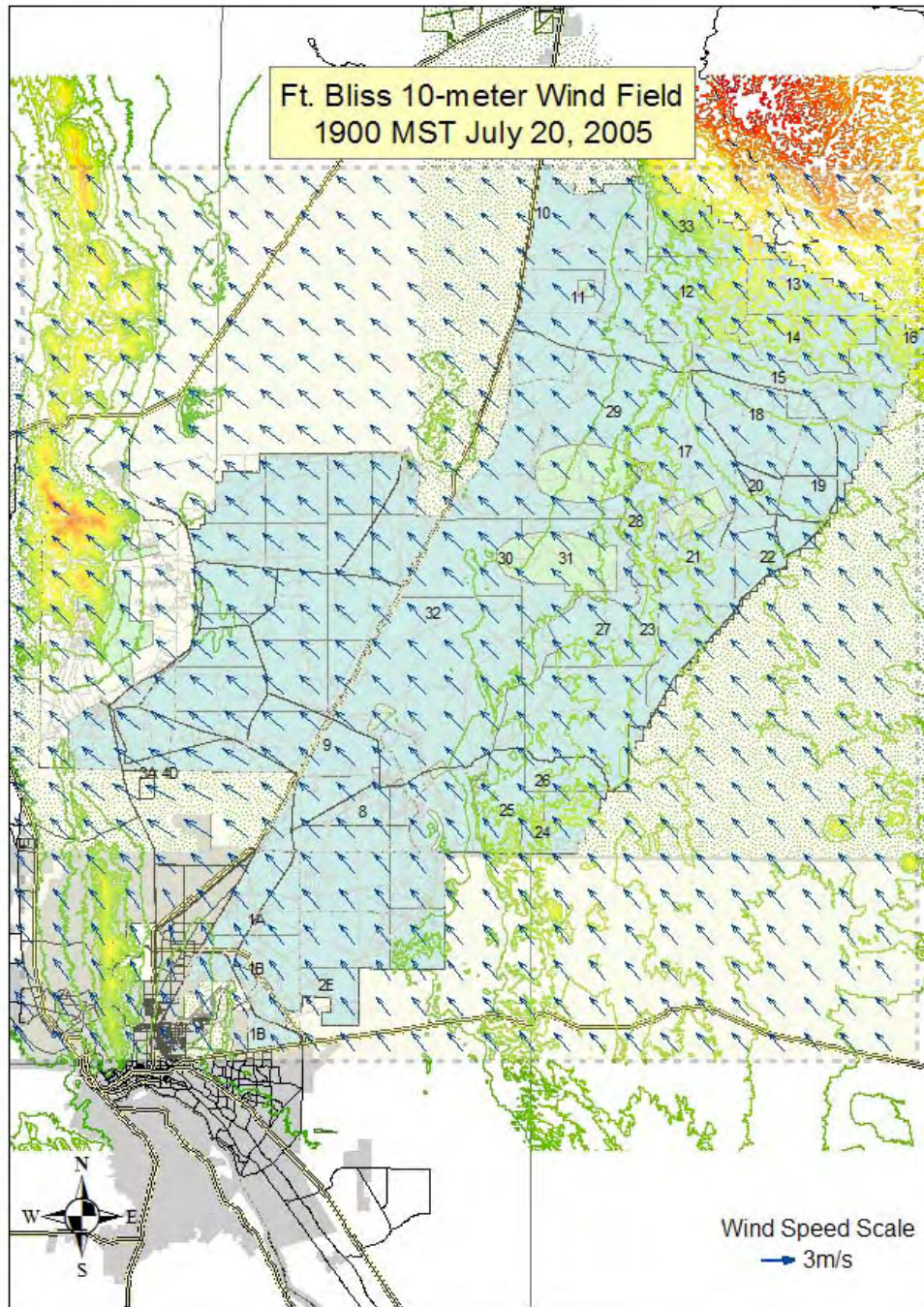
This appendix contains 25 screen captures of the 10-m above-ground wind fields predicted by the CALMET module within DUSTRAN. Wind fields are shown at 0700, 1000, 1300, 1600, and 1900 MST for the 5 days included in the current simulations (July 20 through 24, 2005). Header captions within each figure indicate the day and time represented by a given plot. The arrow on each vector indicates wind direction while the scaling of vector length indicates wind speed. A reference vector whose length represents a wind speed of 3 m/s is shown on each plot.

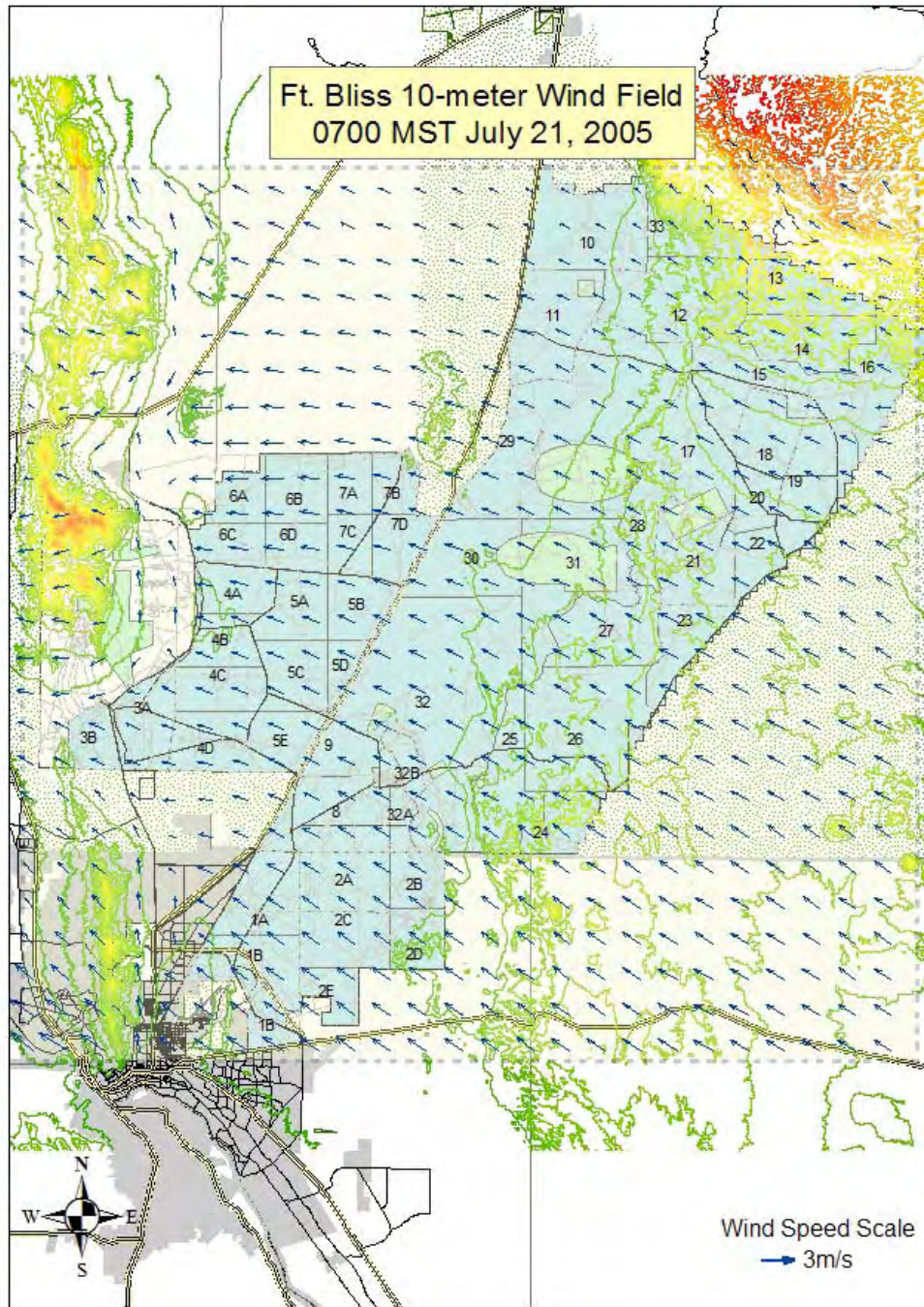


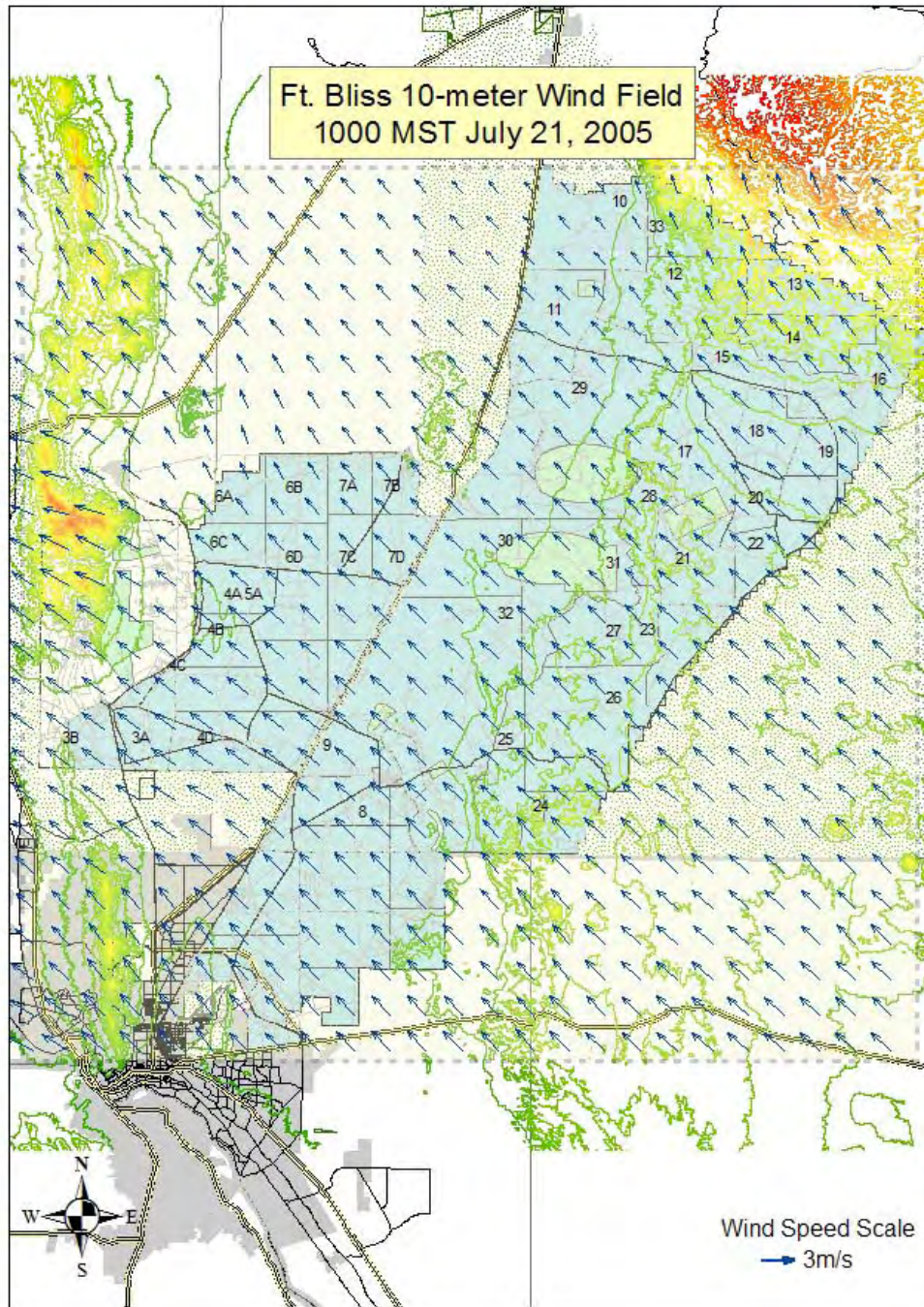


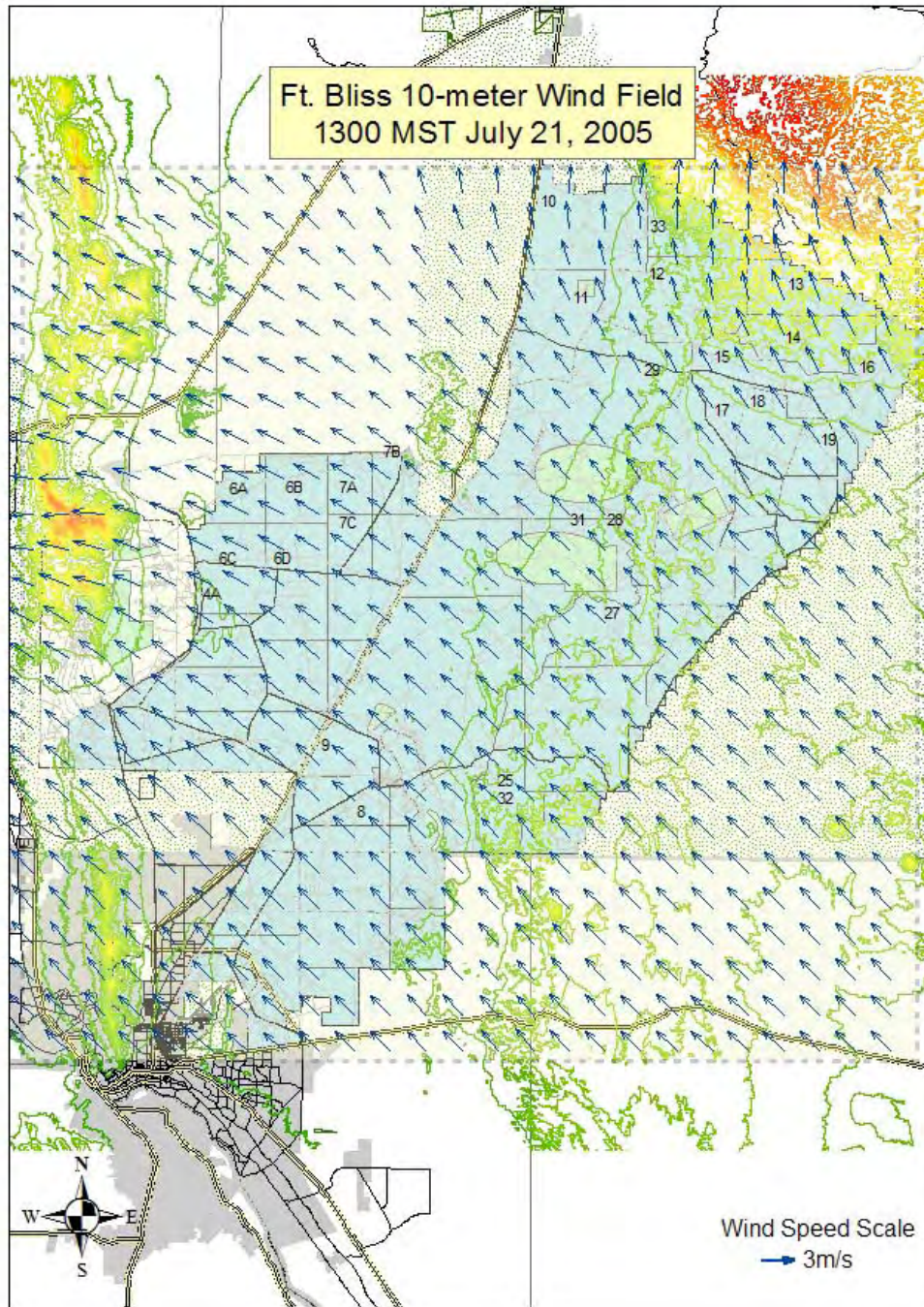


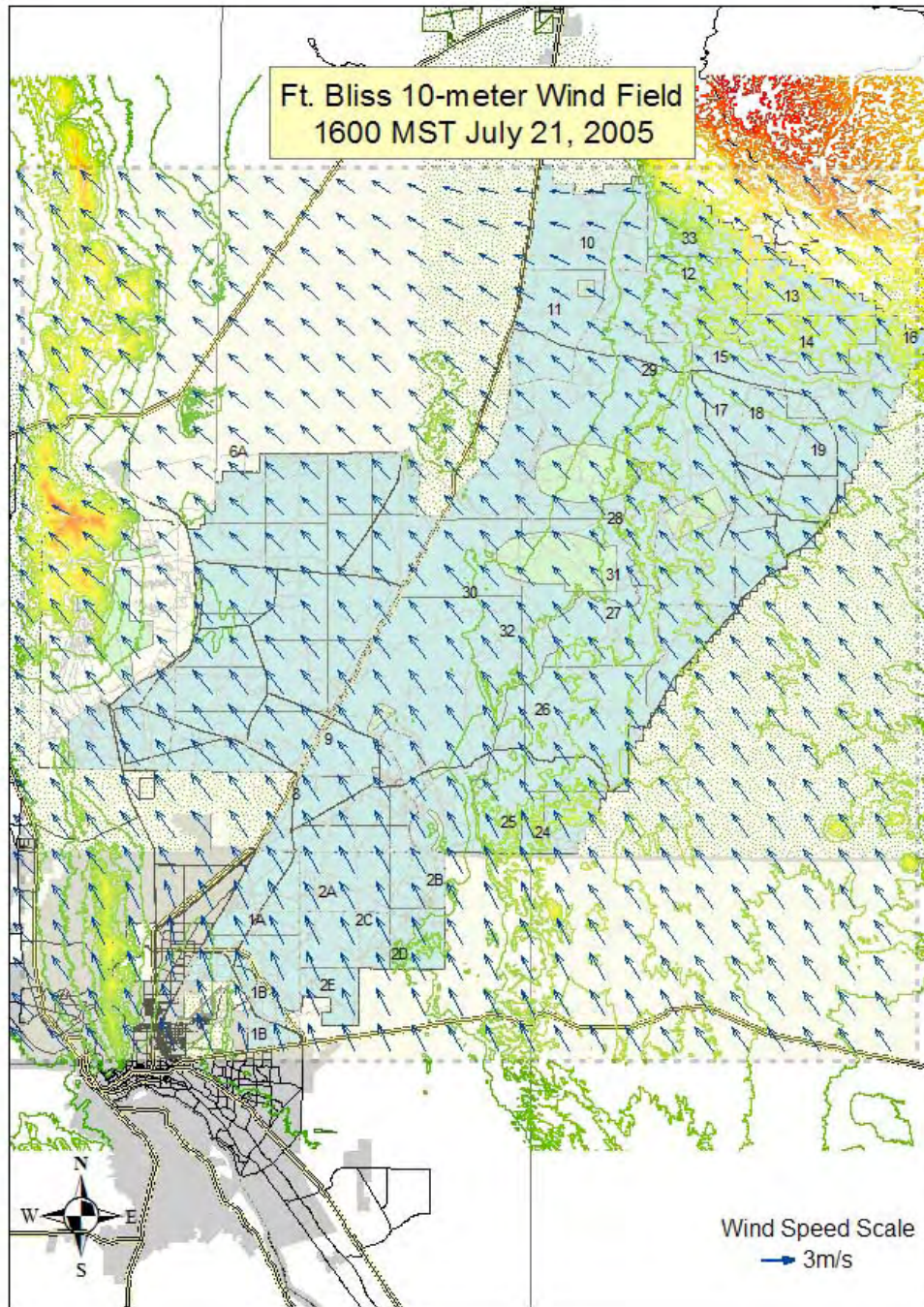


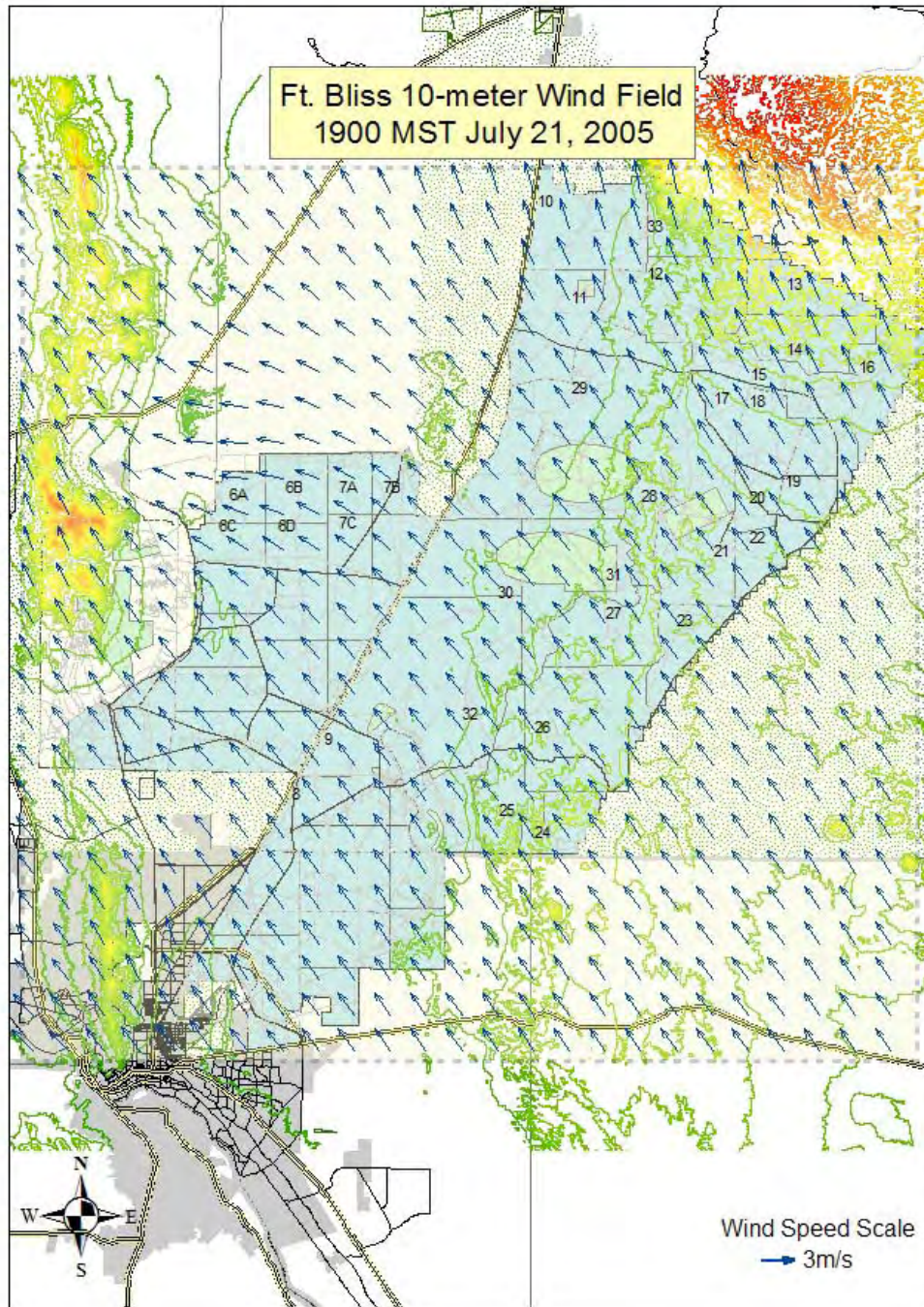


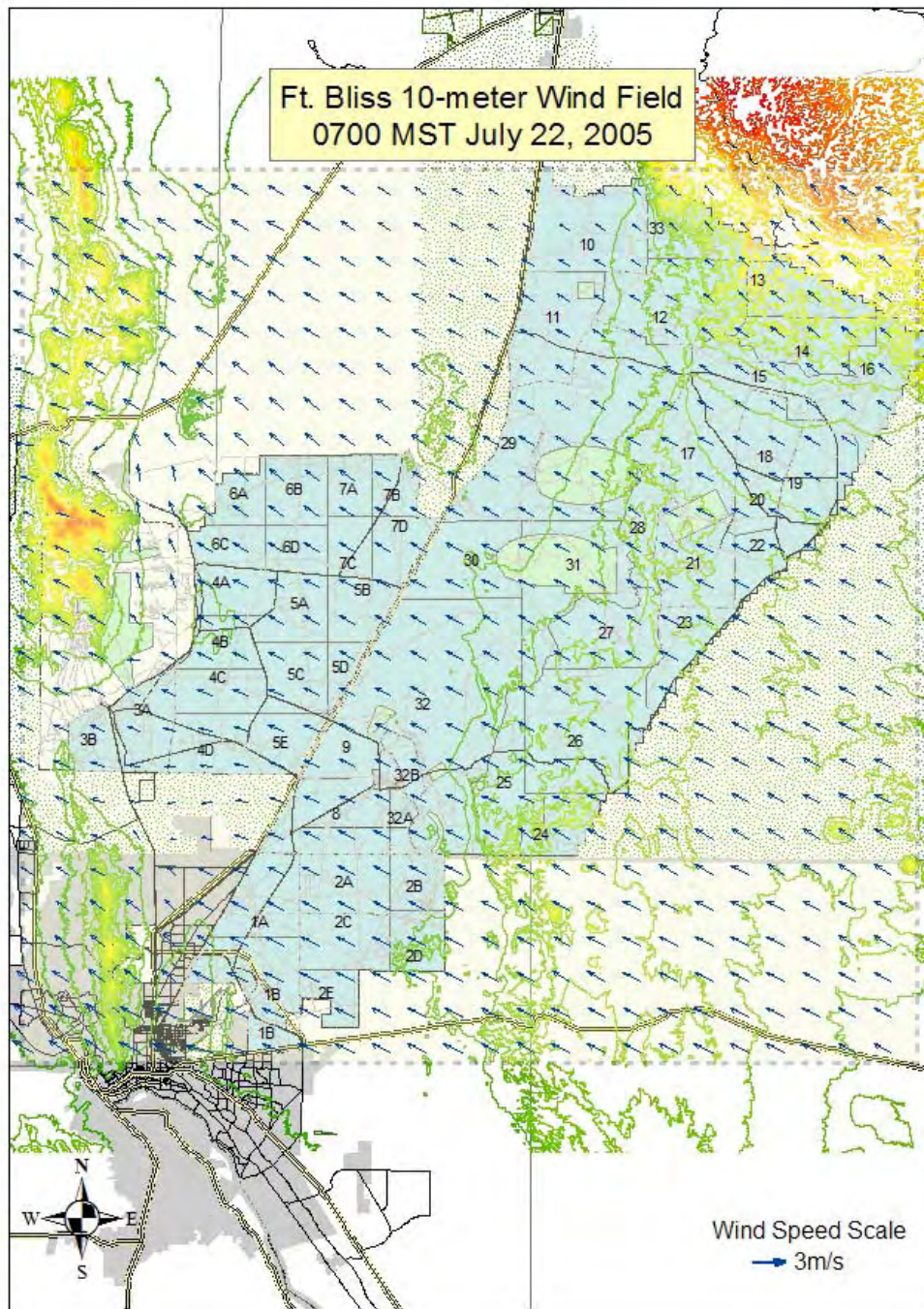


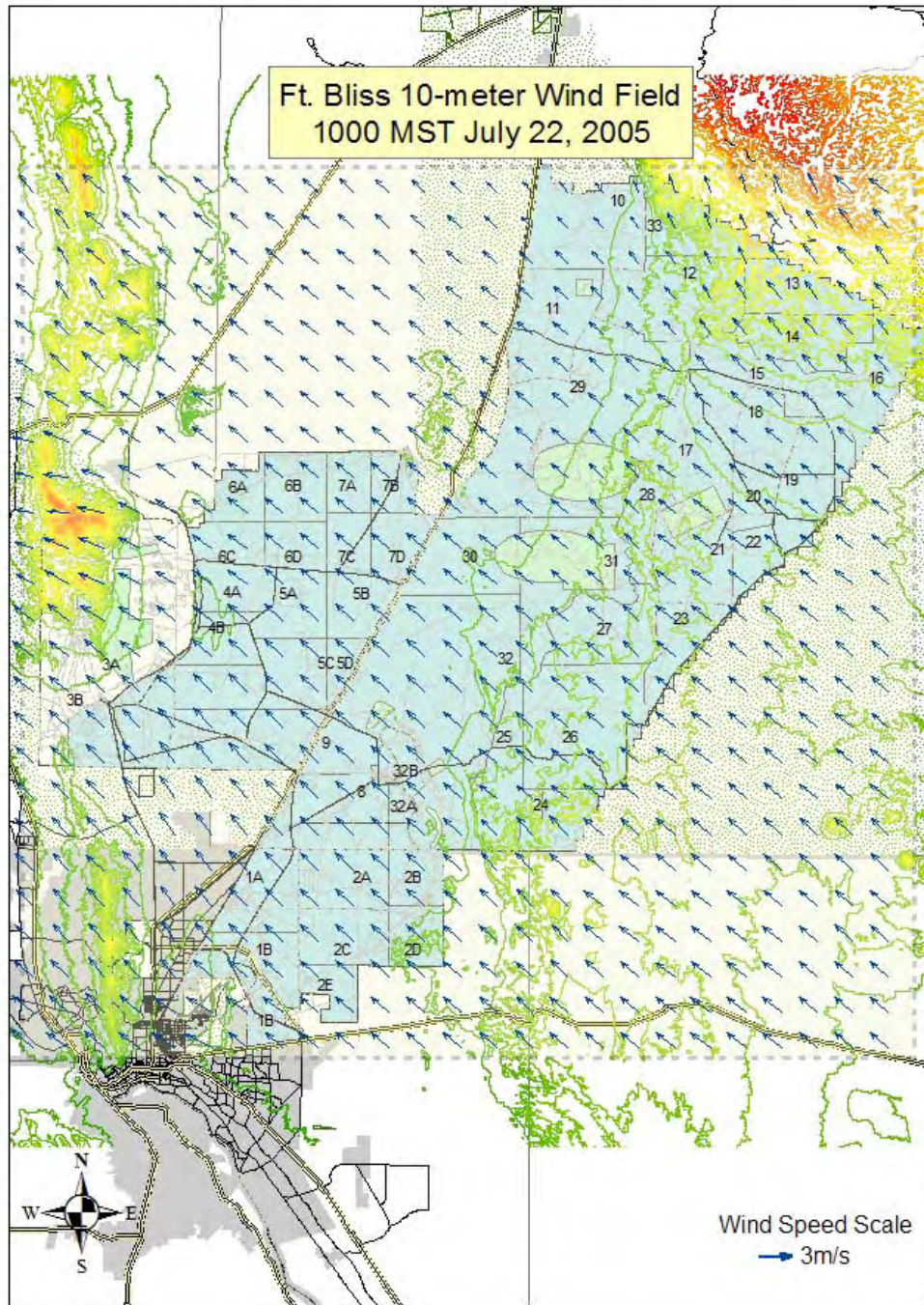


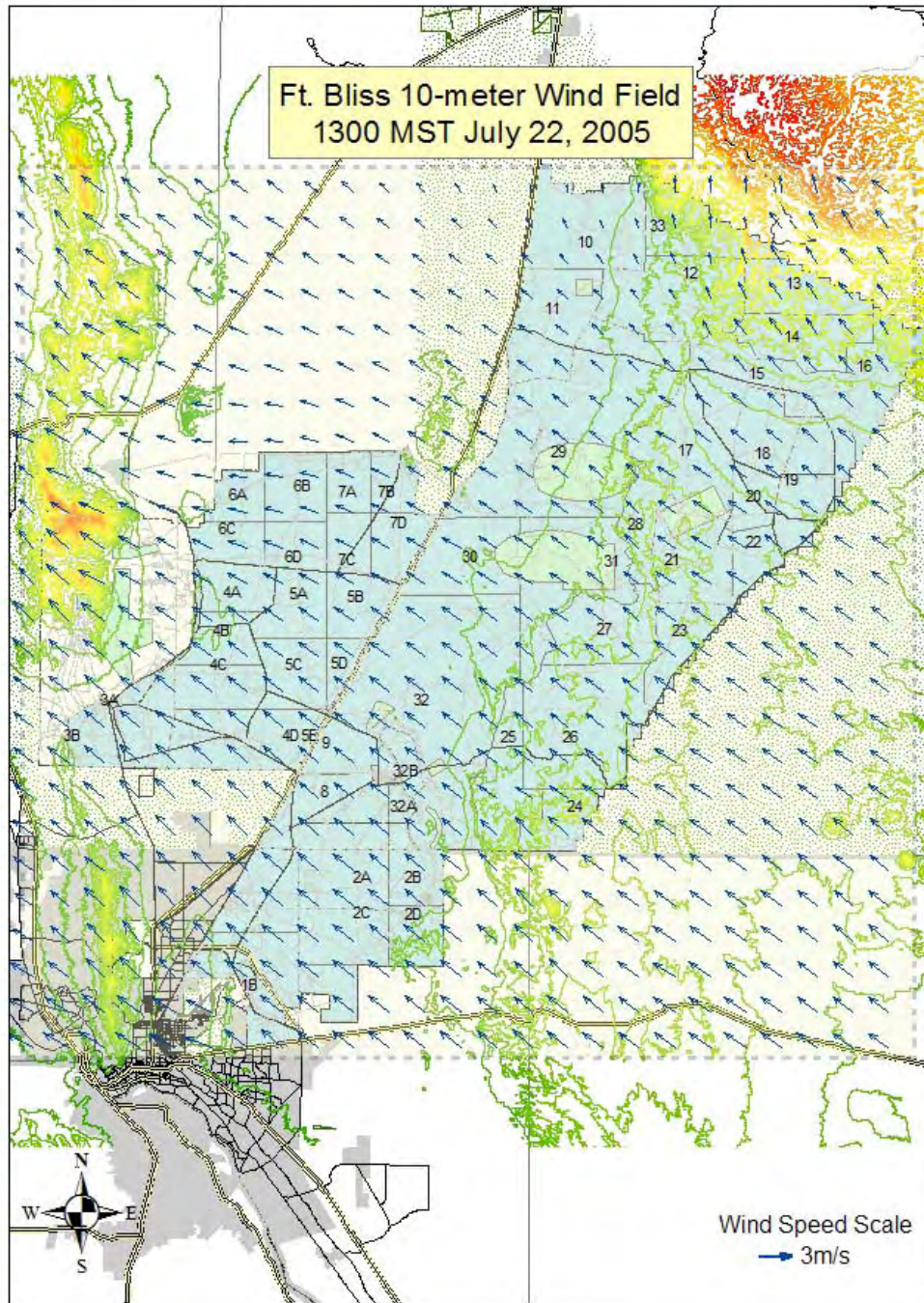


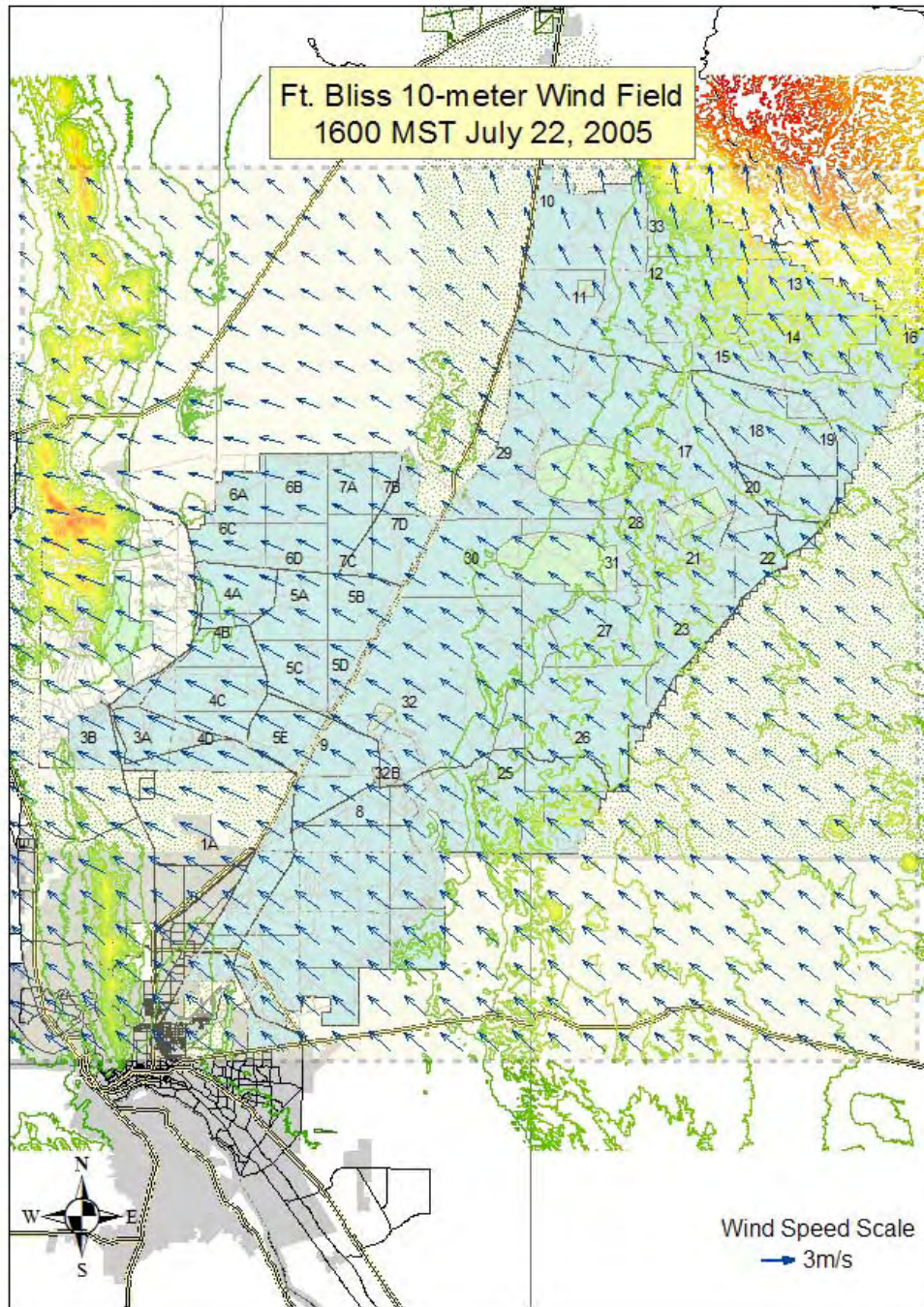


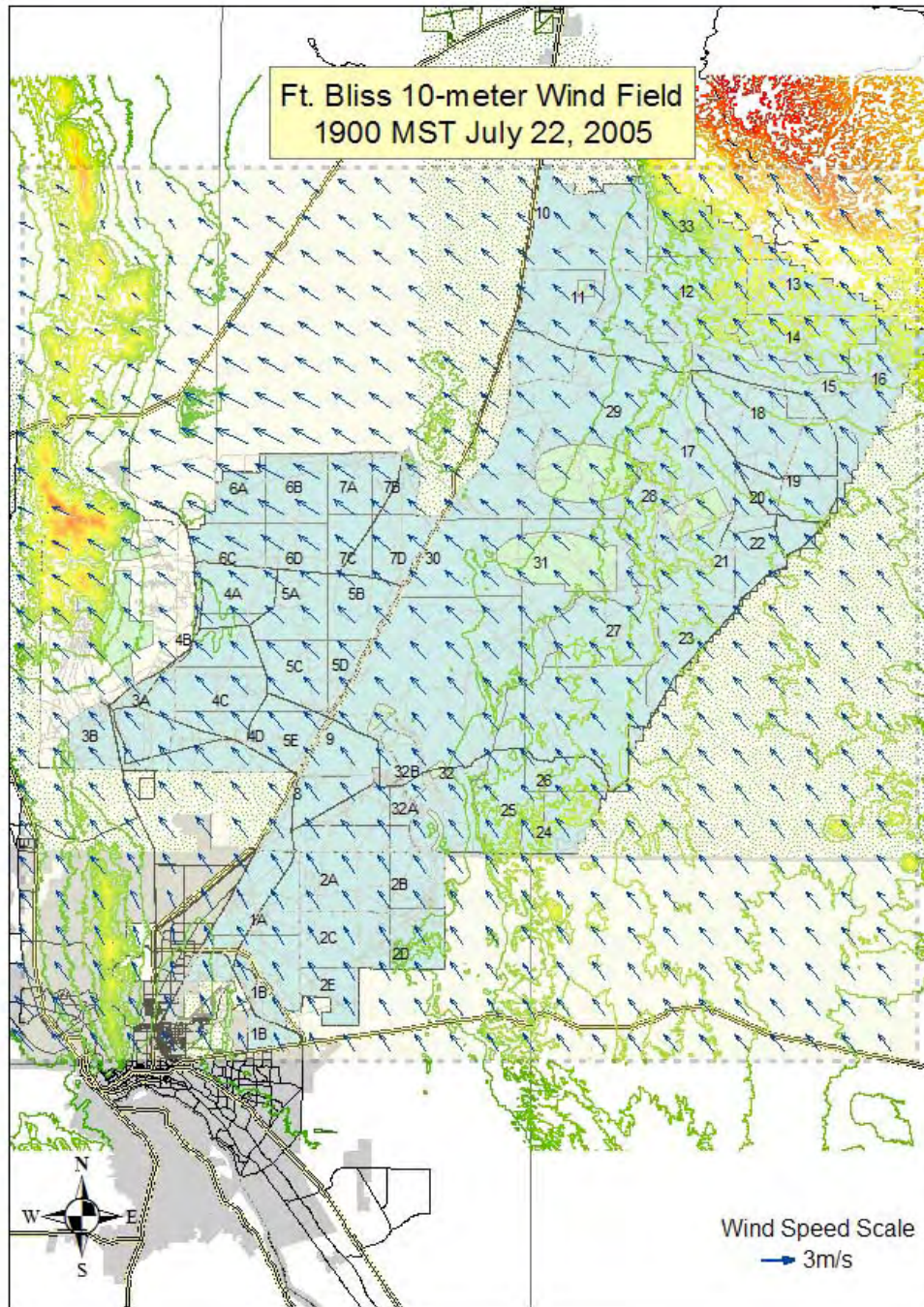


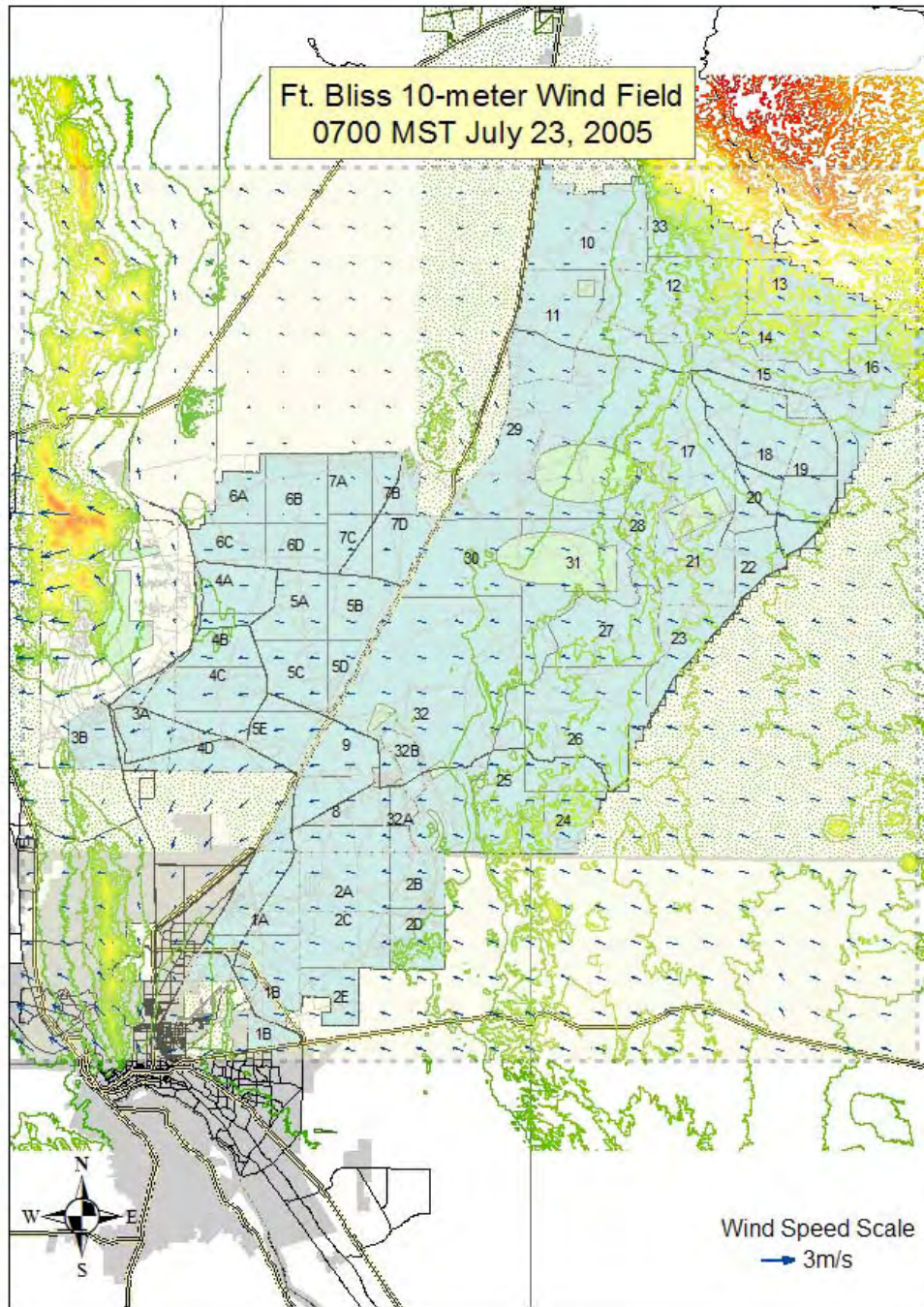


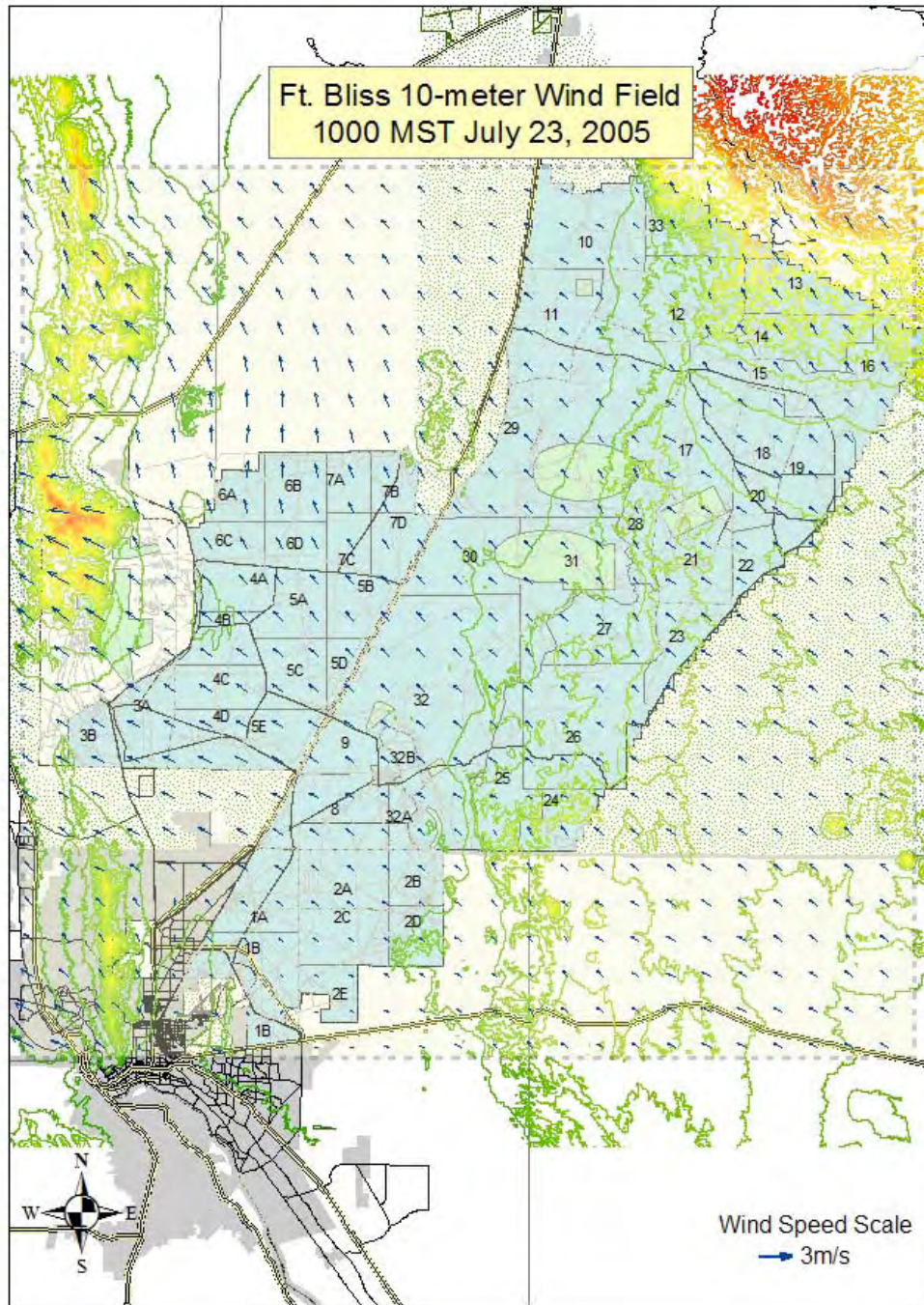


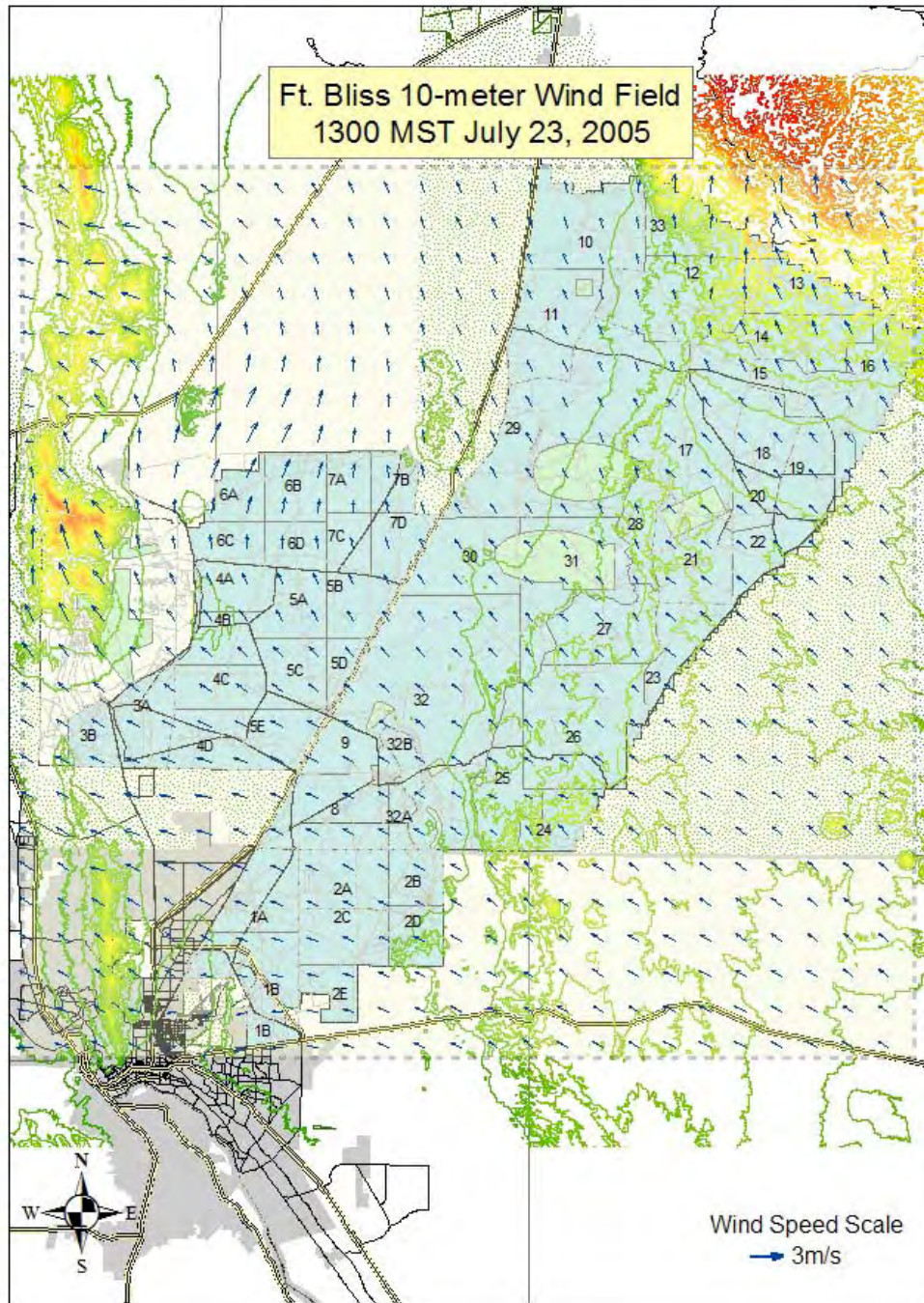


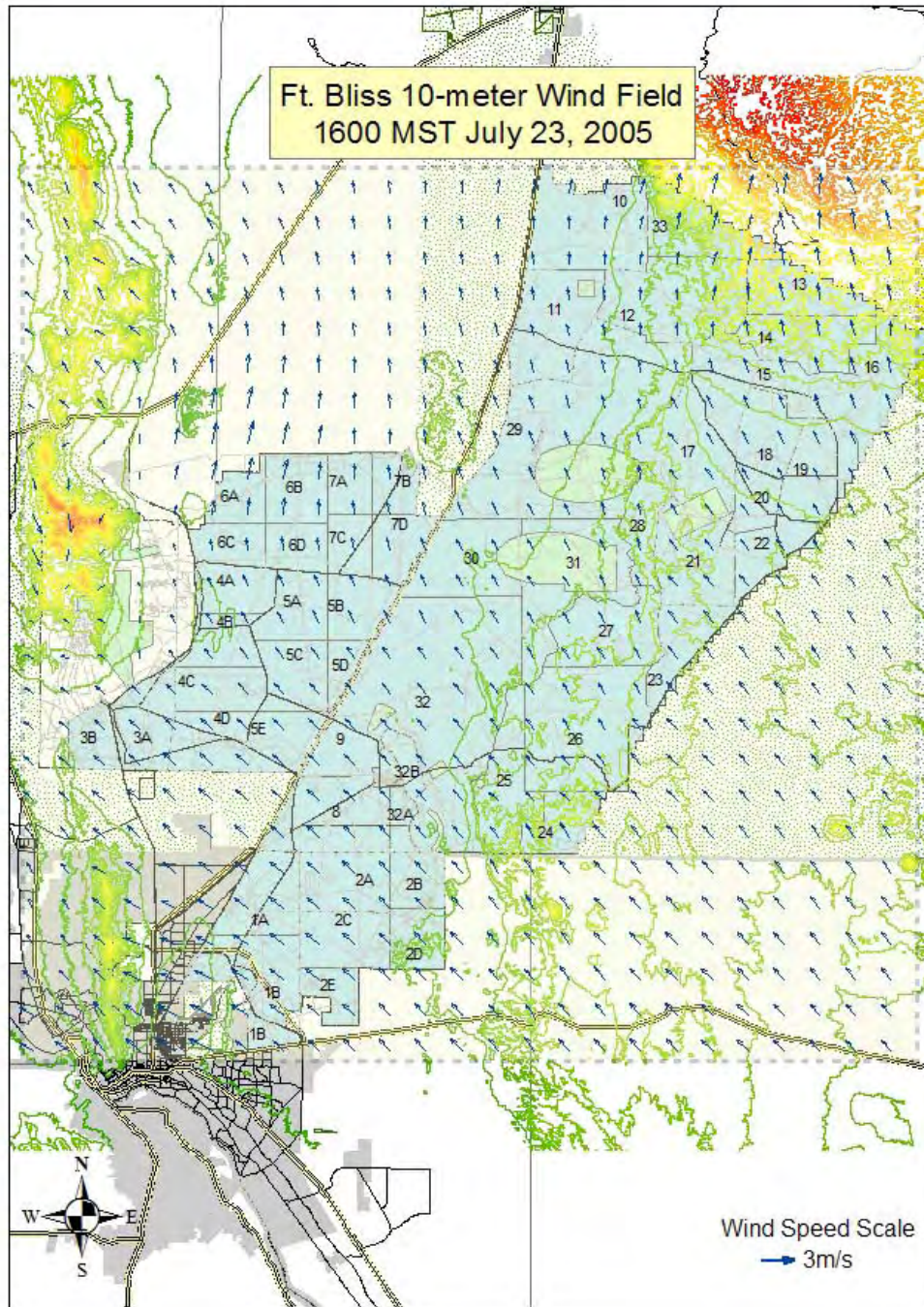


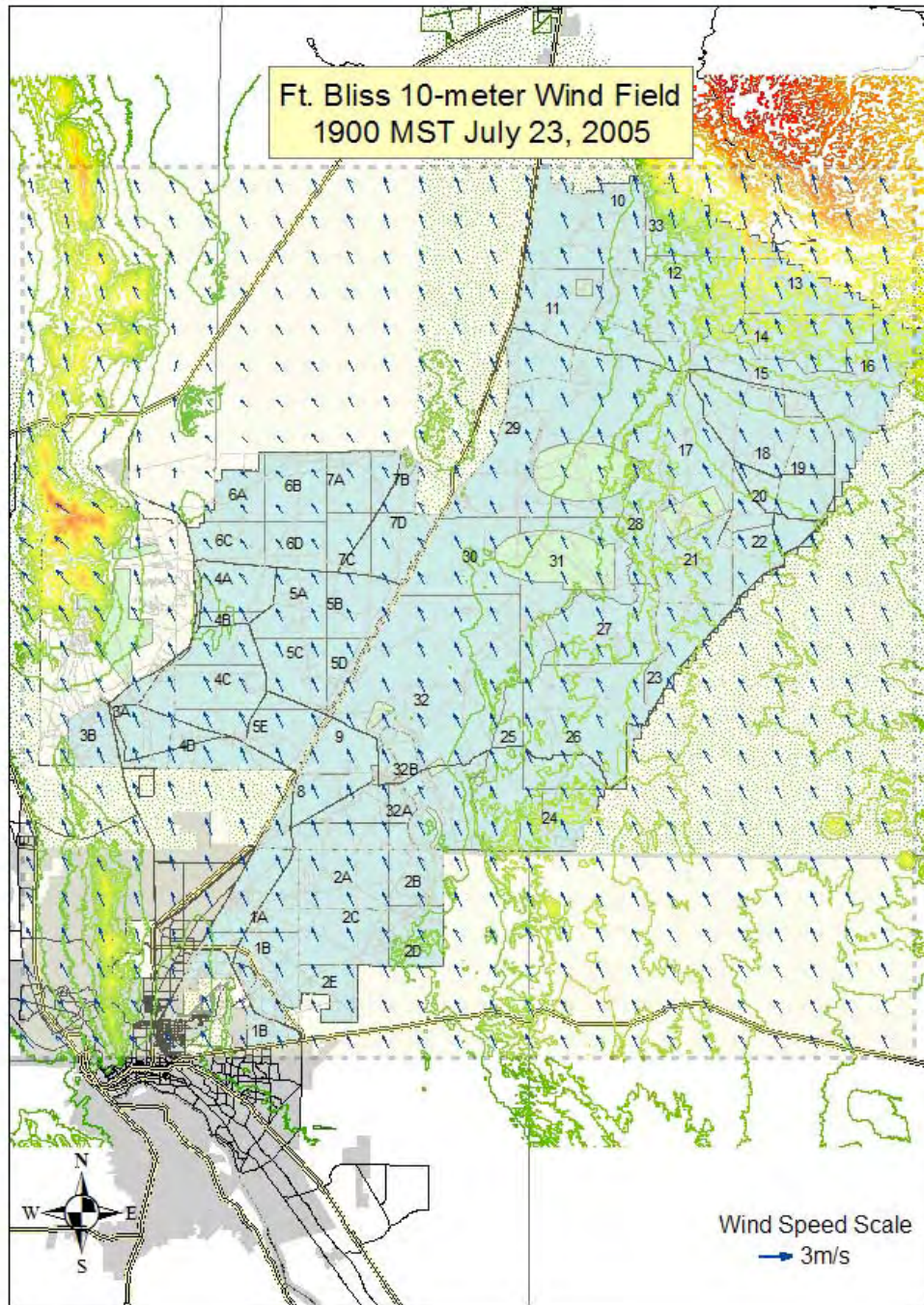


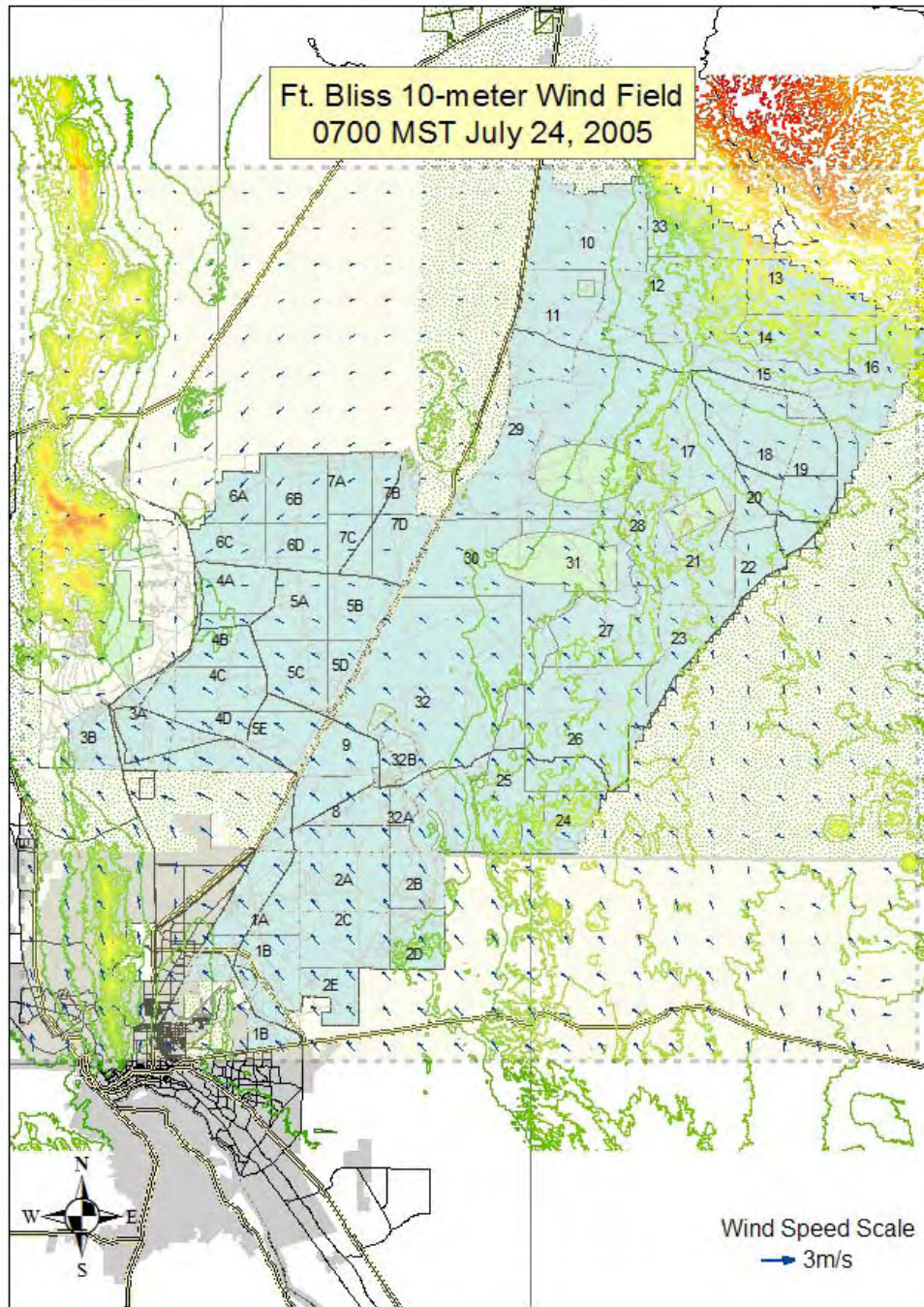


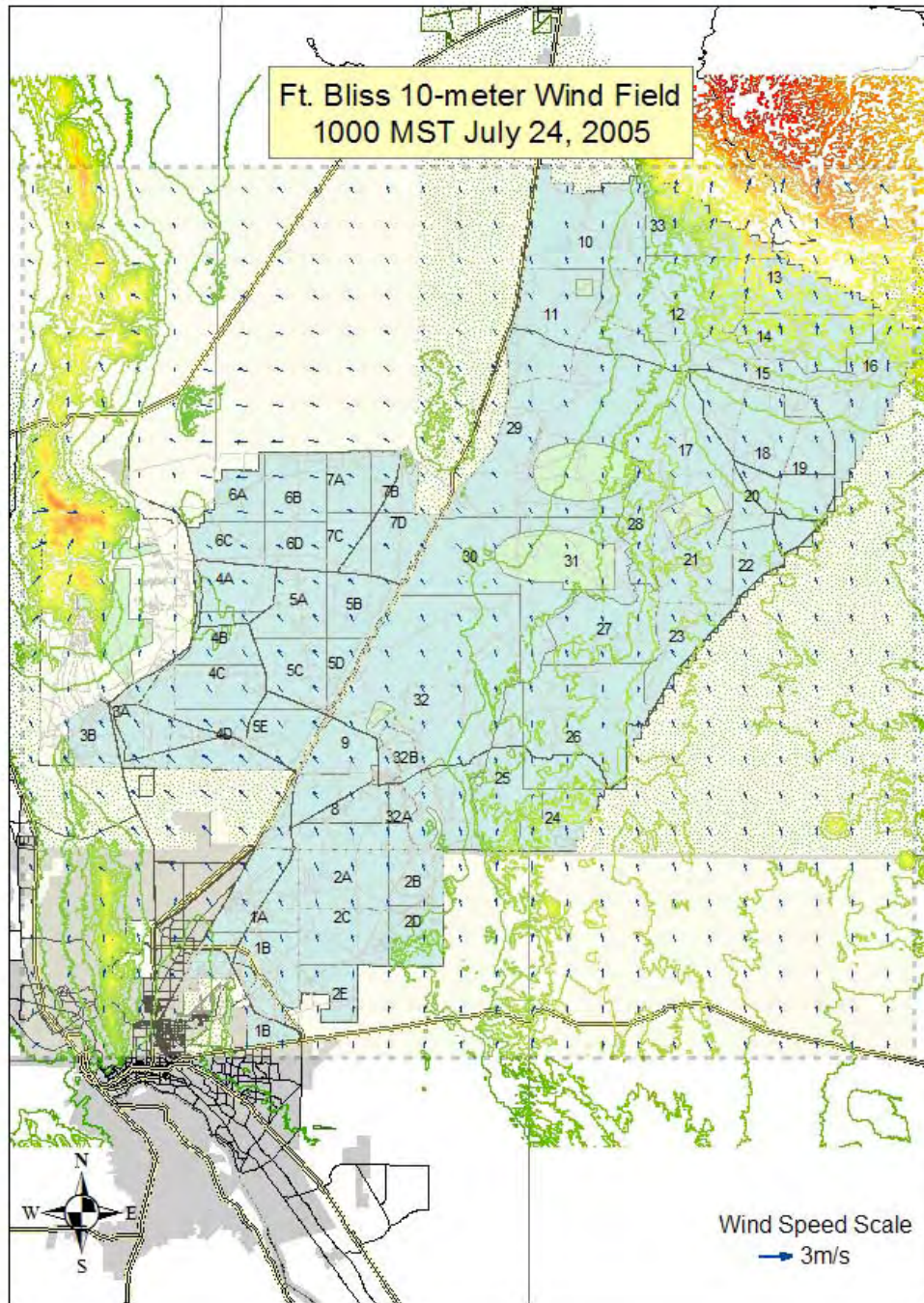


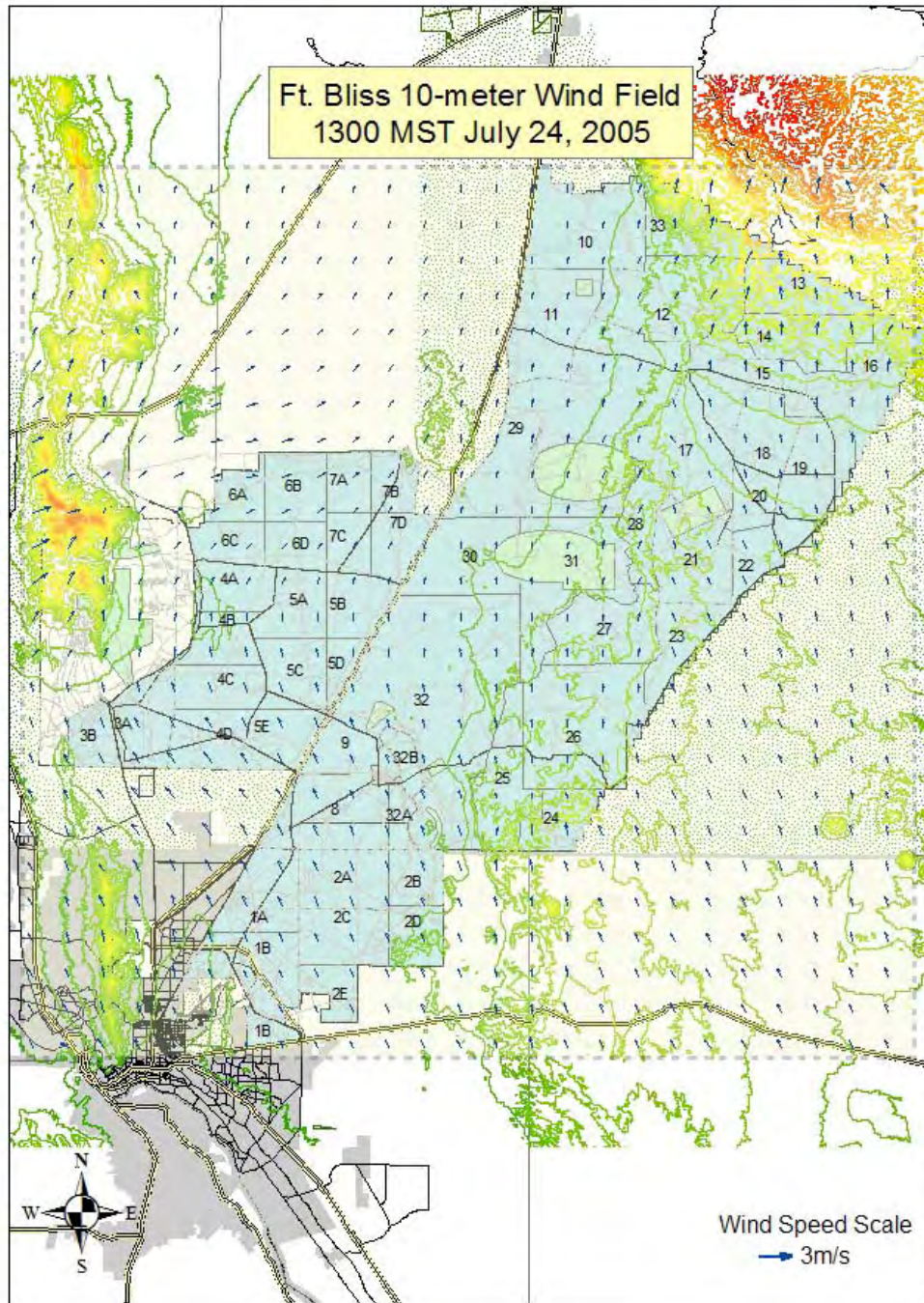


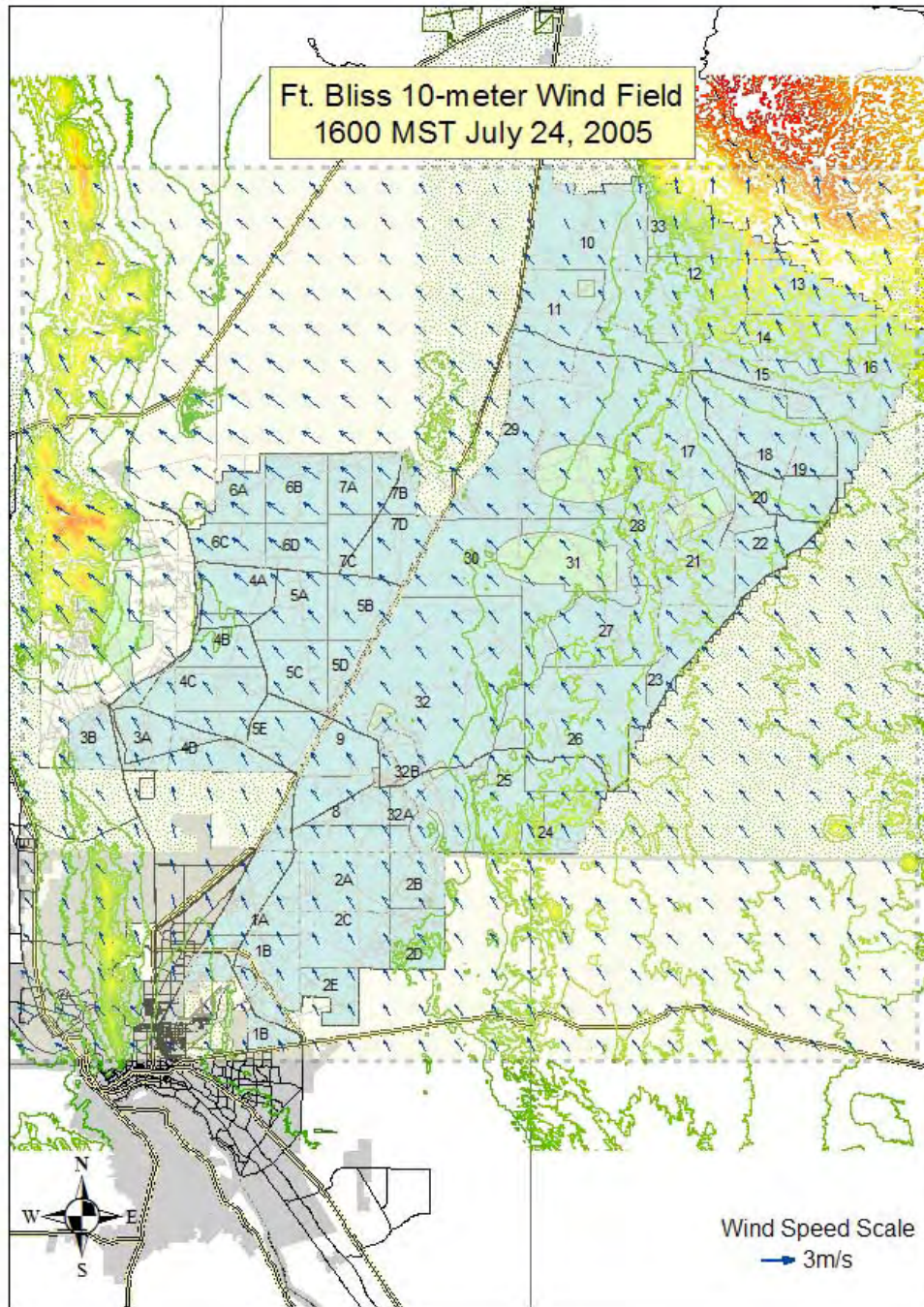


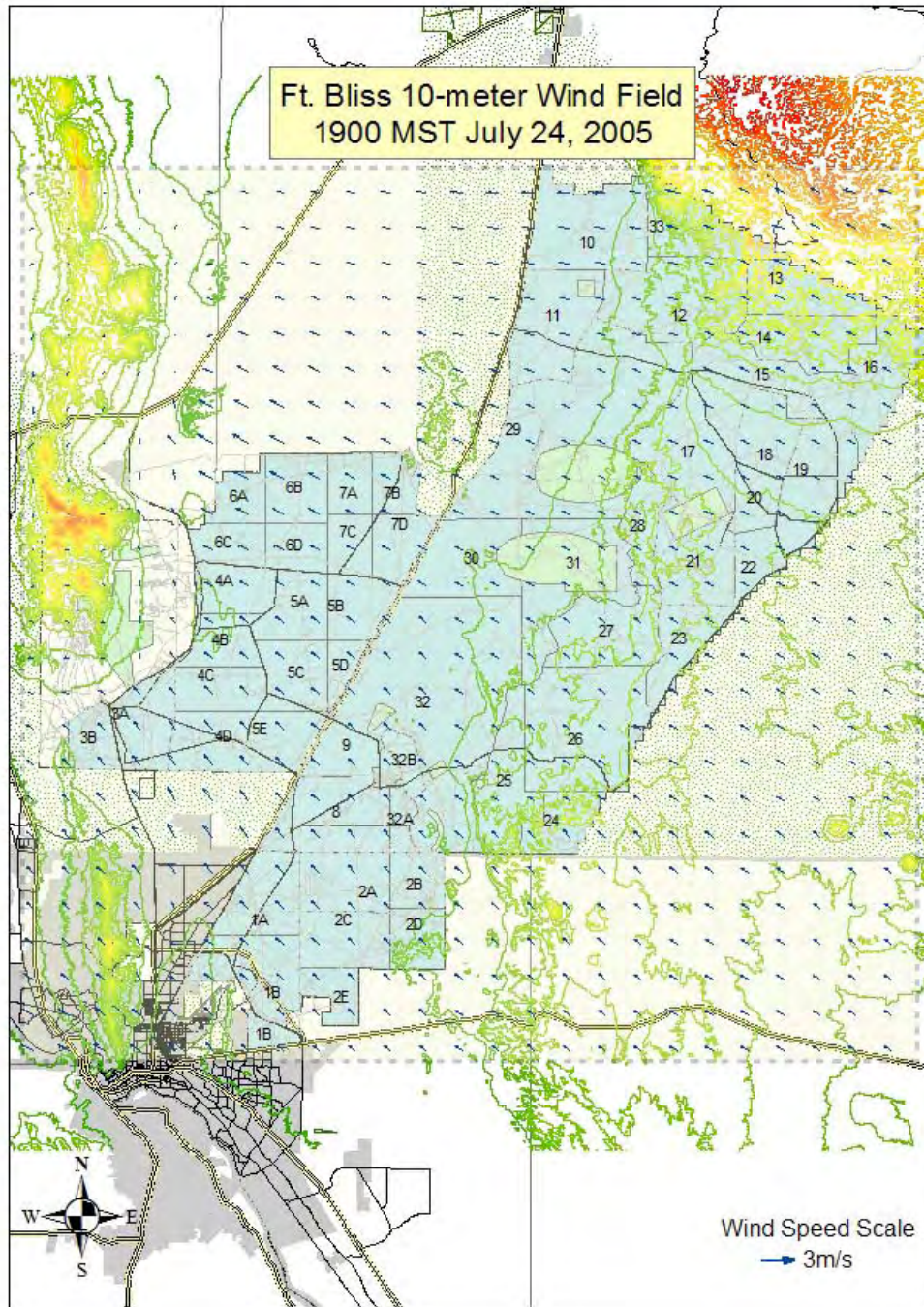










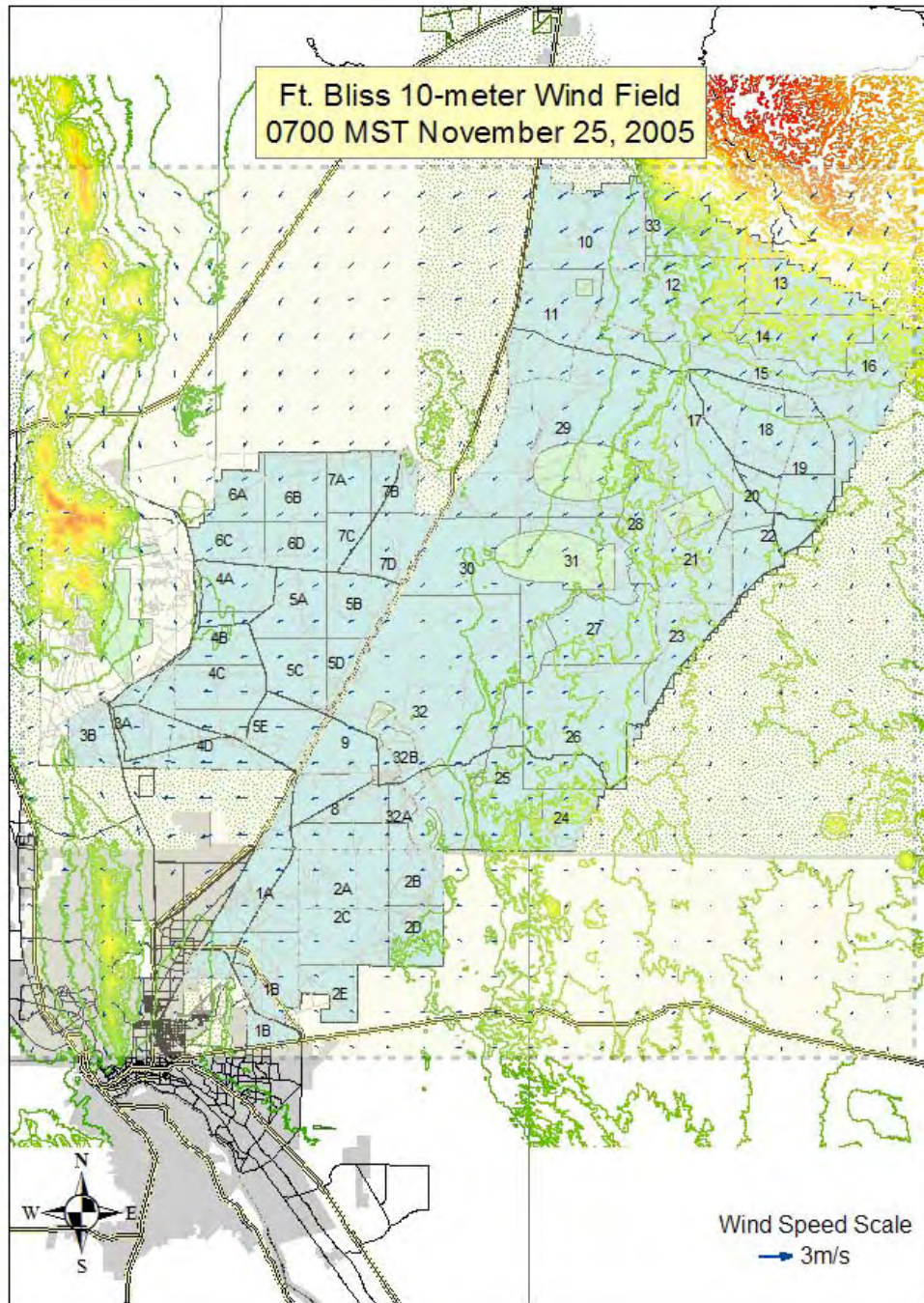


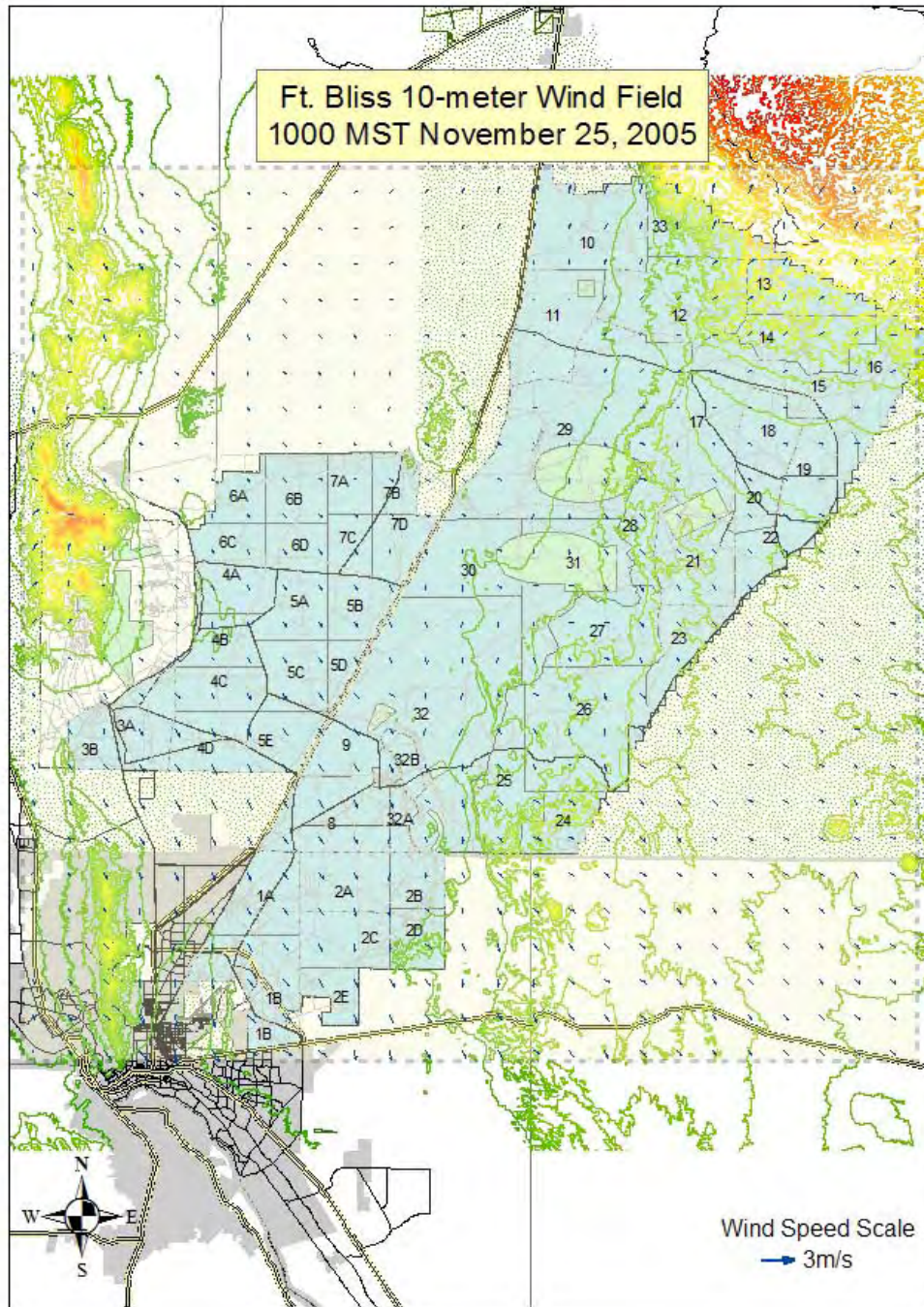
Appendix K

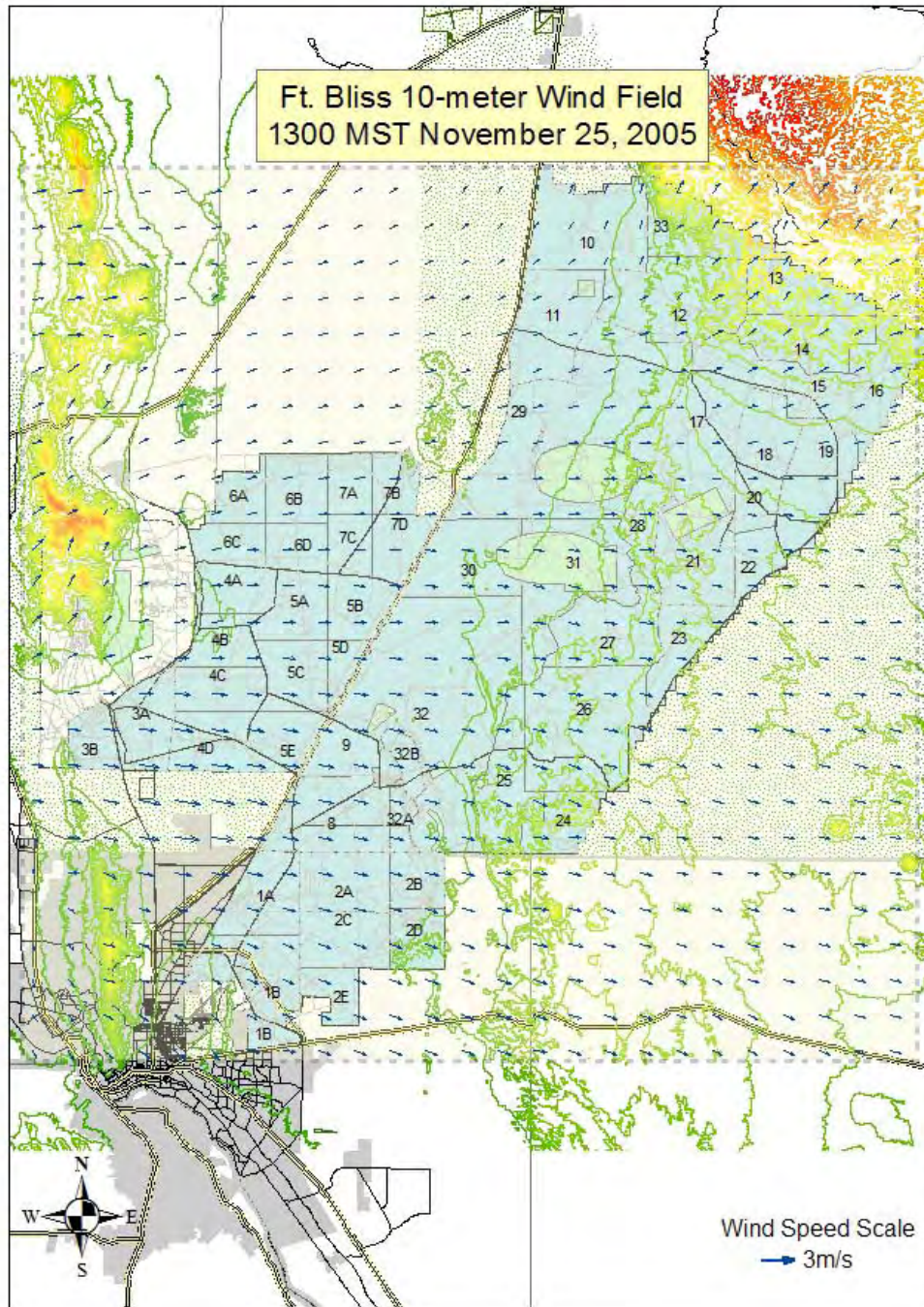
DUSTRAN 10-m-Above-Ground Wind Fields for November 25–29, 2005

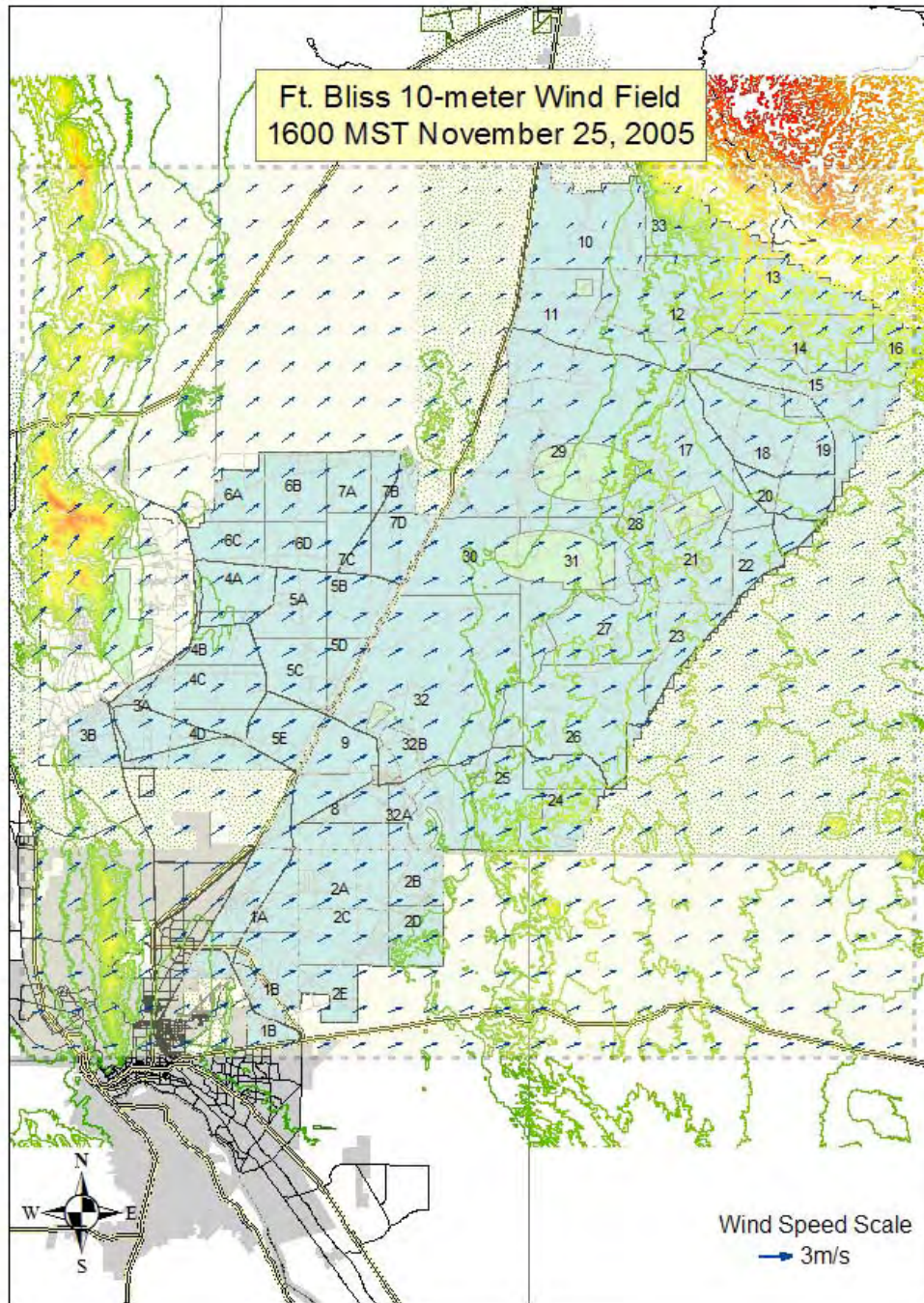
Appendix K: DUSTRAN 10-m-Above-Ground Wind Fields for November 25–29, 2005

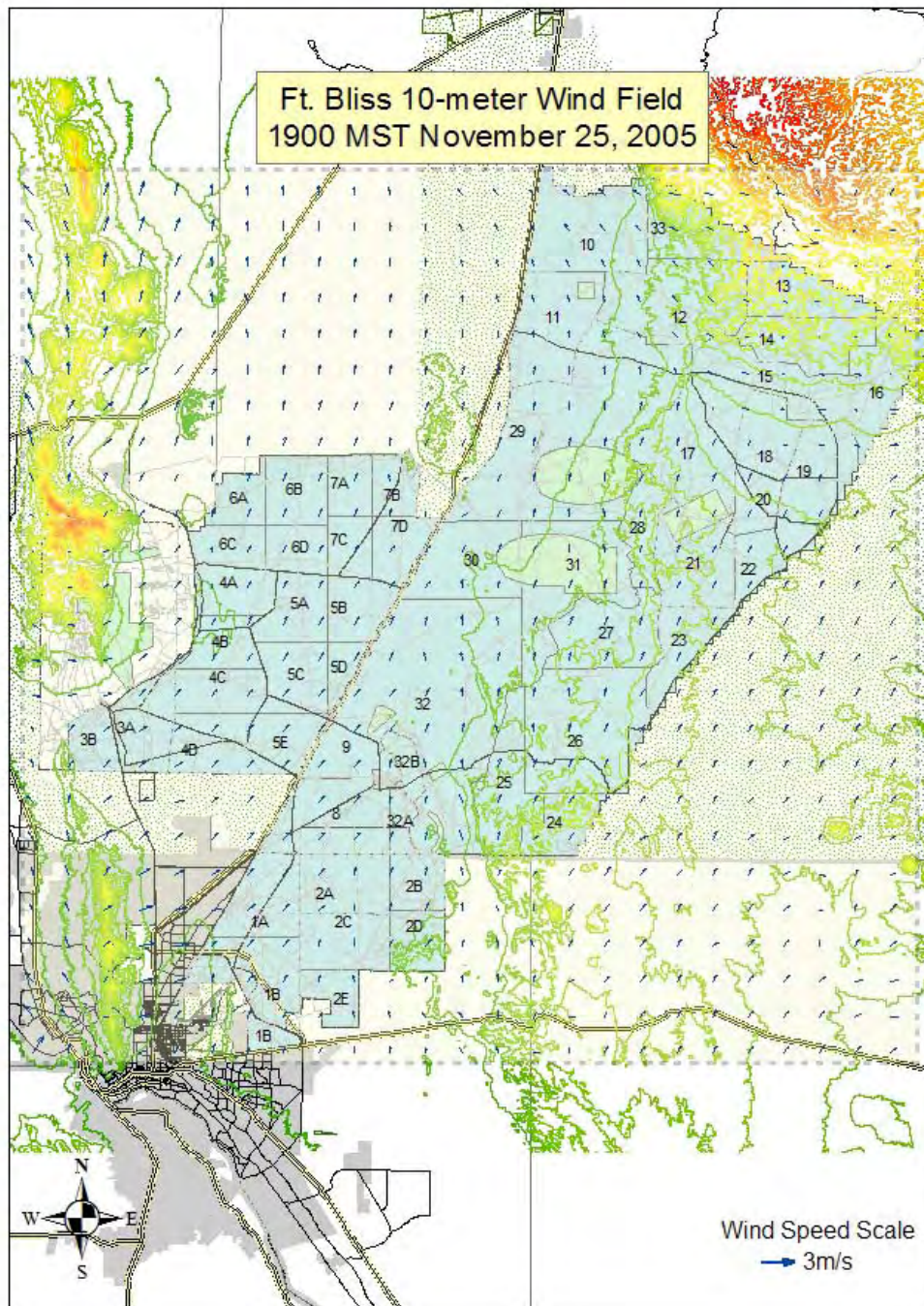
This appendix contains 25 screen captures of the 10-m above ground wind fields predicted by the CALMET module within DUSTRAN. Wind fields are shown at 0700, 1000, 1300, 1600, and 1900 MST for the 6 days included in the current simulations (November 25 through 29, 2005). Header captions within each figure indicate the day and time represented by a given plot. The arrow on each vector indicates wind direction while the scaling of vector length indicates wind speed. A reference vector whose length represents a wind speed of 3 m/s is shown on each plot.

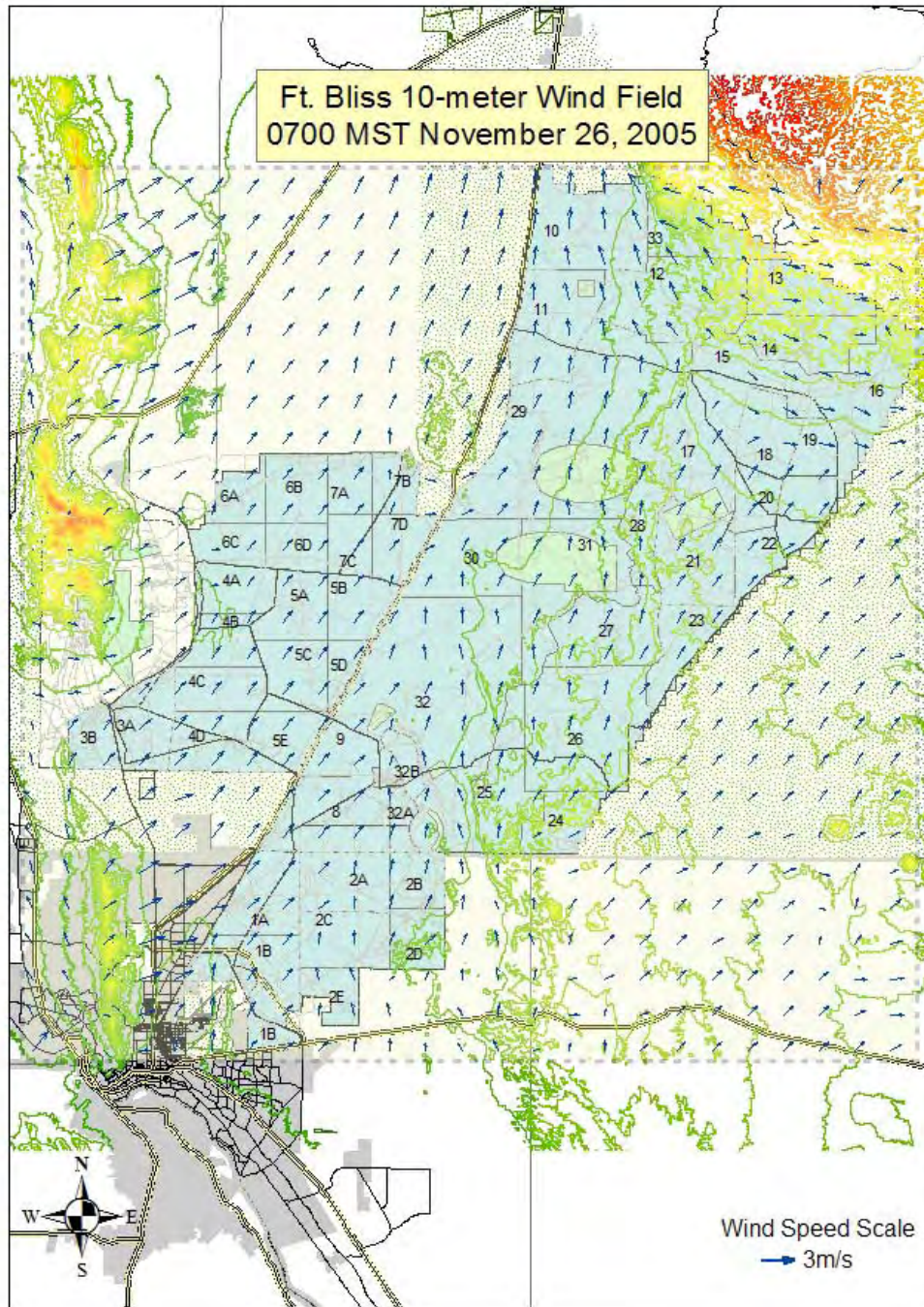


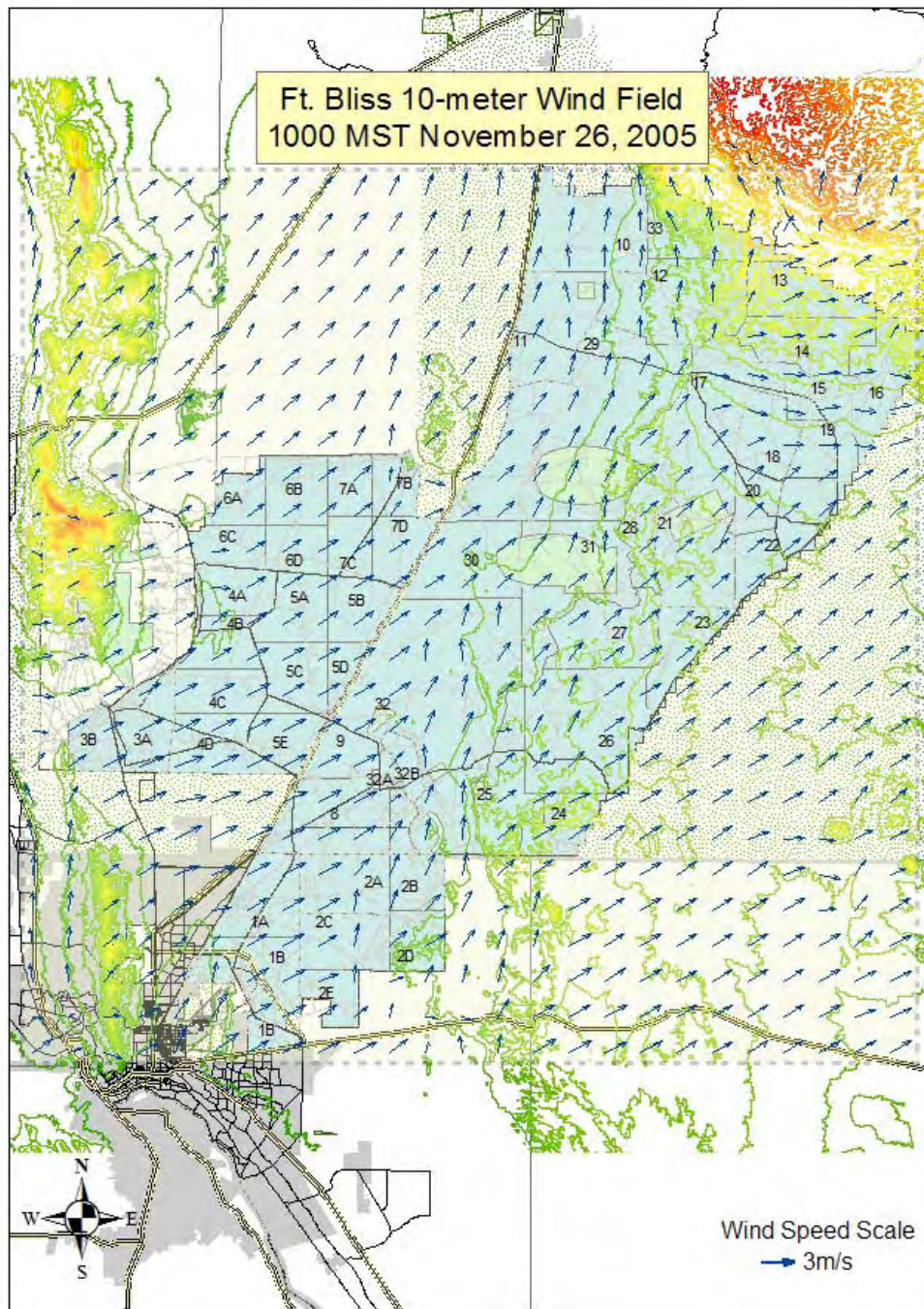


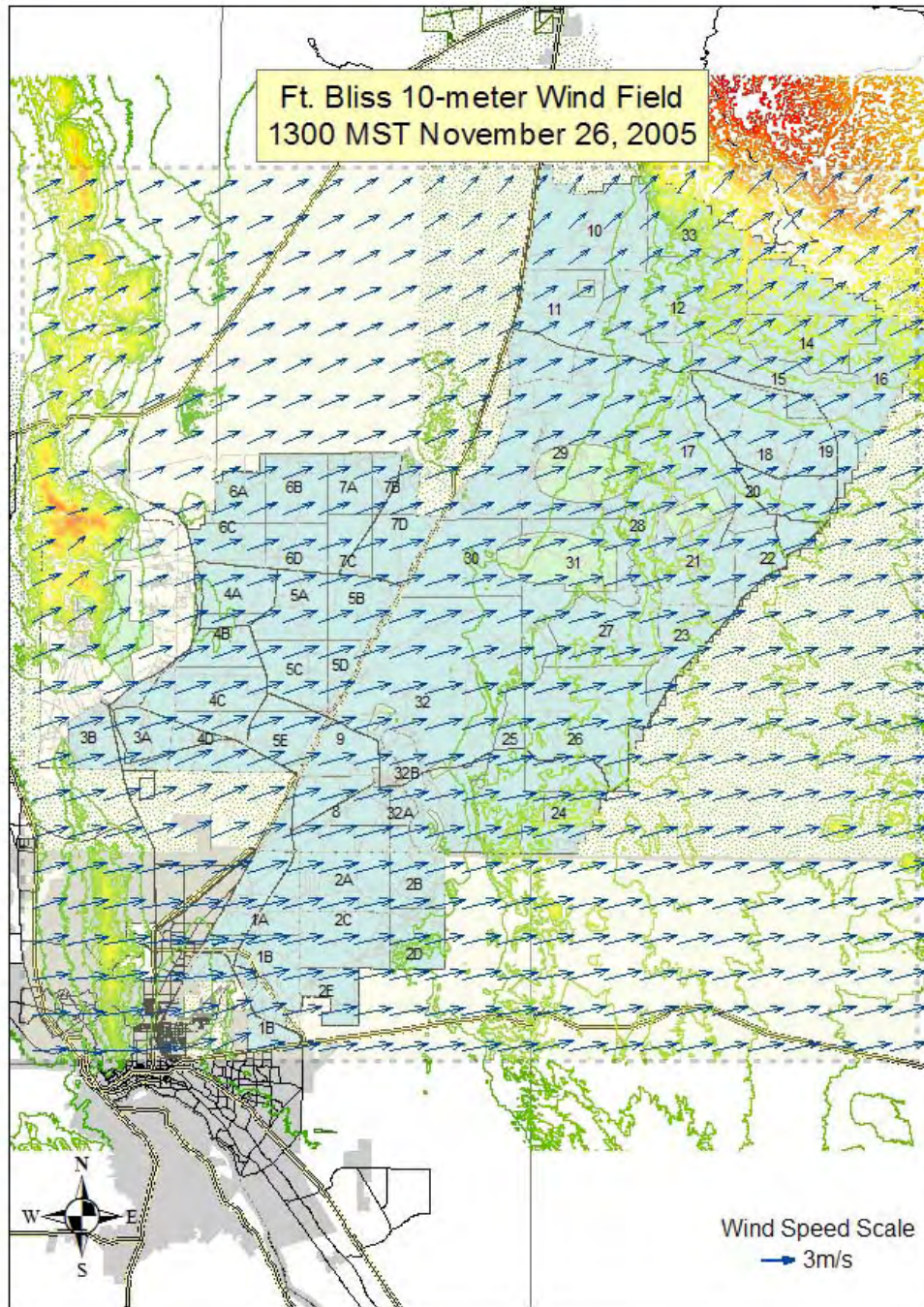


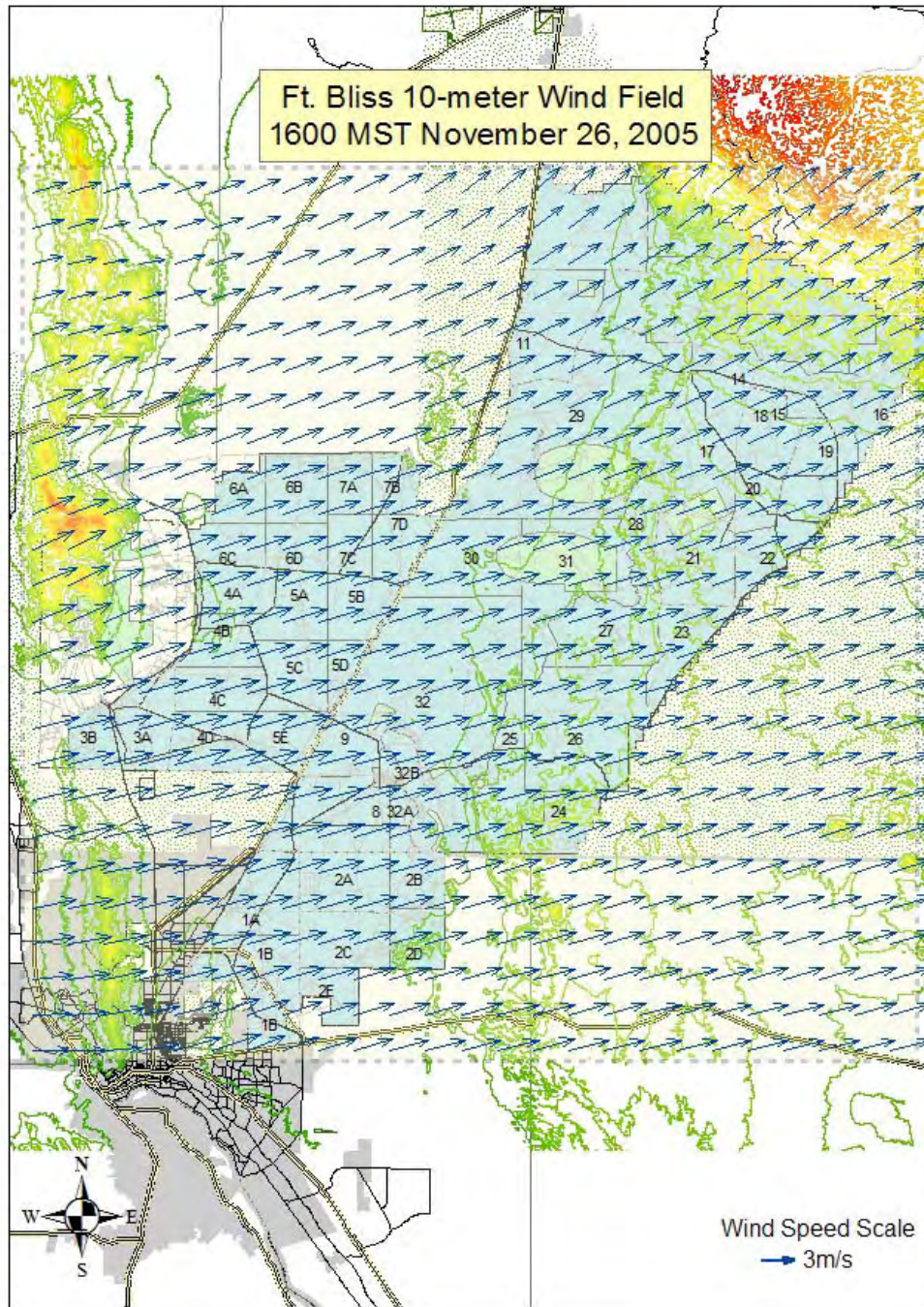


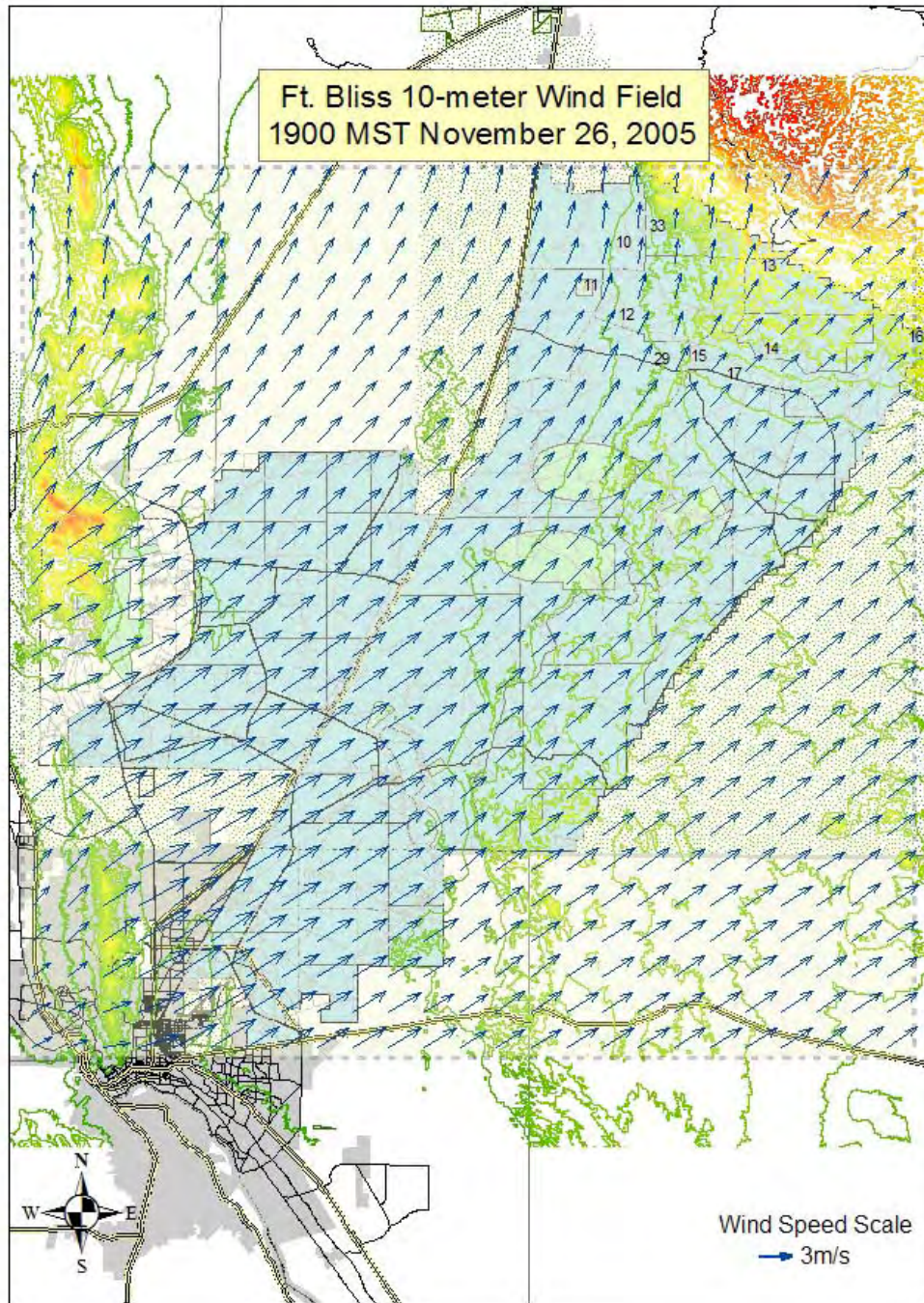


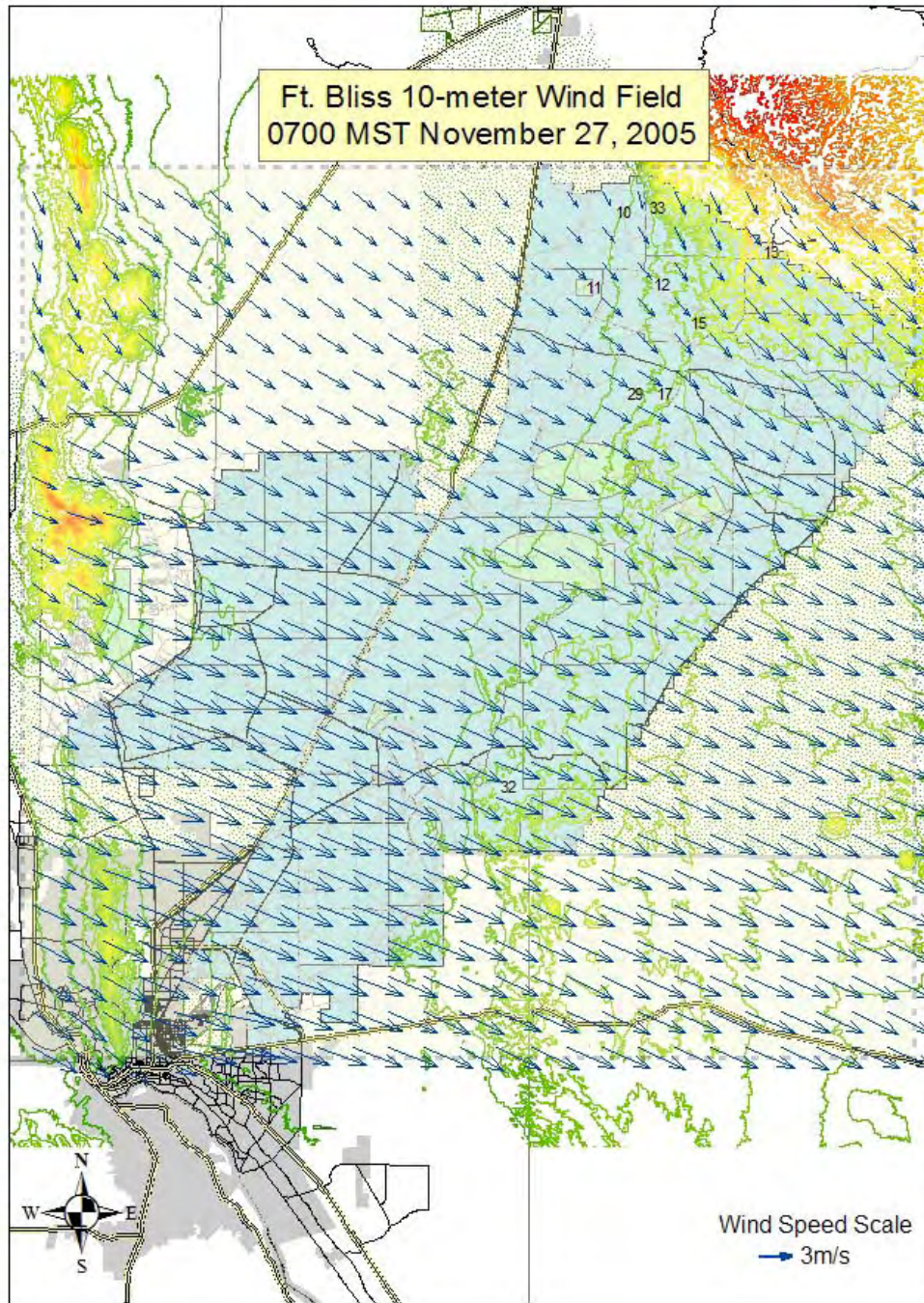


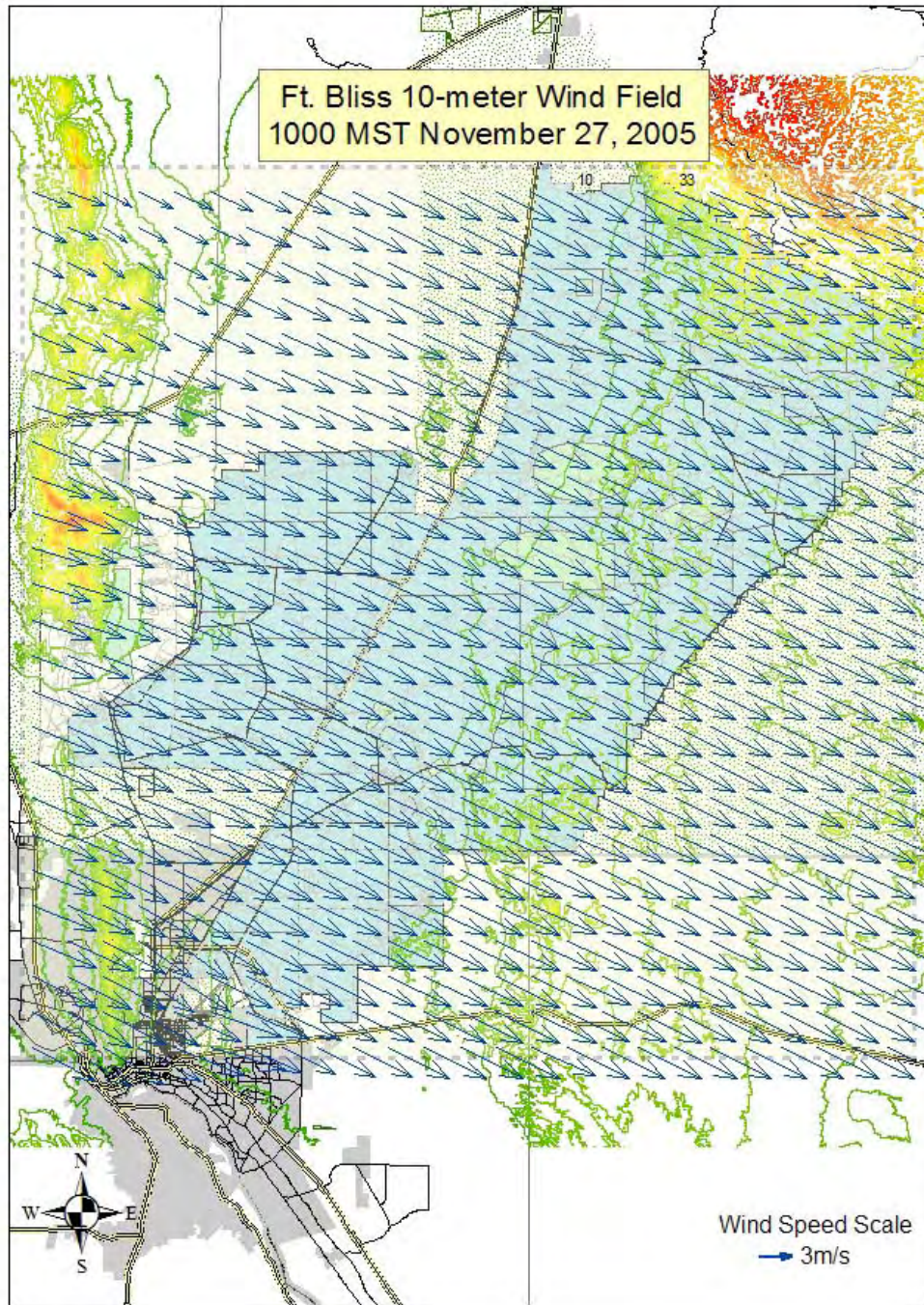


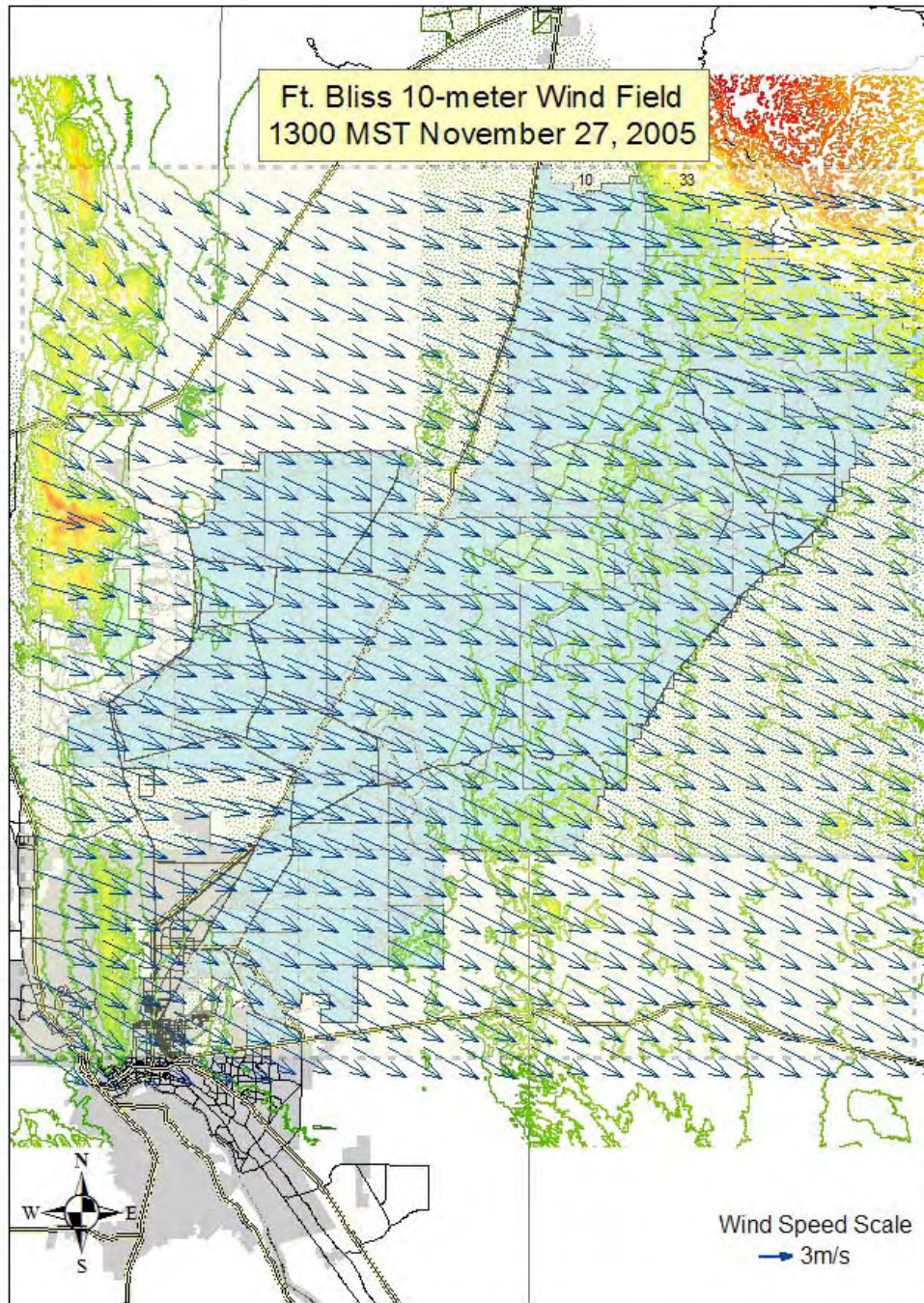


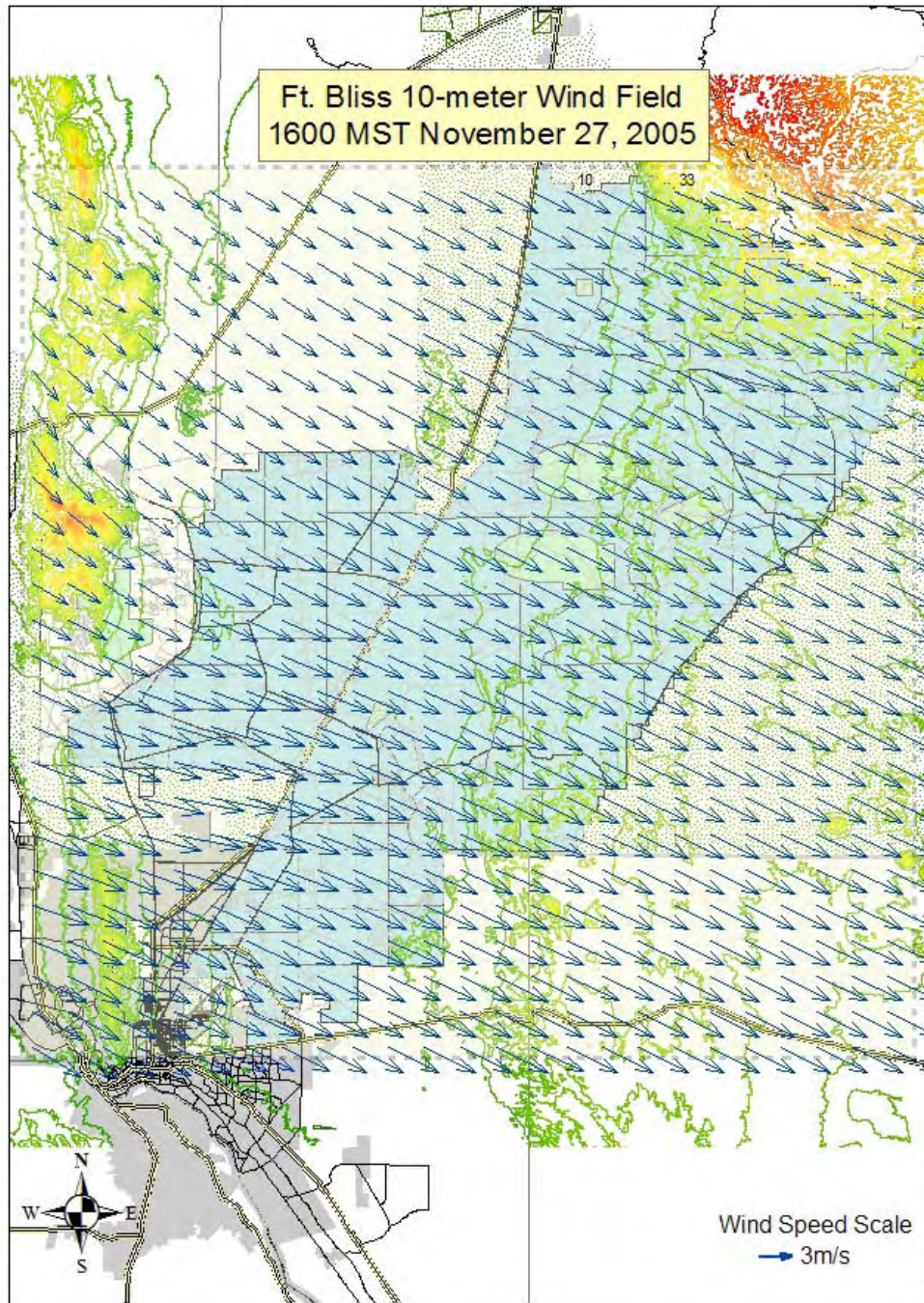


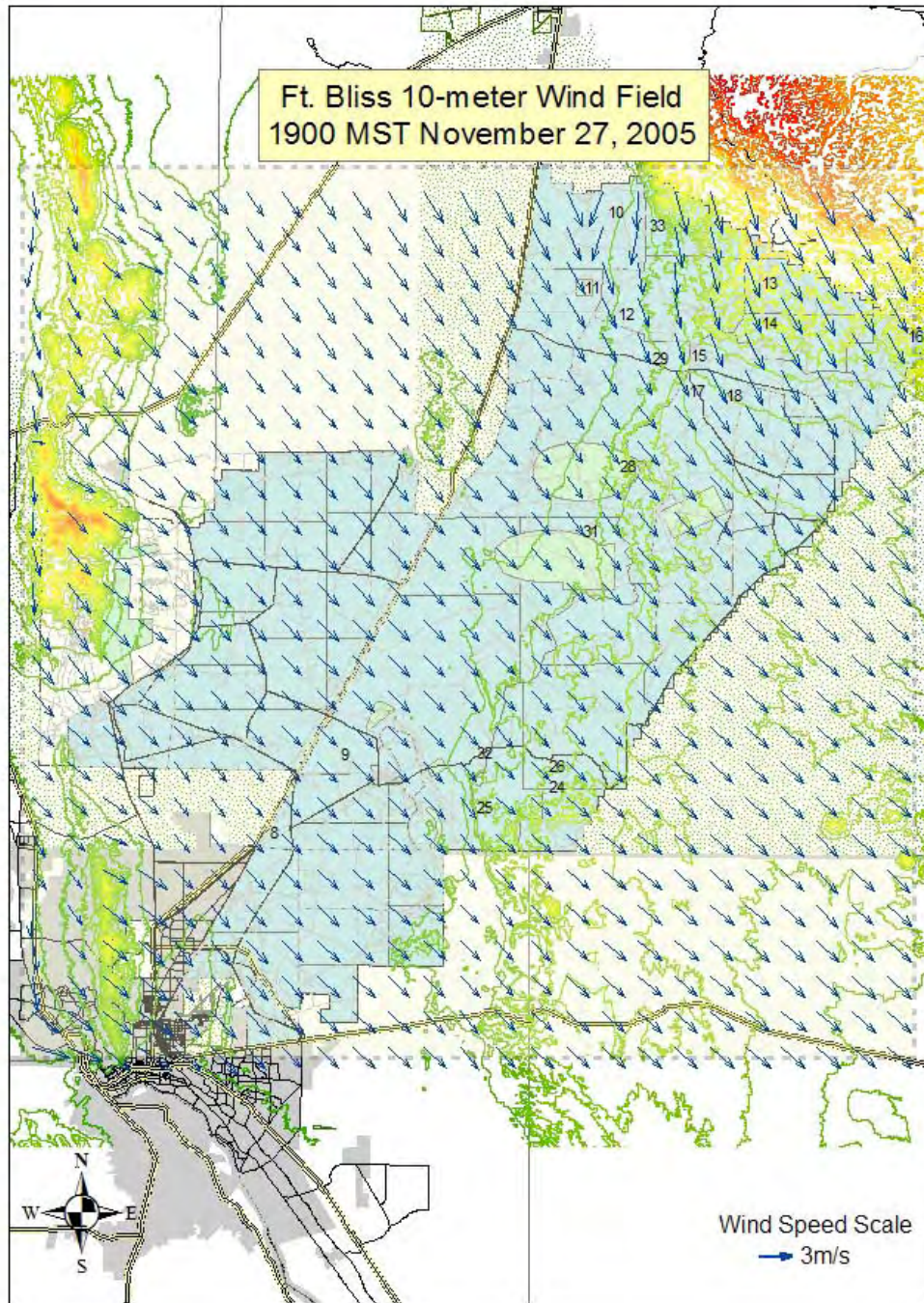


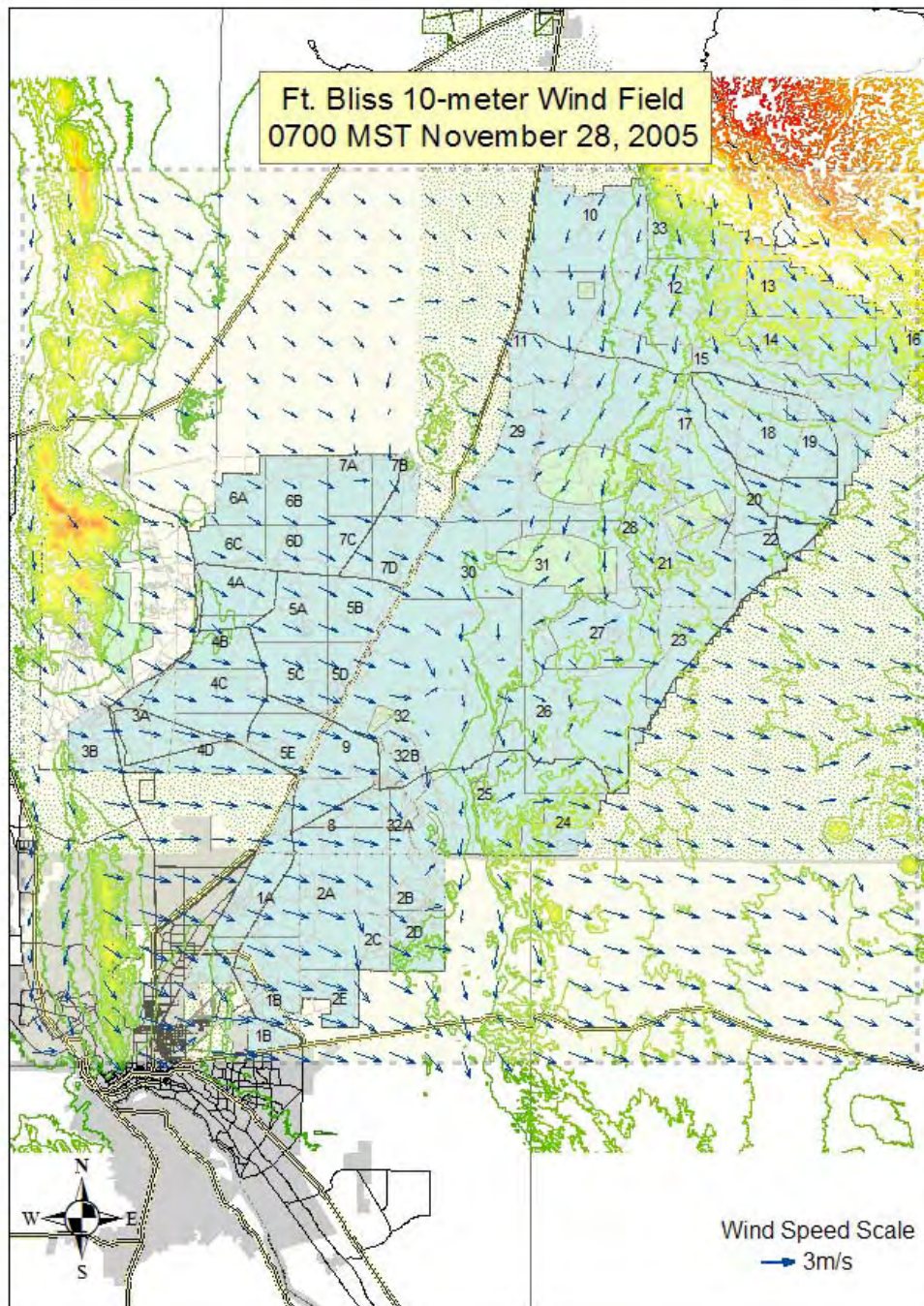


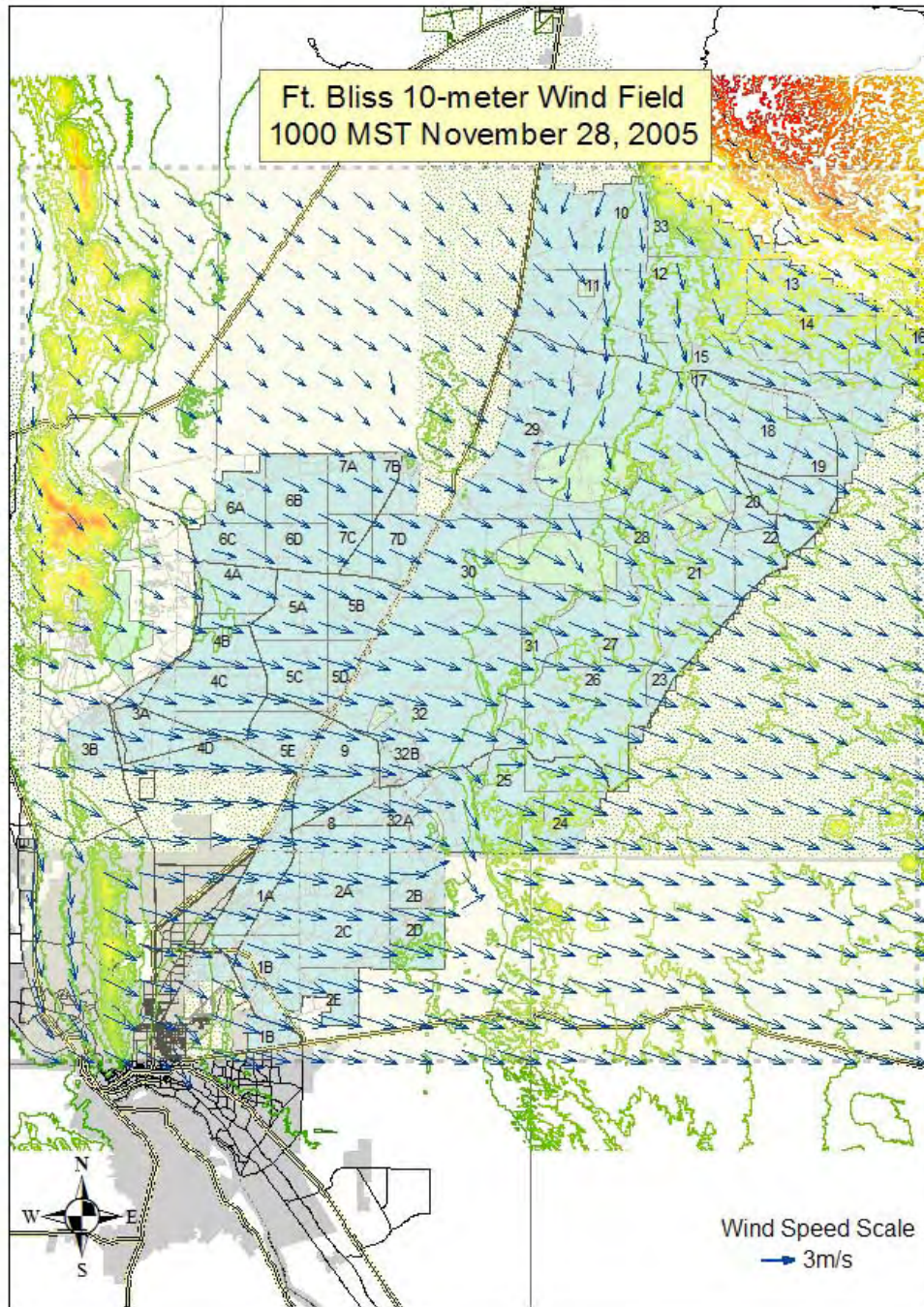


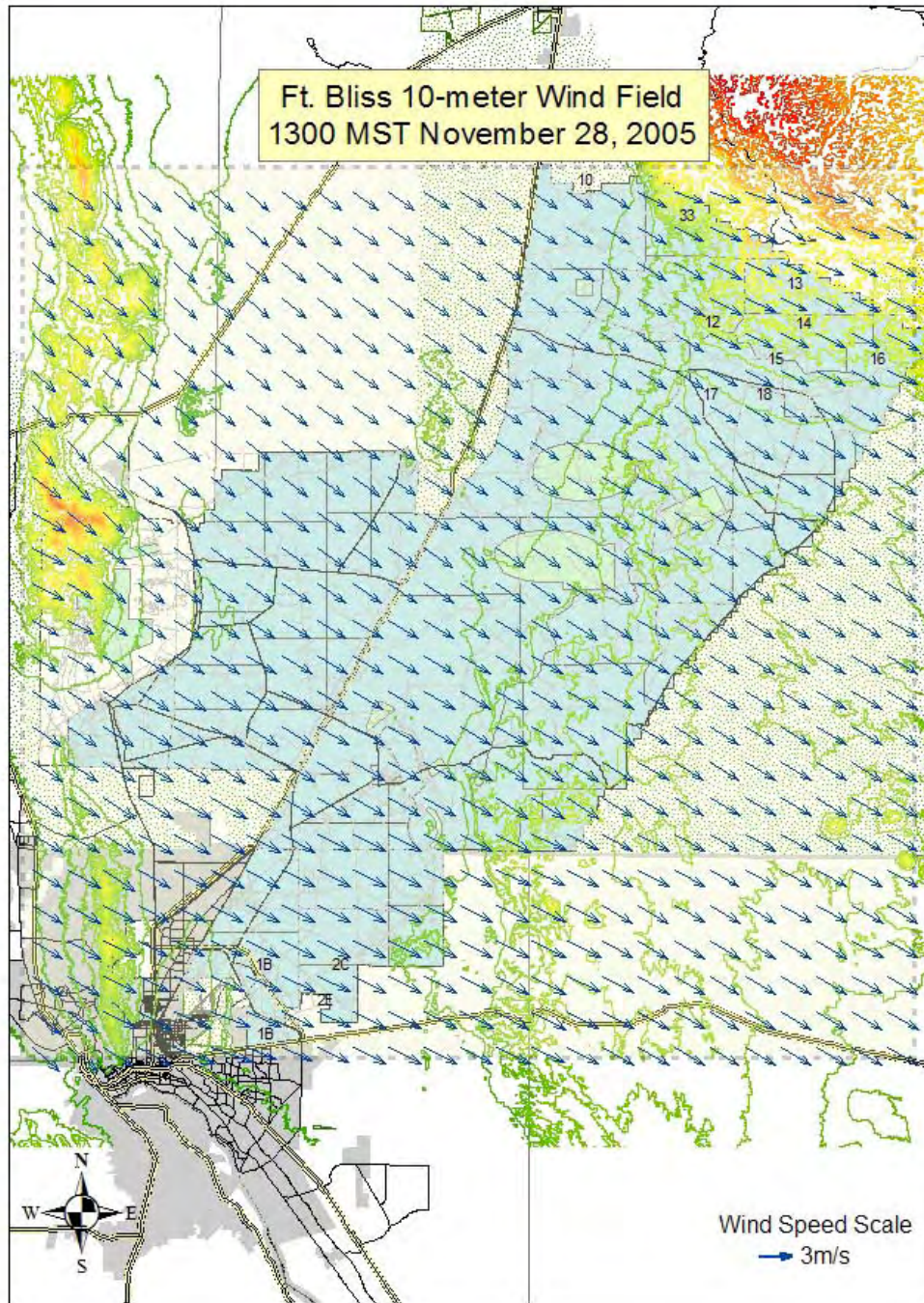


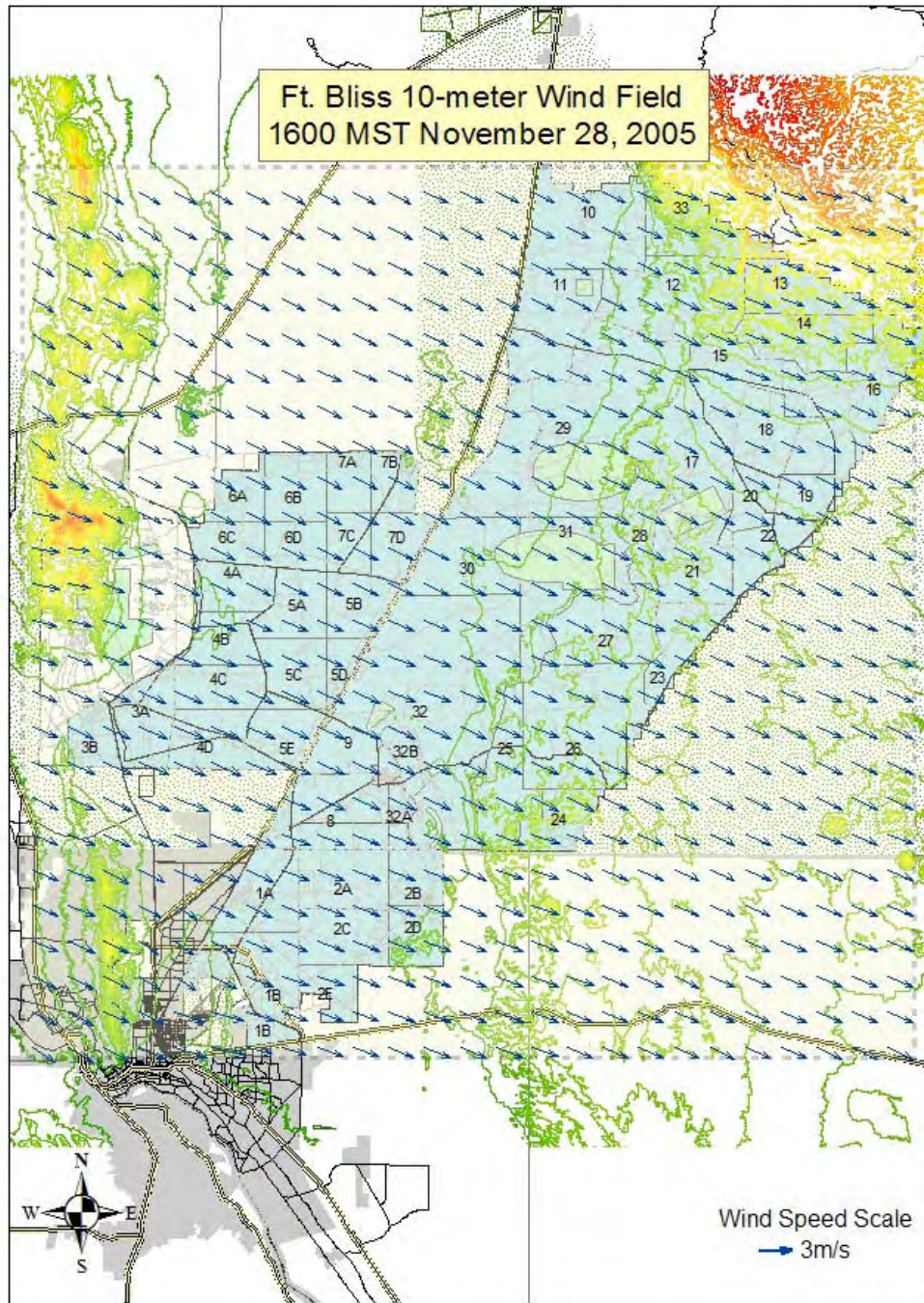


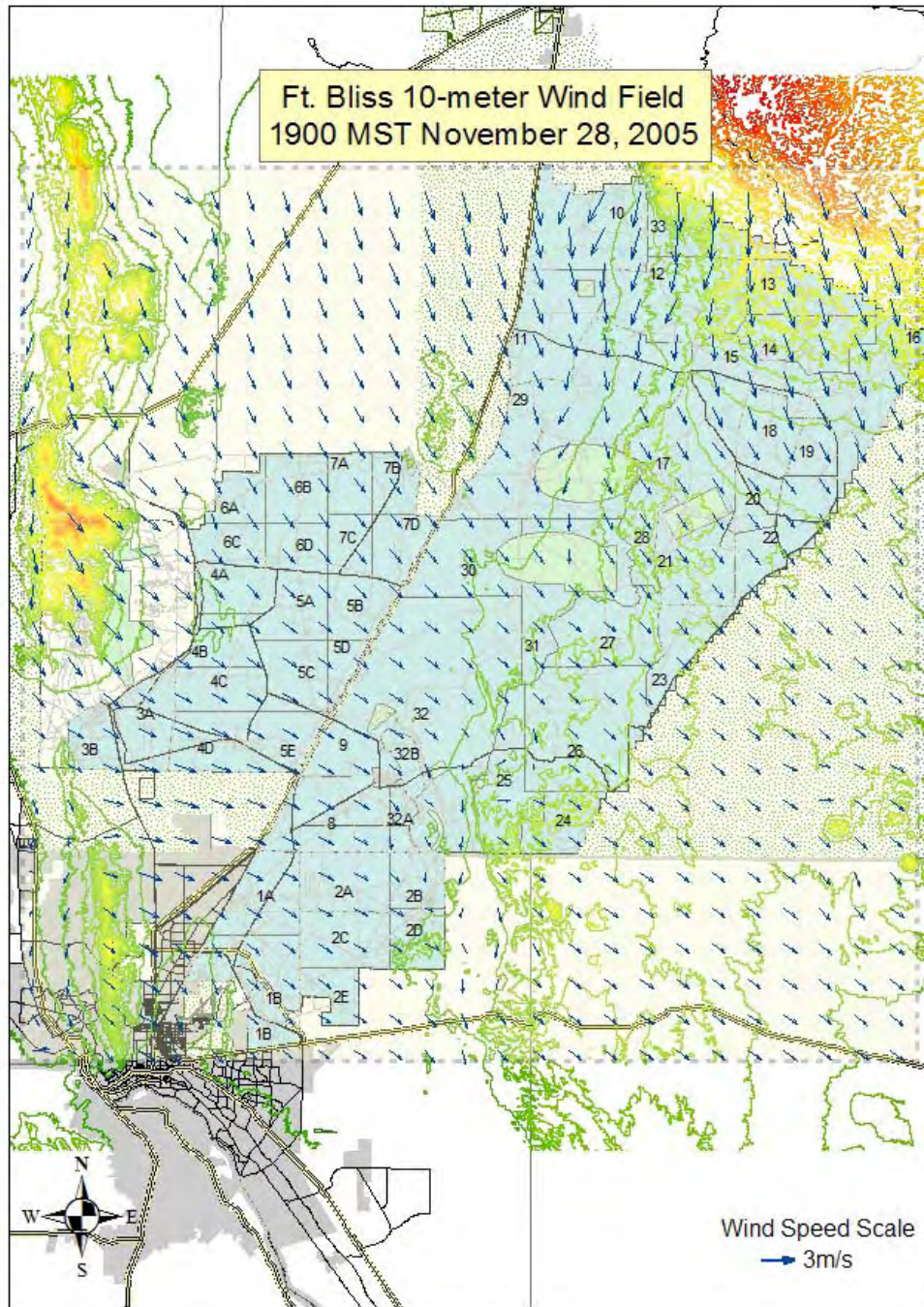


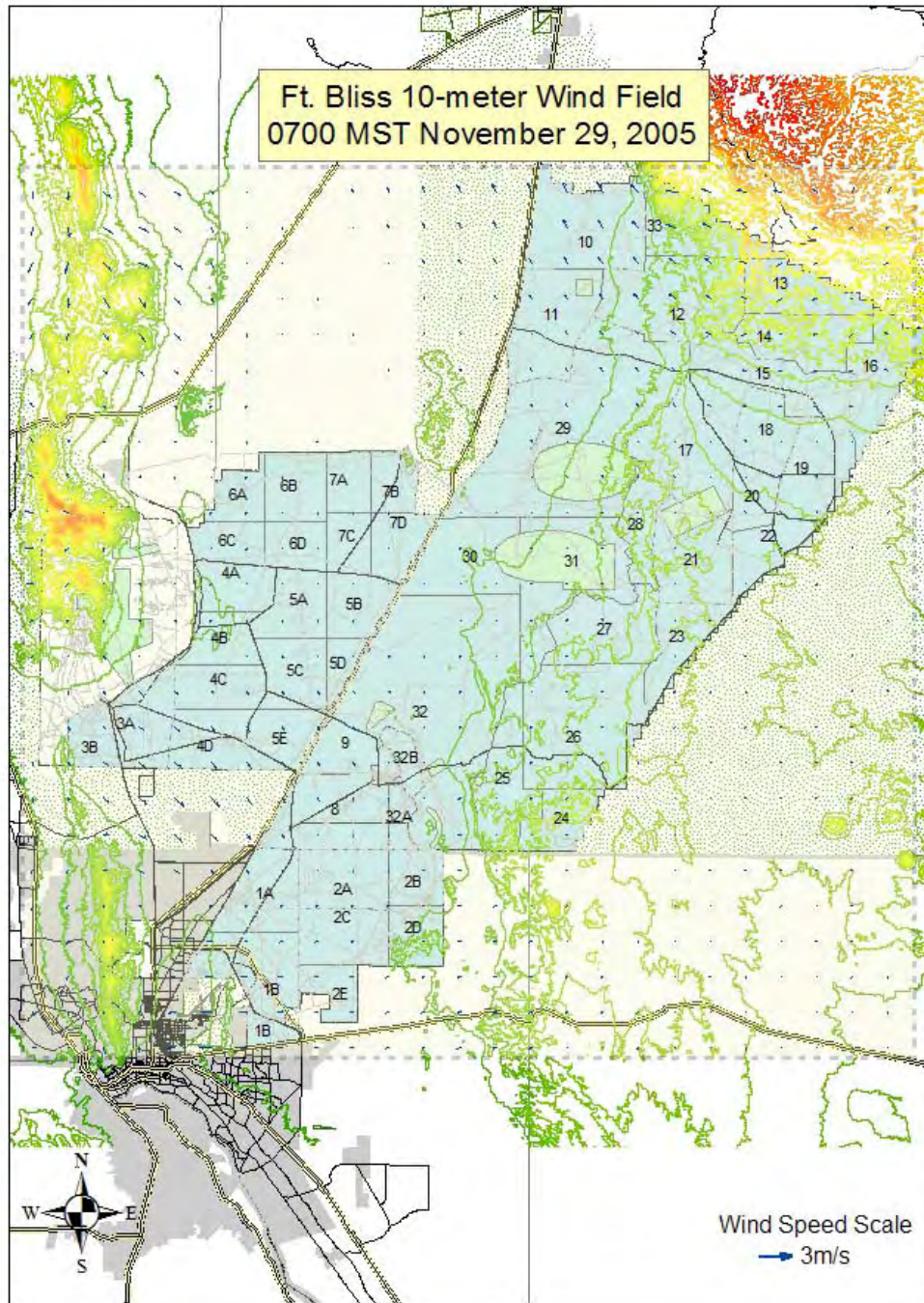


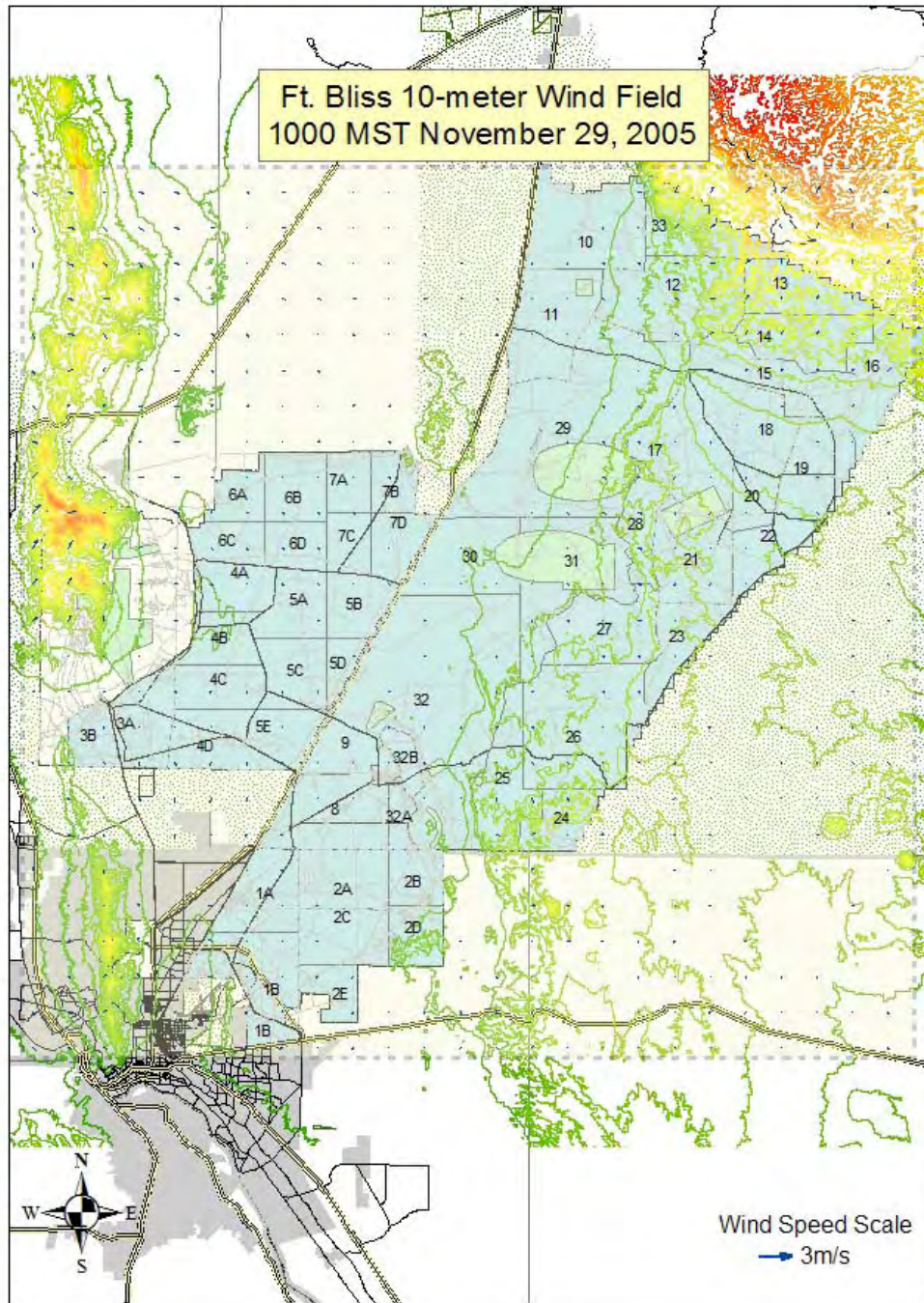


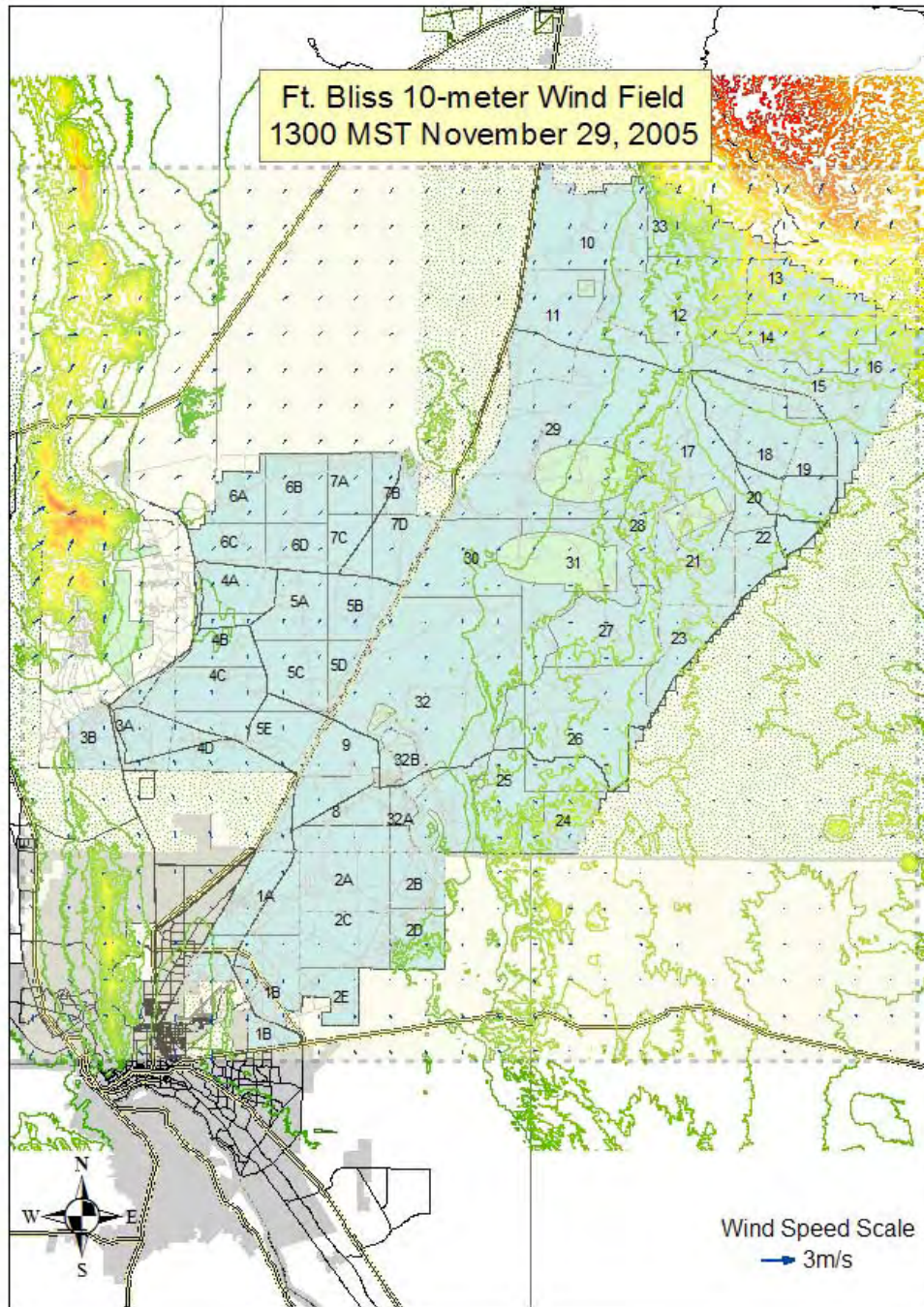


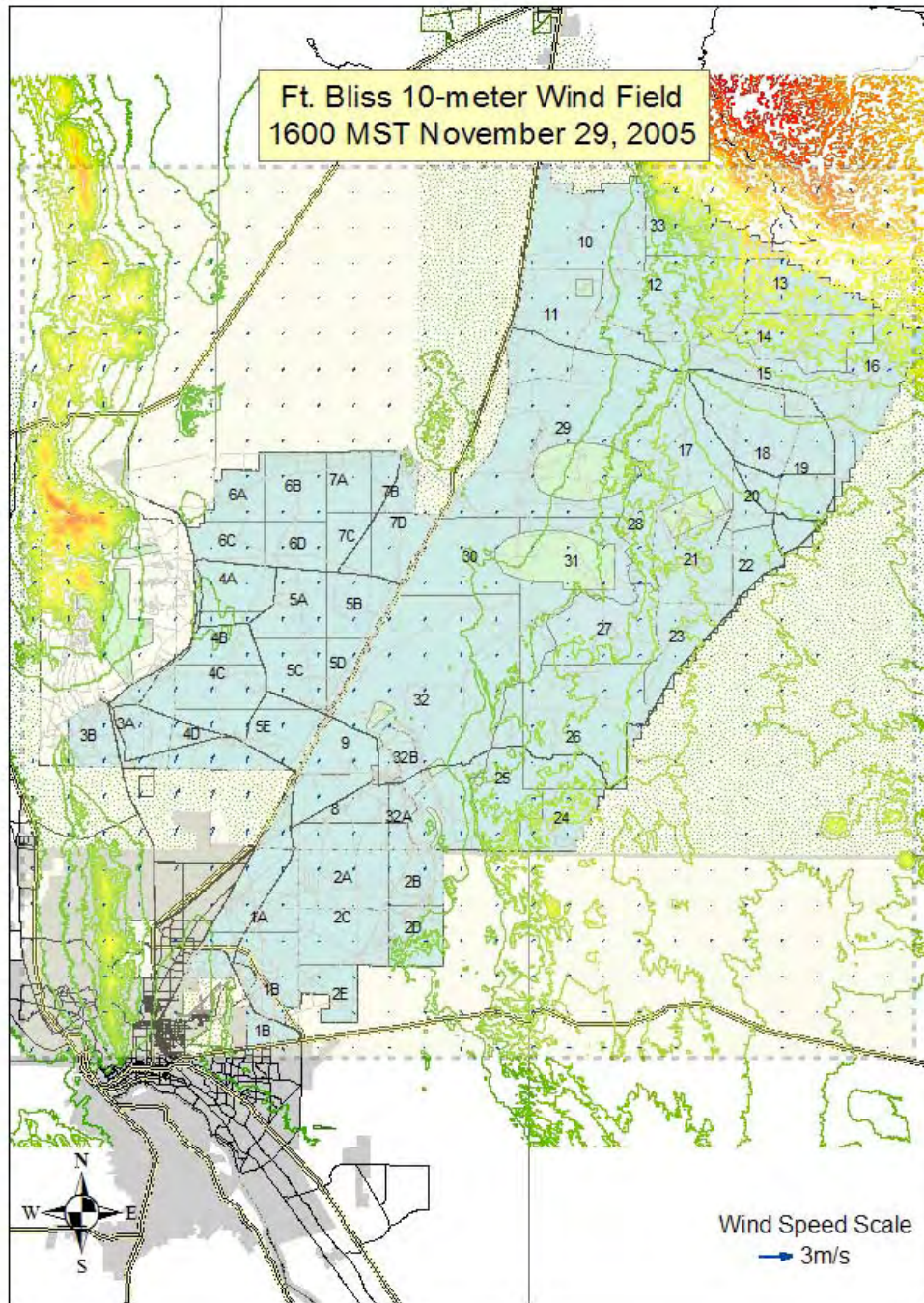


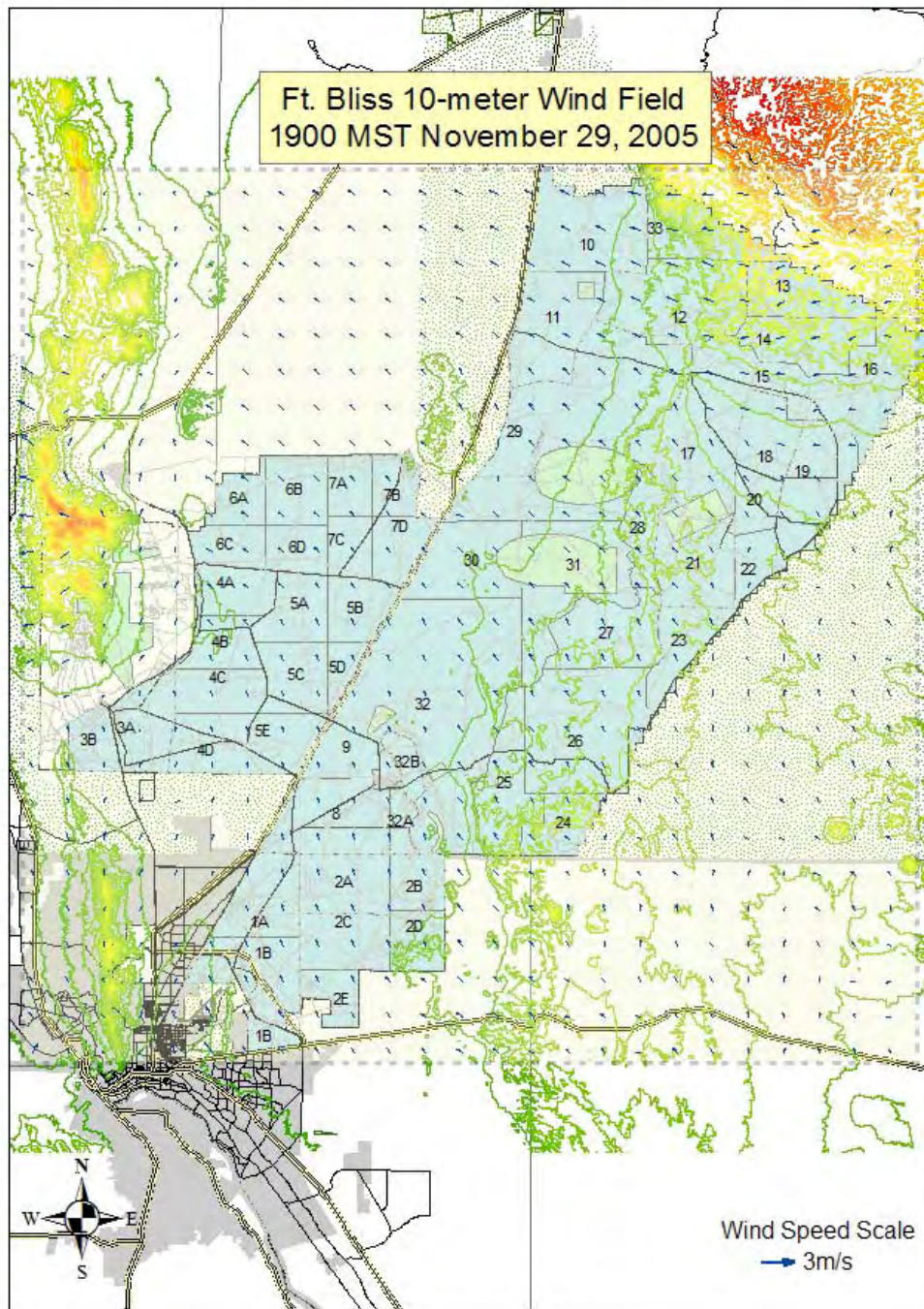












Distribution

**No. of
Copies**

**No. of
Copies**

OFFSITE

ONSITE

2 Jesus D. Moncada
Fort Bliss, Directorate of Environment
IMSW-BLS Attn: Moncada
Bldg. 622-South, Taylor Road
Fort Bliss, Texas 79916
(915) 568-1838

8 Pacific Northwest National Laboratory
K. J. Allwine K9-30
E. G. Chapman K9-30
R. K. Newsom
J. P. Rishel
F. C. Rutz
T. E. Seiple
Information Release (2) P8-55